

DESTRUCTION OF PLUTONIUM USING NON-URANIUM FUELS IN
PRESSURIZED WATER REACTOR PERIPHERAL ASSEMBLIES
by

Paul Chodak III

B.S., Chemical Engineering
Worcester Polytechnic Institute, 1985

RECEIVED

JUL 11 1997

© STI

M.S., Environmental Engineering
Virginia Polytechnic Institute, 1992

SUBMITTED TO THE DEPARTMENT OF NUCLEAR ENGINEERING IN PARTIAL
FULFILLMENT OF THE REQUIREMENTS FOR THE DEGREE OF
DOCTOR OF PHILOSOPHY IN NUCLEAR ENGINEERING AT THE
MASSACHUSETTS INSTITUTE OF TECHNOLOGY

MAY 1996

The Government reserves for itself and
others acting on its behalf a royalty free,
nonexclusive, irrevocable, world-wide
license for governmental purposes to publish,
distribute, translate, duplicate, exhibit,
and perform any such data copyrighted by
the contractor.

Signature of the Author _____
Department of Nuclear Engineering
6 May 1996

Certified by _____
Michael J. Driscoll
Professor Emeritus of Nuclear Engineering
Thesis Supervisor

Certified by _____
Neil E. Todreas
Professor of Nuclear Engineering
Thesis Supervisor

Certified by _____
Marvin M. Miller, Ph.D.
Senior Research Scientist, Department of Nuclear Engineering
Thesis Reader

Accepted by _____
Jeffrey P. Friedberg
Chairman, Department Committee on Graduate Students

DISTRIBUTION OF THIS DOCUMENT IS UNLIMITED

MASTER

19980420 001

DESTRUCTION OF PLUTONIUM USING NON-URANIUM FUELS IN PRESSURIZED WATER REACTOR PERIPHERAL ASSEMBLIES

by

Paul Chodak III

Submitted to the Department of Nuclear Engineering on May, 6th 1996 in Partial
Fulfillment of the Requirements for the Degree of
Doctor of Philosophy in Nuclear Engineering.

ABSTRACT

This thesis examines and confirms the feasibility of using non-uranium fuel in a pressurized water reactor (PWR) radial blanket to eliminate plutonium of both weapons and civilian origin. In the equilibrium cycle, the periphery of the PWR is loaded with alternating fresh and once burned non-uranium fuel assemblies, with the interior of the core comprised of conventional three batch UO_2 assemblies. Plutonium throughput is such that there is no net plutonium production: production in the interior is offset by destruction in the periphery. Using this approach a 50 MT WGPu inventory could be eliminated in approximately 400 reactor years of operation. Assuming all other existing constraints were removed, the 72 operating US PWRs could disposition 50 MT of WGPu in 5.6 years. Use of a low fissile loading plutonium-erbium inert-oxide-matrix composition in the peripheral assemblies essentially destroys 100% of the ^{239}Pu and $\geq 90\%^{total}Pu$ over two 18 month fuel cycles. Core radial power peaking, reactivity vs EFPD profiles and core average reactivity coefficients were found to be comparable to standard PWR values. Hence, minimal impact on reload licensing is anticipated. Examination of potential candidate fuel matrices based on the existing experience base and thermo-physical properties resulted in the recommendation of three inert fuel matrix compositions for further study: zirconia, alumina and TRISO particle fuels. Objective metrics for quantifying the inherent proliferation resistance of plutonium host waste and fuel forms are proposed and were applied to compare the proposed spent WGPu non-uranium fuel to spent WGPu MOX fuels and WGPu borosilicate glass logs. The elimination disposition option spent non-uranium fuel product was found to present significantly greater barriers to proliferation than other plutonium disposal products.

Thesis Supervisor: Michael J. Driscoll
Title: Professor Emeritus of Nuclear Engineering

Thesis Supervisor: Neil E. Todreas
Title: Professor of Nuclear Engineering

Thesis Reader: Marvin M. Miller
Title: Senior Research Scientist, Department of Nuclear Engineering

DISCLAIMER

This report was prepared as an account of work sponsored by an agency of the United States Government. Neither the United States Government nor any agency thereof, nor any of their employees, makes any warranty, express or implied, or assumes any legal liability or responsibility for the accuracy, completeness, or usefulness of any information, apparatus, product, or process disclosed, or represents that its use would not infringe privately owned rights. Reference herein to any specific commercial product, process, or service by trade name, trademark, manufacturer, or otherwise does not necessarily constitute or imply its endorsement, recommendation, or favoring by the United States Government or any agency thereof. The views and opinions of authors expressed herein do not necessarily state or reflect those of the United States Government or any agency thereof.

DISCLAIMER

Portions of this document may be illegible electronic image products. Images are produced from the best available original document.

ACKNOWLEDGMENTS

I would like to express my sincere appreciation and thanks to my thesis supervisors, Professors Michael J. Driscoll and Neil E. Todreas for their patience, guidance and support throughout the course of this work. They provided me with a great deal of advice and encouragement which was always welcomed and enlightening. In addition my special thanks goes to Senior Research Scientist Dr. Marvin Miller for his insightful comments during the writing of this thesis.

I must also thank Idaho National Engineering Laboratory (INEL) for allowing me to use their new MOCUP code. The code was indispensable; without it I'd still be running depletion calculations! To the guys at INEL, DR. Chuck Wemple and Rich Moore, I owe a special debt of gratitude for their unending support.

The research was performed under appointment to the Nuclear Engineering/Health Physics Fellowship program administered by Oak Ridge Institute for Science and Education under contract number DE-AC05-76OR00033 between the U.S. Department of Energy and Oak Ridge Associated Universities. I'd like to thank the Department of Energy for supporting my doctoral program studies at MIT through their Nuclear Engineering Fellowship Program. The program was superbly administered by the folks at Oak Ridge Associated Universities.

Finally, I would be remiss if I failed to acknowledge the contributions of my wife. Carolyn, we have both grown so much. The road was long and challenging but you were always there. Thank you.

TABLE OF CONTENTS

Abstract	2
Acknowledgments	3
List of Figures	9
List of Tables	13
CHAPTER ONE: INTRODUCTION	16
1.1 Scope and Objectives	16
1.2 Background	19
1.2.1 Plutonium Isotopic Grades and Definitions	19
1.2.2 Plutonium Sources and Stockpiles	23
1.3 Proliferation Concerns	23
1.3.1 Plutonium as a Nuclear Explosive Material	23
1.3.2 Distinction between a "Nuclear Weapon" and a "Nuclear Explosive" ..	25
1.3.3 Proliferation Threat Scenarios	29
1.3.4 Safeguards, Security and Verification Considerations.....	33
1.4 Summary and Conclusions.....	40
CHAPTER TWO: SUMMARY AND QUALITATIVE COMPARISON OF WEAPONS GRADE PLUTONIUM DISPOSITION OPTIONS.....	42
2.1 Fundamental Considerations for WGPu vs. RGpu dispositon.....	44
2.2 Reactor Burning of Plutonium	48
2.2.1 Current Light Water Reactors	50
2.2.2 Advanced Light Water Reactors	55
2.2.3 CANDU Reactors	56
2.2.4 Plutonium Consumption - Modular High Temperature Gas Reactor .	58
2.2.5 Other Reactors	60
2.3 Non-Uranium Plutonium Enriched Fuel in PWR Periphery	62
2.3.1 A Non-Uranium Fuel	64
2.3.2 PWR Peripheral Cycle Description	66
2.4 Comparison of Options	66
2.4.1 Definition of Reactor Disposition Options.	69
2.4.2 Throughput, Discharge Isotopes and Destruction.....	71
2.5 Summary and Conclusions.....	71
CHAPTER THREE: QUANTIFYING PROLIFERATION RESISTANCE	74
3.1 Background	75
3.1.1 NAS Proliferation metrics	76
3.1.2 Discussion of NAS Metrics	80
3.1.3 Inherent Barriers	81

3.2 Disposition Product Host Matrix Proliferation Barrier Metrics	82
3.2.1 Fissile Density	82
3.2.2 Chemical Barriers	83
3.2.3 Radiation Barrier	87
3.3 Plutonium Weapons Usability Metrics	88
3.3.1 Critical Mass	89
3.3.2 Neutron Emission Rate	89
3.3.3 Plutonium Isotopic Composition	90
3.3.4 Decay Heat	90
3.4 Scoring and Ranking Algorithm	91
3.4.1 Minimum Threshold.	92
3.4.2 Metric Contribution Weighting	93
3.4.3 Individual Metric Scoring ...	93
3.4.4 Barrier Type Evaluations	96
3.4.5 Overall Ranking of Plutonium Product Forms	97
3.5 Example Implementation of Proposed Metrics	98
3.5.1 Description of Reference Cases	98
3.5.2 Metric Value Results	100
3.5.3 Metric Scoring Results	103
3.5.4 Barrier Type and Overall Scoring Results	106
3.6 Summary and Conclusions	109
 CHAPTER FOUR. NON-URANIUM PLUTONIUM FUELS	112
4.1 Introduction	113
4.1.1 The Ideal Pu Burnup Fuel	113
4.1.2 Design Variables and Assumptions	113
4.2 Required Material Properties	117
4.2.1 Basis for Fuel Performance Requirements	117
4.2.2 Thermal Performance Criteria	119
4.3 Non-Uranium Plutonium Fuel Neutronic Considerations	122
4.3.1 ^{239}Pu compared with ^{235}U	122
4.3.2 Effects of ^{240}Pu and ^{241}Pu Content	124
4.3.3 Special Considerations for Non-Uranium Fuels	125
4.3.4 Use of Burnable Poisons	127
4.3.5 Thorium as a Fertile Material	131
4.3.6 Clad Composition	132
4.4 Literature Survey of Non-Uranium Plutonium Fuels	132
4.4.1 Thorium-Pu and Cerium-Pu Fuels	134
4.4.2 Zirconium and Aluminum Matrices	134
4.4.3 Tungsten-Pu Fuels	135
4.5 Fuel Matrix Selection	136

4.6 Selected Fluorite and Dispersion Matrices	140
4.6.1 PuO ₂ -ThO ₂	140
4.6.2 Stabilized Zirconia and Ceria	141
4.6.3 Alumina Fuel Matrix	142
4.6.4 TRISO Fuel Matrix	144
4.6.5 Application of Thermal Performance Metrics	146
4.7 Fabrication Technology	147
4.7.1 Oxide Fuel Fabrication	150
4.7.2 - TRISO Fuel Fabrication	151
4.8 Peripheral Assembly Fuel Cycle	152
4.9 Conclusions	155

CHAPTER FIVE. COMPUTATIONAL CODES, MODELS AND TECHNIQUES	155
5.1 Code Descriptions	156
5.1.1 MCNP-Origin2 Coupled Utility Program (MOCUP) Depletion Calculations	156
5.1.2 Selection of Key Nuclides	160
5.2 Benchmark Calculations	161
5.2.1 Description of Benchmark Specifications	161
5.2.2 Benchmark Results	164
5.2.3 Discussion of Benchmark Results	169
5.2.4 Conclusions of Benchmark Calculations	172
5.3 Models and Techniques	173
5.3.1 34 Pin Model Power Radial Power Profile Calculations	174
5.3.2 Pin Cell Depletion and Reactivity Coefficients	177
5.3.3 Analysis of Depletion and Pin Power Peak Information	180
5.3.4 Calculation of Core Average Reactivity Coefficient Calculations	183
5.54 Summary	187

CHAPTER 6. NON-URANIUM FUEL AND PERIPHERAL PWR CYCLE RESULTS	189
6.1 Proposed Fuel and Cycle	190
6.1.1 Importance of the Fuel's Inert Matrix Diluent.....	191
6.1.2 Plutonium Cycle and Throughput	194
6.2 Radial Power Peaking and Depletion of Oxide5 Fuel	195
6.2.1 Depletion Through Two Cycles	195
6.2.2 Summary of Radial Power Peaking and Depletion Results	203
6.3 Oxide5 and Whole Core Reactivity Coefficients	204
6.3.1 Fuel Temperature Reactivity Coefficient	205
6.3.2 Moderator Temperature Coefficient Results	210
6.3.3 Inverse Boron Worth and Void Coefficient	213

6.3.4 Summary of Reactivity Coefficient Result	214
6.4 Other Results	214
6.4.1 High Plutonium and Poison Loading	214
6.4.2 Comparison of Thorium and non-Thorium Fuels	217
6.4.3 Summary of Other Results	221
6.5 Summary and Conclusions	221
 CHAPTER 7. SUMMARY AND CONCLUSIONS	224
7.1 Scope and Objectives	224
7.2 Background and Motivation for Work	225
7.3 Summary of Proposed US WGPu Disposition Options and the RGPU Mission	227
7.4 Quantification of the Proliferation Resistance Inherent in Disposition Products	229
7.4.1 Definition of Metrics	229
7.4.2 Example Computation and Comparison of Proliferation Resistance in Spent WGPu MOX, a Borosilicate Glass Log and Spent Non-Uranium Fuels	230
7.4.3 Discussion of Example Proliferation Resistance Calculations	233
7.5 Material and Neutronic Considerations and Selection of a Non-Uranium Fuel Matrix	235
7.5.1 Non-Uranium Plutonium Fuel Neutronic Considerations	235
7.5.2 Narrowing the Field	238
7.5.3 Thermal Performance Criteria	239
7.6 Computational Codes, Models and techniques	242
7.6.1 Depletion Calculations	242
7.6.2 Models and Techniques	245
7.6.3 Calculations of Core Average Reactivity Coefficients	245
7.7 Results	247
7.7.1 Description of the PuO ₂ -Er ₂ O ₃ -inert Matrix and Peripheral Cycle	249
7.7.2 Radial Power Peaking and Depletion Cycle Results	250
7.7.3 Oxide5 Core Average Reactivity Coefficient Results	255
7.7.4 Conclusions on Oxide5 Performance	265
7.8 Conclusions	264
7.9 Future Work	265
 APPENDIX A: NOMENCLATURE	267

APPENDIX B: EXAMPLE PLUTONIUM DISPOSITION PRODUCT INHERENT PROLIFERATION RESISTANCE BARRIER METRIC CALCULATIONS	269
B.1 WGPU Non-Uranium Fuel Raw Metric Values	269
B.2 Conversions of Metric Values into Metric Scores	273
APPENDIX C: WEIGHTING TO DETERMINE CORE AVERAGE REACTIVITY COEFFICIENTS	282
REFERENCES	286

LIST OF FIGURES

Figure 1.1	Critical Mass of Uranium and Plutonium as a Function of Isotopic Mix.....	17
Figure 3.1	Overview of Individual Metric Scoring	94
Figure 3.2	Example Critical Mass Metric Scoring Function	95
Figure 3.3	Overview of Barrier Type Scoring	96
Figure 3.4	Scoring of Overall Proliferation Resistance of a Plutonium Disposition Product	97
Figure 4.1	Fuel Temperature Profile	120
Figure 4.2	Comparison of ^{239}Pu and ^{235}U Thermal Fission Cross Sections	124
Figure 4.3	^{240}Pu Absorption and ^{241}Pu Fission Thermal Cross Sections	125
Figure 4.4	Fuel Constituent and Crystalline Matrix Selection Logic Flow Chart	138
Figure 4.5	Typical Fuel Fabrication Flow Sheet	148
Figure 4.6	TRISO Fuel Fabrication for the GA-PCMHTGR	151
Figure 5.1	MOCUP, MCNP, ORIGEN Depletion Information Flow Scheme	158
Figure 5.2	Detailed Flow Chart of MOCUP, MCNP, ORIGEN and User Supplied Files	158
Figure 5.3	MCNP PWR Pin Cell Cross Section	163
Figure 5.4	Benchmark PWR Pin Cell Reactivity vs Burnup	165
Figure 5.5	Hi. Ref., Lo. Ref. and MOCUP Reactivity Difference vs Burnup.....	165
Figure 5.6	Benchmark Reactivity vs Burnup	167
Figure 5.7	Hi. Ref., Lo. Ref. and MOCUP Reactivity Difference vs Burnup	168
Figure 5.8	Comparison of CASMO and MOCUP Normalized Actinide and Fission Product Weight % vs Burnup	169
Figure 5.9	MCNP 34 Pin Row, Two Assembly Model	175
Figure 5.10	Example Pin Radial Power, Thermal and Fast Flux 34 Pin Model Results	177

Figure 5.11	MCNP PWR Pin Cross Section	178
Figure 5.12	Pin Power - Depletion Algorithm	180
Figure 5.13	Example Reactivity vs Burnup Profiles	181
Figure 5.13	Pin to Pin Power Peak for PuO ₂ Assembly with Three Pu Pin Compositions	182
Figure 5.14	1/8 th Symmetry MCNP Core Model	186
Figure 6.1	Comparison of Reactivity Profiles of Similarly Loaded Fuels with Dissimilar Inert Matrices	192
Figure 6.2	Power Profile for Fresh 3.9 w% UO ₂ and Oxide5	195
Figure 6.3	Progression of Radial Power Peak for Oxide5 Through the First Cycle	196
Figure 6.4	Radial Power Shift as a Result of Rotating the Oxide5 Assembly at EOC One.....	198
Figure 6.5	Progression of Radial Pin Power Peaking Through the Second Cycle	200
Figure 6.5a	Oxide5 & UO ₂ Reactivity vs Burnup	201
Figure 6.6	UO ₂ and Oxide5 Pin Cell FTCs vs Burnup	206
Figure 6.7	Number Weighted and Reference PWR Core Average FTCs vs Burnup	206
Figure 6.8	Power Weighted and Reference PWR Core Average FTCs vs Burnup	207
Figure 6.9	Square Power Weighted and Reference PWR Core Average FTCs vs Burnup	207
Figure 6.10	UO ₂ and Oxide5 Pin Cell MTCs vs Burnup	208
Figure 6.11	Erbium Composition vs EFPD	208
Figure 6.12	Number Weighted and Reference PWR Core Average MTC vs Burnup	209
Figure 6.13	Power and Square Power Weighted and Reference Core Average MTC vs Burnup	210
Figure 6.14	UO ₂ and Oxide5 Pin Cell and Reference PWR Core Average IBW vs Burnup	211

Figure 6.15	Number and Power Weighted Core Average IBW vs Burnup	211
Figure 6.16	UO ₂ and Oxide5 Pin Cell Void Coefficients vs Burnup	212
Figure 6.17	Number and Power Weighted Core Average Void Coefficients vs Burnup	212
Figure 6.18	HTGR-1 Reactivity vs Burnup	215
Figure 6.19	Alumina and TRISO Reactivity vs Burnup	218
Figure 7.1	Critical Mass of Uranium and Plutonium as a Function of Isotopic Mix.....	226
Figure 7.2	Example Critical Mass Metric Scoring Function	231
Figure 7.3	Fuel Constituents and Crystalline Matrix Selection Logic Flow Chart	238
Figure 7.4	Fuel Temperature Profile	239
Figure 7.5	MOCUP, MCNP, ORIGEN Depletion Information Flow Scheme ...	243
Figure 7.6	MCNP 34 Pin Row, Two Assembly Model	245
Figure 7.7	Pin Power - Depletion Algorithm	245
Figure 7.8	Radial Power Profile for Fresh 3.9 w% UO ₂ and Oxide5	250
Figure 7.9	Progression of Radial Pin Power Peak Through the First Cycle	251
Figure 7.10	Radial Power Profile Shift between First and Second Cycles Due to Oxide5 Assembly Rotation	253
Figure 7.11	Progression of Radial Pin Power Peaking Through the Second Cycle	254
Figure 7.12	Oxide5 & UO ₂ Reactivity vs Burnup	255
Figure 7.13	Erbium Composition vs EFPD	255
Figure 7.14	UO ₂ and Oxide5 Pin Cell FTCs vs Burnup	256
Figure 7.15	Number Weighted and Reference PWR Core Average FTCs vs Burnup	257
Figure 7.16	Power Weighted Core Average FTCs vs Standard PWR Values	257
Figure 7.17	UO ₂ and Oxide5 Pin Cell MTCs vs Burnup	258
Figure 7.18	Power and Square Power Weighted and Reference Core Average MTC vs Burnup	258

Figure 7.19	UO ₂ and Oxide5 Pin Cell and Reference PWR Core Average IBW vs Burnup	259
Figure 7.20	Number and Power Weighted Core Average IBW vs Burnup	260
Figure 7.21	UO ₂ and Oxide5 Pin Cell Void Coefficients vs Burnup	261
Figure 7.22	Number, Power Weighted and Reference PWR Core Average Void Coefficient vs Burnup	261
Figure B.1	Example Metric Scoring Function	274
Figure B.2	Fissile Density Scoring Function	274
Figure B.3	Dissolution Scoring Function	275
Figure B.4	Separation Scoring Function	276
Figure B.5	Radiation Scoring Function	276
Figure B.6	Isotopic Scoring Function	277
Figure B.7	Critical Mass Scoring Function	277
Figure B.8	Neutron Emission Scoring Function	278
Figure B.9	Decay Heat Scoring Function	278

LIST OF TABLES

Table 1.1	Isotopic Composition of Grades of Plutonium	20
Table 1.2	Comparison of Weapons Characteristics of Plutonium Isotopes with ^{235}U ..	25
Table 1.3	Facilities Under Safeguards or Containing Safeguarded Material	37
Table 2.1	Advantages and Disadvantages of the PC-MHR	60
Table 2.2	Selected Typical Reference Reactor Designs	67
Table 2.3	Summary Comparison of Throughput, Discharge Isotopics and Destruction Capability	69
Table 3.1	NAS Risk Evaluation Criteria	78
Table 3.2	Inherent Plutonium Disposition Product Barrier Metrics	91
Table 3.3	Example $\text{ZrO}_2\text{-PuO}_2\text{-Er}_2\text{O}_3$ Fuel Composition	100
Table 3.4	Raw Metric Values	101
Table 3.5	Metric Scores	104
Table 3.6	Metric Weights, Contributions and Barrier Type Scores	107
Table 3.7	Final Scores and Ranking of Products	109
Table 4.1	Assembly/Core Design Variable	115
Table 4.2	Assembly Geometry	116
Table 4.3	General Fuel Performance Requirements	118
Table 4.4	Reference UO_2 Properties	118
Table 4.5	Summary of Proposed Thermo-physical Performance Criteria	121
Table 4.6	Cross Sections of Key Fuel Cycle Nuclides	123
Table 4.7	Comparison of Non-Uranium Plutonium and Standard Uranium Fuel Nuclear Design Characteristics	126
Table 4.8	Candidate Burnable Poison Cross Sections and Ratios	129
Table 4.9	Summary of Burnable Poison Uses	131
Table 4.10	Candidate Non-Uranium Plutonium Fuels	133
Table 4.11	Candidate Oxide Host Ceramics	138
Table 4.12	Peroskovites, LnAl_2O_3	139

Table 4.13	Unirradiated PuO ₂ and ThO ₂ Properties	141
Table 4.14	Unirradiated ZrO ₂ and CeO ₂ Properties	142
Table 4.15	Unirradiated Graphite and SiC Properties	146
Table 4.16	Summary of Recommended Fuels Thermo-physical Performance	161
Table 5.1	Selected Fission Products	162
Table 5.2	Benchmark Pin Cell Specifications	163
Table 5.3	Pin Cell Nuclide Densities	164
Table 5.4	Pin Cell Model Specifications	167
Table 5.5	Comparison of Relative Errors @ 10 GWd/MT	167
Table 5.6	Westinghouse Core Assembly Design Parameters	174
Table 5.7	MCNP Model Pin Cell Specifications	179
Table 5.8	Summary of Pin Cell Reference Parameters and Associated Reactivity Coefficients	184
Table 5.9	Summary of Reactivity Calculations	184
Table 5.10	Correlation of Required Information, Codes and Models	188
Table 6.1	Neutronic Performance Criteria for Plutonium Disposition Fuel Producing an Elimination Option	190
Table 6.2	Composition of Example Alumina and TRISO Fuels	192
Table 6.3	Composition of Recommended Non-Uranium Fuel: Oxide5	193
Table 6.4	Erbium Cross Section and Abundance Data	193
Table 6.5	OX1 and OX2 Pu Destruction	198
Table 6.6	Oxide5 Assembly Pin Power Over Two 440 EFPD Fuel Cycles	202
Table 6.7	Summary of Discharge Properties and Fuel Cycle Feasibility Performance of Oxide5	203
Table 6.8	Summary of Core Average Reactivity Coefficient Results	213
Table 6.9	HTGR-1 Depletion Isotopic Summary	216
Table 6.10	Non-Fertile Alumina Fuel Composition	218
Table 6.11	Comparison of Fertile Production of Fissile Material in UO ₂ and Alumina Fuels	219
Table 6.12	TRISO and Alumina Fuel Depletion Isotopes	219

Table 6.13	Thorium TRISO Fuel Composition	220
Table 6.14	Summary of Oxide5 Neutronic Performance	222
Table 7.1	Summary of US WGPu Reactor Disposition Options	228
Table 7.2	Inherent Plutonium Disposition Product Barrier Metrics	230
Table 7.3	Raw Metric Values	231
Table 7.4	Metric Score Summary	232
Table 7.5	Metric Weights, Contributions and Barrier Type Scores	233
Table 7.6	Overall Ranking of Inherent Proliferation Resistance	233
Table 7.7	Comparison of Non-Uranium Plutonium and Standard Uranium Fuel Nuclear Design Characteristics	237
Table 7.8	Summary of Proposed Thermo-physical Performance Criteria	241
Table 7.9	Summary of Recommended Fuels Thermo-physical Performance	241
Table 7.10	Summary of Reactivity Coefficient Calculations	246
Table 7.11	Neutronic Performance Criteria	248
Table 7.12	Composition of Recommended Non-Uranium Fuel: Oxide5	249
Table 7.13	OX1 and OX2 Pu Destruction Data	252
Table 7.14	Summary of Oxide5 Neutronic Performance	263
Table B.1	Inherent Plutonium Disposition Form Barrier Metrics	269
Table B.2	Separation Metric Calculation	272
Table B.3	WNF Discharge Isotopic Neutron Emission and Decay Heat Calculations	272
Table B.4	Spent LEU, Spent MOX, and Borosilicate Glass Log Isotopes	272
Table B.5	Raw Metric Values	273
Table B.6	Metric Score Summary	279
Table B.7	WNF Barrier Type Score	280
Table B.8	Metric Weights, Contribution and Barrier Type Score	281
Table B.9	Overall Scores of Inherent Proliferation Resistance	281

CHAPTER ONE: INTRODUCTION

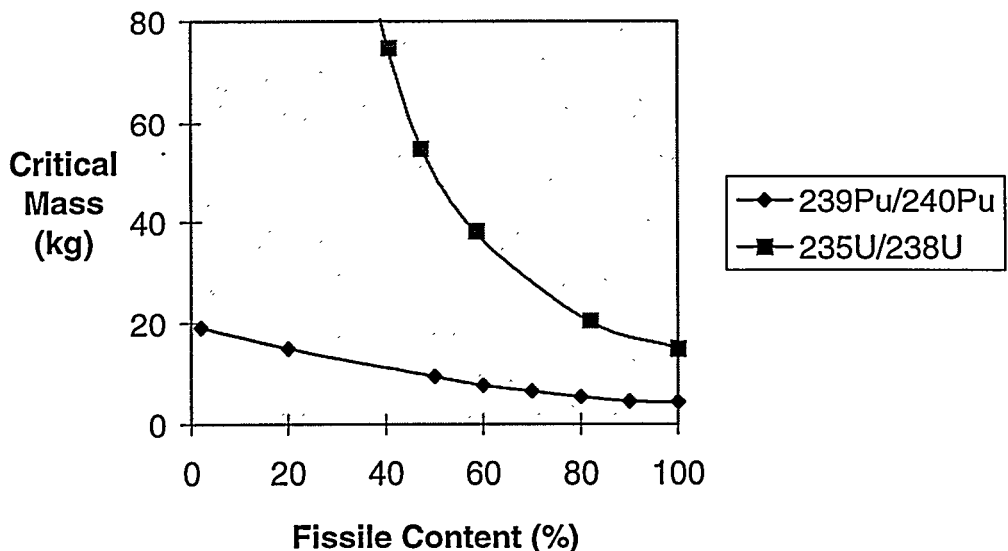
1.1 Scope and Objectives

Plutonium of nearly any isotopic composition can be used to produce an explosive critical mass.¹ Figure 1.1 plots the critical mass of uranium and plutonium in a simple weapon design consisting of a metal sphere surrounded by a thick neutron reflecting uranium metal shell [R-2]. Approximately 10 kilograms of plutonium with an isotopic content typically found in once-through light water reactor spent fuel would be sufficient to build such a simple nuclear explosive. The basic information required to assemble a nuclear weapon has been public for many years [T-2]. Therefore, physical control of plutonium and other weapons usable fissile materials is the primary means of limiting the proliferation of nuclear destruction capabilities. By the year 2000, the world inventory of all plutonium (Pu) will be 1600-1700 metric tons (MT). This inventory is projected to continue to grow by 60-70 MT per year [N-1]. The reliability of international safeguards in deterring and detecting diversion of plutonium for non-peaceful purposes is a function of the size and physical form of the stockpile which must be safeguarded. For example, plutonium in the form of fuel

¹ High concentrations of ^{238}Pu and ^{242}Pu in a plutonium mix make those compositions much less practical for use in nuclear explosives. However, these exceptions are inconsequential since the vast majority of the world's plutonium is of an isotopic composition which makes it of practical use in producing a nuclear yield.

assemblies which can be counted are easier to safeguard than plutonium in the separations part of a reprocessing plant where it is dissolved in various radioactive solvents [M-2]. Measurement and monitoring uncertainties applied to large stockpiles make it nearly impossible to comply with the IAEA guideline of timely detection of the diversion of a significant quantity of fissile material, and can be sufficient to allow accumulation of enough material to produce several weapons.² Consequently, many experts have called for a reduction of world inventories of plutonium [N-1, V-1].

Figure 1.1 Critical Mass of Uranium and Plutonium as a Function of Isotopic Mix [R-2]



^{239}Pu has a 24,000 year half life and it decays to ^{235}U with a 700,000,000 year half life. Both ^{239}Pu and ^{235}U are excellent material with which to build a nuclear weapon. Thus, nuclear transmutation, primarily through fission reactions, is the only way to irrevocably reduce the stockpile of nuclear weapons material. Light water reactors (LWR) are the primary vehicles through which large quantities of materials can be transmuted and PWRs are the dominant LWR variant. Thus, transmutation of plutonium in PWRs is one of the weapons grade plutonium (WGPu) disposal options recommended by the National Academy

² The IAEA defines a significant quantity as 8 kgs of Plutonium [M-2].

of Science (NAS). Mixed uranium-plutonium dioxide (MOX) fuels are already used to burn plutonium in the PWRs of several nations. Unfortunately, neutron capture in the ^{238}U also present produces ^{239}Pu , thereby reducing the maximum net plutonium destruction possible. Non-uranium fuels do not produce any plutonium and so eliminate more plutonium than mixed oxide fuels for the same reactor power level and capacity factor. Total plutonium destruction in a light water reactor with a mixed oxide core destroys only approximately 30% of the total plutonium loaded while non-uranium fuel plutonium disposition options destroy nearly twice that amount [D-4].

This thesis examines the feasibility of using non-uranium fuel in a pressurized water reactor radial blanket to eliminate plutonium of both weapons and civilian origin. Several constraints are considered including effect on the risk of proliferation, acceptability of resultant core physics parameters and fuel manufacturing feasibility. Elimination is defined as substantially complete destruction via transmutation. Large scale use of non-uranium fuels for plutonium disposal will require a significant research and development effort. The goal of this work is to suggest a starting point for that development.

The first chapter reviews background information and defines the terms that frame the debate over plutonium disposal. Chapter two presents a brief summary and a qualitative comparison of the various disposition options being considered for WGpu in addition to the proposed non-uranium peripheral PWR scheme. Next, a series of metrics are presented for quantifying the relative proliferation resistance of the plutonium forms associated with the disposal options. The fourth chapter discusses the general neutronic considerations of non-uranium fuels and outlines the search for non-uranium fuel matrices with acceptable properties. Chapter 5 reviews the computational tools and methods used to develop and analyze fuel performance. Analysis of the results are presented and discussed in chapter six. The final chapter summarizes the thesis, draws final conclusions and identifies future work.

1.2 Background

This section provides a picture of what kinds and how much plutonium exists in world stockpiles. The two basic types of plutonium, referred to as “reactor grade” and “weapons grade”, are defined. Then the custodians, sizes and rates of growth of current world stockpiles of each type are outlined.

1.2.1 Plutonium Isotopic Grade Definitions. Plutonium is generally classified as being of either of two grades: weapons grade or reactor grade. These grades correspond to the traditional separation between the two primary sources of plutonium: military weapons programs and the civilian nuclear power industry. Reactor and weapons grades of plutonium are defined according to their isotopic content. The Department of Defense defines plutonium grades based on ^{240}Pu weight percent: weapons grade plutonium (WGPu) contains less than 7 weight percent (w%) and reactor grade plutonium (RGPu) contains greater than 19 w% [D-7]. Berkhout et al (1993) provide a concise description of typical compositions and key properties as listed in table 1.1 [B-1]. RGPu is defined here to include the range of isotopic compositions found in typical commercial spent low enriched uranium (LEU) and MOX fuels. WGPu is defined in accordance with the generally accepted US and Russian definition of plutonium that contains $> 94\% \text{ }^{239}\text{Pu}$ [V-1].

The isotopes of RGPu can vary considerably depending on the power history of the host material. Plutonium is formed via neutron capture in ^{238}U , followed by two relatively rapid beta minus particle decays producing ^{239}Pu . The higher isotopes of plutonium are primarily formed via subsequent ^{239}Pu neutron capture reactions. $^{240\&242}\text{Pu}$ have relatively low thermal fission cross sections and their concentrations tend to build up with fluence. In contrast, ^{241}Pu is an excellent fissile material with a large thermal fission cross section. Most of the RGPu is found in once-through LEU spent fuel and has an isotopic composition similar to the values listed in table 1.1 [B-1]. As plutonium is recovered and recycled as

MOX, the relative content of the higher isotopes increases. The reduction in ^{239}Pu and increase in $^{240,241\&242}\text{Pu}$ concentrations as a result of a second cycle can be seen by comparing the spent LEU and MOX fuel compositions found in table 1.1. With additional cycles the production and destruction rates of plutonium isotopes reach a quasi-equilibrium. Typical equilibrium spent MOX fuel plutonium compositions contain about 1-3% ^{238}Pu , 35-40% ^{239}Pu , 30-35% ^{240}Pu , 15-19% ^{241}Pu and 10-14% ^{242}Pu .

This distinction between weapons and reactor grade plutonium is an attempt to emphasize the separation between non-peaceful and civilian uses of nuclear technology. Unfortunately, as we will see, the distinction is one more founded in policy rather than in physics. First we will look at the sources of plutonium.

Table 1.1 Isotopic Composition of Grades of Plutonium

Isotope	Half Life	Reactor Grade ^a Spent Fuel LEU ^b	Reactor Grade ^a Spent Fuel MOX ^c	Weapons Grade ^d	Decay Heat	Neutron Emission	Delayed Neutron Fraction
	years	atom percent	atom percent	atom percent	kW/ton	neutrons/ sec-kg	
^{238}Pu	87.7	1.3	2.3	0.012	560	2.6×10^6	0.0021
^{239}Pu	24,100	60.3	38.1	93.8	1.9	22	
^{240}Pu	14.4	24.3	32.7	5.8	6.8	9.1×10^5	
^{241}Pu	376,000	8.3	16.9	0.23	4.2	49	0.0049
^{242}Pu	430	5.0	8.3	0.022	0.1	1.7×10^6	
^{241}Am		0.8	1.7	0.13	114	1.2×10^3	
Radiation hazard relative to ^{239}Pu		190	290	34			
Maximum storage time of separated Pu (yrs) ^e		7	3	No Limit			
Neutron emission rate ($\text{s}^{-1}\text{t}^{-1}$)		3.3×10^5	5.0×10^6	5.3×10^4			
Pu Decay Heat (kW/t^{-1}) after 10 years of storage		14.3	24.4	2.4			

a. Plutonium stored for two years after separation
b. Fuel irradiated in a PWR to 33 Mwd/kg and stored for 10 years before reprocessing
c. Fuel irradiated in a PWR to 43 Mwd/kg and stored for 10 years before reprocessing
d. Weapons Material Stored for ten years
e. The period of time the material could be stored before becoming unacceptable for use in MOX fabrication facilities. Assuming plutonium separated after 10 years fuel storage and a maximum ^{241}Am content of 2.5%.

1.2.2 Plutonium Sources and Stockpiles. Unlike highly enriched uranium which is almost entirely under the stewardship of United States (US) and Former Soviet Union (FSU) militaries, the vast majority of the world's stockpile of plutonium is under civilian control. Spent fuel is the largest single source of plutonium containing some 1100 metric MT of RGPu and is produced at a rate of 60-70 metric MT/year [N-1]. Separated RGPu stockpiles are also growing.

In the 1970's, the projected growth in energy demand and the fraction of that demand which would be supplied by nuclear power were overestimated. In addition, it was anticipated that fast breeder reactor programs would prosper and require plutonium fuel. Based on these estimates, shortages in available uranium reserves were anticipated. Consequently, large capital intensive programs were begun to expand reprocessing capacity and close the nuclear fuel cycle. In the intervening period since these programs were begun, energy demand leveled off, nuclear power plant construction stagnated and large new uranium reserves were discovered. In addition, fast breeder reactor programs have been delayed and scaled back in response to public concerns, technical problems and the below expected growth in energy demand [N-3]. The result has been a long term glut in the uranium market driving down the price of uranium U_3O_8 , the raw material for LEU LWR fuel, from typical market prices of \$30-50 per pound in 1978 down to \$7.25 per pound in 1995 [B-3].³ Consequently, the additional reprocessing and remote fabrication costs associated with MOX fuel make it economically unattractive, and less than 1/5th of the plutonium in spent fuel has been recovered [B-1].

Through 1990, 120.5 MT of civilian RGPu had been separated. Of this, only 35.7 MT were used in fast breeder reactors and 12.3 were used for MOX in light water reactors. As of 1992, 86 MT of separated plutonium were in storage worldwide [N-1]. Despite realization that plutonium cycles will neither be cost effective nor required to extend fuel reserves in the foreseeable future, plutonium reprocessing programs are likely to continue in

³ The price of one pound of U_3O_8 was \$7.25 in March 1995 and has only recently doubled over the last year due to worldwide increase in nuclear power and reduced Russian output [J-1].

Europe, Russia and Japan due to the momentum of long range contracts and capital investments [N-1]. New reprocessing plants whose construction was begun in the 1970's and early 1980's are just now opening their production lines. This additional new capacity adds to the existing separated RG⁹²Pu production-consumption mismatch. Following current reprocessing production plans, approximately 20 MT of separated RG⁹²Pu will be added to the stockpile annually [S-3]. Consequently, civilian separated RG⁹²Pu stockpiles are projected to increase to between 110 and 170 MT by early in the next century.

Another major source of plutonium comes from military nuclear weapons programs. These programs ran reactors whose sole function was to produce WG⁹²Pu. LEU fuel was driven to very low burnups in LWRs to optimize the production of the desirable ²³⁹Pu isotope relative to the higher plutonium isotopes. The fuel was reprocessed and the plutonium recovered for use in the construction of nuclear arsenals. Over the period from 1944 to 1994 the US produced or acquired 111.4 MTs of WG⁹²Pu [D-3]. Strategic Arms Reduction Treaty (START) agreements between the US and FSU call for nuclear arms reductions down to 1,000-2,000 tactical weapons and 3,000-3,500 strategic weapons. To reach these objectives the US must retire approximately 15,000 weapons and the FSU as many as twice that number [B-1]. Forty-five and ninety MT of plutonium pits may be made available for disposal through US and FSU weapon dismantling programs, respectively. There is approximately another 70-120 MT in combined plutonium scrap material inventories. The US recently declared 38.3 metric MT of WG⁹²Pu to be excess to national security needs [D-3]. This amounts to 50% of the total US weapons plutonium inventory. Estimates of between 100 and 200 MT of WG⁹²Pu pits and residual WG⁹²Pu scraps will be added to the separated plutonium stockpile by the year 2000.

It is worth reiterating that either reactor or weapons grade can be fashioned into a weapon which is capable of producing a nuclear fission explosion. Hence, the distinction implied by the names of these two grades is somewhat misleading as will be discussed in the next section.

1.3 Proliferation Concerns

The information necessary to build a nuclear weapon has been public for many years and the necessary equipment and non-nuclear components are accessible worldwide [T-3]. Once a would-be nuclear bomb maker has possession of sufficient quantities of plutonium, little else stands in the way of producing a device capable of producing a nuclear fission explosion. This section discusses the value of RGPu as a raw material for nuclear explosives and proliferation threat scenarios. First the nuclear explosive properties specific to plutonium are reviewed. Then the distinction between a RGPu nuclear “explosive” and a WGPu nuclear “weapon” is considered. Finally, the current weapons reduction verification methods are discussed for their potential application to plutonium stockpile reduction through burning as fuel in multiple LWRs.

1.3.1 Plutonium as a Nuclear Explosive Material. Unlike uranium, all plutonium isotopes can sustain a fast chain reaction and so the critical mass for all plutonium isotopic compositions is finite; plutonium poses a unique proliferation threat. The age of the earth is equivalent to over 10,000 half lives of the longest lived plutonium isotope; thus, plutonium is essentially not found in nature.⁴ ^{239}Pu production in LEU fuels is the primary source of plutonium. Higher plutonium isotopes are produced from ^{239}Pu via sequential neutron captures. ^{238}Pu is produced by ^{242}Cm alpha decay. Thus, most plutonium is predominantly composed of ^{239}Pu as can be seen in table 1.1. Unfortunately, ^{239}Pu is also the preferred isotope for making a nuclear weapon. It is worth digressing to belabor the contrast between plutonium and uranium weapons properties.

^{238}U will not sustain a fast chain reaction. Consequently, 233 & ^{235}U can be diluted with ^{238}U to produce pure uranium which is not weapons usable; pure uranium with less than 6 weight percent (w%) fissile isotopes cannot be used to produce a nuclear fission explosive [T-2]. As a practical limit, uranium enrichment of greater than 20 w% is required to make a weapon of reasonable mass and volume [M-3]. Thus, uranium of less than 20w% 233 & ^{235}U must first be enriched to be of use for a nuclear weapon.

⁴The half life of ^{242}Pu is 376,000 years and the age of the earth is estimated here as 5 billion years.

Enriching uranium has historically not been the method of choice for obtaining weapons material. Gaseous diffusion technology was closely guarded in contrast to plutonium reprocessing technology which was made public in 1955 [M-7]. In addition, gaseous diffusion was capital intensive and consumed large amounts of energy which made it difficult to conceal. However, the physical plant equipment size and power requirements of modern gas centrifuge enrichment technology are much lower than those gaseous diffusion. Thus, construction and operation of gas centrifuge enrichment plants are more difficult to detect than gaseous diffusion plants. However, the difficulty in importing gas centrifuge technology remains a formidable barrier [M-7]. The chemical separation of plutonium from spent fuel is still easier to accomplish than uranium enrichment to weapons usable levels. Thus, preventing the diversion of plutonium remains the primary barrier to proliferation.⁵

All of the plutonium isotopes can be used to produce a bare metal critical mass. J. Carson Mark (1990) provides an excellent discussion of the characteristics of plutonium isotopes relevant to weapons use, some of which are listed in table 1.2 [M-1]. $^{239\&241}\text{Pu}$ are both fissile and have substantial fast neutron cross sections. Their cross sections differ somewhat but they have a similar bare metal critical mass. ^{241}Pu is less desirable than ^{239}Pu because it beta minus decays to produce ^{241}Am which emits a hard gamma and also leads to the production of ^{238}Pu . ^{238}Pu is fissionable with a very low threshold energy. Above 0.5Mev, ^{238}Pu has a larger cross section than ^{239}Pu so that even though it produces only 2.75 neutrons/fission, as compared to the 3.0 neutrons/fission of ^{239}Pu , it has a similar critical mass. However, ^{238}Pu is the least desirable isotope for weapons use because of its relatively large spontaneous fission probability and alpha emissions, which produces significant decay heat. As shown in table 1.1, small quantities of ^{238}Pu significantly increase the neutron flux of spent MOX and LEU RGPU compared to WGPU. In addition to being a handling hazard, a larger neutron flux reduces the probable nuclear yield.⁶ The ^{240}Pu fission cross section has a threshold of a few hundred kilovolts. The high fission threshold of ^{240}Pu reduces its

⁵ Development of enrichment capability is time consuming and is assumed not to be the first choice of a sub-national/terrorist proliferator. As is covered in section 1.3.3, this thesis focuses on a subnational proliferation threat.

⁶ For more discussion on the effect of neutron flux on nuclear yield. see section 1.3.2.

fissionability in a scattering environment such as an oxide. However, ^{240}Pu has a larger cross section than ^{235}U above 1 Mev, and in a metal system, the bare critical mass of ^{240}Pu is smaller than that of 94% enriched ^{235}U . Above 1 Mev, the fission cross section of ^{242}Pu is similar to ^{240}Pu but ^{242}Pu 's fission threshold is significantly higher making it a less effective weapons material. In addition it suffers the same spontaneous fission properties as ^{238}Pu although to a lesser extent. Unfortunately, even in very high burnup materials there is sufficient ^{241}Pu to offset the problems caused by ^{242}Pu .

Table 1.2 Comparison of Weapons Characteristics of Plutonium Isotopes With ^{235}U				
Isotope	Fission Behavior	1 Mev Range Fission Cross section (b)	Approximate # Neutrons Per Fission	Bare Metal Critical Mass (Kg)
^{238}Pu	Threshold (75 ev)	2.3	2.75	15
^{239}Pu	Fissile	2.2	3	15
^{240}Pu	Threshold (0.3 Kev)	1.9	3	40
^{241}Pu	Fissile	1.9	3	15
^{242}Pu	Threshold (100 Kev)	2.0	3	177
^{235}U	Fissile	1.6	2.45	52

a. Threshold energies are defined as the lowest energy above the thermal range for which the fission cross section exceeds 1 barn over a significant spectrum range.

The preceding discussion leads to the conclusion that although RGPU is less desirable than WGPU for making a weapon, both isotopic compositions support production of a nuclear fission explosive. In fact, RGPU material has a significantly lower fast critical mass than pure ^{235}U . The US successfully tested a RGPU nuclear weapon in 1977 [L-1]. The differences between RGPU and WGPU lay in the relative degree of the associated handling hazards and the reliability of the yield. The following discussion is a brief description of basic nuclear weapon design and mechanics.

1.3.2 Distinction Between “Nuclear Weapon” and “Nuclear Explosive”. Nuclear weapons in the arsenals of the Non-Proliferation Treaty (NPT) nuclear weapons states can reliably obtain a high percentage of their design yield. Yield is defined as the explosive power and is usually

measured in equivalent MT of high explosive. A weapon design yield fissions a significant portion of the weapons material, producing a large yield. In contrast, a fizzle yield equates to the minimum energy that must be produced if the system goes fast critical. Complete fission of 1 kilogram of uranium or plutonium produces a 17 kiloton yield. The weapon which destroyed Nagasaki produced a twenty kiloton yield. The Nagasaki weapon was a very simple implosion device consisting of a 6 kgm of WG⁹³Pu spherical core surrounded by a natural uranium metal tamper/reflector which was in turn surrounded by conventional high explosives. This design can be used as a generic model for discussion of weapon mechanics. A qualitative description of how a nuclear fission weapon works is followed by a quantitative discussion of the effects of the higher neutron flux associated with RG⁹³Pu.

The explosion process is initiated by the detonation of the high explosives. The force of the explosion initiates a shock wave which compresses the tamper and the core. Core compression increases plutonium sphere density and a critical geometry is achieved (i.e. critical mass $\propto 1/\rho$). The core continues to compress and begins to generate neutrons at an increasing, exponential rate as it becomes supercritical. The tamper reflects some of the neutrons which might otherwise leak out of the assembly back into the core. The compression continues until the energy generated by the fission begins to vaporize all the material, building up pressure, forcing the weapon apart and making the plutonium subcritical. The period of compression is called the assembly phase and is followed by the weapon rapidly exploding apart, which is the disassembly phase of the detonation. The mean time between fissions is approximately 10^{-8} seconds. Roughly 40-50 generations of fissions are required to generate sufficient energy to cause the expansion of the core [L-1]. The energy builds up in a few hundredths of a microsecond reaching temperatures around several hundred million degrees Kelvin and pressures of 10^8 bar. Expansion of the initial core radius by approximately 1 cm will reduce the probability that a neutron produced by fission will go on to cause another fission sufficiently to quench the chain reaction. There is time for only a few generations of fissions once the disassembly phase begins. The majority of the yield is generated during the disassembly phase.

The greater the compression or degree of supercriticality achieved prior to the disassembly phase, the more material that will be fissioned and energy released during the disassembly phase and the greater the yield of the weapon. Thus, yield is a function of the speed of assembly and the point of the start of the chain reaction during the assembly phase. The faster the assembly, the greater the degree of compression achieved when disassembly begins. A greater compression produces less leakage and higher maximum supercriticality. A longer delay to the onset of a chain reaction allows more time for assembly, increasing the degree of supercriticality. Greater supercriticality results in more fission during the disassembly phase.

A sustained chain reaction is one in which at least as many neutrons are produced as are consumed in any given neutron life cycle. Criticality is defined as the state at which the system produces as many neutrons as are lost to leakage and non-fission absorptions. Thus, the chain reaction can begin any time from the point of initial criticality, and is initiated by a sufficient number of neutrons causing fission. The chance that sufficient neutrons will cause fission, initiating the chain reaction, is proportional to the state of criticality and number of neutrons present. A higher neutron flux requires a lower state of criticality to initiate the chain reaction. This increases the probability that the chain reaction will be initiated earlier in the assembly phase resulting in a lower total yield. It is worthwhile to quantify these concepts.

The exponential increase in neutrons produced and energy released in the assembly phase can be expressed as $e^{\alpha t}$. The value of the time constant α , is zero for an exactly critical system and can reach $1-3 \times 10^8 \text{ sec}^{-1}$ for highly supercritical systems [M-1]. Alpha increases until the start of the disassembly phase. As the density of the weapon decreases during disassembly, the value of α drops off rapidly to zero. The higher the value of α which can be achieved prior to the start of the disassembly phase, the greater the total release of energy. For a system achieving a small degree of supercriticality, the fraction of the total fissile material which will be consumed is proportional to the value of α^3 at the point of initial disassembly [S-2]. In a core with a mass of approximately 10 kgs, disassembly begins when

αt reaches 40 to 45 where t is the time from the point of criticality [M-1]. The smallest possible explosion α value or smallest possible yield, is achieved when the chain reaction begins just as the system reaches criticality or $\alpha = 0$. This situation corresponds to a fizzle yield. As the neutron source is increased the probability of a fizzle yield increases. This relationship is represented by:

$$P = e^{-\left[\frac{1}{2} \bar{N} v'\right]} \quad (1-1)$$

where v' is the probability that any one neutron will start a chain reaction, N is the number of source neutrons produced in the time interval t from criticality ($v'=0$) to when v' equals its maximum value, and, P is the probability of not having predetonation up to that time [S-2]. The value of v' corresponds to the degree of supercriticality and the yield produced. The greater the peak value of v' , the more critical the system and the greater the probability of predetonation. For example, a material with a neutron source of 10^4 neutrons/second with an assembly which compresses 10 cm producing a final value of $v'=0.03$ and a compression velocity of 10^5 cm/sec has an $N=1$. Its chance of predetonation prior to achieving a $v'=0.03$ is $(1-e^{-0.015})$ or approximately 1.5%. If the neutron source is tripled to 3×10^4 neutron/sec, or $N=2$, the chance of predetonation will be approximately 4.4%. For the same system if the desired peak value of $v'=0.3$, the probability of predetonation would increase to 15% and 36.2% respectively. From table 1.1 WGPu, once-through spent RGPU and recycled spent MOX have N values of 5.3, 33 and 500. Thus, we would expect the probability of predetonation prior to a $v'=0.03$ to be 7.6%, 39.0% and 99.9% respectively. The reliability of the yield is significantly greater for WGPu than for spent RGPU or MOX plutonium isotopes. However, as seen in the difference in predetonation probability for $v'=0.03$ and $v'=0.3$, the effect of increased neutron sources on the predetonation probability diminishes for lower yields. The difference between an explosive constructed with WGPu versus RGPU becomes one in which the design yield is the typical yield, with very severe predetonation being rare

for WGPu, to one in which the typical yield is a band from one to a few times larger than the fizzle yield for RGPu.

However, a typical yield for a very unsophisticated RGPu explosive is likely to be on the order of 1 kiloton [M-1, T-2, L-1]. This is sufficient to level a significant portion of a major city and cover the rest in radioactive fallout. To a significant extent, the higher spontaneous fission probability of RGPu vs WGPu can be compensated for by using a more sophisticated design than that used in the first plutonium weapon. The predetonation problem caused by use of RGPu can be compensated for by a faster assembly phase and by fissioning a higher percentage the plutonium, giving the same yield for a smaller amount of material. For example, if both the assembly time and the amount of fissile material were halved, then the probability of predetonation would be decreased by a factor of 4. Better grades of conventional explosives will produce a more rapid compression, decreasing the value of N . Improvement in high explosives technology has resulted in the reduction of the weight of explosives required in US nuclear weapons from hundreds or thousands of pounds (5000 pounds for the Nagasaki bomb) to a range of 15 to 45 pounds [H-7]. Using a reflector similar in design to the one used in the Trinity device combined with the improved explosives available today could allow Trinity level yields (17 kilotons) with RGPu [L-1].

Thus, a nuclear weapon may be produced by using WGPu with an unsophisticated design or RGPu with a sophisticated design. A nuclear explosive is defined as device which has a low probability of producing its design yield. Unfortunately, the distinction may be insignificant when considering a terrorist threat scenario. The next section discusses potential proliferation threat scenarios.

1.3.3 Proliferation Threat Scenarios. In order to assess the effectiveness of plutonium disposal alternatives it is necessary to understand the proliferation threats that they are designed to counter. There are two distinct sources of plutonium weapons material which pose a proliferation threat: WGPu and RGPu. The immediate concern for proliferation is the disposal of WGPu. However, discussion of WGPu proliferation threats should include

consideration of the broader question of management of growing world inventories of separated RG⁹³Pu and spent fuel. In order to frame the discussion of different threat scenarios it is necessary to define some of the pertinent terms.

International programs for nuclear weapons fissile material control consist of safeguard and security measures. The purpose of safeguards is to detect any diversion of plutonium in peaceful use for weapons purposes. Security measures are designed to prevent diversion or theft of weapons materials for unauthorized uses. International safeguards are the responsibility of the International Atomic Energy Agency (IAEA), while security is the responsibility of the state in which the nuclear facilities are located.⁷ The threat of diversion of weapons material is differentiated from the threat of theft in that theft implies that the material is taken against the owner's will by a sub-national or terrorist group. Verification, which may include but is not limited to IAEA safeguards, is the process or procedures used to independently confirm that countries are fulfilling their treaty obligations such as the NPT and the Intermediate-range Nuclear Forces Treaty (INF). The NAS listed three types of WG⁹³Pu threats: diversion, theft and harmful implications of the management of WG⁹³Pu disposal [N-2].

National diversion of plutonium can be carried out either covertly or overtly. Covert diversion would include gradual siphoning off of weapons material from disposal process streams. The rate of plutonium removal from process streams might be kept within the tolerances of measurement uncertainties and so go undetected. Over time, large volumes of material will be processed allowing the diversion of significant quantities to unauthorized purposes. Overt diversion scenarios range from outright abrogation of the specific treaty requirements to violation of the intent. Neither the INF nor START include provisions for the verification of the elimination of warheads. The treaties limit the maximum number of deployed nuclear weapons and are focused on the dismantlement and destruction of weapons delivery systems. Neither the disposition of the warheads contained in these delivery vehicles nor the fissile material contain in the warheads are addressed. Existing multi-

⁷ Section 1.3.4 has a more detailed discussion on the interface of state and IAEA safeguards and security.

warhead launch vehicles are generally not loaded to their maximum warhead capacity. Consequently, warheads can be added to existing launch vehicles and or weapons material can be reused thereby significantly reducing the time required to reconstitute nuclear arsenals. A dramatic change in the political environment could lead a weapons nation to add warheads to remaining launch vehicles allowed by the treaties or onto new launch platforms not covered by the treaties. In these ways, a nation could rapidly scale up its nuclear arsenal to pre-treaty capabilities. This is known as the “Breakout” threat scenario.

Theft of weapons materials can be accomplished forcibly, overtly but not forcibly or covertly [N-2]. Another nation or sub-national group might directly and forcibly steal weapons material from a weapons nation or use an agent to effect the theft. Overt but non-forcible theft refers to a scenario in which national authority is lost leaving the material open for procurement by an outside group. Finally, the covert theft scenario requires the complicity of people inside the custodial organization. The faltering economic stability of Russia and other FSU nations are of greatest concern for this scenario. Fissile material controls in FSU states rely almost entirely on the physical security provided by the custodians of the material. Their material inventory systems are considered weak [N-1, V-1]. As the economic situation in these countries deteriorates, there is a growing incentive for custodial personnel to facilitate the theft of the highly valuable weapons material. This theft scenario applies to proliferation of nuclear weapons capabilities to other nations as well as non-national proliferation to sub-national groups.

It is important to view the impact of plutonium disposal in as broad and comprehensive a manner as possible. Disposal has the potential to decrease or increase the world nuclear proliferation threat. The NAS list potentially harmful influences of WGPu management on specific non-proliferation areas [N-2]. These harmful influences can also be applied to the larger picture of all plutonium: WGPu plus RGPu. WGPu disposal has the potential to weaken the institutions currently managing nuclear weapons in the FSU and US. WGPu management may provide incentives or disincentives for further arms reductions. Thus, a forthright and cooperative effort in good faith could go a long way toward building

the trust to move forward in the reduction of the global nuclear weapons threat. Weak and ineffective WGPu disposal may lead other nations to lose faith in the intentions of the nuclear weapons states and seek nuclear weapons capability. Finally, the way in which WGPu is dispositioned will have an impact on the way in which RGPU is handled in the future.

In the 1970's under former US President Carter, reprocessing was banned in the US because of the concern that it would legitimize and expand separation and use of RGPU in civilian fuel cycles. Such an expansion was considered a grave proliferation risk due to the potential for diversion of plutonium recovered during reprocessing of spent fuel. However, the rest of the world did not follow the US lead and the separation and use of RGPU has grown as discussed in section 1.2.1. The growth of the plutonium fuel cycle has been limited only because it is not economically justifiable in the near term. This is evidenced in the US where the reprocessing ban has since been repealed but reprocessing has not occurred. It can be argued that by removing itself from the development of reprocessing and plutonium fuels technology, the US has nullified its ability to influence the proliferation resistance of the plutonium economy. Similarly, a less than robust and comprehensive course of action in WGPu disposal will have ramifications on the US's ability to frame the solution to the growing world plutonium stockpiles.

The final dimension in considering the effectiveness of disposal alternatives to counter threat scenarios is time. The longer it takes to reduce the stockpile of available WGPu to the minimum level required the greater the risk of proliferation. Since WGPu in the form of metal "pits" is more attractive for weapons use than RGPU, which is usually stored in the form of spent fuel or PuO₂ powder, its availability poses a greater overall threat. Therefore, disposal of WGPu deserves the greatest immediate attention. The political instability in the FSU states underscores the need to move forward with final disposal of WGPu. However, consideration must be also given to the broader picture of growing total world inventories of RGPU both in spent fuel and separated form.

The scenarios discussed above are derived from consideration of WGPu disposal. The reduced reliability of yield and increased handling hazards associated with RGPU

weapons make it a less likely material of choice for building a national nuclear arsenal. Consequently, diversion and breakout scenarios are less credible threat scenarios when considering RGPU. However, the distinction between a nuclear weapon and a nuclear explosive discussed in section 1.3.2 becomes unimportant when considering a sub-national or terrorist type theft scenario threat. It follows that the theft scenario threat posed by WGPU is not much greater than that of separated RGPU [N-1]. There is no technical solution to thwart the will of a nation to develop or enhance its nuclear weapons capability. Knief states that "... little short of an act of war can prevent a determined state with the necessary resources from developing nuclear explosive capability." [K-4]. The other category of proliferators are terrorist organizations. This thesis seeks to address the need for reducing the world inventory of both WGPU and RGPU. Consequently, countering a non-national theft scenario is the primary focus of this work.

Any scheme for reducing the world's plutonium stockpile should include an integral system for verification of final plutonium disposal. This verification system must track the fate of all plutonium handled with sufficient certainty to satisfy international scrutiny and oversight. In the case of WGPU, this task is complicated by the concurrent requirement to protect sensitive weapons information. The next section begins by discussing current safeguards, security and verification practices as background for proposing how they may be extended to encompass the destruction of plutonium in light water reactors using non-fertile fuel.

1.3.4 Safeguards, Security and Verification Considerations. In recognition of the proliferation threat posed by civilian plutonium, the NAS states in its 1994 Disposition of Excess Weapons Plutonium Report that "..., safeguards and security for civilian separated plutonium and HEU should be increased to a level comparable to those applied to plutonium in military stocks." [N-1]. The NAS also calls for "international management" of all weapons usable materials, which includes civilian plutonium. There is a growing awareness of the need to bring all plutonium, WGPU, spent fuel RGPU and separated RGPU,

under more stringent control [B-1, N-1, M-3, V-1]. Proposed plans to bring about such changes include:

- ◊ Halting production of all fissile materials for weapons uses
- ◊ Nations possessing fissile materials to provide detailed and verifiable declarations of all such materials
- ◊ Internationalize storage of all excess fissile materials and bring all materials under safeguards
- ◊ Extend registration and declarations to include all civilian plutonium in storage
- ◊ Agree on international approaches to manage and verify the reprocessing and use of plutonium
- ◊ Systematically and verifiably reduce the world fissile material stockpiles to specific levels through transfers to non-weapons uses

The first steps are already being taken. Weapons reduction agreements were accompanied by an almost complete halt in weapons plutonium production. In September of 1993, President Clinton proposed a ban on the production of all fissile material for weapons and the placement of all excess weapons and all civilian fissile material under international safeguards. The US no longer produces any weapons material and the Russians have shut down all but three of their plutonium production reactors. Russia deems the three reactors necessary for power production and has agreed to shut them down by the year 2000. France and the United Kingdom have also halted production of weapons material. The US has recently issued a detailed inventory of all of its WGPu and declared 38.2 MT available for disposition as excess material [D-2]. Discussions are underway to extend the scope of disarmament programs beyond simple dismantlement of weapons to the less easily reversed verification of reduction in the inventories of WGPu. It is important to look at how such reductions might be verified. Schemes to reduce the world inventory of plutonium must be compatible with heightened security and safeguards requirements. Acceptance of such a

scheme may further depend on whether or not the destruction of plutonium can be independently verified. It is valuable to first look at the existing system of safeguards.

The purpose of national safeguards is to prevent theft of fissile material from national or private ownership. International safeguards build on national safeguards, and are also concerned with the diversion of fissile material by the owner. In practice, this means that the records supplied by the custodial facilities are subject to independent verification.

Most nations have systems for accounting for the location, quantities, uses and transfer of fissile materials. However, the quality and extent of safeguards and security standards vary from nation to nation as well as from facility to facility within a nation. NPT non-nuclear weapons states are required to open all their nuclear facilities to IAEA inspection. Non-NPT states (e.g., India, Pakistan & Israel) do not have international safeguards on all their nuclear facilities, but they may have placed individual facilities under safeguard measures as part of nuclear supply vendor agreements. NPT nuclear weapons states are not required to open any of their facilities to IAEA inspection. However, many have made voluntary agreements to submit some of their nuclear facilities to IAEA inspections. The IAEA safeguard procedures are a function of the type of nuclear facility. Table 1.3 indicates an idea of the extent of IAEA oversight and the types of nuclear facilities with custody of plutonium [N-1].

IAEA safeguards build upon the safeguard programs of the custodial state; however, their authority is very limited. The IAEA safeguard requirements outlined in the 1980 Convention on Physical Protection of Nuclear Material are vague [N-1]. The IAEA has produced its own guidelines which are more specific, but they are not binding. In practice, the security of fissile materials is dependent on the custodial state. States also maintain material accountancy programs which are independently verified during IAEA inspections. IAEA safeguard policy dictates the frequency of IAEA inspections based on the type of weapons material handled in the facility. The strategy is to ensure "timely" detection of diversion. Timely detection is defined as detection within sufficient time to prevent conversion of diverted material into a weapon. For example, the time required to convert

metallic plutonium into a weapon is estimated at 7-10 days. The conversion time for low enriched uranium is estimated to be one year. Thus, facilities which handle metallic plutonium are subject to very frequent inspections relative to those that handle low enriched uranium [M-7]. The intent of IAEA verification inspections is to deter diversion by making the risk of IAEA detection great. However, detection of diversion becomes difficult for facilities which handle bulk materials.

Unlike individual components such as fuel assemblies which can be individually counted, measurement processes for bulk materials such as PuO₂ powder, are only accurate within a percentage of the amount measured. Thus, it is not possible to exactly account for all the weapons material in bulk material facilities. The precision to which IAEA verification of custodial material accountancy records can be achieved becomes a function of the throughput of the facility. For example, the 880 MT/yr. throughput of the planned Rokkasho reprocessing facility at Aomori in Japan will result in plutonium accounting to within plus or minus 256 kg/year [M-7]. Such variance in material accountancy leaves a large margin through which to divert plutonium. Consequently, there is a strong emphasis on facility containment and surveillance (CS) measures to augment material accountancy.

In portal perimeter monitoring, facilities containing fissile material are enclosed in a security perimeter. Access to the facility is restricted through a minimum number of gates and the flow of vehicle traffic in and out is limited to plutonium transportation vehicles. Everything entering and exiting the perimeter is monitored for fissile material. The US Nuclear Regulatory Commission currently requires portal monitoring systems at US nuclear facilities be able to detect as little as 3 gms of unshielded ²³⁵U or 0.5 gms of unshielded Pu. In addition the system must be able to detect 100 grams or more of lead which might be used for shielding. All transfers of material are logged by oversight personnel. Material balances are checked to ensure no unauthorized diversion takes place. Bulk material is placed in smaller discrete packages which can easily be counted. These packages are sealed to prevent tampering with package contents and tagged with a unique identification code for definitive tracking.

**Table 1.3 Facilities Under Safeguards or
Containing Safeguarded Material**

Facility Category	Non-Nuclear Weapon States	Non-NPT States	Nuclear Weapon States	Total
Power Reactors	151	13	2	166
Research Reactors	134	22	2	158
Conversion Plants	6	3	0	9
Fuels Fabrication	33	9	1	43
Reprocessing Plants	5	1	0	6
Enrichment Plants	5	1	1	7
Separate Storage Facilities	35	6	5	46
Other Facilities	54	4	0	58
Subtotal	423	59	11	493
Other Locations	290	28	0	318
Non-Nuclear Installations	0	3	0	3
Total	713	90	11	814

* Safeguarded facilities as of the end of 1992.

Tagging includes microscopic photography of exterior surfaces of the package or spray painting signatures. Both tagging schemes provide a unique tracking code which is virtually impossible to duplicate [T-3]. Seals prevent undetectable tampering with package contents. The IAEA currently seals packages by wrapping them in bundles of optical fibers. Illumination of one end of the fibers produces a unique and complex pattern on the other end. The pattern is recorded and referenced to the tagging code. Opening the package requires disturbing the pattern of the optical fibers and thus irretrievably alters the illumination pattern. Thus, unauthorized package tampering, especially during transport when it is most vulnerable, can be detected. Alternately, containers can be sealed using spot welds. Photographs of the welds record the unique surface patterns. Attempts to open the package will disrupt these patterns which are referenced to the associated package tag. Package contents can be verified passively or actively.

Remote detection and monitoring of warheads is done via fingerprinting of each type of warhead. Fingerprinting refers to identifying the distinctive physical characteristics for specific types of nuclear warheads to allow their detection and identification. There are three techniques for detecting the presence of fissile materials via radiation: passive detection of radioactive decay emissions, active gamma irradiation (x-ray imaging) of an object, or inducing fission in the material. All isotopes of uranium and plutonium undergo decay. The energy of the emissions are a function of the energy level of the parent nuclide. Thus, specific isotope content can be determined. Only neutron and gamma emission are penetrating enough to be of practical use in the detection of fissile material. Neutrons are emitted from spontaneous fission of the even plutonium elements or from (alpha, n) reactions from actinide alpha decay interacting with light nuclide contaminants. Gammas are emitted with most decays and spontaneous fission. Only those above energies of 0.1 Mev penetrate sufficiently to be of practical use in detection of fissile materials. As part of the fingerprinting process, the gamma peaks with the greatest signal to background noise ratio are selected. WG Pu warhead detection with hand held portable detectors out to approximately 25 meters from the source has been reported [F-2]. This detection figure can be increased three fold using collimators and background shielding. However, shielding can be used to defeat passive detectors.

Active gamma ray interrogation techniques can be used to overcome some shielding. The Gamma ray energies used are penetrating enough traverse through the material but yet not so penetrating that the absorption differential between fissile and shielding material cannot be detected. X-raying techniques are used in portal monitoring with devices capable of imaging entire vehicles. However, this approach can be defeated by increased shield thickness.

The least desirable from a hazard standpoint but potentially the most effective method for detecting fissile material is inducing fission. Thermal energy neutrons are preferentially absorbed by the fissile material resulting in some fissions. Either the prompt gammas or the fission neutrons generated can then be detected. However, a thermal neutron source strong

enough to be effective would be very large and impractical [F-2]. Alternatively, a high energy neutron source can be used. This prevents using prompt fission neutron emissions for detection. However, either delayed neutrons or gammas can serve as the detected emission.

Fission product radiation from spent fuel increases background radiation beyond the level which will allow passive gamma detection of residual plutonium. However, if sufficient ^{242}Pu is present, passive neutron emission rates may be sufficient. Alternatively, high or low energy neutron induced fission techniques might be effective. As a last resort, the fission products could be separated from the rest of the fuel, allowing straightforward determination of the residual plutonium. Fingerprinting and analysis of the spent fuel should be part of the fuels development program. Fingerprint patterns could be developed as a function of burnup and initial plutonium composition.

Reactor burning plutonium disposal schemes will require fuel fabrication and reactor site portal perimeter monitoring. In addition, cycles requiring reprocessing will require monitoring of the reprocessing facility. The quantities of plutonium entering the facilities could be tracked and the amount leaving could be verified through sampling and assay of a portion of the product materials. For example, plutonium dioxide discretely packaged and fuel rods could serve as entering and exiting plutonium flow media. Entering discrete plutonium dioxide packages would be tracked as described above. The fuel rods could be tagged via surface microphotography to uniquely identify individual rods and/or fuel assemblies. Photographs of spot welded seals would prevent undetectable tampering with rod contents. Thus, each rod could be tracked. Material balances between incoming plutonium dioxide and outgoing fuel rods would provide verification that no material was being diverted in the fuel fabrication process. Random sampling of fresh and spent fuel rods could be used to verify the final destruction of plutonium.

Fresh fuel decay emissions could be passively monitored to verify plutonium content. The higher neutron emission rate of RG Pu over WG Pu would make it even easier to verify rod contents. RG Pu composition varies. Fingerprinting would be carried out on a batch-by-batch basis. The level of monitoring could be scaled as necessary to provide the required

assurances that no material was being diverted. Since fresh fuel allows passive detection, it might be possible to reduce the level of monitoring down to individual rods as part of the fabrication process. Spent fuel composition could be verified by tracking of physical presence in reactor for a given time period. On-site international oversight would be limited to outage periods to verify when the non-uranium WGPu fuel was loaded and discharged. Alternately, the unique tagging and sealing of the rods might provide sufficient assurance to eliminate the need for tracking of the rods through the fuel cycle. Fresh rods could be shipped out from a central processing facility, irradiated, and then returned to the central processing facility for verification of residual plutonium content. Again, virtually any level of spent fuel plutonium destruction verification desired, from checking each individual rod to random sampling of whole core loads, could be achieved. However, the cost and practicality of transportation when applied to examining all spent fuel pins irradiated in a multiple reactor scheme could prove prohibitive. Finally, since the initial plutonium composition is known, the final composition can be calculated for a known fluence history. Fluence exposure could be determined via the use of fluence test pieces permanently affixed to the fuel pins.

1.4 Conclusions

The world inventory of plutonium is already large and is growing rapidly at a rate of 70 MT/year. Total plutonium stockpiles will reach 1700 MT by the year 2000. The bulk of this plutonium is protected by the radiation barrier of the spent fuel in which it resides. However, noting that the radiation barrier provided by spent fuel is temporary, the NAS recommends that the investigation into long term management of the plutonium in spent fuel should begin now [N-1]. Separated RGPu is being produced at the rate of 20 MT/year. This rate far exceeds consumption and will result in a stockpile of approximately 170 MTs by the year 2000. In addition, the INF and START treaties will liberate approximately 100 MTs of WGPu for disposal.

Plutonium is uniquely suited to supporting fast chain reactions. It cannot be denatured to prevent its use as weapons material. Only chemical rather than enrichment barriers can be imposed by plutonium processing. Thus, the primary barrier to the proliferation of plutonium nuclear devices is physical control. Measurement and monitoring uncertainties are such that if the amount of bulk plutonium safeguarded grows too large, diversion can be accomplished without detection. Thus, as the world inventory increases, so does the risk that physical control over significant quantities of plutonium will be lost.

A credible nuclear device capable of a yield in the range of one kiloton can be produced using RG_{Pu}. A one kiloton yield would have a lethal range roughly one third that of the Hiroshima explosion [N-2]. Thus, a very simple RG_{Pu} metal sphere (with uranium reflector) weapon design could be used to destroy a significant portion of a large city and cover the rest in radioactive fallout. Furthermore, the difficulties in producing such a weapon with RG_{Pu} are not appreciably greater than those encountered with WG_{Pu}. For RG_{Pu}, the nuclear proliferation scenario of plutonium theft by a non-national entity is more credible and is selected as the threat of concern for this thesis.

Experts are calling for world-wide management of plutonium including reduction of stockpiles to the minimum levels consistent with needs. The only way to irrevocably reduce stockpiles is to destroy the plutonium through fission and transmutation. The most promising method for effecting large scale transmutation of plutonium in a timely manner is through light water reactors. It appears likely that current monitoring and verification procedures can be adapted to the verification of plutonium destruction in reactors. The next chapter will summarize and compare proposed WG_{Pu} disposal options.

CHAPTER 2 SUMMARY AND QUALITATIVE COMPARISON OF WEAPONS GRADE PLUTONIUM DISPOSITION OPTIONS

Although there is little concern over the control of US stockpiles, political instability and economic hardship places the security of FSU states' WGpu at risk. By default, secure storage will be required until long term solutions can be agreed upon and implemented by the US and FSU states. Ideally, the storage and inventory of the WGpu would be subject to both stringent security and bilateral safeguards.

Currently considered long term plutonium disposition options can be roughly divided into two major categories: vitrification and reactor burning. Vitrification of WGpu involves transforming it from its current metal pit form, into a radioactive glass waste form which is unusable in a nuclear explosive without chemical processing.¹ Thus, vitrification makes the plutonium difficult to extract and use. The second category involves fissioning the plutonium, extracting the resultant energy, in one of a host of potential nuclear reactors. The plutonium is thus converted from a metal pit form to radioactive spent fuel. The reactor options can be subdivided into alternative reactor designs and fuel cycles. Of interest here are the current light water reactors (CLWR), advanced light water reactors (ALWR), Canadian deuterium uranium

¹ There are other so called clean glass vitrification options which do not involve the addition of radioactive fission products. However, the general consensus, as led by the NAS, is that a radioactive barrier should be included in vitrification products [N-1, N-2].

reactors (CANDU), the General Atomics Plutonium Consumption - Modular High Temperature Gas Reactor (PC-MHR) and other reactor (OR) designs including liquid metal reactors, molten salt reactors and accelerator based conversion (ABC) designs as vehicles for plutonium disposition. There are several key issues to be considered in the evaluation of WGPu disposition alternatives.

As discussed in chapter one, the most certain way to mitigate the threat of proliferation via the use of plutonium is to reduce the size of the world's stockpile of plutonium and maintain it at the minimum level which supports nuclear programmatic requirements consistent with a high degree of assurance of detecting and preventing any unauthorized diversion using available safeguard and security methods. Reducing the world inventory of plutonium requires transmuting the plutonium in reactors, chiefly through fission reactions. This chapter briefly describes and compares the primary reactor disposition options being considered for WGPu plutonium. Focusing the plutonium disposition debate solely on WGPu produces a different set of criteria with which to evaluate disposition options than might otherwise develop if the focus included separated and spent fuel RGPu inventories. The greater and immediate risk posed by excess WGPu may be just cause for a narrow WGPu focus in the near future. However, the larger threat posed by all plutonium must be addressed in the not too distant future.

This chapter serves three purposes. The first is to develop the distinction between a WGPu and a RGPu disposition mission. The second is to establish a baseline reference of WGPu disposition options and examine how effective the WGPu options are for a RGPu disposition mission. Finally, the advantages of the proposed plutonium elimination option in accomplishing a RGPu mission are presented.

The first section of this chapter examines the distinction between considering WGPu as a waste for disposal or a resource and the distinction between the criteria which apply to a strictly WGPu inventory as compared to all-plutonium disposition missions. The next section briefly describes and qualitatively compares the various disposition options. These

descriptions are not detailed. Details of the various options can be found in the Department of Energy Plutonium Phase I and II Plutonium Disposition Study Reports, reactor option vendor reports and the NAS Committee on International Security and Arms Control Panel on Reactor Related Options Report [A-4, A-5, D-4, G-2, G-3, G-4, G-5, N-1, N-2, W-1]. Then, a description of the proposed plutonium elimination option using non-uranium fuel in the peripheral assemblies of PWR core is presented. The final section of this chapter compares the throughput, plutonium destruction capability and discharge isotopics of representative reactor designs in each option category.

2.1 Fundamental Considerations for WGPu vs. RGPu Disposition.

Plutonium is a hazardous material, in terms of being a radiotoxic health hazard, and potentially dangerous in that it can be used to produce a very powerful explosion with a yield on the order of kilotons of equivalent high explosives. Plutonium is also a source of commercial energy. Complete fissioning of one hundred MT of WGPu produce approximately 10^8 MWd; this is equivalent to all the energy generated by operating US LWRs over a three year period [N-4].² It is also roughly enough plutonium to fuel all currently operating US LWRs with a one-third mixed oxide fuel in a once through cycle for three years. However, plutonium is more radiotoxic than uranium and requires remote fuel fabrication processes. In addition, plutonium fuel processing and use requires additional IAEA safeguards above those required for handling of normal LEU fuel; this would be especially true for WGPu MOX fabrication [M-7]. Consequently, PWR MOX fuel costs three time more to fabricate than LEU fuel. [D-8] The NAS estimated that burning 50 MT of US WGPu would cost 500 million dollars more than if LEU were used to generate the same power even if the WGPu metal were supplied free of charge [N-1]. There are also storage and security costs in maintaining the plutonium awaiting fuel fabrication. Consequently, WGPu has a negative net economic value and reactor burning options cannot be justified based on an economic need to take advantage of its energy value.

² Assuming US LWR output of 9.92×10^4 MWe-d [N-4].

For RGPU MOX, reprocessing costs add an additional 5% onto the MOX fabrication costs; thus, RGPU is currently also a net economic liability [D-8]. However, reactor transmutation is the only way currently available to destroy plutonium on the scale that is required. Furthermore, only LWRs are numerous enough to be able to reduce or even stop the growth of RGPU stockpiles. In addition to security and economic considerations, there are questions regarding the impact on proliferation policy.

Proponents of disposal of WGPu as a glass waste assert that using Pu in reactors legitimizes the use of civilian plutonium and could be perceived as a reversal of this country's non-proliferation policy against the use of plutonium in nuclear fuel cycles. Reactor disposition advocates argue that the destruction of plutonium for the express purpose of reducing its proliferation risk could be proposed to the world as a direct effort to further nuclear disarmament. As such, reactor disposition would be perceived as a confirmation rather than a reversal of US policy. Furthermore, the NAS states that disposition of WGPu does not require reprocessing of spent fuel and so does not necessarily resurrect the contentious debate over whether or not reprocessing should be allowed in the US [N-2]. However, reprocessing is required for an RGPU disposition mission. There are other fundamental differences between RGPU and WGPu disposition missions which add to the list of considerations in choosing between reactor and waste glass disposition options.

The key emphasis of any plutonium disposition scheme is to minimize the risk of proliferation. However, the relative importance of the criteria by which risk is measured is a function of the scope of the mission. WGPu is less than 7% of the total world plutonium stockpile and, with the exception of three Russian reactors scheduled to be shut down as soon as alternate energy sources can be found, is no longer being produced. Of the 91 MT of WGPu produced in the US, 33.5 MT is scrap and residue material leaving 68.5 MT that is either in nuclear weapons or stored in metal pit and weapon component form at Pantex in Amarillo, Texas [N-2]. Thus, the existing US WGPu stockpile is predominantly in a metal pit form and of a relatively consistent isotopic composition. Furthermore, the US and Russian military are

the principal custodians of WGPu. Thus, disposition of excess WGPu is a well defined and finite problem. WGPu can be dispositioned through a concentrated program centered around a small number of processing facilities involving a very restricted number of participants. On the other hand, RGPu makes up approximately 94% of the world plutonium inventory and is being produced at a rate of 60-70 MT/yr. Spent fuel RGPu is produced by and is in the custody of hundreds of private electric utilities all over the world. Responsibility for the security of this RGPu falls predominantly on the individual custodians. Spent fuel material designs and burnups are specific to the many different reactor designs used to burn the fuel. Thus, the isotopic composition of the RGPu is variable. Most RGPu is in spent fuel form but a large stockpile of separated RGPu also exists. Unlike WGPu, RGPu must first be recovered from spent fuel via reprocessing before it can be eliminated, thus adding another layer of complexity to the mission. RGPu will continue to be produced for the foreseeable future. Thus, a more long term solution is required which will probably entail the involvement of many commercial and government entities. These differences between WGPu and RGPu disposition missions manifest themselves in defining the criteria for determining the relative attractiveness of the potential solutions.

The NAS defines two clear but qualitative standards for WGPu disposition: the stored weapons standard and the spent fuel standard, respectively [N-1]. The stored weapons standard means that during processing the security of the plutonium should be maintained as close as possible to that which applies to stored nuclear weapons in the arsenals of the US and FSU. Nuclear disarmament should reduce the nuclear weapons threat relative to not disarming. Thus, separated WGPu must be secured as if it were still incorporated in a whole nuclear weapon. The current storage standards for separated RGPu are less stringent than those for WGPu. However, there exists a general consensus that separated RGPu security standards should be tightened [N-1, V-1]. The spent fuel standard requires that the final WGPu disposition product be roughly as inaccessible as the plutonium found in typical LEU spent fuel. The radiation barrier in spent fuel is credited with providing the bulk of the inaccessibility of plutonium. To a lesser degree, the degraded isotopes associated with the irradiation of the WGPu to the RGPu

isotopic compositions found in spent fuel is also assumed to detract from the attractiveness of plutonium for nuclear weapons use. The spent fuel standard rests on the logic that since WGPu makes up less than 6% of the total global stockpile of plutonium; reducing its attractiveness to that of the plutonium found in spent fuel eliminates the additional risk posed by WGPu over the far larger stockpile of RGPU. Thus, the standards for the disposition of only WGPu are limited in scope and are not directly applicable to a RGPU mission.

Based on the logic behind the spent fuel standard, there is no additional advantage to making the WGPu more inaccessible than RGPU in spent fuel; hence, no additional credit should be given to an option because it produces a product which makes the WGPu more proliferation resistant than spent fuel. This directly contrasts with how RGPU mission (i.e. a mission to minimize the total proliferation risk due to all plutonium) options would be valued. A RGPU option which produced a more inaccessible or unattractive final plutonium form would be more desirable in direct proportion to how much more inaccessible it made the plutonium.

In considering the WGPu-only mission, the time it takes to reach the various stages of inaccessibility in a disposition process emerges as an important criteria for differentiating the attractiveness of the options. The risk of proliferation grows in an integral sense with accessibility of a given plutonium host form and the time it stays in that form. The quicker the disposition scheme can process WGPu metal into a final product meeting the spent fuel standard the lower the overall risk. The DOE solicited vendor proposals for completing WGPu disposal within a specific time from the decision to proceed [D-4]. Vendor proposals were targeted at completing a 50 MT WGPu disposition mission within 25 years for new reactor designs (i.e. ALWRs, MHTGRs and ORs) and within the remaining plant lifetime for existing reactor proposals (i.e. CLWRs and CANDU). The time required to complete design, construction, qualification and licensing of all reactor and MOX fabrication facilities deducts from the time available to complete plutonium burning fuel cycles. Thus, for the WGPu mission reactor, throughput is particularly important. A lower throughput forces the use of more reactors to complete the mission within the specified time frame. Increasing the

number of reactors required to complete the mission drives up the cost and transportation risks associated with the option. The urgency specific to the WGPu mission and resultant short duration time scale has a strong impact on the relative worth of potential disposition schemes. The spent fuel standard can be achieved without resorting to new technology. Consequently, the time delay associated with the development of new technology is unwarranted and diminishes the relative merit of any option involving new technology. In contrast, RGPU disposition schemes will need to continue until RGPU is no longer produced. In order to be able to maintain the desired stockpile size, it would be necessary to be able to destroy plutonium at a rate equivalent its production rate. Thus, the RGPU mission would be one of establishing an equilibrium; as such, the sensitivity of the relative risk reduction associated with the time it would take to implement a given option is diminished. As the importance of time is reduced the relative proliferation risk associated with the final plutonium form becomes more important for the RGPU mission. Although the growing stockpiles of separated RGPU may be of an immediate concern, the much larger quantity of RGPU in spent fuel has a radiation barrier that will make it somewhat inaccessible for the immediate future. Consequently, for the RGPU mission it may well be worth a reasonable implementation time delay to develop a new disposition technology which produces a final product that is significantly more proliferation resistant than the spent fuel standard. The time scales over which WGPu and RGPU disposition will take place are fundamentally different. The following sections summarize and compare reactor disposition options using these considerations as a framework.

2.2 Reactor Burning of Plutonium

This section reviews the options for using CLWR, ALWR, CANDU, PC-MHR and OR designs for plutonium disposition. Only highlights regarding the maturity of the technology, experience base and potential obstacles are discussed. More detailed descriptions can be found in the Department of Energy Plutonium Phase I and II Plutonium Disposition Study Reports, reactor option vendor reports and the NAS Committee on International Security and Arms Control Panel on Reactor Related Options Report [A-4, A-5, D-4, G-2, G-3, G-4, G-5, N-1, N-2, W-1]. The DOE-solicited vendor reports address three

possible WGPu disposition missions: spiking, spent fuel and elimination. The purpose of the spiking mission is to process the WGPu into a proliferation resistant form as rapidly as possible. WGPu fuel is loaded into a reactor and irradiated only long enough to build up a sufficient radiation barrier to deter theft. The spiked fuel is then unloaded and stored. After all WGPu has been spiked, the spiked fuel is reloaded into the core and irradiated to meet the spent fuel standard. This option is economically unattractive for three reasons. Since the “spiked condition” discharge burnup is low, fresh fuel is consumed at a rapid rate. Thus a significantly larger capacity and thus more expensive MOX fabrication facility would be required for spiking. The frequent refueling shut downs of the plant would greatly diminish one of the key advantages of a reactor burning option: namely, the ability to offset disposition costs through the generation of electricity revenues. There would also be significant additional storage facility costs for spiked fuel awaiting reload. The NAS concluded that the incremental risk reduction gained by the more rapid development of a radiation barrier would be more cost effectively acquired through increased physical and institutional security and safeguards [N-2]. The spent fuel mission is simply to degrade fresh WGPu reactor fuel to the spent fuel standard without the additional “as rapidly as possible” spiking constraint. The NAS considers a self protecting radiation barrier to be the key deterrent to recovery of plutonium rather than total plutonium content or plutonium isotopes. Thus, the key distinction between the spiking and spent fuel option is the economic benefits of allowing longer fuel cycles to produce spent fuel with larger discharge burnups. However, the DOE has also stipulated a $^{240}\text{Pu}/\text{Total Pu}$ ratio of greater than 0.20 which is not met by the spiking option. At greater than 20% ^{240}Pu the surface flux due to spontaneous fission is considered sufficient to deter use of the plutonium in a nuclear explosive. Finally, the spiking mission has no value as a RGPu disposition mission, and hence will not be considered further. The third class of disposition option, called the elimination option, involves producing spent fuel with essentially no residual plutonium. As is presented in the following subsections describing the categories of reactor disposition options, reactor vendor plutonium disposition calculations have not demonstrated the ability to complete an elimination mission without repeated reprocessing of spent fuel.

2.2.1 Current Light Water Reactors: The US PWR, BWR and Russian VVER1000 units now operating are classified here as Current Light Water Reactors (CLWRs).³ There are 100 LWRs in the US and 400 worldwide [N-5]. LWR disposition options use WGPu mixed with depleted uranium or natural uranium to produce mixed oxide fuel (MOX). The US pioneered RGPU MOX research in the 1950's and 1960's but abandoned the research in the mid-1970's as part of a non-proliferation policy of not promoting a civilian plutonium economy. The European community continued MOX development and use.

Germany, France and Belgium use 1/3 MOX core loads extensively in their LWRs. Japan plans to begin burning 1/3 MOX core loads in 10 of its light water reactors by the year 2000 [A-2]. Belgium provides a significant portion of the worlds MOX fabrication capacity. Great Britain does not use MOX in its reactors but plans to expand its MOX fabrication capacity to compliment its reprocessing services to other nations. The NAS evaluated MOX technology to be very mature [N-2]. Thus, CLWR technology is considered a very mature option for disposition of WGPu. The rate limiting step in burning MOX in CLWRs will be the development and qualification of MOX fabrication capacity in the US and Russia.

The US has no operating production scale MOX fabrication facilities and is currently examining the feasibility of converting one of five nuclear sites originally designed for other uses to support the WGPu disposition campaign [B-2]. In an effort to reduce MOX fabrication costs, the suitability of the existing capabilities at each site, such as secure plutonium storage vaults, waste treatment, an active protection force, perimeter control systems, and the existing licensing basis are used as evaluation criteria. Location is also a large factor in selecting a MOX fabrication site. Collocation of the pit processing, MOX fabrication facility and the reactor which will burn the WGPu MOX would minimize the risk due to transportation theft. Furthermore, locating all of these facilities on a government site is likely to make the licensing process, which could be the rate limiting process, significantly

³ Russia also has an older fleet of RBMK reactors. However, the safety standards of these reactors are substantially below international standards and they are slated to be shut down as soon as replacement power can be constructed. Thus, RBMK reactors are not likely to play a significant role in plutonium disposition.

easier. The Fuel Manufacturing and Evaluation Facility (FMEF) at Hanford is particularly attractive because the Washington Nuclear Project reactor units #1 (WNP1), #2 (WNP2) and #3 (WNP3) are also nearby. WNP3 is a 75% complete System 80 reactor which could be readily modified to burn a full MOX core. WNP1 is an incomplete PWR located on the Hanford reservation. WNP2 is an operating 1155 MWe BWR-5 which could be loaded with a full MOX core and is located on the US Government owned Hanford site. The Fuel Processing Facility (FPF) on the DOE Idaho Falls site already contains many of the capabilities needed for a MOX fabrication facility. The FPF and FMEF are to be the focus of the next phase of the DOE study to determine where best to establish a MOX fabrication plant. However, all of the candidate facilities will require sufficient work and licensing re-evaluation which might make building a completely new site potentially competitive.

Russian MOX fabrication capacity is also insufficient for WGPu disposition. Russia has a small scale operational MOX fabrication facility which has been feeding its BN600 liquid metal reactor. A new larger scale MOX fabrication facility located at the military reprocessing Mayak facility is 50% complete. Work was stopped due to a lack of available funding to complete the project. The NAS estimates insufficient funding will be the major obstacle to MOX disposition of WGPu in Russia [N-2]. There are additional obstacles to the WGPu MOX disposition in CLWRs.

With the exception of 3 Combustion Engineering System 80 reactors, CLWRs are not specifically designed to handle a full MOX core load. Initial studies found that without some modification, CLWRs were generally limited to a core loaded with 1/3 MOX and 2/3 UO₂. There are several differences between ²³⁹Pu and ²³⁵U which can limit CLWRs to a 1/3 MOX core load:⁴ ²³⁹Pu has a smaller delayed neutron fraction reducing the time margin for reactor control, the spectrum of Pu fuel tends to be more epithermal, reducing control absorber worths, the ²³⁹Pu 0.3 ev resonance produces less negative temperature coefficients of reactivity, the higher average neutron flux energy and increased gamma radiation produced

⁴ See Chapter 4 section , for a more detailed discussion on the differences between the use of ²³⁹Pu and ²³⁵U as the primary source of fissile material for power production.

by MOX results in more irradiation damage and heat up of the vessel and internals and the larger decay heat generation rate for MOX fuels increases the load on post shutdown and emergency cooling systems [N-2]. From a WGPu disposition mission perspective, a 1/3 core loading limitation increases the number of reactor-years it would take to disposition the WGPu. The following expression relates MOX throughput (e.g. MT/yr.) to reactor characteristics and MOX loading parameters:

$$\text{MOX Throughput} = \frac{(\text{thermal power})(\text{capacity factor})(\% \text{ of core MOX})(\text{Pu enrichment w\%})}{(\text{average fuel exposure at discharge})} \quad (2.1)$$

More reactor sites mean greater transportation requirements and an increased risk of theft or diversion. In addition, a 1/3 MOX core generally results in net plutonium production in CLWRs. The spent WGPu MOX meets the spent fuel standard but the world inventory of plutonium expands. Thus, 1/3 MOX core loading is unsuitable from a world plutonium inventory reduction perspective.

There are three System 80 Combustion Engineering (CE) reactors operating in Palo Verde, Arizona which were originally designed with the additional control absorber and supporting systems to burn full MOX cores. The additional control rod locations have since been filled with instrumentation but a full MOX capability could be recovered with minimal alteration to the existing systems. Depending on which reactors were selected, between two and three CLWRs could disposition 50 MTs of WGPu in their remaining lifetime. More recent vendor calculations indicate that sufficient margin exists in the designs of many US CLWRs to allow full WGPu MOX operation with little reactor system modification. These reactor vendor calculations have not been independently verified and the maximum allowable enrichments are limited compared to ALWR designs. A higher allowable enrichment has important impacts on total WGPu disposition program time and cost. Increased enrichment increases throughput, thus reducing the total time to complete the WGPu disposition mission. Secondly, a higher enrichment means that fewer total MTs of MOX must be fabricated and a lower maximum fabrication capacity is required. This reduces the capital and operating costs

for MOX fabrication. Up to a point, the additional reactivity and reduced negative temperature coefficient magnitude resulting from higher WGPu enrichments can be compensated for by adding burnable absorbers with appropriate resonance peaks, such as Erbium-167.⁵ However, increasing the WGPu enrichment also increases the residual fissile plutonium content in the spent fuel. A high fissile content in the spent fuel may make it more difficult to dispose of due to long term repository criticality concerns. Additional fresh fuel enrichment will also increase the decay heat load of the spent fuel, potentially decreasing repository capacity [N-2] Augmenting the maximum allowable enrichment will incur additional reactor modification costs suggesting that a compromise between modification cost and time versus increased throughput is required. No US LWR is currently licensed to burn either full or 1/3 MOX core loads. The time and effort required to obtain NRC licensing is likely to be considerable. Vendors are working with utility owners who are interested in the possibility of burning plutonium in their reactors [E-2].

Several utilities have indicated they would be interested in disposition of WGPu provided they were properly compensated. Compensation from the US government may include furnishing of free MOX fuel, reimbursement for all additional operational costs and government-provided security and government taking title of the spent fuel. Specific proposals have included private entity purchasing of two or three collocated reactor units from utilities with government cost-plus reimbursement of capital and operating costs and outright government acquisition of one or two commercial units which are either partially complete or were economically driven to close down prior to the end of their licensed lifetime. It is important to remain cognizant of the fact that the larger volume of the RGPu disposition mission could not be handled in such a limited way.

Maintenance of minimum global stockpiles of RGPu would require processing of much larger quantities of RGPu; at a minimum, 60-70 MT/year would have to be dispositioned just to arrest further RGPu stockpile growth. This can be compared to the total global WGPu disposition program of 100 MTs over a few decades. RGPu reduction requires

⁵ See Chapter four, section 4.3.4 for more details of burnable absorber uses.

a broader effort involving many more entities than is required for WGPu disposition. Elimination of RGPU via LWR MOX burning requires repeated recycling. With each recycle the actinide content will grow, making fuel fabrication more and more difficult. As a practical point of reference, current MOX reprocessing practices do not routinely exceed two recycles [N-2]. PUREX process recycling of MOX fuel produces a pure plutonium product stream thereby increasing the chances of diversion. WGPu MOX disposition eventually reaches the point where the quantity of plutonium remaining can not support criticality in a single reactor. Thus, a partial MOX load is required resulting in an exponentially decreasing plutonium destruction capacity. Thus, MOX disposition of WGPu or RGPU is not suitable as an elimination option.

In summary, CLWRs are attractive because they are already operating. Expanding existing licenses to allow burning of MOX is likely to be less difficult than siting and licensing an entirely new reactor. However, there are several obstacles to the use of CLWRs for WGPu and/or RGPU disposition. Building the required MOX fabrication capacity is likely to be the limiting task in disposition of WGPu in US and Russian CLWRs. The limiting step in building the MOX fabrication capacity is licensing and approval. Collocation of a MOX fabrication and reactor site reduces transportation risks and is desirable for the WGPu disposition mission. However, the much larger capacity required to maintain a constant RGPU stockpile will require several fabrication facilities and multiple reactors. One-third MOX core loading increases the number of reactor-years required to disposition 50 MT of WGPu by a factor of three. Such partial loading also results in net production of plutonium contrary to an RGPU mission. It may be possible to use some existing reactors with 100% MOX cores with minor modifications. However, the enrichments possible are likely to be limited, thereby reducing throughput. Full RGPU loading will probably require reactor modifications. The allowable enrichments may be increased through the use of burnable absorbers but the resulting fissile content of the spent fuel will also increase. A relatively large fissile content in the spent fuel may be a long term repository criticality issue making disposal difficult and the spent fuel more attractive for plutonium recovery. Finally, MOX burning in CLWRs is not suitable for eliminating plutonium. The repeated

reprocessing that would be required over a long time period would likely result in an overall increase in the net proliferation risk. ALWRs also use MOX fuel but some of the other disadvantages of CLWR plutonium disposition can be avoided through the use of ALWRs.

2.2.2 Advanced Light Water Reactors. ALWRs can be classified as either an evolutionary or passive safety type design. Evolutionary reactors are generally the next generation vendor designs which include experience based improvements in safety, reliability and ease of construction over current LWRs. US evolutionary LWR capacities range from 1300-1400 MWe and their designs are very mature. Evolutionary ALWRs are being built outside the US. The ABB-CE System 80+ and the ABWR have received Nuclear Regulatory Commission design certification and are in the final stages of the design licensing process. Passive safety type ALWR designs combine natural modes of heat transfer and material properties to prevent short term severe core damage without operator action in the event of a design basis accident. They are typically 600 MWe or less in size resulting in a higher bus bar cost. Passive Safety ALWRs are more revolutionary in design than are the evolutionary ALWRs and are consequently less mature. Assuming the evolutionary reactor designs are deemed sufficiently safe, the passive safety type ALWRs offer no advantages over the evolutionary type for plutonium disposition and their smaller size reduces the potential maximum throughput. Between 4 and 9 passive safety ALWRs are required to disposition 50 MT of WGpu in 25 years as compared to 2 evolutionary ALWRs. Thus, passive safety type ALWRs will not be considered further.

Evolutionary ALWRs for plutonium disposition are designed with features such as more control rods and control rods with greater absorptive cross sections to boost total control rod worth, increased cooling of core internals to mitigate gamma heating, larger chemical shim systems, a thicker core support barrel to mitigate fast neutron flux, and larger spent fuel and emergency cooling systems to handle the larger plutonium spent fuel decay heat loading. These features give ALWRs the advantage of sustaining full MOX core loading with plutonium enrichment in the neighborhood of 6-7 w% and achieving plutonium

destruction ranging from 22-36%. Thus, the overall throughput of plutonium can be increased and the total MOX fabrication requirements to complete the disposition mission are reduced. From the perspective of a RGPU stockpile reduction and maintenance mission, higher initial enrichment results in spent fuel with a higher fissile plutonium content. The net destruction of plutonium is improved only slightly because the higher plutonium content displaces some uranium. However, ALWR MOX fuel still contains significant amounts of ^{238}U which breeds new ^{239}Pu . Thus, ALWRs offer little advantage over CLWRs for an RGPU disposition mission.

Burnable poison such as erbium, gadolinium and boron must be added to the MOX fuel to offset the unwanted physics impact of high plutonium enrichments. This is a new MOX fuel form which is not part of the existing experience base. Consequently, it will require testing and qualification before it can be licensed for use. Thus, additional fuel testing and development is required in order to take advantage of the additional throughput capacity of ALWRs.

ALWRs have several disadvantages relative to CLWRs. There are no ALWRs in the US or Russia. They must be sited, licensed and built. In the US there is strong public resistance to construction of new reactors bolstered by the economic reality of a lack of demand for additional base load generating capacity in the near future. The Russians do not have the capital necessary to bring their CLWRs up to international safety standards much less build new ALWRs of foreign design. The next section discusses the viability of using CANDU reactors for plutonium disposition.

2.2.3 CANDU Reactors. There are 22 operating CANDU reactors with output varying from 515 to 881 MWe. Each Bruce A reactor provides 769 MWe at a capacity factor of 80%. CANDUs employ on-line refueling and a deuterium moderator to maintain criticality with natural uranium and avoid the need for enrichment. On-line refueling allows the low excess reactivity and short core residence times of natural uranium fuel without power interruption. The deuterium moderator reduces parasitic neutron absorption losses relative to water,

improving the neutron economy, which increases the maximum achievable discharge burnup. CANDU reactivity control systems are more flexible and have a greater capacity to add more control absorbers than CLWRs or ALWRs. This enables them to operate with full MOX cores and higher enrichments without the need for any system modification. CANDU discharge burnups are typically only 20% of CLWR spent fuel burnups. CANDU's have a more thermalized neutron spectrum which increases the ^{239}Pu destruction potential. The shorter residence time and lower operating temperatures of natural uranium CANDU fuel has allowed for a relatively thin cladding. In a WGPu disposition mission role where higher enrichments have a positive economic advantage, the maximum residence time of the fuel in the core is limited by the thin cladding. Cladding water-side corrosion limits the maximum allowable residence time which in turn limits the ability to take advantage of the higher WGPu enrichments allowed by the more flexible CANDU reactivity control system. The discharge burnup for the WGPu fuel is limited to approximately 9,700 MWd/MT. Proposed CANDU MOX fuel of 1.2 w% and 2w% enrichment is located in the intermediate and outermost rings respectively, and contains about 0.19 Kgm WGPu/bundle. A new "CANFLEX" CANDU fuel design is capable of sustaining a discharge burnup of 17,000 MWd/MT. The corresponding WGPu MOX enrichments are 2.1 w% in the intermediate ring and 3.6 w% in the outer ring which equates to 0.38 Kgm WGPu/bundle. The CANFLEX design has the same external dimensions but with each bundle containing 43 fuel elements vice the 37 elements in the standard design. Thus, the power density in each element is reduced thus allowing each element to go to higher burnups without degradation. The dysprosium content and diameter of the inner two rings is increased while the plutonium content is increased and the diameter of the pins in the two outer rings is decreased compared to the standard CANDU fuel bundle design. Using CANFLEX fuel each reactor would dispose of 9 bundles/day producing the same 1050 Kg/yr. throughput. Thus, the real advantage of the CANFLEX fuel is that increasing the enrichment reduces the total amount of MOX fuel that must be fabricated to complete the WGPu disposition mission, which saves on fuel costs. The calculated total plutonium destruction with the MOX fuel was 34%. Using non-uranium fuel and on-line shuffling where each fuel bundle makes multiple passes

through the core in a plutonium “destruction” mode, 80% plutonium destruction is estimated [A-3]. Using a non-fertile fuel without shuffling produces 60% net plutonium destruction. A rigorous development, testing and qualification regime would have to be completed before the novel non-uranium fuel design plutonium destruction mode could be implemented.

Canada has no MOX fabrication facilities nor is there any significant experience base for CANDU MOX fuels. However, the fuel is simpler, operates under less demanding conditions and would likely be less expensive to produce. The partially complete Hanford FMEF plant is favored as the production site for the Bruce A station CANDU unit’s MOX. The MOX would be fabricated in the US and transported to Canada. The spent MOX would then be returned to the US. This reactor disposition scheme has the shortest duration between the time of decision to the time when the first WGpu MOX enters the reactor. The time it would take to produce and qualify the MOX is the limiting factor. There are no CANDUs licensed to burn MOX and there is a Canadian tradition against enrichment and nuclear weapons technology. Gaining the Canadian public’s acceptance for this disposition plan could also be a significant hurdle. The political viability of shipping US WGpu out of the security of US soil is uncertain. The lower burnup and smaller size of the CANDU spent fuel might make it a greater proliferation theft risk.

2.2.4 Plutonium Consumption - Modular High Temperature Gas Reactor (PC-MHR).

The General Atomics Modular High Temperature Gas Reactor (MHR) is an advanced reactor designed primarily for inherent passive safety. It is gas cooled with TRISO particle ceramic fuel loaded into vertical channels cut into large graphite moderator blocks. Each 31.4" high hexagonal graphite fuel block consists of several axial channels. Into some of these channels are placed fuel rods, with the remainder serving as the single phase helium coolant conduits. Standard refractory TRISO-coated fuel particles with a plutonium oxide kernel, porous graphite buffer inner coat, silicon carbide barrier middle coating and an outer dense pyrolytic carbon protective layer, are compacted with carbon into fuel elements which

are inserted into the fuel bearing channels. The resultant spent fuel is considered suitable for disposal.

Various configurations and compositions of plutonium loaded TRISO fuels were tested in both the Dragon and Peach Bottom reactors to burnups up to 747,000 mega-watt-days per metric ton of heavy metal, (MWd/MT) with a fast neutron fluence of 1.5×10^{25} n/m², E > 0.18 Mev [G-2]. Peach Bottom fuel with up to 88% enriched PuO₂ kernels demonstrated performance on par with HEU kernels except that the performance was more sensitive to the O:Pu ratio. General Atomics is proposing the PC-MHR which is an adaptation of their direct cycle Gas Turbine MHR for the disposition of WGPu. The gas turbine uses a direct cycle to boost the thermal efficiency and thus reduce the busbar costs of electricity generation. The plutonium consumption versions use a non-fertile PuO₂ kernel TRISO particle fuel with a O:Pu ratio of 1.6. Er₂O₃ compacts are loaded in separate channels as a lumped burnable poison. The PC-MHR destroys 90% of the ²³⁹Pu and 63% of the total Pu loaded with a 24 month residence time average burnup of 590,000 MWd/MT Pu. The non-uranium fuel enables the PC-MHR to achieve a total plutonium destruction level that is nearly a factor of three higher than can be achieved with LWR once-through MOX cycles. In its review, the NAS pointed out several advantages and disadvantages of the PC-MHR as a disposition option, as listed in Table 2.1.

TRISO fuel silicon carbide, (SiC), and pyrolytic carbon, (PyC), layers strongly enhance the fresh fuel chemical barrier to WGPu recovery. The NAS Panel on Reactor Related Options report noted that manufacturing TRISO fuel "... as soon as possible, before it could be used in a reactor, would provide a more significant safeguard than would fuel fabrication for most other reactors." [N-2]. The Panel further noted that because of its higher burnup and non-plutonium producing nature, TRISO "... spent fuel would pose a less attractive target for a potential proliferator than most other types of spent fuel." Since the fuel and the moderator are combined in single graphite block units, the plutonium density is lower than in standard LWR oxide fuel. A larger mass of the fresh fuel would have to be stolen to accumulate a critical mass, improving the proliferation resistance of the fuel.

However, a lower plutonium density fuel also correlates with a larger volume of spent fuel for final disposal.

Table 2.1 Advantages and Disadvantages of the PC-MHR

<u>Advantages</u>	<u>Disadvantages</u>
1. Tougher to recover WGPu from fresh SiC coated fuel than fresh MOX fuel	1. Need funding for a new reactor design acceptance and licensing
2. Much higher ^{239}Pu and $^{\text{total}}\text{Pu}$ destruction than LWR MOX options	2. Must develop, test and qualify plutonium TRISO fuel
3. Spent fuel Pu has less attractive isotopes for explosive than MOX LWR spent fuels	3. New fabrication technology and facility required
4. Spent fuel has more physically dilute Pu	4. Must redesign core for higher burnups
5. Spent fuel multiple coatings tougher to reprocess than MOX	5. Must overcome utility skepticism resulting from Colorado Fort St. Vrain and German THTR
	6. Lower spent fuel radiation barrier

The critical path for the PC-MHR is qualification of the PuO_2 kernel TRISO fuel. The DOE concluded that the PC-MHR technology was not yet mature with considerable development and testing yet to be done [D-4].

2.2.5 Other Reactors. There are existing and conceptual reactor designs which could be brought to bear on the plutonium disposition problem. These include current and advanced liquid metal reactors (LMRs), molten salt reactors (MSRs) and accelerator based conversion schemes (ABC).

There are nine operating LMRs which are typically fueled with 20-40w% enriched plutonium and uranium fuels. Great Britain the US and Germany have all canceled their LMR programs but France, Japan and Russia have active LMR programs. The US EBR-II (16.5 MW_e) and the FFTF (400 MW_{th}) facilities are too small to make a significant contribution to the WGPu disposition mission. In addition, FFTF has been shut down and funding for the EBR-II has been canceled. France's 1200 MWe Superphenix reactor is by far

the largest LMR in the world. Of the current LMRs only the Superphenix is capable of disposition of plutonium at a significant rate. Unfortunately, Superphenix's availability has been low and France now intends to convert this plant into a research facility. Japan has postponed its planned deployment of commercial LMRs and recent technical problems at Japan's new 280 MW_e Monju facility have brought the viability of that project into question. The 280 MW_e Monju facility would only be capable of a maximum disposition rate of 10-15 tons of WG⁹⁰Pu every 20 years. The Russian 56 MWe BN600 LMR was designed to burn HEU and conversion to using an all MOX core is not considered technically feasible. The small size and poor reliability of current LMRs resulted in a NAS recommendation against their use for WG⁹⁰Pu disposition [N-2]. However, it is worthwhile to consider the possibility of using future advanced LMRs for RG⁹⁰Pu disposition.

LMRs use a fast flux spectrum and so are theoretically capable of fissioning close to 100% of the plutonium. In the once-through mode, the higher fissile plutonium loading required to maintain criticality in a fast spectrum results in spent fuel with a higher weight percent of fissile plutonium. Although it would meet the NAS spent fuel standard, the isotopic content would be higher in ²³⁹Pu than the residual plutonium in MOX spent fuel produced from plutonium of the same initial isotopic composition. Consequently, recycling would be required to eliminate plutonium. In the recent past, advanced LMR programs were ongoing in the US, Russia, and Japan, with a collaborative Western European effort between France, Germany and Great Britain. The US GE Integrated Fast Reactor (IFR) design used a Pu-Zr-U metal alloy fuel in a 330 MWe passive decay heat removal design. The design included an innovative non-aqueous pyroprocessing facility on the reactor site. Molten uranium and plutonium were recovered together with some residual fission products in a proliferation resistant mix which would then be remotely fashioned into new metal fuel elements. An LEU fuel reprocessing technology which did not effect the complete separation of a pure plutonium stream would be significantly more proliferation resistant than PUREX. Development of such reprocessing would be an invaluable technology in support of a RG⁹⁰Pu disposition mission. However, the IFR project was canceled in 1994. Completion of the IFR is estimated to take 10-15 years after licensing and technical approvals were obtained. The

construction of two 50% complete Russian 750 MWe BN800 LMR was halted due to lack of funds. The BN800 is designed to use a full MOX core. Completion of the BN800 reactors is likely to require western funding and a minimum of 10-15 years. Germany and Great Britain have withdrawn their support for the collaborative design of the European Fast Reactor and the Japanese have indefinitely postponed the construction of their 670 MWe loop design demonstration fast breeder reactor.

The capital costs for advanced LMRs are likely to be significantly greater than those of ALWRs or other reactor technologies. Their designs are significantly less mature and their past reliability record is not promising. LMRs use enriched fuel which is a more natural fit for RG⁹⁰Pu or WG⁹⁰Pu disposition. However, even with free enrichment, LMR fuel is still significantly more costly than LWR fuel. LMRs have no real advantages over LWRs in a plutonium disposition mission and their maturity is significantly lower. Thus, it would seem unwise to rely on LMRs for WG⁹⁰Pu or RG⁹⁰Pu disposition.

Molten salt reactors (MSR) and accelerator based conversion (ABC) schemes are still in the conceptual phases and are the least mature options. The advantage of MSRs are that liquid fuel allows for continuous on-line reprocessing, facilitating near total plutonium elimination. Similarly, ABC designs can produce near total destruction of plutonium. Both designs are a minimum of decades away from fruition and so will not be considered further here.

2.3 Non-Uranium Plutonium Enriched Fuel in PWR Periphery

Light water reactor burning of WG⁹⁰Pu in MOX fuel will reduce it to no more a proliferation threat than the far more extensive world stockpile of reactor grade plutonium. However, RG⁹⁰Pu can be used to produce a multi-ton nuclear yield in an unsophisticated explosive design. Thus, converting all the WG⁹⁰Pu into spent fuel does not address the largest part of the plutonium proliferation threat posed by a sub-national group. The 100 MT of WG⁹⁰Pu to be declared surplus makes up approximately only 6% of the world's plutonium

inventory. Short of destruction, the unique characteristics of plutonium prevent achieving absolute assurance against it being chemically processed and subsequently used to generate a nuclear explosion. In order to truly minimize the sub-national proliferation threat, both WGPu and RGPu must be burned beyond the NAS spent fuel standard. The immediacy of the WGPu problem leads the NAS to reject the development of new technology for WGPu disposition but the NAS also states that “Further steps should be contemplated, however, to move beyond the spent fuel standard and reduce the security risk posed by all the world’s plutonium stocks, military and civilian, separated and unseparated; the need for such a step already exists and will increase with time” [N-1]. Elimination of plutonium in a once-through reactor deep burning fuel cycle would be a final solution. This section presents the plutonium disposition scheme which is the subject of this dissertation.

2.3.1 Non-Uranium Fuel. There are two reasons for using non-uranium fuel rather than MOX. ^{238}U breeding of ^{239}Pu prohibits substantially complete plutonium destruction in a once-through LWR MOX fuel cycle. The PUREX reprocessing technology and equipment required to produce a pure plutonium stream from MOX fuel cycles is well defined and uses equipment common to a wide variety of non-nuclear chemical processes [S-4]. MOX spent fuel does not provide a credible chemical barrier to plutonium recovery. A novel fuel and cycle designed to maximize plutonium destruction can improve the overall proliferation resistance of plutonium cycles. It is interesting to note that all of the LWR WGPu disposition options being considered by the DOE or the NAS employ a MOX fuel cycle. Non-uranium fuel enhanced the destruction capability of both the CANDU and PC-MHR reactor disposition options to 63% and 80% as compared to CLWR and ALWR destruction capabilities of 22-36%. Use of CANDUs for the WGPu mission requires transferring WGPu across national borders and there are a relatively few CANDUs in the world for the RGPu disposition mission. The PC-MHR reactors do not currently exist and even if they were exclusively chosen to meet future energy needs, it would be many years before they would exist in numbers comparable to LWRs. An appropriately composed non-uranium LWR fuel would provide most of the PC-MHR benefits listed in table 2.1 while avoiding all the cost and uncertainty of a new reactor technology. Finally, none of the reactor WGPu MOX

disposition options are able to effect a true elimination option without relying on repeated recycle. Consequently, a non-uranium fuel designed to eliminate plutonium in a once-through cycle in existing LWRs is of interest.

2.3.2 PWR Peripheral Cycle Description. PWRs comprise over two thirds of operating US commercial reactors. Thus, it would be convenient to be able to achieve a deep burn of plutonium in PWRs. A PWR fuel cycle using non-plutonium producing fuel in the peripheral assemblies of a PWR is proposed.

A true plutonium elimination option requires that the plutonium fuel be subcritical for a period of time while the remaining plutonium is transmuted. The reactor must be able to drive the subcritical plutonium fuel near the end of its residence time without unacceptable power peaking or loss of core criticality. In commonly used three batch low leakage core fuel management, the twice burned UO_2 assemblies are placed on the core periphery because they generate less power. These assemblies are, by themselves, subcritical and produce only about 30% of core average power during their third cycle. Producing fewer neutrons in the core periphery reduces vessel fluence as well as improving overall neutron economy. The non-uranium plutonium fuel is specifically designed to yield a large net plutonium destruction while operating in PWR peripheral assembly locations. The fissile density of the fresh plutonium fuel is similar to twice burned UO_2 fuel. This lower plutonium enrichment reduces residual plutonium, degrades discharge plutonium isotopics and further enhances neutron economy. Driving well burned plutonium fuel on the periphery of the core to eliminate plutonium is an extension of low leakage management. Using the peripheral locations also produces less of a disruption to core average physics parameters.

Peripheral assemblies constitute approximately 20-25% of the core and have a smaller contribution to overall core properties due to their lower average power density. Thus, the impact of ^{239}Pu properties on core characteristics is reduced. The lower power density of the peripheral assemblies also reduces the performance requirements of the fuel. Using only peripheral assemblies allows greater flexibility in matching the fuel design with the fuel cycle needs. Early fuel management schemes placed the freshest assemblies on the core periphery

to minimize power peaking. The shift to current low leakage management was accommodated through changes in fuel design rather than with reactor modification. Similarly the extension of this trend is accomplished in the present instance using a non-uranium plutonium fuel and an alternate peripheral loading pattern.

The proposed fuel would have a core residence time of two 18 month cycles. The first cycle that the non-uranium plutonium assemblies are introduced into an equilibrium PWR core, they are loaded in every other peripheral location. During the first cycle the interior plutonium pins see a much larger thermal flux due to the self shielding of the plutonium fuel assembly. At the end of the first cycle the once burned non-uranium plutonium fuel assemblies are rotated 180° to expose the exterior pins to the larger thermal flux found on the inner half of the assembly. Thus, the plutonium assemblies are burned more evenly, increasing plutonium destruction. The UO_2 assemblies which remained in the periphery during the first cycle are replaced with fresh plutonium assemblies. At the start of the second cycle, the once burned and fresh non-uranium plutonium fuel assemblies are loaded in an alternating pattern in all the peripheral locations of the core. This staggered loading pattern reduces the total driving power load on the core (i.e. the reactivity penalty of the peripheral assemblies) and minimizes power peaking in the UO_2 assemblies adjacent to the periphery.

Chapter 4 presents a more detailed discussion of the potential composition, development, testing and fabrication requirements of the non-uranium fuel. Chapter 6 presents the results of calculations of the physics, throughput, discharge isotopics and plutonium destruction capability of the proposed cycle. Section 2.4 compares the performance of the vendor-proposed reactor plutonium disposition options. These results serve as a comparative baseline with which to evaluate the results of using this peripheral PWR non-uranium fuel cycle for plutonium disposition.

2.4 Comparison of Options

This section compares the throughput, discharge isotopes and plutonium destruction produced by the proposed reactor disposition options. The first subsection defines the specific reactor designs for which the results are presented. The second subsection presents the results and discusses their significance. All of the options require construction of fuel fabrication and plutonium pit conversion facilities. LWRs have an edge over the non-MOX options in that there is a large MOX experience base. A discussion of the feasibility of fabricating non-MOX plutonium fuels is deferred to chapter 4.

2.4.1 Definition of Reactor Disposition Options. There are several CLWR and ALWR options proposed for plutonium disposition. For comparison purposes it is sufficient to look at a typical current and advanced PWR and BWR design, for a total of 4 LWRs. The PC-MHR and CANDU options are mature technologies and are also considered. Table 2.2 summarizes the representative designs selected. All of the reference designs considered are full plutonium core options.

The three Palo Verde ABB-CE system 80 reactors are used as the representative reference CLWR-PWR design. These reactors were specifically designed for use with full MOX cores with features such as extra control rod worth, greater decay heat removal capabilities, more-shielded pressure vessels and better cooling of core components. The System 80 reactors were designed with 97 control rod locations as compared with 101 rod locations for the evolutionary ALWR System 80+. The lower control rod worth of the System 80 reduces the allowable enrichment to 4.5 w% WG_{Pu} as compared with the 6.7 w% used in the 80+ disposition design. The core average burnup of the spent fuel is 32,500 MWd/MTHM as compared to 42,600 MWd/MTHM for the 80+. Two of the Palo Verde System 80 control rod locations are being used for instrumentation because they were not required for UO₂ core operations. Very few modifications to the existing Palo Verde reactor

designs will be required: the existing rod locations will have to be reclaimed for control rod use or the boron enrichment will need to be increased. These system 80 plants have an average remaining lifetime of 32 years. The three Palo Verde reactors can disposition 50 MTs of WGPu in 11.1 years of operation while two can accomplish the mission in 16.7 years.

The GE BWR-5 design is the reference CLWR-BWR design. This design is considered representative of the 27 GE BWR-4,-5 &-6 designs now operating. Full MOX cores with fuel rod enrichments between 1 and 4.2 w% WGPu and a loading of 5.33 Kgs of WGPu/bundle are proposed. All rods contain gadolinium as a burnable absorber. One-third of the core is replaced every 18 months resulting in a 4.5 year residence time and a discharge burnup of 37,600 MWd/MT. It takes 66.1 reactor-years to disposition 50 MTs of WGPu in BWR-5s, which represents approximately 12% of the GE BWR-4,-5 &-6 remaining reactor-years. For the reference case 3 BWRs are used to disposition the WGPu.

Table 2.2 Selected Typical Reference Reactor Designs

Reference Type	Reference Design	Power Rating (MW _e)	Fuel Type
CLWR - PWR	ABB-CE System 80	1270	MOX
CLWR - BWR	GE BWR-5	1155	MOX
ALWR - PWR	Westinghouse PDR 1400	1400	MOX
ALWR - BWR	GE ABWR	1300	MOX
MHTGR	GA PC-MHR	286	PuO ₂ TRISO
CANDU	AECL Bruce A	769	MOX

The Westinghouse PDR1400 was submitted to DOE as a larger alternative to the PDR600 to increase the plutonium throughput. The PD600 is an adaptation of the commercial AP600 design for the plutonium disposition mission. The MOX fuel is 6.6 w% WGPu using a zirconium-diboride integral fuel burnable absorber coating, high soluble boron

concentrations and glass burnable absorber rods to meet safety criteria. Two PDR1400 reactors are required to disposition 50 MTs of WGPu in 25 years.

General Electric's ABWR was originally designed for full MOX core operations. The first of two new units being built in Japan was recently completed. NRC design certification of the US version was completed in 1995 and final design licensing is underway. The average fuel bundle plutonium content is 5.3 w% with gadolinium used as an integral burnable absorber. Gd_2O_3 has been burned in BWR MOX fuel before but not at the high weight percents proposed for this option. Two ABWRs disposition 50 MTs of WGPu in 25 years.

The General Atomic PC-MHR is a inherently passively safe design. Although the maturity of the PC-MHR is not at the level of ALWR designs, it is based on experienced gained from 35 years and 50 gas cooled reactors. The 590,000 MWd/MT burnup required to effect the plutonium disposition mission appears much larger than the typical 40,000 MWd/MT burnups of the LWR options. However, qualification of the TRISO fuel performance and manufacturing quality assurance makes the critical path for deployment of this option significantly longer than that of any of the other vendor reactor options proposed. Fourteen PC-MHR 14 reactors are required to disposition 50 MTs in 25 years due to its lower power rating.

AECL's CANDU proposal is based on using the four-unit Bruce-A reactor site for WGPu disposition. The Bruce-A plants are located in Ontario, 160 kgms from the US-Canadian border. Each of the CANDU's 480 fuel channels contain 13 fuel bundles. In the existing fuel design, each fuel bundle contains 37 fuel elements concentrically arranged. MOX would be substituted for natural uranium in the outer two rings and depleted uranium with 5 w% dysprosium as a burnable absorber would be used in the two central rings. Two reactors consume 15.5 bundles per day so that each reactor will disposition 1.05 MT/year.

Two of the four reactor units could be used to disposition 50 MT of WGPu in slightly more than 6 years of reactor operations. Thus, the CANDU option is the fastest WGPu reactor disposition option by almost a factor of two.

2.4.2 Throughput, Discharge Isotopes and Destruction. Table 2.3 presents the results of the vendor reference design calculations for disposition of 50 MT of WGPu in 25 years [A-4, A-5, D-4, G-2, G-3, G-4, G-5, N-1, N-2, W-1]. The small size and greater fraction of plutonium destroyed in the PC-MHR correlates to the low throughput relative to the other designs. There is no diluent metal in the TRISO kernel so that the discharged heavy metal is mostly plutonium. The BWR-5 produces the best discharge isotopes and plutonium destruction of the CLWR options due to its higher discharge burnup. The discharge isotopes of all of the MOX options are similar to each other and typical of RGPU.

Table 2.3 Summary Comparison of Throughput, Discharge Isotopes and Destruction Capability

Metric	Reference Designs					
	System-80	BWR-5	PDR1400	ABWR	PC-MHR	CANDU
Throughput (MT WGPu/Rx-yr)						
	1.5	1.06	1.56	1.2	0.28	1.05
Discharge Isotopes (kgm Isotope /kgm total Pu Mass)						
²³⁸ Pu	0	0.010	0.02	0.006	0.003	0.001
²³⁹ Pu	0.609	0.421	0.54	0.590	0.275	0.513
²⁴⁰ Pu	0.234	0.353	0.227	0.270	0.302	0.375
²⁴¹ Pu	0.137	0.151	0.151	0.105	0.327	0.086
²⁴² Pu	0.027	0.066	0.062	0.028	0.093	0.024
Destruction Fraction (kgm loaded/kgm discharged)						
²³⁹ Pu	0.49	0.71	0.53	0.61	0.89	0.63
Total Pu	0.22	0.36	0.18	0.38	0.64	0.34
Average Burnup (GWd/MTHM)						
	32.5	39.2	40.0	39.0	590.2	9.7
% Pu in HM Reload Fuel						
	3.7	2.0	1.1	4.1	96.1	1.0
Discounted (4%) Life Cycle Cost (Revenue) in \$M - Government Ownership						
	not avail.	not avail.	(759)	(552)	(1324)	not avail.
Discounted (4%) Life Cycle Cost (Revenue) in \$M - Utility Ownership						
	not avail.	1313	1111	1113	(660)	1481

Government owned option cost data was not available for any of the existing reactors nor was it available for the utility owned option for the System 80 reference case. The general trend

is that if the government takes ownership, it theoretically could recoup upfront capital costs through electricity revenues. The utility owned options are based on a cost-plus fee for service type arrangements and so the government cannot make money on the disposition. The 48% thermal efficiency of the proposed PC-MHR direct cycle design produces significantly lower busbar generation costs and yields better life cycle costs.

All of the reactor options provide several proliferation barriers to the reuse of the processed plutonium for weapons use. Conversion of the metal pit into an oxide fuel provides a chemical barrier and increases the critical mass required. Nuclear transmutation destroys some of the plutonium, hence reduces the amount of plutonium available for weapons use. The resulting fission products provide a strong radiation barrier forcing remote handling and sophisticated processing of the spent fuel to recover the plutonium. Finally, even if recovered, the residual plutonium isotopes are degraded in favor of the higher isotopes making it less attractive for use in making a nuclear explosive. All of the reactor options meet the spent fuel standard and the ≥ 20 w% ^{240}Pu for WGpu disposition standard. It is appropriate to digress here to consider the non-reactor option of vitrification.

Vitrification of WGpu with or without high level fission product waste does not reduce the world inventory of plutonium or does it isotopically degrade the plutonium. The advantage of vitrification is that it would take less time from the point at which a decision is made to establish a radiation barrier. In this respect, the incremental risk reduction provided by vitrification over the time required to complete reactor disposition may be seen as analogous to spiking. The magnitude of this incremental risk reduction must be weighed against the failure to reduce the world inventory of plutonium or isotopically degrade the plutonium. The other advantage of vitrification is that it can not possibly be construed as a endorsement of the civilian plutonium fuel cycle. The value of this advantage must be viewed in the historical light of the impact of the mid-1970's decision of the US not to reprocess. Vitrification is not at all applicable to a RGpu disposition mission; it would not make sense to reprocess spent fuel to produce a RGpu disposition product that was not more proliferation resistant than the spent fuel from which the plutonium was extracted in the first

place. As such, vitrification of WGPu may be viewed as a lost opportunity to build momentum for the ultimate goal of reducing and then controlling the world stockpile of plutonium to a manageable level.

The spent fuel standard relies primarily on the radiation barrier as the key deterrent to recovery of plutonium. The DOE has also stipulated a $^{240}\text{Pu}/\text{Total Pu}$ ratio of greater than 0.20. At greater than 20% ^{240}Pu the surface flux due to spontaneous fission is considered sufficient to deter use of that plutonium for weapons use. Little distinction is made regarding the weight percent of residual plutonium in the spent fuel. However, a weapon with a most likely yield of greater than one kiloton can be produced with plutonium of greater than 20 w% ^{240}Pu , and the radiation barrier of spent fuel is temporary. Higher fresh fuel enrichments are desirable because they reduce the total cost of MOX fabrication to disposition a fixed amount of plutonium. However, for the same burnup a higher initial enrichment produces a spent fuel with a higher plutonium w%. Although the incremental increase in risk may be difficult to quantify, fresh fuel with a high WGPu enrichment generally will produce spent fuel with a greater plutonium content than standard LWR spent fuel.

2.5 Summary and Conclusions

The WGPu plutonium disposition mission is fundamentally different than the RGPU mission. The WGPu mission is smaller and more well defined and involves reducing the relative risk of WGPu to that of RGPU. This mission can be accomplished with relatively few facilities and participants. Since WGPu is no longer being produced, the disposition mission is also finite in length. In contrast, the RGPU mission involves reducing and then maintaining the world stockpile of all plutonium at a level which will permit achieving an acceptable level of non-proliferation assurance. This mission requires the elimination of orders of magnitude more plutonium than the WGPu mission. It is also indefinite in length as it will be required as long as plutonium continues to be produced. Consequently, the goal

is one of establishing an equilibrium between plutonium production and destruction at the desired total plutonium stockpile level. Non-proliferation experts are already recommending such a RGPU mission [N-2, V-1].

Some very clear conclusions can be drawn regarding fuel technology for WGpu and RGPU disposition missions. All of the reactor options will require significant fuel and fuel fabrication qualification programs. The LWR MOX fuel development programs can draw on the large European experience base. However, the large enrichments and burnable poison loading proposed for the ALWR options are not part of the MOX experience base and will require significant fuel test programs to demonstrate reliability. There is little CANDU MOX experience but the less rigorous operating conditions and simpler design of CANDU fuels are not likely to present significant technological hurdles. The non-uranium PC-MHR fuel permits achievement of better discharge isotopes and plutonium annihilation fractions than MOX fuel options. However, TRISO fuel is less mature than MOX options. Thus, from a fuel technology perspective the MOX options are least risky but also do not offer the potential to substantially eliminate plutonium. Consequently, MOX fuel is preferable for a WGpu mission where the time to reduce the plutonium to the spent fuel standard is key. The PC-MHR TRISO fuel form or the CANDU non-uranium fuel is preferable for a RGPU disposition mission. A fuel and reactor technology which would permit large scale plutonium elimination is the most preferable for a RGPU mission.

CLWR reactor technology is very mature with only minor modifications required for full MOX core burning. CLWRs are already built and licensed, although the extension of licensing to burn MOX may be problematic. On average, CLWRs have a lower throughput which is a disadvantage for the WGpu mission. They offer less potential recovery of upfront capital costs due to their shorter remaining reactor life span over which electricity revenues can be collected. ALWRs provide a better opportunity to recoup capital costs but they also entail greater economic risk due to larger upfront capital costs. CANDU is the most mature reactor technology requiring no modifications to burn a full MOX core. However, it requires transporting WGpu across international borders. The more mature reactor technologies are

preferable for a WGPu mission because there is less schedule risk and the cost differential between options is not significant relative to the risk of proliferation. There is less distinction from a RGPU perspective. It is the fuel composition and cycle design that determine the capacity for plutonium destruction in a given reactor rather than the reactor technology itself. However, many reactors will be required to handle the magnitude of RGPU that is involved in the RGPU mission. Consequently, PWR reactors are preferable for RGPU disposition.

The MOX reactor options are the most mature and can convert WGPu to meet the spent fuel standard. However, the capability to destroy plutonium is limited by the use of ^{238}U bearing fuel. They can not go beyond the spent fuel standard without repeated recycling which would extend the RGPU elimination mission. In consequence, MOX disposition is not suitable for a RGPU option. The PC-MHR offers the ability to go beyond the spent fuel standard but it requires an extensive fuel development program in addition to new reactor technology; however, it does meet the standards of an elimination option.

The non-uranium fuel peripheral-loading PWR solution proposed here produces a true plutonium elimination option in a once-through PWR cycle. Such a solution would be applicable to WGPu or RGPU disposition missions. However, no additional advantage is gained by going beyond the spent fuel standard unless all plutonium is to be considered for disposition. Thus, the delay required to develop non-uranium fuel is not justified for the WGPu mission, although such fuel could be used for the later stages of this process, which is projected to last at least 25 years. The solution offered here provides a technique for establishing a plutonium elimination regime on the scale required to complete the RGPU disposition mission using existing PWRs. Thus, it has the advantage of not requiring any new reactors. One key disadvantage of the RGPU mission approach is that it will require reprocessing of spent fuel. However, spent fuel is already being reprocessed at an increasing rate around the world. Hence, the appropriate goal may be to make such reprocessing more proliferation resistant. This chapter made some qualitative comparisons between disposition options. The next chapter presents a scheme to quantitatively evaluate the proliferation resistance of the final plutonium product.

CHAPTER THREE: METRICS FOR QUANTIFYING INHERENT PROLIFERATION RESISTANCE OF PLUTONIUM DISPOSITION PRODUCTS

The NAS report on Reactor related plutonium disposition options proposes several qualitative criteria for evaluating the nuclear weapons proliferation risk associated with WGPu disposition options [N-2]. Many of these metrics are also relevant for a RGPU disposition mission. This chapter summarizes these metrics as background from which a quantitative subset of metrics are derived. These new metrics are focused on quantifying the inherent proliferation barriers specific to WGPu or RGPU host forms because they are more technical and independent of the policy aspects of the disposition options and so not subject to rapid change. Inherent barriers are those barriers which result only from the properties of the actual physical product of the disposition option. Thus, inherent barriers are also the most readily measured to support objective evaluation criteria. It is assumed that the proliferator has possession of the disposition product material which contains plutonium. Consequently, no institutional barrier, physical security or safeguard metrics are considered here. In the interest of being conservative, the criteria are weighted to account for the lowest common denominator threat scenario: a capable sub-national terrorist group interested in producing a crude nuclear explosive.

The author recognizes that such quantification of proliferation resistance is controversial. However, it is important to be able to gauge approximately how proliferation resistant the end product of a disposition option is relative to other products and the spent fuel standard. Such quantification can not only help in selecting which options are most useful for plutonium disposition but it can also illuminate where the emphasis on future improvements to fuel cycle proliferation resistance can be made. This chapter details an approach to accomplishing that task. It is offered as a logical and objective starting point for discussion and modification rather than the definitive method. Development of metrics and an algorithm for applying them requires making assumptions and judgments. Some of these assumptions and judgments are subject to debate. Hence, a strong effort is made to identify and address each of these as they enter into the process.

Section 3.1 summarizes the NAS criteria which include the entire array of barrier types. Section 3.2 and 3.3 propose quantitative metrics for evaluation of the proliferation barriers resultant from only the physical properties of the disposition product which hosts the processed plutonium. Section 3.4 proposes a scheme for implementing the metrics to arrive at an overall ranking of disposition product's relative proliferation resistance. A example application of these metrics is provided in section 3.5. Appendix A contains detailed example calculations supporting this application.

3.1 Background.

The section reviews some of the proposed criteria for evaluating the proliferation risk associated with WGPu dispositioning. All of the disposition options require several stages of activity, from weapons dismantlement to final placement of the disposition plutonium product. The risk associated with each option is determined by the

cumulative risk of each of the stages comprising the option. This cumulative risk is heavily biased by the least secure stage in the process. In turn, the risk associated with each stage is a function of specific characteristics such as the physical form of the plutonium, the plutonium inventory and the time to complete the stage. Thus, there are several levels and categories of evaluation possible. Risk is generally assessed on a comparative basis between options. However, two absolute standards for risk have been identified in the WGPu debate: the stored weapons standard and the spent fuel standard.

The stored weapons standard applies to the material and the process up to the point when the plutonium host form meets the spent fuel standard. It would be difficult to maintain exactly the same level of security achievable with stored weapons for plutonium actively being processed. Stored weapons are under lock and key with military controlled access while plutonium being processed is accessible to and handled by many workers. Thus, the goal of security and safeguards measures is to reduce the risk to the maximum extent possible so as to approach the stored weapons standard. The spent fuel standard requires plutonium in the final disposition product to be roughly as inaccessible as plutonium in spent fuel. From that point on, the security measures taken for spent fuel apply. With these two standards in mind the NAS proposes metrics which cover all the stages of the disposition process.

3.1.1 NAS Metrics. The NAS states that the primary goal of WGPu management and dispositioning should be the mitigation of risks to international and national security. This section reviews these criteria to provide a context for introducing new metrics proposed in the following sections. A more detailed description of the NAS evaluation scheme is provided in their 1995 reactor related options report for the management and disposition of excess weapons grade plutonium [N-2].

The NAS proposes specific criteria and an algorithm for applying them in a stage-wise manner, ultimately arriving at a set of risks associated with the disposition option. Consequently, these criteria cover all aspects of the disposition process. They are categorized into four general areas: time and quantity dependent risks, intrinsic barriers, implementation-dependent barriers, and overall risk in the overt and covert theft and diversion threat scenarios defined in chapter 1. Table 3.1 presents a summary of the NAS criteria [N-2]. A value is assigned for each individual criteria for each stage of a disposition option. The NAS does not definite a single quantitative number to characterize the overall risk of an option. Time and quantity criteria are used to assess the risk associated with how long material spends in between the two absolute standards. These are the only metrics which are quantified via measurement of real disposition option properties. The plutonium is most vulnerable between the time it is taken from a stored weapon to the time it meets the spent fuel standard. The larger the integral of the inventory over time for a particular stage of processing, the greater the risk. Plutonium density criteria are used to gauge how much of the process stage material must be stolen or diverted to constitute a significant quantity. Intrinsic barriers refer to those barriers provided by the physical properties of the plutonium material found in each process stage. The 0-4 scale corresponds to a negligible (=0), small (=1), medium (=2), large (=3), and very large (=4) barrier rather than an actual measurement of the associated property. Thus, the value assigned is the result of a qualitative assessment. The relation between scale values is not necessarily linear nor is it consistent between criteria. The 0-4 scale for the radiological barrier of plutonium host forms is linear with each unit change equal to an order of magnitude difference in the radiation field. The isotopic barrier scale uses HEU as the reference zero value, WGPu is assigned a barrier reference value of 1, typical RGpu is assigned a barrier reference of 2, high burnup RGpu with weight percent of ^{240}Pu greater than 40% is assigned a barrier reference of 3 and uranium with less than 20 weight percent ^{233}U or ^{235}U is assigned a barrier reference of 4. Larger contents of ^{240}Pu and ^{242}Pu increase the critical mass and

make it more difficult to produce a non-fizzle yield. ^{238}Pu complicates design problems by generating heat and ^{241}Pu produces ^{241}Am . Chemical barriers refer to the chemical form of the plutonium.

3.1 NAS WG Pu Risk Evaluation Criteria [N-2]		
Criteria	Type of Measurement	Units/Scale
Time and Quantity		
Start Date	Quantitative	Date
End Date	Quantitative	Date
Integrated Inventory	Quantitative	Kg-yrs
Dilution	Quantitative	Kg material/Kgm Pu
Intrinsic Barriers		
Isotopic	Qualitative	0-4 scale
Chemical	Qualitative	0-4 scale
Radiological	Qualitative	0-4 scale
Mass/Bulk	Qualitative	0-4 scale
Implementation-Dependent Barriers		
Location	Qualitative	0-4 scale
Containment	Qualitative	0-4 scale
Institutional	Qualitative	0-4 scale
Overall Threat Scenario Vulnerability		
Overt Diversion	Qualitative	High-Medium-Low
Covert Diversion	Qualitative	High-Medium-Low
Overt Theft	Qualitative	High-Medium-Low
Covert Theft	Qualitative	High-Medium-Low.

Metallic plutonium is the most convenient chemical form for producing a weapon. Other forms such as oxides, carbides and nitrides generally increase the critical mass of the weapon. The presence of admixture impurities such as neutron absorbers, fission products and chemical spoilers make processing of the raw material into metallic form more difficult. Under the NAS scheme, plutonium metal is assigned a chemical barrier value of zero, pure plutonium oxide is assigned a chemical barrier

value of one, MOX is assigned a chemical barrier value of two and plutonium imbedded in spent fuel or a vitrified waste form is assigned a chemical barrier value of four because the radiation barrier makes processing much more challenging. The radiological hazard metric gives credit for both penetrating gamma emissions requiring additional process shielding and alpha and beta emissions which present inhalation and ingestion hazards. Natural, depleted or LEU is assigned a radiological barrier value of zero, HEU is assigned a radiological barrier value of one, WGPu in metal of oxide form is assigned a radiological barrier value of two, metallic RGpu is assigned a radiological barrier value of three and plutonium in spent fuel or mixed with high level waste is assigned a radiological barrier value of four. The Mass/Bulk criteria assess how easily the plutonium host material can be smuggled out of a facility. If the material can be carried and easily concealed by a single individual, such as small amounts of metallic or oxide HEU and WGPu, it is assigned a barrier value of zero. If the material is readily portable by one person but more difficult to conceal it is assigned a barrier value of one. If the material can be moved by one person but can not be concealed, such as a fuel element weighing less than 10 kilograms the material is assigned a barrier level of two. If a forklift is required for movement, such as for assemblies weighing more than 100 Kgs, a barrier value of three is assessed. Finally, material forms of 1,000 kilograms or more requiring a crane to be moved are credited with a mass/bulk barrier value of four. The next major category of barriers are those dependent on implementation.

Implementation dependent barriers assess the risk associated with the physical location, containment and institutional barriers erected around the process stages of a disposition option. The risk associated with the location of the disposition stage is assigned as follows: transportation is considered the riskiest stage and assigned a score of zero, multiple sites disposition is assigned a score of 1, process at a single site or storage at multiple sites is assigned a score of two, and the least risky location criteria value is assigned to storage at a single site with a score of 3. One point is added to the

location criteria value if the site is remote or otherwise hard to get to. Containment criteria assess how difficult it is to defeat packaging to gain covert access to the plutonium-containing material. Institutional criteria deal with the level of human and hardware security provided. The final category of criteria assess overall risk relative to the specific threat scenarios defined in chapter one.

Overall threat scenario criteria account for the influence of issues specific to each disposition option which do not lend themselves to any of the other categories. The effectiveness of the barriers in each stage is evaluated with respect to each specific threat scenario. Sub-sections 3.1.2 and 3.1.3 review the properties of the NAS metrics and define what is meant by inherent proliferation resistance.

3.1.2 Discussion of NAS metrics. Time and quantity criteria can be influenced by how the technology of a specific option is implemented. For example, the time and quantity criteria risk for a MOX fabrication stage could be reduced by increasing the throughput capacity of the fabrication facility. The fabrication capacity is limited by cost considerations rather than technology and so the associated risk is not limited by the technology. Similarly, implementation dependent barriers and overall threat scenario barrier criteria risks are not unique for a given disposition option. The risks characterized by these metrics is a function of how the disposition option is carried out. As such, the measured risk is part of a set of values that can be derived by examining all reasonably conceivable ways to carry out the disposition option. These types of barriers are based on economics and policy and are beyond the scope of this investigation. However, a set of barriers exist which are fundamentally different because they are more particularly defined by the technology of the option. For example, while MOX spent fuel isotopes will vary depending on burnup such variation is limited by reactor physics and safety constraints. Unlike MOX, non-fertile fuel can be used to eliminate essentially all the Pu. Thus, there is a much greater contrast produced by differences in

the technology of the option than how the option is carried out. The plutonium isotopes produced by a disposition option can be called an inherent proliferation barrier.

3.1.3 Inherent Barriers. The key difference between inherent barriers and other sorts of proliferation barriers is that inherent proliferation barriers remain even if the proliferator has possession of the disposition product plutonium host material. For example, the plutonium isotopes of a disposition option product can provide an inherent barrier to proliferation. In the extreme case of an elimination option, if the small amount of residual spent fuel plutonium that exists is primarily ^{238}Pu and/or ^{242}Pu then for all practical purposes the plutonium is useless as a raw nuclear explosive material. The inherent barrier metrics proposed here are a subset of the NAS metrics. They quantify and develop the NAS intrinsic barriers. In order to evaluate these barriers it is necessary to define several quantitative metrics for each barrier type.

These quantitative metrics measure the physical properties of disposition product which provide the barriers to proliferation. They are equally applicable to WGPu and RGpu disposition options. Multiple metrics are defined for each barrier type described above. Ideally each metric would uniquely evaluate some aspect of its associated barrier. A certain degree of coupling among the metrics is unavoidable. However, careful definition can minimize the overlap.

It is convenient to group the proposed technical criteria into two barrier types: those which measure the barriers associated with the plutonium host form matrix and those which measure the barriers associated with trying to use the plutonium resident in the host form matrix to make a nuclear explosive. These two barrier types are designated disposition product host matrix and plutonium weapons usability barriers, respectively.

Section 3.2 and 3.3 propose specific metrics to evaluate the inherent proliferation barriers of candidate plutonium disposition products.

3.2 Disposition Product Host Matrix Proliferation Barrier Metrics

The inherent proliferation resistance of processed plutonium host forms cannot be quantified in absolute terms. Any host can be manipulated to retrieve the plutonium and make a nuclear device. The goal then becomes one of quantifying the relative difficulty involved in reconstituting weapons usable material from a given plutonium host form. The proliferation barriers presented by the disposition product host matrix can be quantified using metrics which measure the quantity, chemical, and radiation barriers inherent in the plutonium host form. Quantity relates to how much of the host material must be diverted before enough plutonium has been acquired to construct an explosive. The lower the fissile plutonium content, the more material that would have to be stolen. Chemical barriers resist chemical separation of plutonium from its host matrix. Metrics measuring the inherent chemical barrier presented by a host form are perhaps the least straightforward properties to measure. They quantify the relative difficulty involved in developing a suitable purification process for retrieving the plutonium from the host matrix via chemical separation. Radiation barrier metrics address the radiation hazard associated with handling a host form before plutonium separation can be achieved.

3.2.1 Fissile Density. A lower concentration of plutonium in the host material means that production of a nuclear explosive will require accumulation and processing of more material. It is assumed that as the volume or mass of material that must be stolen increases so does the difficulty in accomplishing the task covertly. If the metric were simply defined as the volume or mass of material that must be stolen to accumulate sufficient plutonium to produce a nuclear explosive, it would have a strong dependence on the critical mass and the plutonium isotopes; material with a larger fraction of neutron

absorbers and a lower ^{239}Pu w% results in a larger critical, mass requiring a larger volume or mass of material to be stolen. This interdependence is minimized by defining the metric as a fissile density in kgs $^{239\&241}\text{Pu}$ per cubic meter. The lower the fissile density the greater the proliferation barrier. This metric does not include any consideration for packaging. The material can be packaged at every stage of the process to optimize the barrier to theft regardless of the option chosen. For example, fuel assemblies can be encapsulated in canisters with tamper proof seals until they are loaded individually into the reactor. Thus, the bulk and mass are more a function of the packaging used rather than the technology of the option. Packaging can be mechanically removed and so is not considered an inherent proliferation barrier. Once the proliferator possesses a sufficient quantity of the disposition product, it will be necessary to chemically process the material to retrieve the plutonium.

3.2.2 Chemical Barriers. Absolute chemical barriers do not exist. The commercial nuclear industry regularly separates plutonium and uranium from spent fuel which contains virtually the entire periodic table of elements. However, the key is to measure the relative proliferation resistance. A plutonium host matrix which is more difficult to penetrate and which contains a significant amount of chemical spoilers may take longer to process than a straight MOX matrix. A chemical barrier is defined here as any element or material which resists chemical separation of plutonium from its host form. Residual impurities in the recovered plutonium can detract from its usefulness in nuclear explosives in two ways. A strong neutron absorber can inhibit the chain reaction by consuming neutrons which would otherwise lead to more fissions and a strong neutron scatterer can reduce the energy of fast neutrons below the threshold required to cause the fission of the non-fissile plutonium nuclides.

Determining how best to measure the relative chemical proliferation barrier of a plutonium host form is an inexact process. The proliferation resistance depends on what

chemical method is used to separate the plutonium from the rest of the host matrix elements. Unfortunately, there is an extremely long list of possible techniques which can be employed. However, most fuel reprocessing is accomplished through aqueous processes. The PUREX process is universally used for LWR spent fuel reprocessing [B-3]. Non-aqueous pyroprocesses involve extreme temperatures and are designed specifically to be able to handle short-cooled spent fuel which creates a serious solvent degradation problem in PUREX type processes [S-4]. There is an ample stockpile of well cooled spent fuel and it is assumed that a proliferator would choose the least radioactive plutonium host that could be found. Thus, there would be no reason to pursue pyroreprocessing technology. Other non-aqueous processes have extremely challenging equipment material requirements or other disadvantages. It is assumed that these factors will tend to lead the proliferator to some form of aqueous based purification scheme. Thus, the analysis focus is on resistance to aqueous type purification processes with particular emphasis on PUREX type processes.

Separation via an aqueous process will involve two steps: dissolution of the host matrix solid lattice into its constituent ions followed by separation of solvated ions. Consequently, two chemical barrier metrics are proposed: dissolution resistance and separation resistance. Dissolution resistance quantifies the difficulty involved in dissolving the host matrix and getting the plutonium into solution to facilitate further processing. The greater the solubility of the matrix material the lower its dissolution resistance. Solubility data can be found tabulated in units of gms per liter and are used here as a measure of dissolution resistance. Other dissolution metrics are possible.

Experimental data could be generated to quantify the integral time and temperature required to dissolve a given amount of plutonium host matrix products in the solvent considered most likely to be used. However, there are far too many solvents to be all-inclusive here. Standard PUREX processing begins with a nitric acid dissolution step.

Thus, the solubility of the matrix in nitric acid at a common temperature is used to assess dissolution resistance. The solubility of each matrix in other solvents can similarly be included in an evaluation to increase the range of validity of the results.

Once the proliferator destroys the host matrix and gets the plutonium into solution, there remains the task of separating the plutonium ions from the rest of the host matrix ions. Distribution coefficients provide a definitive measure of the separability of different ions by specific solvents under very specific conditions. When tabulated values for applicable conditions can be found, the distribution coefficients can be directly used as the metric. For the PUREX process, the values of the distribution coefficients for the ions of interest between the tri-butylphosphate and aqueous phase can be used as a measure of the separation resistance. For the present purposes, the distribution coefficient (D) values for specific ions are normalized to plutonium. The closer an ion's normalized D value is to unity, the greater the resistance it offers. Summing the contributions of all the ions found in a plutonium host form yields a dimensionless metric value of the separation resistance.

There are a variety of aqueous separation schemes that may be employed by a would-be proliferator. Distribution coefficients are only applicable for a specific set of conditions and so are limited in their robustness for evaluation of resistance to separation. The ionic radii of the metals present in the host matrix can be used as a more generally applicable metric for assessing the resistance to plutonium separation.

There are several characteristics of ions in solution which describe their behavior, including enthalpy of solution, acid-base behavior, stability and rate constants and redox potential. These parameters quantify the stability of an ion in solution and describe how it may react to changes in the solution environment. Trends in these properties are known to correlate to a varying degree with the radius and charge of the ion of interest. For

example, lanthanide(III) and actinide(IV) cation solvent exchange rate constant trends follow a simple electrostatic interaction framework [B-4]. As the ionic radius increases, the rate constant decreases. Similarly, solvent-ion stability constants are found to be very dependent on the ionic radius. In order for larger cations, such as plutonium, to be readily extracted, the complexing ligand must be able to form several secondary chelating bonds which in effect wrap around the ion. This requires that the active site of the ligand be closely matched with the ionic radius of the cation. If the radius is too large or too small, insufficient bonding will take place and the cation will not be easily removed to the target solvent phase. The rate and solvent-ion stability constants are of particular importance for aqueous plutonium extraction techniques. Predicting the behavior of ions solely based on simple electrostatic trends is a major simplification. However, we are only interested in whether this matrix constituent is likely to behave more or less like plutonium ions when compared to another constituent. In the absence of distribution coefficient data, the extent to which the ionic radius and charge of a candidate element are similar to that of plutonium may be adequate to indicate how similar its solution behavior is to that of plutonium.

The ionic radii and charge can be used to compare chemical barrier resistance as follows. The quotient of each host metal ion radius and plutonium's ion radius is calculated. The quotients are determined for each of the plutonium oxidation states, +3, +4, +5, +6, exhibited by each non-plutonium metal ion. The absolute value of the difference between exact ion radii agreement, i.e. 1.0, and the actual value is multiplied by 100 and then its metal weight percent of the total non-plutonium metal mass. The weighted quotient differences for each non-metal are summed to produce a total weighted value for each oxidation state. Perfect agreement with plutonium would yield a zero value for each oxidation state. The average of the total weighted quotients is taken to produce a single number for each host form. The larger the final average value, the lower the chemical separation barrier between plutonium and the other metals in the host matrix.

The final barrier presented by the plutonium host matrix is potentially the most formidable: the radiation barrier.

3.2.3 Radiation Barrier. The RG₃Pu in spent fuel can be used to make a nuclear explosive and the PUREX process is well defined and uses widely available equipment. Consequently, the radiation barrier in spent fuel is the primary inherent deterrent to theft and processing of spent fuel for plutonium recovery. A radiation field which will generate a lethal dose in a short period of time may actually prevent a terrorist group from being able to handle the host form. A radiation field of that magnitude forces the use of shielding and remote handling procedures which greatly complicate the initial steps of the separation process. A large radiation field can also significantly degrade the solvents used in the separation processes further complicating the task of recovering the plutonium. On the other hand, a weaker radiation field which may only increase the exposed individuals' risk of developing cancer may not be an effective deterrent against terrorist organizations. Thus, while it is difficult to estimate what dose a terrorist might be willing to accept, there is some threshold value above which remote handling will almost certainly be required and below which exposures due to handling might be tolerable. The NRC and IAEA guidelines require less stringent security for plutonium containing materials producing a radiation field of greater than 100 Rad/Hour at 1 meter because they are considered to be sufficiently self-protected [K-4]. (Note that a dose of 450 rem is the LD50/30 limit for a general human population)¹ The NRC & IAEA threshold of 100 rad/hr is adopted here. However, radiation barriers are temporary in nature; the radiation field generated by spent fuel of typical burnup decays to 100 Rad/Hr in approximately 160 years [N-1]. Thus, both the magnitude of the radiation field and the estimated time it will remain above some threshold are important. The radiation metric is defined as the number of years that a host

¹ An LD50/30 radiation dose is defined as the dose which would cause the death of 50% of those exposed within 30 days of the exposure.

form will retain a radiation field above 100 rad/hr at 1 meter. No credit is given for alpha and beta emissions and their associated inhalation and ingestion hazards because they are considered more long term chronic hazards rather than capable of producing a lethal dose preventing the completion of chemical processing. Concern for long term health problems are not a strong deterrent against a terrorist or sub-national threat.

Assuming the proliferator is able to separate the plutonium from its disposition product host matrix, the properties of the recovered plutonium may present additional barriers to its use in a nuclear explosive.

3.3 Plutonium Weapons Usability Metrics

The plutonium weapons usability barrier metrics are based on the assumption that the proliferator has separated pure plutonium from the disposal product matrix. The associated metrics assess the level of difficulty in producing a nuclear explosion from the recovered plutonium. It is assumed that plutonium which would allow the proliferator to build a weapon with a lower critical mass and a higher reliability is more attractive. Low critical mass and a high probability for producing a maximum yield suggest three metrics for assessing how readily the plutonium in the host matrix can be used to create such a nuclear explosive: critical mass, surface neutron flux and plutonium isotopes. In addition, the decay heat produced by the plutonium presents a fourth plutonium weapons usability barrier. Note that decay power and critical mass are definable functions of isotopes: hence there is a certain degree of redundancy in the selection of metrics. This can be allowed for in the weighting process used to combine metrics. Redundant metric categories are retained because different manifestations of isotopic content relate directly to physical attributes relevant to construction of a practical explosive. The relative nuclear explosive value of a material is directly related to its critical mass.

3.3.1 Critical Mass. Nuclear weapons operate in a fast (vice thermal) spectrum; the potential of a host form to be brought fast critical is what must be quantified. Nuclear explosive devices compress a subcritical mass to achieve supercriticality and the resultant explosive release of energy. There are three considerations in determining the ground rules for calculating the critical mass: compression, weapon design and geometry.

The first judgment is whether to use the nominal or compressed density. Estimating the degree of compression that could be achieved in a crude design is at best an inexact process. Fortunately, compression is essentially a geometrical alteration which can be accomplished on any host material; the effects of compression are not unique to the plutonium being considered. Since we are interested in relative properties, the uncompressed mass is an equally valid metric and is somewhat more straightforward to measure. Next, the configuration of the plutonium must be considered. Technical aspects of the design of the weapon such as use of a tamper and reflector can have a large impact on the physics of the detonation. The reflector/casing design are not inherent properties of the WGPU host material and therefore provide no relative resistance information. Hence, a bare unreflected system is assumed. Finally, a spherical configuration has the lowest neutron leakage and thus represents the lowest possible critical mass geometry. Accordingly in the present work, the bare, unreflected, spherical, uncompressed critical mass measured in kilograms is used to measure the nuclear explosive value of the plutonium found in the disposition product. The second weapons usability metric proposed is the neutron emission rate

3.3.2 Neutron Emission Rate. The likelihood that a nuclear explosive will not reach its optimum yield depends on the subcritical surface neutron flux from spontaneous fission and alpha-neutron interactions of plutonium nuclides. As discussed in section 1.3.2, a higher neutron flux makes sub-maximum yield more likely but does not prevent the device from achieving fast criticality and generating a nuclear explosion. Thus, the surface

neutron flux gives a rough indication of the likely magnitude of the explosion relative to its theoretical maximum yield. The primary contributor to the neutron surface flux is from spontaneous fission of the even plutonium isotopes. The concentration of nuclides which spontaneously fission is the same for all non-irradiated WGPu host forms; thus, this metric is essentially zero for all but spent fuel and RGPu host forms. The neutron emission rate for plutonium metal can be readily estimated and used directly as a metric in units of neutrons/ sec-Kg Pu.

3.3.3 Plutonium Isotopic Composition. The third weapon usability metric considers the isotopic makeup of the plutonium which is resident in the host matrix. WGPu is highly enriched in fissile material with an isotopic mix of approximately 93.5% ^{239}Pu , 6.0% ^{240}Pu and 0.5% ^{241}Pu . The isotopics of all other grades of plutonium are inferior for weapons use. Section 1.3.1 provides a detailed analysis of the effects of each plutonium isotope on the dynamics of nuclear weapon physics and design. ^{239}Pu and ^{241}Pu are the key fissile nuclides for weapons use. The isotopic metric is defined as grams of $^{239+241}\text{Pu}$ per gram of total plutonium. WGPu isotopics are considered optimum for weapons use and consequently WGPu is defined as presenting no isotopic barrier to weapons use. Since plutonium is a synthetic element, the isotopics can only be diluted through the WGPu-neutron interactions. Fresh fuel and vitrification host forms provide no isotopic barrier. The fourth weapons usability metric is the plutonium decay heat.

3.3.4 Decay Heat. The decay heat generated by plutonium complicates the explosive design. If the decay heat is low enough, conduction through the explosive and convection plus radiation at its surface may be sufficient cooling mechanisms. Such is the case with WGPu. A greater decay heat rate may yield temperatures high enough to degrade other weapons materials such as the high explosives. Thus, either the device would have to be assembled just prior to detonation or an active cooling system would be required. The decay heat is essentially zero for WGPu host forms such as clean glasses and fresh reactor

fuels which do not contain any irradiation products. To maximize the independence of the decay heat metric, it is measured in units of watts per kilogram of plutonium rather than in units of watts per critical mass. The product of this value and the critical mass can be readily obtained to produce the total heat which must be dissipated in a design.

The metric values are defined to allow objective measurement, but how they are applied and combined to draw conclusions about the relative inherent proliferation resistance of individual disposition products is also critical. It is necessary to define a logic-based algorithm for using these metrics.

3.4 Scoring and Ranking Algorithm

This section describes an algorithm for applying the metrics defined in the previous sections to arrive at a conclusion regarding the inherent proliferation resistance of disposition products. An example evaluation is presented in section 3.5. Table 3.2 summarizes the proposed metrics defined in sections 3.2 and 3.3.

3.2 Inherent Plutonium Disposition Product Barrier Metrics		
Criteria	Type of Measurement	Units/Scale
Disposition Product Matrix Barriers		
Fissile Density	Quantitative	kg fissile Pu/m ³ host
Dissolution	Quantitative	gms/liter
Separation	Quantitative	dimensionless
Radiation Barrier	Quantitative	years
Plutonium Weapons Usability		
Isotopic	Quantitative	gms fissile/gm Pu
Critical Mass	Quantitative	kg Pu
Neutron Emission	Quantitative	n/sec-kg Pu
Decay Heat	Quantitative	w/kgm Pu
1. The separation metric is calculated by ratioing separation distribution coefficients if the data can be found. Alternately it is calculated as an ionic radius ratio as described in section 3.2.3.		

The metrics defined above measure specific plutonium matrix properties. Thus, they are objective in nature. In contrast, there are many possible ways in which to combine these metrics to calculate and rank the proliferation resistance of the disposition options. Altering the methods chosen would effect the conclusions which might be drawn as to which option produced plutonium products with the most proliferation resistant inherent barrier. Consequently a fair amount of judgment is implicit in the scheme used to combine the metrics to reach a quantitative conclusion. Thus, the following presents only one possible scheme and the logic used in its derivation.

3.4.1 Minimum Threshold. These metric criteria provide a means of making a relative comparison between options. However, there should also be an absolute minimum. The NAS spent fuel standard is the final disposition form minimum proliferation resistance threshold. A disposition product which falls short of this standard presents a security risk beyond that of spent fuel and will require special security measures.. Thus, the values for each metric corresponding to typical spent fuel should be used as a threshold. The performance evaluation of host forms should detract from the score of a disposition product for sub-spent fuel proliferation performance and award credit for proliferation resistance that is better than that inherent in spent fuel. Giving credit for performance above the spent fuel threshold is only valid for a RGPu mission as discussed in chapter 1. Thus, there is an inherent assumption that it is considered important to deal with all the world's plutonium rather than simply reducing the proliferation risk associated with weapons grade plutonium to the level of the much larger stockpile of RGPu.

Next, some distinction must be made as to the relative importance of each metrics contribution to the disposition product matrix and plutonium weapons usability proliferation barrier types.

3.4.2 Metric Contribution Weighting. Not all the metrics need be given equal weight. For example, the decay heat metric may be of secondary importance in quantifying the weapons usability of a host matrix metal mix. Using a clever design, the proliferator could store the host metal mix containing the plutonium in a cooling medium and assemble the explosive just prior to detonation. In that case, long term decay heat removal would not be required. Similarly, any device, crude or sophisticated, which can produce a nuclear explosion is of concern. Consequently, the relative probability of producing a less than optimum yield as indicated by the neutron emission rate metric is also of secondary importance in measuring proliferation resistance and should be weighted less than other metrics.

Thus, a minimum spent fuel standard threshold and metric weighting should be part of the algorithm. The first step in that algorithm is to convert the all the individual metric values into a set of metric scores normalized to a consistent scale.

3.4.3 Individual Metric Scoring. Figure 3.1 is a example flow chart for determining individual metric values. A metric scoring curve is defined for each metric with ordinate values from -1 to 1. The scoring curve converts the individual metric values into metric scores according to the functionality between the metric value and the impact on the robustness of the barrier.

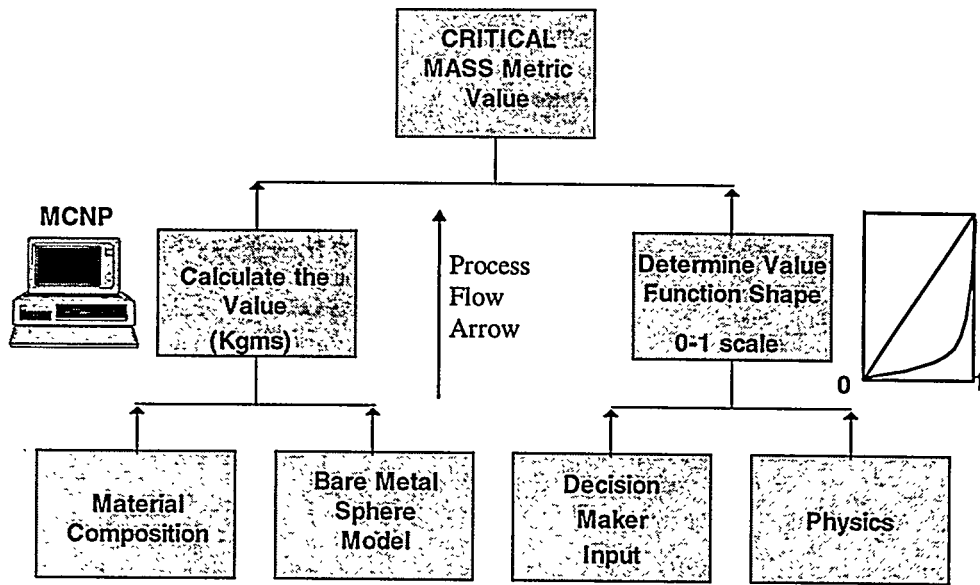


Figure 3.1 Overview of Individual Metric Scoring

The ordinate values can range from the corresponding metric value for spent LEU fuel to the peak metric value for the options being considered. The zero abscissa value equates to a barrier equivalent to that of LEU spent fuel. A disposition product that is not as proliferation resistant as spent fuel for a given metric property receives a negative metric score ; thus, the spent fuel standard is the minimum threshold. Figure 3.2 is an example of a linear metric scoring curve for critical mass. A linear critical mass scoring function assumes the difficulty in creating a weapon increases linearly with the critical mass.

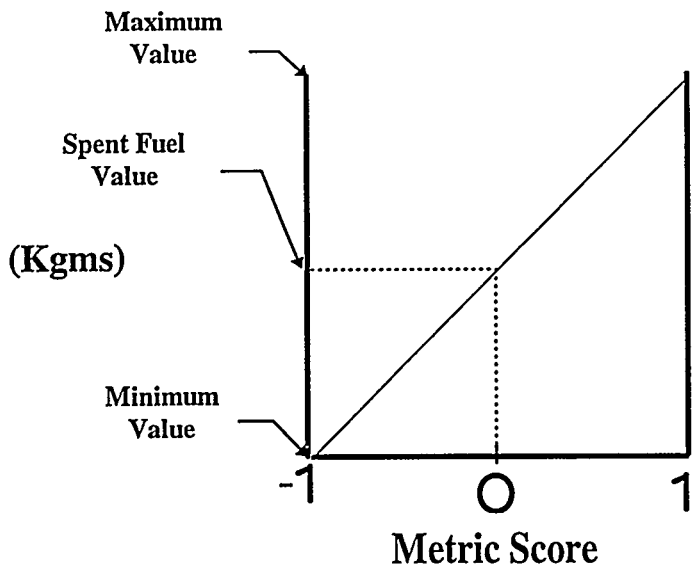


Figure 3.2 Example Critical Mass Metric Scoring Function

Ideally, the linear slope of the scoring function from 0 to 1 should be equal the slope from 0 to -1 to ensure equal relative weighting to the credit and penalty for positive and negative performance, respectively. This is accomplished through proper setting of maximum and minimum values. However, the physical realities of some metrics do not necessarily permit equal slopes. For example, it is not physically real to define a negative critical mass as a minimum ordinate value. Consequently, the slopes from 0 to 1 and from 0 to -1 may not be equal depending on the metric. The driving consideration is to produce a spread in the scores. For example if the maximum critical mass performance were defined as 1000 Kgs and equated to a metric score of +1, then all the disposition products options would have a score of approximately 0. This would only indicate that the disposition option critical masses were closer to that of spent fuel rather than an extreme value of 1000 kgs. Setting too large a range of metric values obscures the differences between the options. Thus, if possible, the range of metric values chosen should be small enough to discern the difference between the options. Similarly, setting the range too small drives all the options to a +1 or -1 score. This is not always avoidable but it should

be minimized. To maximize the objectivity of the metric scoring, anchoring the metric value range on some physically real characteristic such as percentage of the spent fuel value or the actual range of disposition metric values seems to be most logical. However, as will be seen for some metrics in the next section, it is still not always possible to create a spread in all of the metric scores if they are very similar. A discussion of some specific metric scoring functions is provided in section 3.5.2. More complex curves which better correlate the effect on the difficulty level for creating a weapon and the change in the metric value can be envisioned. However, a detailed study of potential metrics scoring functions is beyond the scope of this work.

Once metric scores are determined they can be weighted and combined to produce scores for the disposition product matrix and plutonium weapons usability barrier types.

3.4.4 Barrier Type Evaluations. Single quantitative-value evaluations of the inherent proliferation barrier presented by a plutonium host form are derived for each barrier source: disposition product matrix and plutonium weapon usability. Individual metric values are weighted between 0, of no importance, and 100%, of singular importance. The sum of the weighting factors must equal 100%. The products of the individual metric scores and their weights are summed to determine the score for the barrier type. Figure 3.3 is a flow chart for the scoring of the plutonium weapon usability barrier from the individual metric scores.

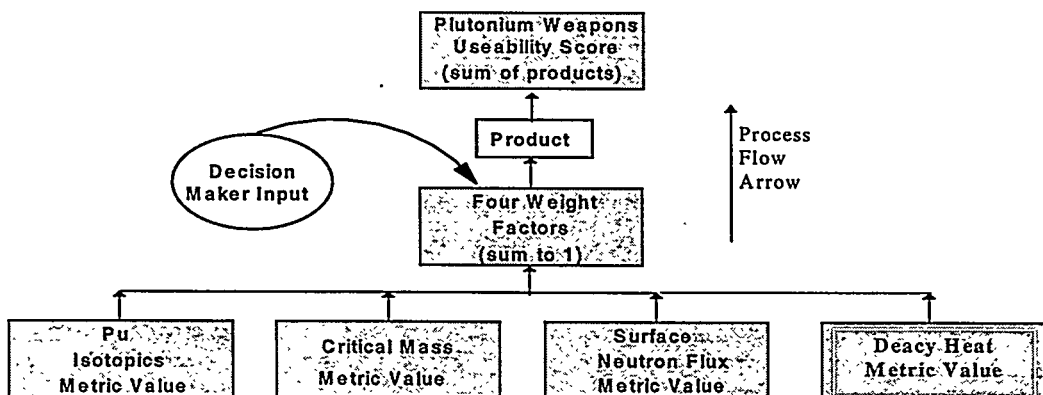


Figure 3.3. Overview of Barrier Type Scoring

3.4.5 Overall Ranking of Plutonium Product Forms. The two barrier type rankings are added together resulting in a single value for each disposition product. The host form with the highest score is the best performer. Each disposition product is ranked between 1 and the total number of host forms being considered for disposition matrix and plutonium weapons usability barrier types. In a comparison between HLW spiked glass, MOX spent fuel and non-uranium spent fuel, each disposition product would have a ranking between 1 and 3 based on their overall barrier type scores. Products which perform the best are ranked number 1 and the one performing the worst is ranked 3. Thus, the relative strength of the proliferation barriers of each option is determined. Figure 3.4 is a flow chart for determining the final score for a plutonium disposition product.

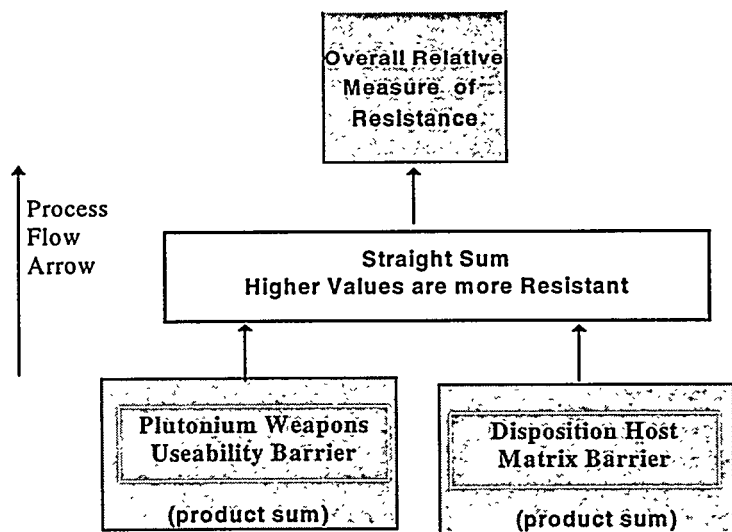


Figure 3.4. Scoring of Overall Proliferation Resistance of a Disposition Plutonium Product

Section 3.5 provides an example application of the metrics and algorithm in comparing HLW spiked WGPu borosilicate glass, spent WGPu MOX fuel and WGPu non-uranium spent fuel.

3.5 Example Implementation of Proposed Metrics

This section uses the metrics and algorithm detailed above to illustrate how to quantify and compare the inherent proliferation resistance of candidate final disposition products. WGPu disposition products are used because the properties of the WGPu disposition products are more readily available.

The intent of this section is to provide a model for how to quantify the relative inherent proliferation resistance of candidate disposition products. This goal is distinct from definitively calculating the absolute proliferation resistance of these disposition products. Many judgments and assumptions are required to complete the necessary calculations. Some of these assumptions and judgments are subject to debate. A strong effort has been made here to identify and address each of these as they enter into the process. The reader is referred to appendix B which contains a detailed example calculation of how the metrics values were derived, scored and combined to produce barrier type scores.

There are two primary disposition options being considered for WGPu: reactor irradiation and vitrification in borosilicate glass [N-2]. A comparison is made between spent MOX fuel assemblies and borosilicate glass logs to one of the non-uranium fuel plutonium disposition assemblies suggested in this thesis. The next section describes these three reference case disposition products.

3.5.1 Description of Reference Cases. The properties of MOX irradiated in the Westinghouse PDR1400 are used as the reference case for comparison [W-1]. LWR MOX fuel disposition options are discussed in detail in chapter 2. The selection of the PDR1400 reactor option is somewhat arbitrary but there is little difference between the spent MOX properties of all the LWR reactor designs. Selection of another design as the reference case would not significantly alter the results of this example comparison.

There are three potential sub-options being considered for borosilicate WGPu vitrification: vitrification with high level fission product waste (HLW), vitrification with Cesium 137 only, and a “clean glass” option.

A significant radiation barrier is established by the incorporation of HLW and ^{137}Cs . Incorporation of only ^{137}Cs rather than the host of nuclides contained in HLW simplifies recovery of the WGPu from the glass. Thus the ^{137}Cs glass can be considered more of a storage form rather than a waste form when compared to that produced by the HLW vitrification sub-option. The Russians regard the WGPu as a valuable energy resource and so are not in favor of treating it as a waste. “Clean glass” does not incorporate nuclides to create a radiation barrier. Instead, chemical spoilers are added to complicate the recovery of the WGPu without requiring costly remote processing. To be conservative, a composite of the glass logs produced by both the HLW and ^{137}Cs -only sub-options is used as the reference product. It is assumed to have a 2,000 Rem/Hr at 1 meter radiation barrier similar to that proposed for the ^{137}Cs sub-option and contain 20 w% HLW. Each log weighs 1800 Kgs and contains 20 kgs of WGPu at 1.1 w%. The spent MOX and glass are compared to a simple zirconia-plutonium dioxide-erbia ($\text{ZrO}_2\text{-PuO}_2\text{-Er}_2\text{O}_3$) non-uranium fuel.

The composition and description of the $\text{ZrO}_2\text{-PuO}_2\text{-Er}_2\text{O}_3$ non-uranium fuel can be found in chapter six and a discussion of the materials aspects of the fuel is found in chapter four. Table 3.3 lists the weight percent composition of the $\text{ZrO}_2\text{-PuO}_2\text{-Er}_2\text{O}_3$ non-uranium fuel.

Table 3.3 Example ZrO₂-PuO₂-Er₂O₃ Fuel Composition

Isotope/Element	weight percent
²³⁸ Pu	0.0003
²³⁹ Pu	2.7394
²⁴⁰ Pu	0.1701
²⁴¹ Pu	0.0068
²⁴² Pu	0.0007
²⁴¹ Am	0.0038
Er	1.3417
Zr	70.4440
O	25.2932

3.5.2 Metric Values Results. This section outlines the calculations and discusses the results of an example application of the metrics proposed in this chapter. Table 3.4 summarizes the measured/calculated raw metric values. Determination of the metric values is generally straightforward with exceptions noted in the discussion of each value. Appendix A contains detailed example calculations.

Fissile density values are higher for spent LEU and MOX because they must be discharged in a near-critical condition. The fissile density of the vitrified log is only limited by the practical constraint of the proportional cost of producing a large number of logs. The non-uranium fuel cycle proposed here drives the plutonium bearing fuel well into the subcritical region and essentially eliminating the plutonium. The result is disposition product with a very low comparative fissile density. Thus, the proliferator would have to process much more of the highly radioactive non-uranium spent fuel to recover sufficient plutonium to create an explosive.

Dissolution values are applicable to a PUREX type dissolution of the disposition matrix in nitric acid. The values listed are the solubility, in gm/liter, of the nitrate form of the matrix constituents in water: UO₂(NO₃)₂ for MOX and LEU and Zn(NO₃)₂ for

non--uranium fuel [L-2]. The dissolution metric is not applicable to borosilicate glass because the plutonium is removed via leaching rather than wholesale dissolution of the matrix. The NAS judged the chemical barriers of a vitrified log to meet the spent fuel standard. Consequently, the vitrified log will be given a dissolution metric value of 0.00 for metric scoring purposes.

Table 3.4 Raw Metric Values

Metric (units in Table 3.2)	Spent LEU	HLW Glass Log	Spent WGPu MOX	WGPu Non-U Fuel
Disposition Product Matrix Barriers				
Fissile Density	158	18.34	97.48	1.55
Dissolution	167	not applicable	167	211
Separation	40	0.12	40	0.37
Radiation Barrier	160	145	160	160 ^a
Plutonium Weapons Usability				
Isotopic	68.6%	94.5%	69.1%	10.2 %
Critical Mass	15.4	12.0	16.6	48.3
Neutron Emission	3.3×10^5	5.3×10^4	4.4×10^5	5.21×10^6
Decay Heat	10.3	2.3	14.4	10.3

a. The non-uranium radiation barrier is assumed to be the same as MOX spent fuel.

Separation metric values are based on distribution coefficients reported for the PUREX process. Values for specific ions were normalized to that of plutonium. The normalized ion coefficients are then weighted by their atom percent in the matrix of each disposition form. The listed value is the sum of the weighted normalized coefficients for each matrix composition. All of the product matrices have fission products which add some difficulty in separation of plutonium. However, PUREX is specifically designed to eliminate low fission product compositions. The slightly higher separation metric value for zirconia is a function of additional difficulty in removing higher concentrations of zirconium. The uranium ion resulting from MOX dissolution and

also found in spent LEU is significantly more difficult to separate than most of the fission products. This gives MOX a metric separation value similar to that of spent fuel which is much larger than that of the vitrified log or non-uranium fuel.

The radiation barrier for all the disposition product forms is similar to that of spent LEU. Typically, 15 year old spent LEU has a radiation barrier of 2,000 rem/hr at 1 meter from midplane of the assembly [N-2]. The radiation barrier of the vitrified log is specifically engineered to be 2,000 rem/hr at 1 meter. The radiation barrier of all these products is controlled by the long lived fission products and/or ^{137}Cs both of which have an average half life of 30 years. Consequently, the radiation barrier reduces by 50% every 30 years. Spent fuel reaches 125 rem/hr by 135 years and approximately 60 rem/hr by 165 years after discharge. The number of years to reach the IAEA self protection limit of 100 rem/hr is approximately 15 years more than that of the vitrified waste form because the vitrified glass log starts out with the same barrier as 15 year old spent fuel.

The weapons usability type barriers rely on the inherent resistance of the separated plutonium. Plutonium is not transmuted by the vitrification process; the final product glass contains WGpu. The isotopes of spent LEU, WGpu MOX and WGpu non-uranium fuels are calculated via manipulation of depletion calculation results. Critical masses are calculated for a bare pure plutonium sphere by varying the radius of the sphere until a multiplication factor of 1.00 results as calculated using MCNP.² The density of metallic plutonium is used to convert the resultant spherical volumes into critical masses. The high ^{242}Pu content and low fissile content of the non-uranium residual plutonium composition results in a critical mass nearly three times that of the other disposition products. Total neutron emissions and decay heat for the residual

² The Monte Carlo Neutron Particle (MCNP) code is described in chapter 5.

plutonium compositions are calculated by taking the sum of the weight percent weighted neutron emission rates and decay heat of each of the plutonium isotopes as listed in table 1.1. Non-uranium fuel has a very high ^{242}Pu content which produces nearly an order of magnitude increase in the neutron emission rate. However, a slightly lower ^{238}Pu content results in a slightly lower decay heat rate.

3.5.3 Metric Scoring Results. Each metric value is converted into a metric score using metric scoring function curves. Accurate establishment of metric scoring functions is beyond the scope of this work. Linear scoring functions from -1.0 to 1.0 with the spent fuel value equivalent to a metric score of zero as described in section 3.5.4 are assumed for all metrics. Since the spent fuel standard was established as the minimum acceptable performance, spent fuel's metric value scores zero by definition. Table 3.5 lists the results of converting the raw metric values into scores and Appendix A contains detailed example calculations.

All the disposition products have a lower fissile density than spent LEU resulting in only positive values. The 1.55 Kg/m³ non-uranium value is the best and so defines the upper bound of the range and equates to a 1.00 score. The difference between spent fuel and non-uranium fissile densities is 156.45 Kg/m³. Taking the inverse produces a linear slope of 6.4×10^{-3} score units/unit difference in density of the option form and spent fuel. Thus, the MOX score is $[(158.0 - 97.5) \times (6.4 \times 10^{-3})] = 0.39$. The score for the vitrified log is similarly calculated.

The dissolution metric scoring function ranges from 0 to one and 0 to -1 are based on the spent fuel metric value, thus defining boundary values of 0 and 334 gm of matrix constituent/liter of H₂O on either end of the ordinate axis. Since a lower solubility is preferable, a -1 metric score equates to the higher solubility of 334 gm of matrix constituent/liter of H₂O. This metric value range produces a linear scoring function slope

of 6×10^{-3} score units/relative difference in solubility. Since the matrix of spent fuel and LEU is the same, the solubility difference is zero and so MOX scores zero. The 211 gm Zr(NO₃)₂/liter of H₂O solubility of a zirconia matrix is larger than that for a UO₂ matrix, producing the negative metric score listed.

Table 3.5 Metric Scores

Metric	Spent LEU	HLW Glass Log	Spent WGPu MOX	WGPu Non-U Fuel
Disposition Product Matrix Barriers				
Fissile Density	0.00	0.89	0.39	1.00
Dissolution	0.00	0.00	0.00	-0.26
Separation	0.00	-1.00	0.00	-0.99
Radiation Barrier	0.00	-0.19	0.00	0.00
Plutonium Weapons Usability				
Isotopic	0.00	-0.82	-0.02	1.00
Critical Mass	0.00	-0.22	0.04	1.00
Neutron Emission	0.00	-1.00	0.10	1.00
Decay Heat	0.00	-1.00	0.51	0.00

a. The non-uranium radiation barrier is assumed to be the same as MOX spent fuel.

The 2.5×10^{-2} score units/unit difference in the separation metric value is set by the low vitrified log value. Both the non-uranium zirconia fuel and the vitrified log have significantly lower separation scores than MOX as a result of their lack of significant quantities of uranium.

There is little difference in radiation barrier metric values. The +1 score is defined as 150% of the spent fuel radiation barrier or 240 years. Likewise, the -1 score is equated to 80 years. As described above, MOX, LEU and non-uranium fuel all have approximately the same radiation barrier resulting in metric scores of 0.00. The vitrified

log's radiation barrier metric value is only 15 years less and so earns a slightly negative score.

It is worth summarizing the results of the matrix level barriers metric scores before moving to the plutonium weapons usability metrics. Although all the options exceed the spent fuel standard for fissile density, the non-uranium spent fuel clearly offers greater proliferation resistance as a result of eliminating more plutonium. The selection of 1.1 w% plutonium in the glass log is based on proposed options but is probably on the low end of loading being considered [N-2]. A lower or higher loading would produce larger and smaller fissile density respectively. The chemical barrier matrix metrics, dissolution and solubility, show that MOX meets the spent fuel standard based mainly on the properties of UO_2 . The glass and non-uranium zirconia matrix options appear less chemically resistant than the MOX. However, these numbers are the most suspect in the group because they are based on data which was not specifically derived for this application and consequently has a limited applicability. Deriving this type of data and developing more definitive metrics is a subject for later discussion in this section. Finally, as expected, all the options meet the spent fuel standard for a radiation barrier and the difference in the barrier metric scores are small. Next the plutonium weapons usability metric score function curves and results are reviewed.

The isotopic scores are calculated with a scoring function slope defined by the metric values. The 0 to 1 abscissa score range equates to ordinate spent fuel metric values of 68.6% and non-uranium fuel value of 10.17 %. The 0 to -1 ordinate range is limited by a maximum of 100% fissile plutonium. Thus, there are two different slopes: 3.18×10^{-2} from -1 to 0 and 1.71×10^{-2} from 0 to 1. Similarly, the critical mass slope from -1 to 0 is limited by a zero critical mass. The positive score slope, from 0 to 1, is set by the 48 kg non-uranium fuel critical mass.

Using a log scale, the range of metric values for neutron emissions results in a slope equal to $[1/(WNF - LEU)] = 8.3 \times 10^{-1}$. The low limit becomes $5.52 - (6.72 - 5.52) = 4.27$ which is greater than the vitrified log emission rate; hence, the vitrified log earns a score of -1. The MOX score $[(5.64 - 5.52) * 8.3 \times 10^{-1}] = 0.10$.

Finally, the decay heat scoring function ordinate range is defined by the low value of the vitrified log decay heat generation, producing a uniform slope from -1 to 0 and 0 to 1 of 0.125 score units/watt.

Summarizing the weapons usability metric score results, the strong additional proliferation resistance secured by substantial destruction of plutonium becomes apparent. The non-uranium spent fuel residual plutonium is mostly ^{242}Pu making it quite useless for nuclear explosive purposes. At the other extreme, the fact that no plutonium is transmuted shows up as a strong weakness of the vitrification option. The MOX option falls between the two as might be inferred since plutonium metrics essentially measure the degree of plutonium transmutation accomplished.

3.5.4 Barrier Type and Overall Scoring Results. Individual metric values and scores are derived above; two steps remain to determine the final ranking of the relative inherent proliferation resistance of the three disposition products. First the proliferation score of the disposition product matrix and plutonium weapons usability barriers types must be determined. Then the options must be ranked in terms of their overall proliferation resistance.

Barrier type scores are the sum of the product of the associated individual metric contributions. The contributions are determined by weighting the importance of each metric in determining the strength of the associated barrier. It is recognized that how the metrics are weighted is subject to great debate. Weighting of the metrics is heavily

dependent on the perspective of the decision maker and many different valid solutions can result. However, as stated at the outset of this section, the goal here is to provide a model for how to quantify the relative inherent proliferation resistance of candidate disposition products. This goal is distinct from calculating the definitive or absolute proliferation resistance. The viewpoint chosen here is to minimize a sub-national or terrorist threat. The weight functions (WF) and contribution of each metric assigned by the author are listed in table 3. 6. The WFs sum to 100% so that

Table 3.6 Metric Weights, Contributions and Barrier Type Scores

	WF	HLW Glass Log	Spent WGPu MOX	WGPu Non-U Fuel
Disposition Product Matrix Barriers				
Fissile Density	0.3	0.27	0.12	0.30
Dissolution	0.1	0.00	0.00	-0.03
Separation	0.1	-0.10	0.00	-0.01
Radiation Barrier	0.5	-0.09	0.00	0.00
Matrix Barrier Score		0.07	0.12	0.18
Plutonium Weapons Usability				
Isotopic	0.4	-0.33	0.006	0.40
Critical Mass	0.4	-0.09	0.014	0.40
Neutron Emission	0.1	-0.10	0.00	0.10
Decay Heat	0.1	-0.10	0.051	0.00
Usability Barrier Score		-0.62	0.07	0.90

the product matrix and plutonium weapons usability barrier types both have an equal total weight of 1. Although the chemical barriers can slow down a proliferator, the fissile density and radiation barriers are considered of greater importance than the chemical metrics. Given an aggressive enough acid and temperature any plutonium host matrix can be dissolved and the unique multiple oxidation states of plutonium facilitate

its separation from all other ions. The NAS estimates that any group possessing the sophistication required to build a nuclear device would also possess the necessary chemical expertise to overcome any chemical barrier that could be engineered into the clean glass option [N-2]. The radiation barrier is considered the primary barrier to spent LEU fuel plutonium recovery. Thus, it is given slightly heavier weighting over the fissile density. Similar primary and secondary weighting of the plutonium weapons usability metrics is also adopted.

A nuclear explosion cannot take place unless the isotopic and critical mass barriers have been overcome. In contrast, neutron emission and decay heat barriers can make weapon design more difficult; they can not prevent detonation. For example, neutron emissions simply reduce the likely yield of a nuclear explosive. However as stated in chapter 1, even a low yield in the range of one kiloton is a substantial terrorist threat. Assembling the weapon just prior to detonation would circumvent decay heat considerations. Thus, the critical mass and the isotopic barriers are more heavily weighted than decay heat and neutron emission barriers.

The metric contributions are the product of the weighting function and the metric score. These contributions are summed to provide total barrier type scores. In turn these barrier type scores are added to quantify the overall relative proliferation resistance of each of the three disposition products. A disposition product which exactly met the spent fuel standard would have an overall score of 0.00. The disposition products are then ranked in order of decreasing total score. These ranking are listed in table 3.7. The top scoring product is ranked number 1 and is the most inherently proliferation resistant product while the lowest scoring product is ranked number 3 and is the least inherently proliferation resistant product. As a result of the enhanced plutonium weapons usability barrier, the non-uranium spent fuel provides significantly superior proliferation resistance. The MOX spent fuel provides the next best performance

and scores slightly above the spent fuel standard (as the reader will recall, the spent fuel standard equates to a score of 0.00). The vitrified waste form is the least proliferation resistant product because of the low barrier to use of the separated plutonium which remains weapons grade. This substandard performance of the vitrified waste form is based on the assumption that both the matrix level and plutonium usability barriers are of equal merit. However, the matrix level barriers would have to be considered approximately 8 times more important than the plutonium usability barrier (an unlikely consideration) for the vitrified waste form to meet the spent fuel standard.

Table 3.7 Final Scores and Ranking of Products

	HLW Glass Log	Spent WGPu MOX	WGPu Non-U Fuel
Matrix Barrier Score	0.074	0.12	0.18
Weapons Usability Score	-0.62	0.07	0.90
Overall Score	-0.55	0.19	1.08
Ranking	3	2	1

3.6 Summary and Conclusions. NAS metrics include all aspects of the disposition process. Thus, they include implementation, policy and economic based risk considerations of specific proposals. However, a subset of metrics quantifying only those barriers to proliferation which are a function of the properties of the final disposition product forms can be defined. These barriers are inherent in the disposition product and so remain even if the proliferator is given access to the plutonium. Thus, the inherent barriers are the most reliable. The set of metrics proposed quantify the proliferation resistance independent of non-technical considerations. Thus, they can be used to determine how plutonium disposition options can be improved to reduce the risk of proliferation. These metrics can be objectively defined based on measurable properties. However, quantifying the inherent relative proliferation resistance of plutonium disposition products requires assumptions and judgments. Specifically, the

weighting of the importance individual metrics make to the cumulative proliferation resistance is heavily subject to the viewpoint of the evaluator. The viewpoint chosen here is minimization of the threat from a sub-national/terrorist type threat. In addition, the view is inclusive of all plutonium , WGPu and RGPu, and so credit is given for proliferation resistance achieved beyond the spent fuel standard. The spent fuel standard is used as the minimum threshold of proliferation resistance so that performance below that provided by spent fuel is penalized. The requirement for inclusive judgments and policy type decisions necessarily dictates that the scheme outlined above can only be a starting point for discussion.

The results of the application of the proposed metrics and evaluation algorithm are as follows. Although all the options exceed the spent fuel standard for fissile density, the non-uranium spent fuel clearly offers greater proliferation resistance as a result of eliminating more plutonium. The selection of 1.1 w% plutonium in the glass log is based on proposed options but is probably on the low end of loadings being considered [N-2]. A lower or higher loading would produce larger and smaller fissile density respectively. The chemical barrier matrix metrics, dissolution and solubility, show that MOX meets the spent fuel standard based mainly on the properties of UO₂. The glass and non-uranium zirconia matrix options appear less chemically resistant than the MOX. However, these numbers are the most suspect in the group because they are based on data which was not specifically derived for this application and consequently has a limited applicability. Finally, as expected, all the options meet the spent fuel standard for a radiation barrier and the differences in the barrier metric scores are small.

The advantages of near complete elimination of plutonium in the non-uranium fuel substantially enhances the plutonium weapons usability barrier. The non-uranium spent fuel residual plutonium is mostly ²⁴²Pu making it quite useless for nuclear explosive purposes. On the other extreme, the fact that no plutonium is transmuted shows up as a

strong weakness of the vitrification option. The MOX option falls between the two as might be expected since plutonium metrics essentially measure the degree of plutonium transmutation accomplished.

As a result of the enhanced plutonium weapons usability barrier, the non-uranium spent fuel provides significantly superior proliferation resistance. The MOX spent fuel provides the next best performance but scores only slightly above the spent fuel standard. The vitrified waste form is the least proliferation resistant product because of the low barrier to use of the separated plutonium, which remains weapons grade. This substandard performance of the vitrified waste form is based the assumption that both the matrix level and plutonium usability barriers are of equal merit. However, the matrix level barriers would have to be considered approximately 8 times more important than the plutonium usability barrier (which appears unlikely), for the vitrified waste form to score overall as well as the spent fuel standard. Chapter four examines the selection of a non-uranium fuel of the type identified here as the preferred alternative.

CHAPTER FOUR: NON-URANIUM PLUTONIUM FUELS

Reduction of the world's stockpile of plutonium will reduce the risk of proliferation relative to a subnational threat. This work proposes to eliminate plutonium by loading it in non-uranium fuel and burning it in a PWR radial blanket. Chapter 2 examined the WGPu options being considered and presented the qualitative logic behind selection of PWRs and non-uranium fuels as the preferred alternative for plutonium elimination. Specifically, non-uranium fuel can destroy plutonium more efficiently than MOX fuels. The metrics in Chapter 3 reinforce these ideas with quantitative measures of the relative risk reduction achievable with the proposed elimination option. This chapter focuses on the particulars of the non-uranium fuel suggested for use in the peripheral assembly elimination option proposed here. To be of practical use, such a non-uranium fuel must meet two sets of performance criteria: acceptable in core neutronic and thermo-physical performance. The fuel's overall performance must support its integration into the current LWR fuel cycle with the minimum perturbation possible. Neutronic considerations include radial power peaking, reactivity vs burnup profiles and depletion cycle composition. Thermo-physical performance must be as good or better than UO₂ in terms of thermal, physical and mechanical integrity over the fuel cycle. A large fuel development and qualification program will be required before the recommended plutonium elimination option could be implemented. The purpose of this chapter is to consider the possible fuel matrix designs and requirements

First, the design variables available for consideration are reviewed. Then the material and neutronic considerations of non-uranium fuels are examined. A survey of candidate non-uranium fuels and their relative advantages and disadvantages is presented. A selection process is presented which leads to the recommendation of specific non-uranium fuels for development. Finally, fabrication methods are considered.

4.1 Introduction

There are many variables which determine fuel performance and the degree of proliferation enhancement achieved. This section lists and discusses these variables. First it is important to identify the characteristics of the ideal plutonium eliminating fuel and cycle.

4.1.1 The Ideal Pu Burning Fuel Cycle. The ideal fuel and fuel cycle combination for plutonium burning would have a high burnup capability resulting in a spent fuel with a negligible plutonium content. Residual plutonium would be comprised primarily of non-fissile isotopes. The fuel should be compatible with both existing and advanced LWRs in order to increase the potential maximum rate of plutonium destruction. A high degree of safety and reliability in service are required for the cycle to be accepted by the commercial industry. In addition, fabrication of the Pu burning fuel should not be significantly more difficult or costly than current fuels if the cycle is to be economically viable. Finally, the spent fuel should be acceptable for geologic disposal without need of further processing. Section 4.1.2 presents the design variables which can be manipulated to achieve this ideal.

4.1.2 Design Variables and Assumptions. Fuel geometry, composition and cycle variables determine performance. Table 4.1 lists these design variables and summarizes the considerations and advantages that can be realized with the appropriate manipulation of each.

The geometry of the fuel assembly can be altered to manipulate the degree of moderation of the fuel. This together with the clad thickness, fuel rod diameter and the fuel

rod pitch can be varied to adjust the magnitude and sign of the isothermal moderator temperature coefficient. Over-moderation produces a more positive (less negative) isothermal moderator temperature coefficient. Increasing the fuel rod diameter, reducing the rod pitch or increasing the cladding thickness will increase the metal to water ratio thereby reducing the degree of moderation. Decreasing the degree of moderation can also be used to shift the neutron spectrum upwards and reduce the reactivity of the plutonium.

The desired plutonium destruction and neutronic characteristics can be achieved with or without altering assembly geometry. However, altering the geometry has thermal-hydraulic implications. Since the least impact possible on existing PWR systems is desired, no changes in geometry are proposed here: the lattice of choice is the widely used Westinghouse 17 x 17 assembly with the dimensions listed in table 4.2.

Composition determines the neutronic, mechanical and thermal properties of the fuel. The composition of both the cladding and the fuel meat itself can be manipulated to achieve acceptable overall performance. Fertile materials can be used to hold down excess reactivity and to produce fissile material. Fissile nuclide production adds positive reactivity as a function of burnup, thereby extending achievable cycle length. Using thorium (Th) to produce ^{233}U may be of particular interest in the development of non-uranium fuels. Unlike ^{239}Pu , ^{233}U can be denatured by adding a small amount of ^{238}U to prevent creating a source of pure ^{233}U .

The type and distribution of burnable poisons can be selected to tailor the reactivity profile of the fuel over core life, the prompt fuel temperature coefficient (FTC) and isothermal moderator temperature coefficient (MTC) and the residual plutonium content. Burnable poison selection was examined and is discussed at length in section 4.3.4. Burnable poisons (BPs) can be homogeneously distributed in the fuel, heterogeneously lumped in fueled or unfueled rod locations or used as a surface coating on fuel. Homogeneous BPs provide a larger negative reactivity insertion per unit of poison than lumped burnable poisons. Consequently, burnout is quicker than for lumped BPs. Homogeneous distribution requires that the BP be compatible with the fuel matrix.

Table 4.1 Assembly/Core Design Variables

Variable	Options	Advantages & Considerations
Geometry Variables		
Rod Pitch	tight pitch	increase epithermal flux => 1. more $^{239}\text{Pu}(n,2n)^{238}\text{Pu}$; 2. more ^{238}U and ^{232}Th capture => inc. conversion 3. lower $\Sigma_f^{239\text{Pu}}$ => inc. loading
Rod Pitch	increase pitch	=> higher flux => more complete Pu burnup
Rod Diameter	increase	=> reduce mod/fuel ratio => more negative MTC
Cladding	thicker	=> allow for high burnup water side corrosion => reduce mod/fuel ratio => more negative MTC
Annular Fuel	use it	=> accommodate high burnup fission prod. gases => reduce peak centerline temperature
Rod Plenum	increase	=> accommodate high burnup FP gases
Burnable Poisons	homogeneous	=> greater BOL reactivity hold down
Burnable Poisons	lumped	=> slower poison burnout
Burnable Poisons	IFBA ^a	=> compromise between lumped and homogeneous
Composition		
Fertile Nuclide Concentrations	^{238}U , ^{232}Th mixture	=> manipulate resonance integral => vary slope of reactivity vs burnup curve
Pu Analogs/ Recovery Spoilers	Th, Ce, Ru, Ti, Zr, Pr, Hf, Np	=> make recovery of pure Pu from the fuel more difficult
Burnable Poisons	B, Dy, Ho, Gd, Er, Hf & Eu.	=> negative contribution to temperature coefficients
Cladding	Zr w/Hf alloy	=> increase hold down reactivity
Cladding	Stainless Steel	=> increase parasitic losses
Cladding	Zirlo/Duplex	=> better durability for increased burnup
Cycle		
Pu Assembly Location	Peripheral	=> lower power density => reduced impact on core physics parameters

a. Integral Fuel Burnable Absorber

Lumped BPs are self shielded and so burn out slower, providing a more constant positive reactivity insertion rate per unit burnup. Integrated Fuel Burnable Absorbers (IFBA) are a

coating of BP on the fuel. IFBAs have the advantage of not requiring incorporation in the fuel matrix and without the need to displace that pin in the assembly. However, unlike lumped or IFBA poison distribution schemes, homogeneous poisons require chemical processing to remove them. This enhances the proliferation resistance of the fuel. In the present work, the desired neutronic performance was achievable without the need for non-homogeneous burnable poisons. Consequently, neither lumped nor IFBA distributions were given further consideration.

Table 4.2 Assembly Geometry

Rod Outside Diameter (cm)	0.950
Diametral Gap (cm)	0.0165
Clad Thickness (cm)	0.0572
Rod Pitch (cm)	1.26
Number UO ₂ Rods per Assembly	264
Square Assembly Width (cm)	21.40

The cycle length and the number of batches used determine the required fissile fuel loading in reload fuel. The goal of this work was to integrate non-uranium plutonium fuel into typical PWR fuel cycles. Consequently, the standard industry practice of a three batch core with an 18 month cycle length was assumed.

Fuel composition is the primary variable which determines fuel performance and is the subject of the remainder of this chapter. The required material performance must be established to provide a background for selection of the appropriate material composition.

4.2 Required Material Properties

This section derives fuel performance requirements. First, the general PWR fuel limit requirements are adopted. These general requirements are then translated into specific minimum acceptable fuel properties based on corresponding UO₂ characteristics.

4.2.1 Basis for Fuel Performance Requirements. A fuel's thermal and mechanical properties enable it to perform satisfactorily. Satisfactory performance can be defined as the maintenance of cladding integrity without the need for a reduction in reactor plant operational status. Transient and steady state design limits are designed to ensure that cladding integrity is maintained. PWR fuel must fulfill the requirements listed in table 4.3 to be deemed satisfactory. The presence of non-uranium fuel in the core should not impose any additional operational or transient restrictions beyond those which normally apply to a standard PWR core. Non-uranium fuel assemblies comprise approximately 25% of the PWR core in a peripheral loading scheme. Consequently, as long as the fuel performs at least as well as standard UO₂ no additional restrictions should be required. Thus, UO₂ characteristics are used as the baseline minimum performance standards. Furthermore, these general criteria can be translated into specific property values that must be better than or equal to those of UO₂ as listed in table 4.4 [T-1]. UO₂ fuel integrity under transient and normal operating conditions is ensured by meeting two design criteria: no incipient melting of the fuel under steady state or transient conditions and a maximum allowable cladding strain of less than 1%. These criteria establish the minimum performance standards for UO₂ fuel in PWRs.

Table 4.3 General Fuel Performance Requirements

Requirement	Operating Conditions	Accident Conditions
Chemical Stability	- compatible with cladding at temperature	- no autocatalytic exothermic reactions with H ₂ O or Air at temperatures less than 1200 °C
Irradiation Stability	- no degradation of properties below limits over expected residence time, fluence - swelling less than UO ₂	- no significant release of energy stored in crystalline lattice
Thermal Conductivity	- greater than that of UO ₂ over service life	- not degraded below that of UO ₂ for peak temperatures or transient temperatures
Specific Heat	- no specific requirement	- comparable to or less than UO ₂
Thermal Stress Resistance	- no specific requirement	- comparable to or better than UO ₂

Table 4.4 Reference UO₂ Properties

Fresh Fuel Property	Value	Associated Design Limit(s)
Thermal Conductivity (200-1000 °C)	3.6 W/m-°C	Steady State and Transient Fuel Peak Centerline Temperature - no incipient melt
Melting point	2800 °C	Steady State and Transient Fuel Peak Centerline Temperature - no incipient melt
Specific Heat @ 100 °C	247 J/Kg-°C	Transient Peak Centerline Temperature - no incipient melt
Linear Expansion Coefficient (400-1400 °C)	1.01E-5 1/°C	< 1% clad strain
Stability Range	no phase change from 20 °C up to melting point	< 1% clad strain
Theoretical density	10.97 gm/cm ³	- minimum porosity for swelling

UO₂ fuel design criteria require no melting of the fuel under transient or steady state conditions. Thus, the peak fuel temperature must be below the melting point of the fuel. The melting point, thermal conductivity, specific heat and power density establish the allowable

steady state temperature profile in the fuel. The specific heat determines the amount of stored energy in the fuel at steady state conditions. The specific heat also determines the amount of energy which can be stored in a transient without exceeding the peak centerline temperature. The linear expansion coefficient and stability range address changes in fuel volume with temperature. Phase changes can lead to fuel expansion, cladding strain and subsequent failure. Thus, a limit of less than 1% cladding strain is established. The crystalline structure of oxide fuels must be stable over the temperature and fluence range expected in a PWR. UO_2 has a fluorite face-centered cubic crystalline structure which is thermally and structurally stable. The fluorite structure is somewhat unique in that it has a large number of vacant sites. This allows UO_2 to incorporate a significant percentage of fission products without alteration of its structure [K-2]. Similar performance is required of a viable non-uranium plutonium fuel. Specific performance criteria can be developed to directly compare key thermo-physical properties.

4.2.2 Thermal Performance Criteria. The non-uranium ceramic material which will incorporate the plutonium and absorber atoms must possess thermo-physical properties which give it in-service performance as good or better than UO_2 . It is therefore worthwhile to develop a set of metrics, based on the discussion above, to compare properties of potential plutonium fuel ceramics to UO_2 . Thermal performance is defined by the licensing and design limits imposed on fuel. Three performance areas are of specific interest: thermal margin to melting, transient time constant for quenching, and stored energy.

1. **Thermal Margin to Melting**: Let T_{CL} , T_{MP} be the normal operating centerline temperature and the ceramic melting point respectively. Figure 4.1 illustrates the relationship of these temperatures:

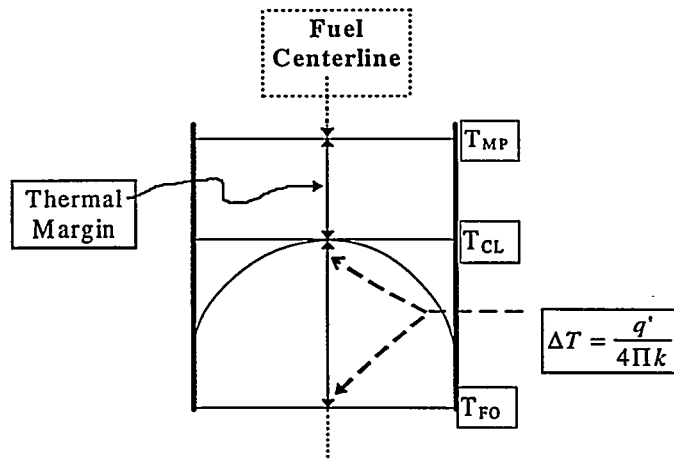


Figure 4.1 Fuel Temperature Profile

ΔT is the difference between fuel outside edge temperature, T_{FO} , and T_{CL} . ΔT is therefore equal to the linear heat generation rate, q' , divided by the product of the thermal conductivity of the material, k , and 4π . The relative thermal margin to melting can be calculated by the following expression:

$$M \text{ margin} = \frac{T_{MP} - \Delta T}{T_{MP}} = 1 - \frac{q'}{4\pi k T_{MP}} \quad (4.1)$$

Thus, for the same q' a material with a larger value of kT_{MP} will have a larger thermal margin to melting.

2. Stored Energy. Stored energy must be removed via emergency cooling systems in the event of a Loss of Coolant Accident, LOCA. The more energy stored in the fuel during normal operations the greater the heat load on cooling systems. The stored energy, E_s , is approximately equal to the product of the heat capacity, c_p , the density, ρ , and the average fuel temperature $\overline{\Delta T} = 1/2(\Delta T)$:

$$E_s \approx \rho c_p \overline{\Delta T} = \frac{q' \rho c_p}{8 \pi k} \quad (4.2)$$

In this expression, one recognizes the thermal diffusivity parameter α as:

$$\alpha \equiv \frac{k}{\rho c_p} . \quad (4.3)$$

Thus, ceramic material α values can be used as a comparison metric. A larger value of α is preferable from a stored energy consideration.

3. Transient Time Constant. The transient time constant characterizes the rate of decay of the fundamental mode during quenching. It is determined by the thermal diffusivity, α , in expressions of the form:

$$P = P_o e^{-\alpha \lambda^2 t} \quad (4.4)$$

Table 4.5 summarizes the above considerations. The ratio of the metric values to that of UO_2 must exceed or equal 1.0 to ensure adequate performance. Section 4.6.4 applies these performance criteria to the recommended fuels matrices identified and described in the intervening sections. It is important to note that the thermal conductivity is a strong function of crystalline structure, purity, fluence and temperature and quoted values vary considerably in the literature. Thus, the values presented are more illustrative of potential performance and must be confirmed as part of the fuel development and testing program.

Table 4.5 Summary of Proposed Thermo-physical Performance Criteria

Thermal Limit or Consideration	Performance Constraint	Metric	Metric Value New Matrix
			Metric Value UO_2
No Fuel Melt	- normal operating thermal margin to melting	kT_{MP}	≥ 1.0
LOCA Performance	- maximum allowable stored energy	α	≥ 1.0

The steady state and transient power density plays a large role in determining the ability of a given set of fuel properties to perform satisfactorily. The power density is in turn determined by the neutronic characteristics of the fuel relative to the fuel around it. Thus it is critical to

understand the neutronic differences between standard UO_2 fuel and non-uranium plutonium fuels.

4.3 Non-Uranium Plutonium Fuel Neutronic Considerations

Plutonium's neutronic properties differ significantly from those of uranium. Although plutonium is the source of 30-50% of the power in UO_2 fuel at the end of a conventional LWR cycle, non-uranium fuel derives nearly all of its power from ^{239}Pu fissions and has a much higher plutonium atom density than end of life UO_2 fuel. This presents some problems at the interface between Pu and UO_2 assemblies. In addition, the absence of ^{238}U in non-uranium Pu fuels necessitates that a substitute diluent must be employed.

4.3.1 ^{239}Pu Compared With ^{235}U . The use of ^{239}Pu instead of ^{235}U as a fissile power source presents several challenges. Table 4.6 lists the cross section properties for key fissile and fertile nuclides. ^{239}Pu has significantly larger thermal absorption, fission and absorption to fission cross section ratio, resulting in a hardening of the neutron spectrum relative to ^{235}U fuel. Consequently, burnable absorber and control rod worths and shutdown margins are reduced. Also, ^{239}Pu atom density must be higher than ^{235}U in UO_2 to achieve the same reactivity. Uniform Pu assembly enrichment can produce unacceptably large power peaking factors at the interface between UO_2 and Pu assemblies. The thermal flux is suppressed at the edge of the Pu assembly. The pins on the interface between the UO_2 and Pu assemblies experience a much larger thermal flux than the more interior pins resulting in unacceptably high power peaking. Thus, the pins at the edge of the assembly would require a reduction in their fissile loading relative to the interior pins. Alternatively, a low fissile density may be used throughout the Pu assembly with an appropriate BP loading to hold down excess reactivity at the interface.

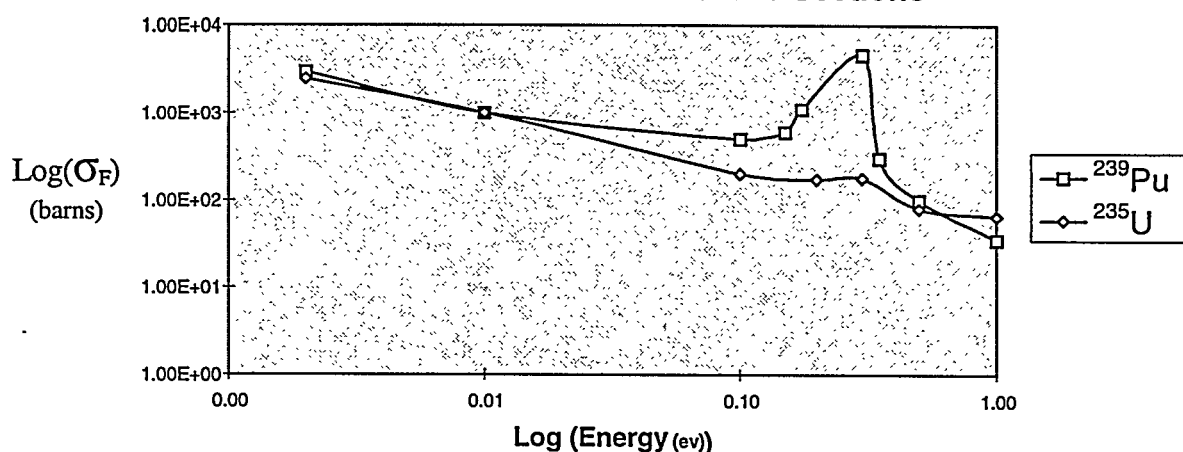
Table 4.6 Cross Sections of Key Fuel Cycle Nuclides (barns)							
	^{232}Th	^{233}U	^{235}U	^{238}U	^{239}Pu	^{240}Pu	^{241}Pu
Thermal ¹							
σ_a	7.4	571	678	2.7	1013	290	1368
σ_c	7.4	46	101	2.7	271	0.06	368
$\sigma_f (\eta)$	1E-6	525 (2.3)	577 (2.1)	5E-6	742 (2.1)	290	1007
Resonance Integral ²							
RI _a	86	884	380	274	445	8493	697
RI _c	85.2	135	130	272	169	8484	116
RI _f	0.58	748	250	1E-03	277	9	581
Notes:							
1. Thermal cross sections are evaluated at 2200 m/s or 0.025ev.							
2. Resonance Integrals are for infinitely dilute conditions.							

A less troublesome consideration is that ^{239}Pu also has 1/3 the delayed neutron fraction of ^{235}U , reducing the reactor reactivity response time and thus the margin for reactor control. Fortunately, studies indicate that the control systems in place have sufficient response margins to accommodate plutonium fueled reactor transients. [N-2]. Peripheral location and lower than average power will also reduce the worth of the subject plutonium fuel as discussed in chapter 5.

Figure 4.2 sketches the fission cross section versus energy profile for ^{239}Pu and ^{235}U on a log-log scale. At 0.01 ev both ^{239}Pu and ^{235}U have (approximately) a thermal fission cross section of 1,000 barns but ^{239}Pu 's only drops to 500 barns at 0.1 ev as compared to 200 barns for ^{235}U . In addition, ^{239}Pu has a nearly 5000 barn fission cross section peak at approximately 0.3 ev. The ^{239}Pu resonance absorption region has both capture and fission reaction components. Any negative prompt feedback provided by capture resonance broadening is offset by increased fission absorptions. Also, an increase in moderator temperature leads to an upshift in the neutron spectrum into a region where $1/v$ control absorbers are less effective. Moreover, the ^{239}Pu fission cross section is still relatively high in the slightly epithermal region and has that 5000 barn peak at 0.3 ev. Thus, there can be a net increase in reactivity in under-moderated

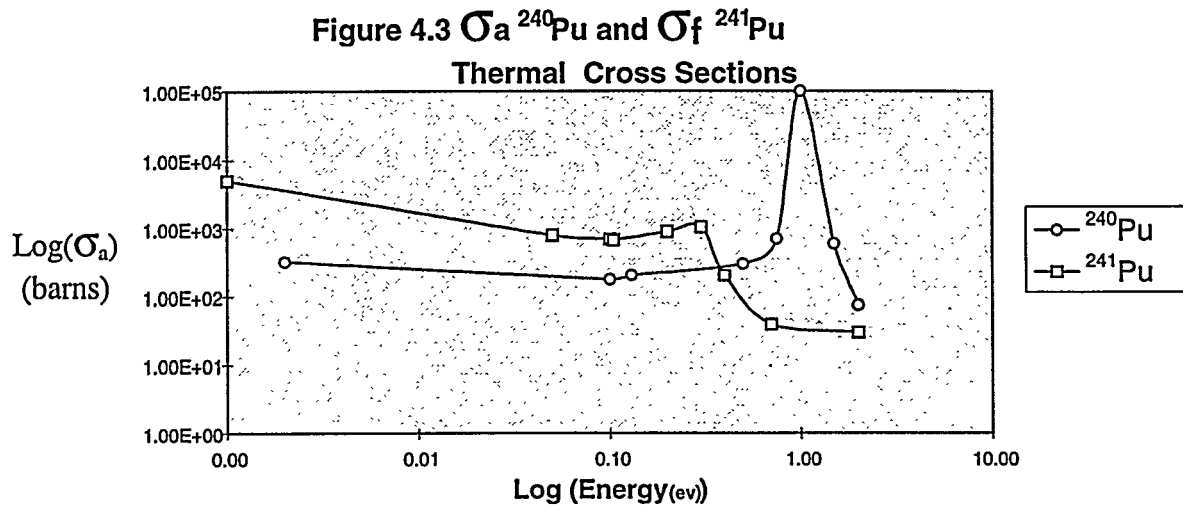
system conditions leading to a less negative or positive isothermal temperature coefficient. ^{239}Pu tends to have less negative prompt fuel and isothermal temperature coefficients compared to ^{235}U enriched UO_2 fuels. Thus, greater non-fissile resonance absorption is required to offset this undesirable effect. ^{238}U is the major resonance absorber in UO_2 fuels but is absent in non-uranium Pu fuels. The presence of ^{240}Pu compensates in RGPu; however, WGPu is > 93 w% ^{239}Pu . Thus, burnable poisons are required for non-fertile WGPu fuels.

Figure 4.2 Comparison of ^{239}Pu and ^{235}U Thermal Fission Cross Sections



4.3.2 Effect of ^{240}Pu & ^{241}Pu Content. ^{240}Pu is both a resonance absorber and thermal poison. Figure 4.3 shows the absorption cross section profile for ^{240}Pu . Its absorption cross section follows a $1/v$ profile from 300 barns at 0.02 eV to 100 barns at 0.3 eV. Thus, it provides some hold down reactivity but the effect is small. Sterbenz et al. [S-1] investigated the effects of variable ^{240}Pu content in a $\text{PuO}_2\text{-ZrO}_2$ fuel. They reported that for a fixed BOL reactivity, an increase from 4w% to 18w% ^{240}Pu loading only increased the allowable loading of plutonium from 7.8 to 11.0 grams. However, the resonance absorption was found to significantly improve the prompt fuel temperature coefficient (FTC). At 4w% ^{240}Pu the FTC was 0.0528 to 0.00 pcm^0K from 600 to 1100 ^0K and -0.167 pcm^0K from 1600-2400 ^0K . At 18w% the FTC improved to a small but negative value of -0.244 to -0.186 pcm^0K over the entire temperature range from 600-2400 ^0K . Only a very slight improvement in the isothermal moderator

temperature coefficient (MTC) from 15 to 10 pcm^0K was noted. The main effect of increasing the ^{240}Pu content is to provide some resonance absorption which helps to make the FTC more negative. This can reduce the required loading of resonance absorbing BPs when burning RGPU which has approximately 24w% ^{240}Pu .



^{241}Pu has even larger fission and absorption cross sections than ^{239}Pu . Consequently, a RGPU in a non-fertile matrix has a less negative reactivity versus burnup slope than comparably loaded WGpu non-fertile fuel. The higher initial content of ^{240}Pu in RGPU results in higher production of ^{241}Pu which mitigates reactivity loss with burnup. Thus, WGpu presents greater neutronic challenges than does RGPU; consequently, modeling and depletion calculations were done using WGpu loaded non-uranium fuel.

4.3.3 Special Considerations for Non-Uranium Fuels. In non-uranium fuel, alternatives must be found to perform the physical and neutronic functions that ^{238}U serves in UO_2 fuel. ^{238}U is the major actinide constituent in the UO_2 pellet which forms the physical matrix of the fuel. A substitute matrix must have comparable thermal and mechanical properties. ^{238}U acts as an neutron absorber to hold down the excess reactivity at the start of a cycle. This allows greater fissile loading and a longer fuel cycle. ^{238}U also helps extends the cycle in MOX fuels by producing additional ^{239}Pu to mitigate the rate of fissile depletion. In addition to these functions, ^{238}U is a resonance absorber with peaks in excess of 5000 barns at ~ 7, 11, and 13 eV. A substitute resonance absorber is required in non-uranium fuels to provide the negative

Doppler reactivity contribution normally provided by the ^{238}U in MOX fuels. Burnable poisons or thorium can be used to provide these functions.

Table 4.7 is a summary comparison of the nuclear design characteristics for a reactor loaded with non-uranium plutonium without poison or fertile material fuel as compared to the same reactor loaded with standard UO_2 fuel with the same BOL reactivity and burned at the same power density to EOL.

Table 4.7 Comparison of Non-Uranium Plutonium and Standard Uranium Fuel Nuclear Design Characteristics

Parameter	Plutonium Core	Reason for Difference	Potential Consequence
Isothermal Moderator Temperature Coefficient (MTC)	1. WGPu compositions are much less negative 2. RGPU compositions are slightly less negative	1. Reduced resonance absorption plus spectral shift 2. Same as above but with increased ^{240}Pu resonance absorptions	1. Unacceptable Transient Behavior 2. Unacceptable Transient Behavior
Prompt Fuel Temperature Coefficient (FTC)	1. WGPu compositions are much less negative 2. RGPU compositions are slightly less negative	1. Reduced resonance absorption 2. same as above but with increased ^{240}Pu resonance absorptions	1. Unacceptable Transient Behavior 2. Unacceptable Transient Behavior
Cold to Hot Reactivity Swing	Reduced	Less Negative MTC	Reduced cold boron requirements
Installed Reactivity	Reduced	Lower allowable fissile loading	Shorter cycle length
Control Rod Worth	Reduced	More epithermal flux	Possible increase in number of rods
Boron Worth	Reduced	More epithermal flux	Increased Boron requirements
Xenon Worth	Reduced	More epithermal flux	Improved stability
Fission Product Poisons	Increased	Increased Yields	Reactivity penalty - shorter cycle
Local Power Peaking	Increased	Increased water worth	More complex fuel management
Delayed Neutron fraction	Reduced	$\beta_{\text{Pu}} < \beta_{\text{U}}$	Unacceptable Transient Behavior

The differences which can not be accommodated within safety margins must be compensated for through the manipulation of fuel design and/or plutonium fuel loading strategies.

4.3.4 Use of Burnable Poisons. Burnable poisons are one potential fuel design solution to compensate for the potentially unacceptable nuclear design characteristics of non-uranium plutonium fuels. Burnable poisons (BP) are used to serve three purposes: to provide beginning of cycle (BOC) excess reactivity control allowing increased fissile loading, to shape the reactivity vs. burnup curve over the cycle, and to provide negative contributions to FTC and MTC through resonance absorption. There are two disadvantages of burnable poisons: unavoidably diminished neutron economy and the potential shortening of the cycle due to residual negative reactivity at the end of the cycle (EOC). The second disadvantage can be minimized by using a (monoisotopic) BP with a large thermal capture cross section. Such a BP can provide maximum BOL excess reactivity control with a minimum number density and will burn out faster, leaving less residual negative reactivity at the EOC. However if the thermal cross section is too large, the poison burns out too quickly causing an unacceptably high excess reactivity peak early in the cycle. A BP with a thermal cross section slightly larger than the fissile nuclide is ideal. When the fissile nuclide depletion rate is slightly less than the total combined BP depletion, the rate of the net loss of reactivity can be slowed.

This description of BP control can be quantified as follows:

Starting from the basic depletion equation:

$$\frac{\partial N}{\partial T} = -\Sigma \Phi \quad (4.5)$$

and assuming that $\frac{\Phi_{BP}}{\Phi_{235U}} = 1$, it can be shown that:

$$\left[\left[\frac{[BP]_t}{[BP]_0} \right] = \left\{ \frac{[F]_t}{[F]_0} \right\} \frac{\sigma_a^{BP}}{\sigma_a^F} \right] \quad (4.6)$$

where $[F]$ is the fissile nuclide density and $[BP]$ is the burnable poison concentration..

Generally, 1/3 of the initial fissile load is necessary just to produce criticality at time $t =$ end of cycle:

$$\frac{[F]_t}{[F]_0} = \frac{1}{3} \quad (4.7)$$

Therefore, if the end of life burnable poison concentration is to be less than 10% of the initially loaded density, then:

$$\frac{\sigma_{a \text{ thermal}}^{BP}}{\sigma_{a \text{ thermal}}^F} \geq 2.5 \quad (4.8)$$

This provides a rough yardstick for measuring the relative acceptability of a given nuclide as a burnable poison.

Table 4.8 alphabetically lists all nuclides with a thermal absorption cross section of greater than 1000 barns or a resonance integral greater than 2000 barns. These cross sections are also ratioed to the corresponding ^{239}Pu thermal and resonance cross sections. The ^{239}Pu thermal and resonance ratio values for those BPs anticipated to have an end of cycle residual density of less than 10% of the initial loading are listed in bold face and highlighted in the last two columns of table 4.7.

A BP resonance cross section which overlaps the 0.3 ev ^{239}Pu cross section is preferable for inserting a negative contribution to FTC in the non-uranium plutonium fuels. In addition, a flatter cross section profile through the thermal energy range, approximately 0-1 ev, can produce a more negative contribution to MTC. Thus, the BP/ ^{239}Pu resonance ratio, the energy of the resonance and the slope of the cross section profile are all contributory factors. Thus, the cross section vs. energy profiles of these poisons can be reviewed to determine their suitability.

Table 4.8 Candidate Burnable Poison Cross Sections & Ratios

BP	% Abundance	Obs.	Res. int.	^{239}Pu ratio	^{239}Pu res. ratio
Dy161	18.9	581	1100	0.57	2.20
Dy162	25.5	180	2800	0.18	5.60
Dy163	24.9	130	1600	0.13	3.20
Dy164	28.2	2700	340	2.64	0.68
Er167	23	670	3000	0.66	6.00
Eu151	47.8	9204	5800	9.01	11.60
Eu153	52.2	350	150	0.34	0.30
Gd155	14.8	61000	1540	59.75	3.08
Gd157	15.7	255000	800	249.76	1.6
Ho165	100	64.5	710	0.06	1.42
Sm149	13.8	4000	3100	3.92	6.20
Sm152	26.7	208	3000	0.20	6.00

Notes:

1. All values are listed in barns
2. Res. Int. = Resonance Integral
3. Ratios are absorption or resonance integral divided by the ^{239}Pu
4. Res. Int. are for infinitely dilute conditions.
5. Thermal cross sections are evaluated at 2200 m/s.

Samarium (Sm) and Holmium (Ho) have large cross sections but can be eliminated for the following reasons. Sm's cross section drops off sharply in the energy range from 1700 barns to < 100 barns from 0.1 to 0.5 ev. Ho has approximately 5000 barn resonance peaks at 4 and 10.5 ev, respectively, but has a strongly negative linear slope from 1000 barns at 2.0E-4 ev to < 10 barns at 1.0 ev. In addition, Ho is one of the least abundant of the lanthanides.

Four burnable poisons stand out as most promising: Gadolinium (Gd), Europium (Eu), Erbium (Er) and Dysprosium (Dy). Gadolinium has a sharply decreasing total cross section of 500,000 barns at 0.0001 ev to 9000 barns at 0.1 ev with resonance peaks of 200 and 1700 barns at 1.1 and 1.15 ev, respectively. Gd's cross section is roughly 1/v from 0.1 to 1 ev and is 600 barns at 0.3 ev. The seven sequential isotopes in the Gd chain lead to some replenishment of the 155 and 157 isotopes. This reduces the rate at which it burns out (but also increases the

end of life residual poison). The major advantage of Gd is that it has a huge thermal cross section which provides superior BOL excess reactivity hold down at low loading. Europium has a very large cross section and its resonance peaks at 0.321 ev and 0.461 ev provide excellent overlap of the ^{239}Pu resonance peak. However, the slope of the cross section through the thermal range is only slightly shallower than Gd. Europium can provide a strong negative contribution to FTC. Erbium has a smaller but flat thermal cross section tail from approximately 1000 barns at 0.004 ev to 125 barns at 0.1 ev and so will require a greater loading than Gd or Eu to achieve the same excess reactivity effect. However, its resonance peaks of 200 and 1500 barns at 0.460 and 0.584 ev, respectively, provide a significant negative contribution to FTC and MTC. Er's flat thermal cross section tail at low thermal energies make it ideal for inhibiting reactivity increase as a result of moderator thermal spectral shifts. The smaller thermal cross section produces less of a reactivity peak as it burns out but results in some residual negative EOL reactivity. Dy's cross section decreases linearly from 6000 barns at 5.0E-4 ev to 110 barns at 1.0 ev and it has a 200 barn resonance peak at 2 ev. Dy has a larger thermal cross section than Eu but significantly smaller than Gd and it does not have the advantage of resonance peaks in the energy range of interest. Table 4.9 summarizes some of the literature on burnable poison use adapted from Ayoub and Driscoll [A-6]. Initial depletion calculations confirmed that Eu burned out too quickly, producing an unacceptable plutonium fuel power peak at approximately mid-cycle. Of the four poisons selected from cross section analysis, Gd and Er appear to be most promising. They are readily mixed with Al_2O_3 and have excellent neutronic properties. Consequently, fuel design efforts focused on the use of these two as homogeneous burnable poisons.

Table 4.9 Summary of Burnable Poison Uses

Absorber	Type(s)	References	Notes
Boron	* As oxide in glass or in Al_2O_3 * ZrB_2 coating (IFBA) on UO_2 pellets * B_4C	[Y-1] [S-7]	* Extensive Experience Base * Available as Enriched ^{10}B * Forms Helium Gas \Rightarrow . not good for homogeneous use
Gadolinium	* Gd_2O_3 admixed with UO_2 * Miscible in Al_2O_3	[T-4]	* Resonance structure enhances MTC
Erbium	* Er_2O_3 admixed with UO_2 * Miscible in Al_2O_3	[J-1], [C-2], [G-7]	* matches low loading Pu fuel depletion
Hafnium	* HfO_2 admixed with UO_2	[P-1]	* Could also be put into Zircaloy clad * May not burn out fast enough * Used in selected control rod applications
Others: Sm, Cd, Eu, In, Ho, Dy.	* Oxides Admixed with O_2	[P-1], [F-5]	* Lack of Experience * Ho & Dy burn out too slowly * Sm & Eu burn out too fast * Cd, In are alloyed with Ag and used in PWR control rods * Dy is proposed for use in the HWR and Pu burning version of the CANDU reactors

4.3.5 Thorium as a Fertile Material. Thorium (Th) by production of ^{233}U can flatten the reactivity vs. burnup profile of non-uranium fuel. It can also function as a chemical spoiler to complete chemical recovery of Pu from fresh fuel or the residual remaining in spent fuel. The thermal absorption cross section for ^{232}Th is roughly three times that of ^{238}U . Thus, Th can be used in place of BPs to hold down excess reactivity, and increases cycle length by increasing the allowable ^{239}Pu loading.

The flux in the Pu fuel assemblies is highly epithermal. Unfortunately, the effective resonance absorption cross section for thorium is slightly less than that of ^{238}U (when heavily self-shielded). The net effect of using ^{232}Th in place of ^{238}U (without lattice re-optimization) is a reduction in the overall conversion ratio relative to MOX and UO_2 fuels. From a proliferation standpoint, some small weight percent of ^{238}U is also required to denature the ^{233}U produced.

4.3.6 Clad Composition. Stainless steel cladding's chemical and mechanical properties are superior to those of Zircaloy. It is not now widely used commercially in LWRs due to its higher capture cross section which results in increased parasitic neutron losses. Enrichment requirements increase from 3.4 to 5 weight percent in switching from Zircaloy to stainless steel clad unit cells.[E-1] This leads to a 7% increase in LWR fuel cycle costs. However, this cost increase does not apply to WGpu dispositioning because there are no enrichment costs. In addition, the reactivity penalty is not critical for peripheral assemblies. Achievement of extensive plutonium destruction via high burns may make the added chemical durability of stainless steel over Zircaloy cladding well worth the reactivity penalty.

4.4 Literature Survey of Non-Uranium Plutonium Fuels

This section summarizes work and related experience on non-U plutonium fuels. A recent OECD report provides an excellent summary of the work on non-uranium fuel development and is summarized in Table 4.10 [P-2].

Table 4.10 Candidate non-Uranium Plutonium Fuels*

Fuel Type	Country	Status	Reactor	Purpose / Comments
Solid Solutions				
PuO ₂ -ThO ₂	Canada	Theoretical	CANDU	- WGpu dispositioning
	Germany	Theoretical	PWR	- Pu/Th fuel cycle
	Japan	Theoretical & Experimental	LWR	- Once-through Pu incineration - Synthesis only in Al ₂ O ₃
PuO ₂ -CeO ₂	France	Experimental	PWR	- Minor actinide incineration - Scheduled for 1996
	Germany & Brazil	Experimental	PWR	- Reduced plutonium production
	Switzerland	Experimental	LWR	- Sol-gel ceramic synthesis
PuO ₂ -HfO ₂	Switzerland	Theoretical	LWR	- BP survey study
PuO ₂ -ZrO ₂	Canada	Theoretical	CANDU	- WGpu dispositioning
	Switzerland	Theoretical & Experimental	LWR	- Sol-gel ceramic synthesis - Irradiation testing has begun
PuO ₂ -Y ₂ O ₃	France	Experimental	PWR	- Minor actinide incineration - Scheduled for 1996
(Pu-RE)O ₂	France	Theoretical	Fast	- Pu incineration
Eutectics/Dispersion				
PuO ₂ -Al ₂ O ₃	Japan	Theoretical & Experimental	LWRs	- WGpu incineration - With ZrO ₂ or ThO ₂ - Experimental synthesis only
	Switzerland	Theoretical	PWR	- Effect of neutron absorbers
PuO ₂ -CeO ₂ in Al ₂ O ₃	MIT	Theoretical	PWR	- Peripheral Once Through Cycle - WGpu & RGPu destruction
PuO ₂ - (Ln)Al ₅ O ₁₂	Switzerland	Experimental	LWR	- Sol-gel ceramic synthesis
PuO ₂ -BeO	Canada	Theoretical	CANDU	- WGpu dispositioning
	Japan	Theoretical	FBR	- once-through Pu incineration
PuO ₂ -MgO	France	Experimental	LWR	- NpO ₂ -MgO production of ²³⁸ Pu
	France	Experimental	Fast	- Pu incineration
PuO ₂ - MgAl ₂ O ₄	France	Experimental	PWR	- Minor actinide incineration
	France	Experimental	Fast	- Pu incineration
	Switzerland	Experimental	LWR	- Sol-gel ceramic synthesis
Pu-W	US (INEL)	Theoretical	LWR	- metal

* See reference [P-2] for literature references for each entry

4.4.1 Thorium-Pu and Cerium-Pu Fuels. There has been substantial use of Th as a fuel material. Both the Elk River and Indian Point reactors used $\text{UO}_2\text{-ThO}_2$ in a solid solution fuel. Indian Point used up to 7 w% $^{235}\text{UO}_2$ fuel in a ThO_2 matrix. ThO_2 irradiation performance was found to be similar to that of UO_2 . Thorium has also been used as in a $\text{UC}_2\text{-ThC}_2$ carbide fuel in the US Peach Bottom and British Dragon high temperature gas reactors. Thoria (ThO_2) and ceria (CeO_2) can form a fluorite solid solution with PuO_2 . Thorium can be used without adding BPs. Ceria is neutronically inert and so requires the addition of rare earth poisons (RE).

Recent work investigating the use of thorium to increase the destruction of WGPu in LWRs reported that a standard 1100 MWe PWR loaded with WGPu ^{238}U MOX consumes ^{239}Pu at a rate of 420 kg/year. However, net total Pu inventory is reduced by only 220 kg/year [G-1]. It is estimated that a thorium MOX core is capable of destroying ^{239}Pu at a rate of 900 kg/year.

Pin cell studies indicate that $\text{PuO}_2\text{-ThO}_2$ fuel has acceptable plutonium loading, a comparable FTC and a more negative MTC as compared to UO_2 [S-1]. WGPu loading of 85.8 gms/rod was possible providing a 4 yr. burnup to 100% total plutonium destruction. At a typical PWR discharge burnup of 33,000 MWd/MT, ^{239}Pu and total plutonium destruction of 72.6 and 55% were realized. However, the plutonium discharge isotopics were comparable to that of a reference uranium MOX fuel.

4.4.2 Zirconium and Aluminum Matrices. Akie et al. investigated inert ceramic matrices for LWR destruction of WGPu [A-1]. Two fluorite-structure ceramics were recommended: $\text{PuO}_2\text{-ThO}_2\text{-Al}_2\text{O}_3$ and $\text{PuO}_2\text{-ZrO}_2(\text{Y}_2\text{O}_3, \text{Gd}_2\text{O}_3)\text{-Al}_2\text{O}_3$. In both matrices, metal oxides are single phase particles dispersed in a second Al_2O_3 , alumina, phase eutectic. The $\text{Y}_2\text{O}_3, \text{Gd}_2\text{O}_3$ are added to stabilize zirconium oxide. Alumina, thoria and stabilized zirconia have a high

solubility for both actinides and fission products. The alumina is used to provide a chemically durable shell for the fuel particles producing a stable waste form suitable for geologic disposal.

Parratte et. al. examined the physics of elemental B, Dy, Er, Hf, Sm, Eu, and Ho as burnable poisons for use in an alumina reactor grade plutonium dispersion fuel [P-1]. Using a PWR pin cell, they looked at reactivity swing, temperature and void coefficient behavior, and total plutonium destruction all as a function of burnup. Control rod worths were examined using a 15x15 assembly with Ag/In/Cd clad in stainless steel. In a once through cycle, they reported 70% destruction of the total plutonium with the residual being 30w% ^{240}Pu and less than 8w% ^{239}Pu . They concluded that it was possible to achieve acceptable reactivity coefficients with a carefully chosen mix of burnable poisons in a non-uranium Pu fuel.

Sterbentz et.al. completed a rough feasibility study of potential fuels for the destruction of WG Pu in LWRs. [S-1] They examined plutonium oxide, aluminum-plutonium and plutonium carbide fuels. The melting point of aluminum-plutonium fuel is too low for standard LWR power applications. It was only considered in a low temperature, low pressure, non-power producing reactor option. Plutonium oxide fuels were favored over plutonium carbide fuels because of their larger operating experience base and more mature manufacturing technology. BOL pin cell neutronic analysis was performed on $\text{PuO}_2\text{-ZrO}_2$ and $\text{PuO}_2\text{-ZrO}_2\text{-ThO}_2$ matrices with Gd, Eu and Er as burnable poisons. They found that LWR BOL reactivity and reactivity coefficient constraints force unacceptably low loading of plutonium unless either thorium or BPs are used. The $\text{PuO}_2\text{-ZrO}_2\text{-ThO}_2$ matrix yielded acceptable BOL reactivity and negative reactivity coefficients for reasonable Pu loading without the need for BPs. $\text{PuO}_2\text{-ZrO}_2\text{-BP}$ compositions with Er, Gd and Eu all yielded negative FTCs but only Er and Eu also yielded negative MTCs. However, $\text{PuO}_2\text{-ZrO}_2\text{-Eu}_2\text{O}_3$ had a positive MTC at lower Eu mass loading. They further concluded that current mixed oxide manufacturing processes and equipment could be used to manufacture a $\text{PuO}_2\text{-ZrO}_2\text{-BP}$ fuel with little modification.

4.4.3 Tungsten-Pu Fuels. Tungsten (W) has a very large resonance to thermal cross section ratio and has been proposed as a substitute to provide the negative Doppler lost by removal of

^{238}U in non-fertile fuels. Tungsten's resonance behavior is similar to that of ^{238}U making it an excellent neutronic substitute. Chang [C-1] proposed several methods for using W to avoid extensive reactor control redesign in burning weapons grade uranium, WGU, and WGPu. Tungsten oxide has a low melting point of 1430 $^{\circ}\text{C}$ but could be used as part of a metal alloy in dedicated WGPu burning reactors operated at low power, temperature and pressure. For high temperature power reactor use, tungsten metal, with a 3410 $^{\circ}\text{C}$ melting point, could be incorporated either as a central pin or in a sleeve arrangement. Alternately power could be derived from the burning of the weapon grade material in an Al_2O_3 Zr -stabilized matrix allowing operation at high temperature.

4.5 Fuel Matrix Selection.

RGPu and WGPu are both highly enriched in fissile isotopes. Hence, PuO_2 must be diluted to achieve acceptable neutronic properties. With the exception of thoria (ThO_2), the host fuel matrices are neutronically inert. Consequently, their fissile, fertile and BP atom densities can be adjusted to produce essentially the same neutronic performance regardless of the host material. Selection criteria lie in their material properties, ease of fabrication and experience base. This section presents filter logic to narrow the field of candidates. Figure 4.4 is a flow chart showing the decision points leading to a recommendation of three candidate fuels for development: zirconia, alumina and TRISO.

The matrix constituent decision path has two major decision points. First the periodic table is reduced to a handful of potential elements based on the requirement that the matrix be neutronically inert (i.e. do not want capture reactions in matrix materials). The second constituent element requirement is that it form the preferred crystalline structures and that the structure be chemically stable and compatible with the cladding. The matrix selection path is more involved.

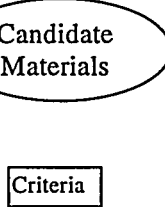
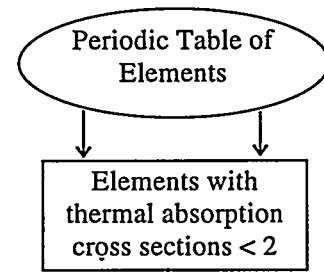
There are many fuel matrices not listed in table 4.9, including silicides, nitrides and carbides which could be investigated for non-uranium plutonium fuel incineration. The goal of this work is limited to identifying a potentially acceptable plutonium elimination fuel for use in current PWRs rather than to develop the best fuel possible. Consequently, the large existing fabrication and performance experience base of oxide fuels give it a huge advantage over other potential fuel matrices. Plutonium fuels require remote handling and fabrication techniques. Such processes are already used for the production of MOX and are more easily adapted for non-uranium oxide fuels. The performance of MOX fuel is more sensitive to variations in the manufacturing process due to plutonium's more pronounced variability in stoichiometry. This makes it more critical to select a fuel which will allow use of the existing MOX experience base to the maximum extent possible in the development of a new non-uranium fuel. The compatibility of oxide fuel with cladding has been investigated in detail and the properties and stability of oxide ceramics are more defined and proven. Thus, an oxide fuel is likely to take less time and expense to develop and qualify.

Exclusion of uranium from the fuel matrix necessitates the use of incorporated burnable poisons to set the desired neutronic properties. Thus, the crystalline structure of the oxide matrix must be able to incorporate plutonium and burnable poisons. Peroskovites, Fluorites, Yag, Rutile and Yag oxides are capable of incorporating actinides and rare earths. The vacancies in fluorite structures make them particularly amenable to the incorporation of fission products. The closer the host cation's radii are to those of the substitution ions the less strain placed on the host phase crystalline structure. Several ceramic oxides are capable of incorporating both the actinides and rare earth burnable poisons. Table 4.10 lists potential host crystalline structures and typical formulas [D-1]. As mentioned previously, fluorites are known to be exceptionally stable as nuclear fuels due to their ability to readily incorporate fission products without phase change. Thus, the fluorite structure is recommended for this application.

Table 4.11 Candidate Oxide Host Ceramics

Structure	Example Formula
Fluorite	$(\text{Zr,Act. or Lanth.})\text{O}_{2+x}$
Peroskovite	$(\text{Sr,Ba})(\text{Ti,Zr})\text{O}_3$
Spinel	MgAl_2O_4
Yag	$\text{Y}_3\text{Al}_5\text{O}_1_2$
Zirconolite	$\text{CaZrTi}_2\text{O}_7$
Rutile	TiO_2 , RuO_2

Matrix Constituent Selection Path



Matrix Selection Path

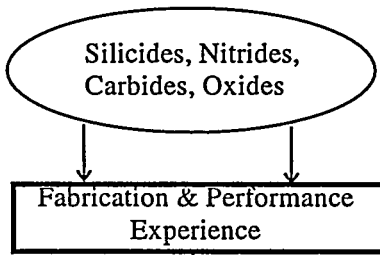


Figure 4.4 Fuel Constituents and Crystalline Matrix Selection Logic Flow Chart

The next level of decision in figure 4.4 is whether or not to disperse the fluorite mix into an inert matrix or to use it directly as a solid solution. The ceramic properties of the fuel can be enhanced if a dispersion matrix is used; the thermal conductivity can be increased, fission product retention enhanced and a more stable spent fuel form produced over that achievable with the fluorite ceramic. Alumina forms a natural fluorite structure with rare earths that can also incorporate a second fluorite PuO_2 phase. In addition, the inert dispersion matrix can host the RE oxides. For example, Peroskovites (LnAl_2O_3) are a particular form of alumina found in nature and are particularly stable with high melting points. The lanthanide series contains the rare earth burnable poisons used to manipulate the fuel's neutronic characteristics as discussed in section 4.3.4. Table 4.11 lists Peroskovites of interest [K-1]. The lanthanides in table 4.11 can be added to help tailor the reactor physics properties of the fuel. There is more experience with TRISO fuels in which one would coat PuO_2 particles with three carbon layers, [A-4, A-5] than for alumina or zirconia fuels.

Table 4.12 Peroskovites, LnAl_2O_3	
<u>Lanthanide</u>	<u>Melting Point, °C</u>
Cerium, Ce	2030
Samarium, Sm	2040
Europium, Eu	2047
Gadolinium, Gd	2069
Dysprosium, Dy	1940
Holmium, Ho	1980
Erbium, Er	1963

Extensive development and testing is required to bring each of these candidates to practical use. A solid solution fluorite fuel can be developed that will meet minimum performance requirements. Dispersion fuel is not widely used nor manufactured. The

potential benefits must be weighed against the potential added cost and time required to develop a dispersion fuel.

4.6 Selected Fluorite and Dispersion Fuel Matrices.

This section describes the two solid solution fluorite and two dispersion fuels selected in section 4.5: $\text{PuO}_2\text{-ThO}_2$, $\text{PuO}_2\text{-}(\text{Zr/Ce})\text{O}_2\text{-REO}_{1.5}$ alumina (Al_2O_3) and TRISO fuel particles in a silicon carbide (SiC) binder material. The proposal is to clad and assemble these fuel matrices to produce an otherwise standard PWR assembly. Consequently, the cladding still serves as the primary fission product barrier as in normal UO_2 fuels. An excellent summary of the properties of alumina, zirconia, graphite and silicon carbide as nuclear fuel matrices is available elsewhere [H-1].

4.6.1 $\text{PuO}_2\text{-ThO}_2$. Table 4.12 provides the properties of PuO_2 and ThO_2 . Comparison with UO_2 properties in table 4.4 shows ThO_2 properties are almost identical to those of UO_2 . Consequently, the solid solution should have properties comparable to MOX. $\text{PuO}_2\text{-ThO}_2$ fuels have been irradiated satisfactorily. PuO_2 and ThO_2 also have a fluorite crystalline structure and can form a solid solution. ThO_2 has the same thermal conductivity and thermal expansion coefficient as UO_2 . PuO_2 has a similar linear expansion coefficient but a lower thermal conductivity than UO_2 . Consequently, MOX fuel has a lower thermal conductivity than UO_2 .

PuO_2 has a more pronounced variable stoichiometry with temperature than does UO_2 [H-4]. PuO_2 evolves oxygen on melting, decreasing its Pu:O ratio to 1.6. This variation in stoichiometry affects the thermal conductivity. Hyperstoichiometric compositions typically have lower thermal conductivities. Thus, the performance of MOX fuel is more sensitive to variations in the manufacturing process. This makes it more critical to select a fuel which will allow use of the existing MOX experience base to the maximum extent possible in the development of a new non-uranium fuel. Pu also reacts with Zr-II [H-2]. The lower mass

number fission product yield peaks at a higher mass than for uranium. Thus, plutonium fissions produce more noble metals such as ruthenium, palladium and rhodium increasing the amount of free oxygen available and subsequently the oxygen potential in the fuel.

Table 4.13 Unirradiated PuO_2 and ThO_2 Properties		
Property	PuO_2	ThO_2
Thermal Conductivity (200-1000 $^{\circ}\text{C}$)	~2 W/m- $^{\circ}\text{C}$	3.6 W/m- $^{\circ}\text{C}$
Melting point	2400 $^{\circ}\text{C}$	3250 $^{\circ}\text{C}$
Specific Heat @ 100 $^{\circ}\text{C}$	253.3 J/Kg- $^{\circ}\text{C}$	291.0 J/Kg- $^{\circ}\text{C}$
Stability Range	up to melting point	up to melting point
Theoretical density	11.46 gm/cm 3	9.56 gm/cm 3

4.6.2 Stabilized Zirconia and Ceria. Zirconia forms a distorted monoclinic fluorite which is not suitable for incorporating Pu. However, it can be stabilized by the addition of a third oxide to form a stable face centered cubic fluorite. The REs that must be added for neutronic performance reasons can also serve to stabilize the zirconia. Degueldre et. al. reported that the heavier the lanthanide, the greater its ability to stabilize ZrO_2 in the preferred fluorite structure [D-1]. Erbium was found particularly effective. The major drawback of the zirconia matrix is the low conductivity of ZrO_2 . It may be possible to overcome this drawback by mixing in a stabilizing Ln oxide of higher conductivity. CaO can also be used to stabilize zirconia and at 15 mol% has been reported to increase conductivity above 2.0 W/m- $^{\circ}\text{K}$ [S-1] at 1500 $^{\circ}\text{K}$. However, it did not increase the conductivity significantly at anticipated temperatures. Annular pellets may also be used to reduce the centerline temperature. An annulus of half the pellet diameter was found to drop the centerline fuel temperature by 600 degrees to 1300 $^{\circ}\text{C}$ at a 400 w/cm power density [D-1].

Cerium is neutronically inert and is unique among the lanthanides in that it forms a fluorite structure and so can be mixed to form $\text{PuO}_2\text{-CeO}_2$ particles. It exists in both the +3 and +4 oxidation states, has an ionic radius similar to plutonium and is a good plutonium ion analog. It can be added to the oxide particle mix to enhance the chemical proliferation

barrier of the fuel. Ceria's thermal conductivity is better than zirconia at 900 $^{\circ}\text{K}$ but drops off to be approximately equivalent at expected operating temperatures. Cerium can be used to stabilize zirconia. However among the lanthanides, it is the least effective stabilizer.

Table 4.14 Unirradiated ZrO_2 and CeO_2 Properties

Property	ZrO_2	CeO_2
Thermal Conductivity (@ 1000 $^{\circ}\text{C}$)	2.0 W/m- $^{\circ}\text{C}$	1.3 W/m- $^{\circ}\text{C}$
Melting point	2770 $^{\circ}\text{C}$	2600 $^{\circ}\text{C}$
Specific Heat @ 100 $^{\circ}\text{C}$	457.2 J/Kg- $^{\circ}\text{C}$	460 J/Kg- $^{\circ}\text{C}$
Linear Expansion Coefficient (20-1400 $^{\circ}\text{C}$)	9.6E-6 $^{\circ}\text{C}^{-1}$	1.1E-05 $^{\circ}\text{C}^{-1}$
Stability Range	up to melting point	up to melting point
Theoretical density	5.85 gm/cm 3	7.28 gm/cm 3

There is a dearth of published data on the irradiation stability of zirconia under a fast fluence. Most of the available data were derived for waste form applications involving alpha damage studies. One available report cited a 21% reduction in ZrO_2 thermal conductivity for a fluence of 2×10^{20} n/cm 2 ($E > 100$ ev). More research needs to be done in this area. Specifically the irradiation stability of ternary zirconia fuel must be explored.

4.6.3 Alumina Fuel Matrix. An alumina, Al_2O_3 , dispersion fuel matrix provides design flexibility in meeting cycle reactivity requirements. PuO_2 is combined with zirconia and/or ceria to form a fluorite crystalline structure. The fluorite particles are homogeneously dispersed in a second aluminate, aluminum-lanthanide, Ln , oxide, phase. An alumina fuel matrix can accommodate the fissile and poison loading required to create the novel fuel neutronic properties necessary for seamless integration into the peripheral location of a PWR. Since the alumina is proposed as a substitute for UO_2 , its mechanical and chemical properties must be comparably or better suited to this application than those of UO_2 . Alumina's thermal conductivity is high for a ceramic, exceeding that of UO_2 by more than a factor of three [G-

1]. Compared to UO_2 , this would reduce alumina's peak centerline temperature and gradient by a factor of three for the same power density. Consequently, fewer problems with temperature gradient driven phenomena such as fission product gas pressure buildup and fission product migration are expected. This is the major advantage of an alumina dispersion fuel as compared to a solid solution $\text{PuO}_2\text{-ZrO}_2$ (stabilized) matrix. Alumina's volumetric specific heat exceeds UO_2 's by 30%; a potential increase in stored energy is offset by the lower temperature. The higher heat capacity will allow the absorption of more decay heat under accident conditions. Alumina's melting point is lower but comparable to that of UO_2 and likely to be well above anticipated transient temperatures which should also be lower due to the higher heat capacity. Linear expansion coefficients are also comparable. The matrix density is not critical; the fissile density can be varied to achieve the desired reactor characteristics. Alumina's chemical stability is excellent for this application. Under normal operating conditions the alumina is clad and therefore isolated from water. There is no autocatalytic reaction under high temperature accident conditions and its corrosion rate in flowing steam up to 1430 °C is on the order of millimeters/year [H-3]. Alumina is used in some LWRs as a burnable poison host and as insulation pellets at the end of fuel pins.

Akie et al. [A-1] have synthesized both non-fertile and thorium loaded alumina matrices for the burning of WG Pu and found that alumina combines well with fission products. Simulated spent fuels displayed excellent durability as waste forms.

Some questions remain regarding the neutron irradiation stability of alumina fuel matrices. Alumina undergoes significant swelling under fluences appropriate to fusion applications. Clinnard, investigating the use of $\alpha\text{-Al}_2\text{O}_3$ as an insulator for fusion applications, reported 3-10 vol% swelling under irradiation of 925 and 1100 °K up to fluences of $1 - 2 \times 10^{26}$ neutrons/meter², (n/m²) [C-3]. In a more definitive study, Clinnard and Hobbs report 1.9-3.5 vol% swelling in $\alpha\text{-Al}_2\text{O}_3$, also referred to as corundum, irradiated at 925 °K to fast fluences, $E > 0.1$ Mev, of 0.3 and 2.3×10^{26} n/m² respectively.[C-2] The anisotropic nature of the swelling is likely to cause grain boundary cracking. In addition, the alumina matrix absorbs and combines with fission products to form new crystals which add

to the strain. However, a subsequent report defined a threshold fluence of $1 \times 10^{25} \text{ n/m}^2$, below which no significant swelling of $\alpha\text{-Al}_2\text{O}_3$ was observed [K-3]. A typical PWR peripheral fast neutron flux of $1 \times 10^{13} \text{ n/cm}^2\text{-sec}$ leads to a fluence of $3 \times 10^{24} \text{ n/m}^2$ each year of continuous operation. Hence in a peripheral location, the 10^{25} fluence threshold would not be exceeded. The addition of lanthanides chemically stabilizes alumina and may also result in additional radiation resistance. UO_2 fuel typically undergoes fission product gas induced swelling and cracking. To minimize potential pellet clad interactions the swelling is (in part) compensated for by cladding design. A similar accommodation in design may be possible for any irradiation-induced swelling encountered in Alumina fuel. Like UO_2 , neutron irradiation degrades alumina's thermal conductivity. A recent report indicates that after 18 months of irradiation the thermal conductivity may decrease to approximately that of ZrO_2 , which is below fresh UO_2 (F-1). These and other material issues must be the subject of a significant fuels development and testing program. Nevertheless, it seems likely that an alumina fuel similar to the design described above would prove satisfactory as a fuel.

4.6.4 TRISO Fuel Matrix Description. Pu-Th O_2 -Zr O_2 kernels or non-fertile Pu O_2 -Zr O_2 -BP kernels can be used to destroy Pu in a PWR. Again, cerium can also be added to enhance chemical proliferation resistance. For the non-thorium variant a lanthanide poison oxide, Ln_2O_3 , similar to that discussed for the alumina matrix, is used to tailor the cycle reactivity profile and optimize the net plutonium destruction. The burnable poison particles would be coated and mixed with the TRISO fuel particles and formed into compacts. The compacts are then loaded into Zircaloy fuel pins. Alternatively, the TRISO and burnable poison particles can be loaded directly into the Zircaloy cladding with compactable graphite or silicon carbide material: the compactable material fills the spaces between the particles to enhance thermal conductivity. Loading the cladding with a compactable material-TRISO particle mix would permit the use of remote vibratory compaction as a fabrication technique

The TRISO particles being considered here are similar in design to those used in the PC-MHTGR reactor dispositioning option described in chapter 2, section 3. The TRISO fuel

matrix has the advantage of being a more tested fuel alternative to an alumina or zirconia fuel matrix. The material performance of TRISO fuel with PuO₂ and PuO₂-ThO₂ kernels has already been tested. Various configurations and compositions from reactor grade to enriched plutonium loaded TRISO fuels were tested in both the Dragon and Peach Bottom reactors to burnups up to 747,000 mega-watt-days per metric ton of heavy metal, (MWd/MT) with a fast neutron fluence of 1.5×10^{25} n/m², E > 0.18 Mev [G-2]. The results were mixed, depending on the Pu:O ratio used and there is some conflict among the conclusions that were drawn. However, since in the present application the cladding is available as a primary fission product retention barrier, the TRISO fuel spheres could be expected to provide more than adequate performance, especially when compared to UO₂. Elimination of the outer silicon carbide layer to reduce cost may even be justifiable since the cladding will be the designated design barrier to fission products release. The maximum strength of the kernel without the layer would be the limiting factor; this would be especially true for vibratory compaction fuel pin fabrication.

Both graphite and SiC properties are very dependent on the manufacturing process. However, modern forms produced for nuclear applications are excellent matrix candidates: table 4.14 lists their properties. Even at EOL fluences their thermal conductivity exceeds that of UO₂ by nearly an order of magnitude. High purity reactor grade graphite irradiated in the Oak Ridge High Flux reactor up to fluences of 3×10^{26} n/m² expanded by only 2 vol% [H-5]. SiC irradiated at 1300 ⁰K is projected to have a useful life of $2-3 \times 10^{26}$ n/m² [H-6]. Stored lattice damage energy is of no practical concern for irradiation temperatures of 500 ⁰C. SiC has a slightly larger absorption cross section than graphite. However, this is not problematic for non-uranium plutonium fuel for this application since RG⁹⁰Pu and WG⁹⁰Pu are diluted to the desired enrichment. Hence there is no associated cost of additional enrichment. SiC may be preferable to graphite due to its greater resistance to oxidation under accident conditions. Graphite can experience an autocatalytic reaction sequence under very restrictive but

plausible conditions of high water vapor content, temperature $> 650^{\circ}\text{C}$, adequate supply of oxygen with a gas flow capable of removing gaseous combustion products.

Table 4.15 Unirradiated Graphite and SiC Properties		
Property	Graphite	SiC
Thermal Conductivity (@ 1000 $^{\circ}\text{C}$)	$> 30 \text{ W/m-}^{\circ}\text{C}$	$> 15 \text{ W/m-}^{\circ}\text{C}$
Sublimation point **	1500°C	1950°C
Specific Heat @ 100 $^{\circ}\text{C}$	$720 \text{ J/Kg-}^{\circ}\text{C}$	$666 \text{ J/Kg-}^{\circ}\text{C}$
Stability Range	up to melting point	up to melting point
Theoretical density	12.0 gm/cm^3	40.1 gm/cm^3
** sublimation in a vacuum		

4.6.5 Application of Thermal Performance Metrics to Recommended Fuel Matrices. Table 4.15 presents the properties and resultant metric ratios for the recommended zirconia, alumina and TRISO (considered as a SiC matrix). Alumina and SiC matrices have acceptable performance metrics. Zirconia's substandard performance is primarily due to its low thermal conductivity. Erbia, which is added primarily for reactivity control and which helps to stabilize zirconia in the preferred mono-clinic fluorite structure, may also improve the thermal conductivity of the zirconia. CaO can also be used to stabilize zirconia and at 15 mol% has been reported to increase conductivity to above $2.0 \text{ W/m-}^{\circ}\text{K}$ [S-1] at 1500°K . However, zirconia's thermal conductivity must be increased by a factor of two to achieve UO_2 margin ratios ≥ 1.0 . Consequently, annular pellets may be required to reduce the centerline temperature. An annulus of half the pellet diameter was found to drop the centerline fuel temperature by 600 degrees to 1300°C at a 400 w/cm power density [D-1].

Table 4.16 Summary of Recommended Fuels Thermo-physical performance						
Candidate Matrix	ρ (gm/cm ³)	T_{MP} ($^{\circ}\text{C}$)	k (W/m-K)	C_p (J/ $^{\circ}\text{K}$ -kg)	$\frac{kT_{MP}}{kT_{MP} - \text{UO}_2}$	$\frac{\alpha}{\alpha_{\text{UO}_2}}$
ZrO_2	5.85	2770	2.0	457.2	0.5	0.5
Al_2O_3	3.97	2000	7.0	775.7	1.4	1.6
SiC	3.22	1950	15	666.6	2.9	5.0
UO_2	10.97	2820	3.6	235.7	1.0	1.0

4.7 Fabrication Technology.

The oxide and TRISO fuel matrices were selected in part due to the potential for easily adapting existing fabrication designs and operations to produce the non-uranium fuel. This section examines the relevant existing fabrication techniques with regard to suitability for this application.

4.7.1 Oxide Fuel Fabrication. Sterbenz et al (1993) provide an excellent overview of the issues regarding fabrication of PuO_2 fuels for WGPu disposition in reactors [S-1]. Figure 4.5 depicts a typical UO_2 or MOX fabrication process. The oval overlays mark steps which will need to be altered to produce a non-uranium fuel. UF_6 feed stock comes from enrichment processes for enriched fuels. U_3O_8 is the feed stock for natural uranium fuels and nitrate solutions of uranium and plutonium are the product of reprocessing. There are three major processes used to produce oxide fuel powders: Co-conversion, Co-precipitation and Integrated Dry Route/Mechanical Blending. The process selected depends on the type of feed stock, the degree of homogeneity required and the desired product solubility.

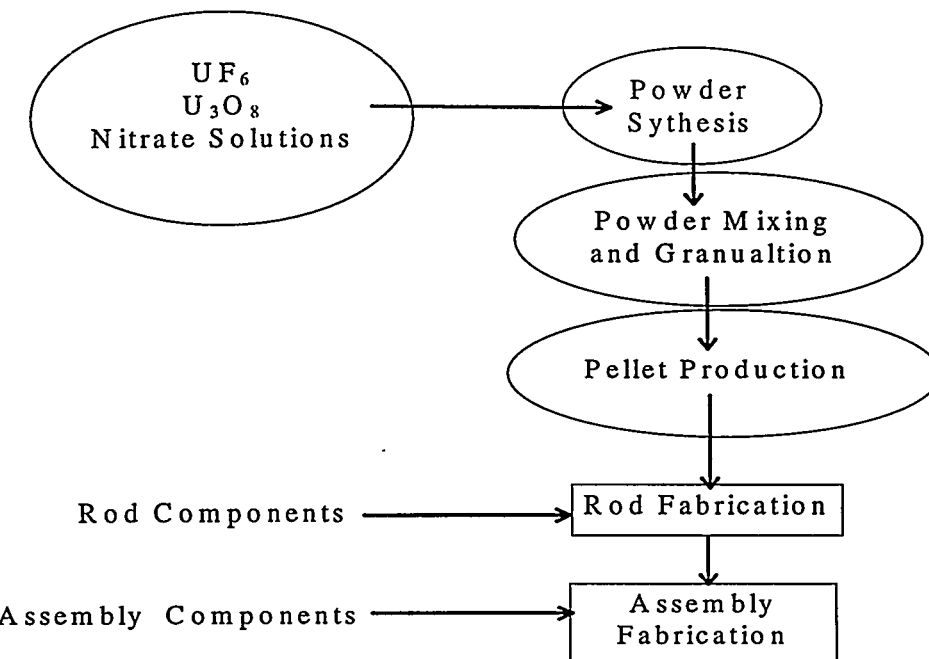


Figure 4.5 Typical Fuel Fabrication Flow Sheet

Co-conversion, also known as thermal microwave denitration, is the most direct method to produce a homogeneous solid solution. Microwaves are used to drive off nitrogen from reprocessing product streams. There is no direct contact between the material and the heating medium so that it is very amenable to remote handling. However, the process is energy intensive. This process would require a nitric acid solution of the Zr/Ce, Pu, BP or Pu,Th mix feed stock to produce the non-uranium solid solution fluorite fuels. These solutions are readily available as product streams from plutonium recycling of PWR spent fuel.

Co-precipitation of UO₂ and MOX fuels is accomplished by the addition of hydroxides to a nitrate solution of the actinides. However, the hydroxides can be gelatinous causing a handling problem. Alternately, oxalates can be precipitated. These techniques are not directly transferable to the PuO₂-(Zr/Ce)O₂-BP_{1.5} ternary fuels. Significant development is likely to be required. This process will be more easily adaptable to production of PuO₂-ThO₂.

In dry route processing, PuO₂ is typically produced through precipitation of Pu from nitrate solution through hydroxide or oxalate precipitation. The precipitate is then fed

through a rotary kiln and an orbital screw blender to produce the powder. For (Ce/Zr)O₂-PuO₂ based fuels the individual oxide powders would be procured and mechanically blended. They would not necessarily form a solid solution. Solid solutions are generally desirable because the product pellet has a poor nitric acid solubility. However, low solubility would make plutonium recovery more difficult and hence enhance proliferation resistance of the fresh fuel. There is a potential problem in that a non-solid solution fuel may have degraded thermal conductivity. The degree of homogeneity is dependent on how finely ground the powders are prior to mixing. Alternately, a pre-pelletizing process can be employed after mixing to increase homogeneity. For example, dry ball milling is a mechanical pulverizing and mixing technique using simple low cost equipment to control the degree of homogeneity. A balance can be struck between desirable solid solution properties such as thermal conductivity and the lower solubility of a of a more dispersion-like fuel

Early MOX fabrication processes added PuO₂ powder to already granularized UO₂ [H-9]. The resulting product was actually an interstitial dispersion of PuO₂ among the original UO₂ granules. However, the thermal conductivity of the pellets was too low. The process was then modified to blend PuO₂ and UO₂ powders. The mix is then pelletized and sintered to produce a UO₂ matrix in which is dispersed fine plutonium-rich oxide particles. The blending process was further modified to enhance PuO₂ solubility by directly micronizing the PuO₂ powder with UO₂. In a once-through non-uranium fuel cycle, proliferation resistance may be enhanced by making the PuO₂ less soluble. These processes may be adapted to produce PuO₂ particles in an alumina matrix.

The alumina can be produced by mixing the appropriate amounts of the oxide constituents. The mixture is then pelletized, sintered and loaded into standard PWR Zircaloy cladding pins similarly to UO₂ pellets. Thus, they can be manufactured in standard MOX fabrication facilities. The alumina pellets produced by Akie et. al. are extremely chemically stable and are not soluble in standard PUREX nitric acid dissolution procedures, thus adding to the chemical proliferation barrier [A-1].

4.7.2 TRISO Fuel Fabrication. General Atomics has designed a TRISO fuel fabrication process as part of their proposal to DOE for WGPu dispositioning studies [G-3]. Although TRISO fuel technology is less mature than MOX technology, it may be more directly applicable to a non-uranium plutonium dispersion fuel. Figure 4.4 shows the proposed steps of the process. Again the ovals indicate steps which will need to be altered for non-uranium Pu dispositioning. The main changes will be the type of kernels fabricated and the introduction of a fuel rod fabrication step. For RGPu fuel the plutonium will already be in a nitrate solution. The extent of changes in the purification and kernel formation processes due to changes in the chemistry of the feed stock are likely to be similar in extent to those required to adapt MOX technology.

The PC-MHTGR uses channels in graphite fuel blocks rather than fuel rods. Rod fabrication would entail loading of the compacts similarly to loading of UO₂ pellets. Alternatively, vibratory compaction of a TRISO particle-graphite/SiC mix poured directly into the fuel rods could be used in place of compacts. Vibratory compaction densities up to 90% have been achieved using systems with three different particle sizes [H-2]. Remote vibratory compaction has been used successfully in extensive long term production of MOX fuel pins for the BOR-60 liquid metal reactor [H-4]. Remote handling capability becomes even more critical if this cycle is to be adopted for the burning of RGPu.

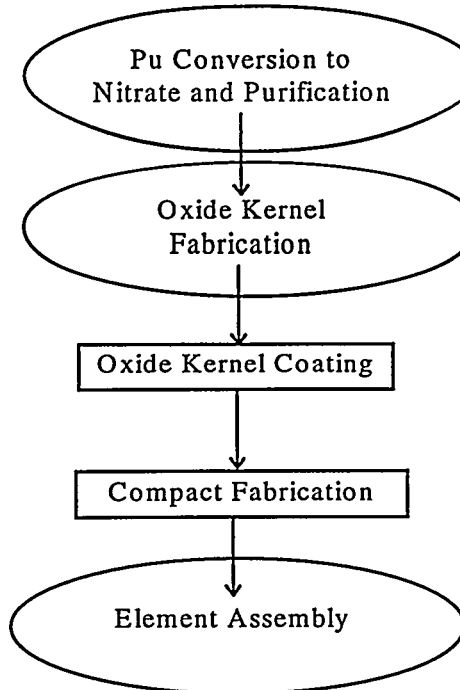


Figure 4.6 TRISO FUEL Fabrication for the GA PC-MHTGR

4.8 Peripheral Assembly Fuel Cycle.

PWRs comprise over two thirds of operating US commercial reactors. Thus, it would be convenient to be able to achieve a deep burn of plutonium in PWRs. A PWR fuel cycle using non-plutonium producing fuel in the peripheral assemblies is proposed. The fuel is specifically designed to yield a large net plutonium destruction while operating in the peripheral assembly locations. Peripheral assemblies constitute approximately 20-25% of the core and have a smaller contribution to overall core properties due to their location. Thus, the impact on core characteristics of the lower delayed neutron fraction and larger fission thermal and resonance cross section of ^{239}Pu relative to ^{235}U is reduced. Using only peripheral assemblies allows greater flexibility in matching the fuel design with the fuel cycle needs, and has been taken advantage of in the past. For example, LWR cycles have shifted from an original cycle management which placed the freshest assemblies on the core periphery, thereby minimizing power peaking, to current low leakage management where the

oldest fuel assemblies are shuffled to peripheral locations to mitigate vessel fluence and gain in overall neutron economy. These changes were achieved through more detailed design of the fuel rather than with reactor modification. It is estimated that current LWRs can be licensed to operate with 1/3 MOX loading in the core interior without modifications [N-2]. This same sort of flexibility could be used to run the novel plutonium fuel assemblies at a higher loading and power to increase the throughput and net plutonium destruction. Conversely, the lower peripheral assembly plutonium loading could be used to enhance discharge isotopes and neutron economy. The usual lower power density of peripheral assemblies would reduce the performance requirements of the fuel. Alumina and TRISO type fuels are examined for use in this peripheral cycle scheme.

4.9 Conclusions

Using ^{239}Pu as the primary BOL fissile species results in a fuel which is substantially neutronically different from $^{235}\text{U}/\text{UO}_2$ fuel. In addition, eliminating uranium from the fuel matrix greatly enhances the ability to destroy plutonium, but it also presents several additional challenges. Table 4.1 lists the many variables which can be manipulated to overcome these challenges. However, initial investigation indicates that the proper mixture of homogeneous burnable poisons can produce acceptable initial plutonium loading, MTC, FTC and reactivity versus burnup profiles. This is further confirmed in the literature. Thus, only the fuel composition needs to be altered to provide the once-through PWR plutonium elimination which is sought.

The fissile, fertile and BP atom densities determine the neutronic performance and hence the degree of plutonium destruction achievable. There are several candidate fuel matrices which could incorporate these neutronically active ingredients while providing the necessary material properties. However, the goal is to select a fuel which will allow the safe destruction of plutonium within existing operating margins. It is also preferable to accomplish this goal with the smallest cost and development effort possible. Development of the “best possible” plutonium destruction fuel possible is neither desired nor required. As

long as its material properties are not or do not degrade to be worse than UO₂'s, the neutronically inert fuel matrix has a negligible effect on the capacity for plutonium destruction. The minimum performance requirements are readily established as "no worse than UO₂" which comprises the bulk of the core. Fluorite oxides have the largest experience base and the most mature manufacturing infrastructure. Consequently, they are selected as the best candidate for containing the plutonium.

A zirconia-plutonium-oxide burnable poison ternary fuel may offer a viable solid fluorite solution option. However the thermal performance drawbacks due to its poor thermal conductivity must be overcome. Alternatively, the plutonium containing crystalline structure can be dispersed in an inert non-fluorite matrix to enhance material properties and fission product retention. Oxide dispersion matrices are preferred because their production should require less modification of existing technology. Alumina is selected as a dispersion matrix over other oxides because of its ability to incorporate fission products, good thermal metric performance and its chemical stability as a spent fuel form. TRISO particles dispersed in a graphite or SiC matrix is selected as a dispersion matrix for potential superior performance and direct applicability of existing technology to non-uranium plutonium fuel kernels. All of the fuel forms selected appear to be able to be manufactured without significant development of new technology.

MOX fuel fabrication techniques and experience bases should be readily adaptable to non-uranium oxide fuel production. For the once-through cycle being proposed, a balance between solid solution and dispersion properties is desirable. If an acceptable balance can be struck, the simplicity and flexibility of the integrated dry route process is preferable to co-precipitation or co-conversion techniques.

Finally, using only the peripheral locations of the PWR allows greater flexibility in tailoring both the plutonium destruction rate and core neutron economy. The resultant impact on current LWR operations and cycles is minimized. Designing a plutonium elimination option which is equally viable in existing as well as advanced PWRs enhances the potential throughput of plutonium. This makes the long term objective of mitigating the risk of

proliferation through first reduction, and then control of the size, of the worlds plutonium stockpile more easily achievable.

CHAPTER FIVE: COMPUTATIONAL CODES, MODELS AND TECHNIQUES

This chapter discusses the models, codes and calculations used to develop and evaluate the non-uranium plutonium oxide fuel in the peripheral PWR fuel cycle advocated here. Chapter 4 discusses some of the specific neutronic challenges presented in using a PWR core partially loaded with non-uranium plutonium fuel. These neutronic challenges are greater for WGPu isotopes than for RGPu. Thus, all calculations were carried out using WGPu isotopes in order to be conservative. Specifically the following data are calculated: pin to pin power peaking factors, discharge isotopes, the fuel reactivity vs. burnup profile, core average reactivity coefficients and whole core reactivity. All the models are based on a PWR core comprised of standard 17 x 17 Westinghouse assemblies. Fuel compositions are developed to support an 18 month fuel cycle with a capacity factor of 0.8. Thus, the base 18 month fuel cycle is repeated at 440 EFPD long periods.

The first section describes the computer codes used and their application to depletion calculations. The second section describes the depletion benchmark calculations and results. The third section describes the use of the computer models and calculation techniques for deriving the required information.

5.1 Code Descriptions

Three computer codes were used to perform depletion calculations: ORIGEN version 2.1, MCNP version 4A and MOCUP [C-4, B-5, M-4]. CASMO-3 was used for depletion benchmark comparison and temperature coefficient calculations. ORIGEN, Oak Ridge Isotope Generation and Depletion code, is a zero dimensional depletion code which employs a matrix exponential method to explicitly calculate the transmutation, decay and production of nuclides. MCNP, Monte Carlo N-Particle Transport code, is a general purpose Monte Carlo code for calculating the continuous energy transport of neutrons, photons and electrons in a three dimensional system. ORIGEN and MCNP are widely used codes and will be discussed here only as is necessary to explain their interaction with MOCUP. CASMO-3 is a multi-group two dimensional transport theory code for burnup calculations on PWR and BWR pin cells and assemblies. It is widely used in industry calculations and will not be described in detail here. The reader is referred to the CASMO-3 manual for details [E-4]. MOCUP, MCNP4A-ORIGEN Coupled Utility Programs, was developed at INEL.

5.1.1 MCNP-ORIGEN2 Coupled Utility Program (MOCUP) Depletion Calculations. A complete description of the MOCUP code can be found in the MOCUP manual [M-4]. This section will describe how MOCUP was used to perform depletion calculations. As the name implies, MOCUP serves as a conduit for passing information between MCNP and ORIGEN. Nuclide-specific cross section information calculated by MCNP is manipulated by MOCUP and provided to ORIGEN. Depletion composition changes effected in ORIGEN are tracked by MOCUP and used to create MCNP input decks. Thus, composition and reactivity changes are calculated as a function of burnup. No modification to either ORIGEN or MCNP is required to treat nuclides explicitly in depletion calculations. This allows accurate depletion of novel fuels and geometries through a series of MOCUP time intervals and ORIGEN time steps. Time intervals refer to the change in burnup between MCNP reaction rate calculations and subsequent ORIGEN nuclide cross section updates. Time steps refer to the individual ORIGEN depletion commands, IRP or IRF, within each

MOCUP time interval. Several ORIGEN time steps are used to complete the burnup specified for a single MOCUP time interval. Figure 5.1 shows the flow of depletion calculation information between MOCUP, ORIGEN and MCNP.

ORIGEN contains one-group cross section libraries and fission product yields for all the nuclides of potential interest. However, these one-group cross section libraries are produced using sophisticated reactor physics codes which collapse multi-group libraries based on specific standard reference reactor geometries and fuel compositions. Consequently, the accuracy of the results that can be produced using these one group cross sections decreases as the actual system being evaluated moves further away from the reference basis for the particular library being used. Consequently, the ORIGEN cross section libraries are of limited use in evaluating new fuel compositions. Fortunately, ORIGEN has a built in feature which allows substitution of user supplied one group cross sections for ORIGEN cross sections. In the present instance, substitute cross sections are derived for the actual composition and geometry from MCNP flux and nuclide reaction rate tallies. A new set of accurate one-group substitute cross sections are generated and supplied to ORIGEN each depletion interval. The cross sections are assumed constant over the depletion interval. The resultant ORIGEN output composition is then incorporated into a new MCNP input and a new set of fluxes and reaction rates calculated. The entire depletion cycle is completed in stepwise fashion.

This approach is not new. Previous work shows that if the time interval over which constant cross sections are assumed is less than 10% of the total End of Cycle (EOC) burnup, the error in the resultant EOC compositions is less than 1% [R-1]. MOCUP automates the process of calculating cross sections and tracking nuclide compositions. This automation makes the process less labor intensive, faster and less prone to clerical errors. Thus, it is more practical to precisely treat individual fission products, thereby eliminating the need for lumped fission product approximations. MOCUP is comprised of three modules, mcnpPRO, origenPRO and compPRO which are used consecutively in each depletion time interval. Figure 5.2 is a detailed flow diagram of the file information through the MOCUP modules, ORIGEN and MCNP.

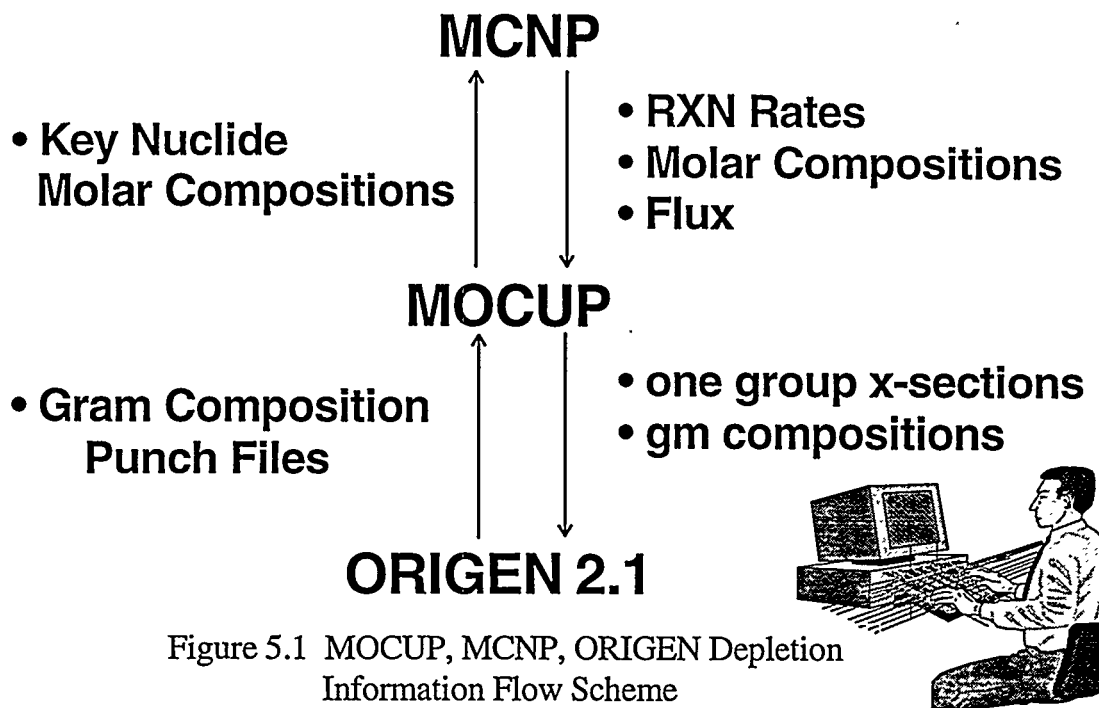


Figure 5.1 MOCUP, MCNP, ORIGEN Depletion Information Flow Scheme

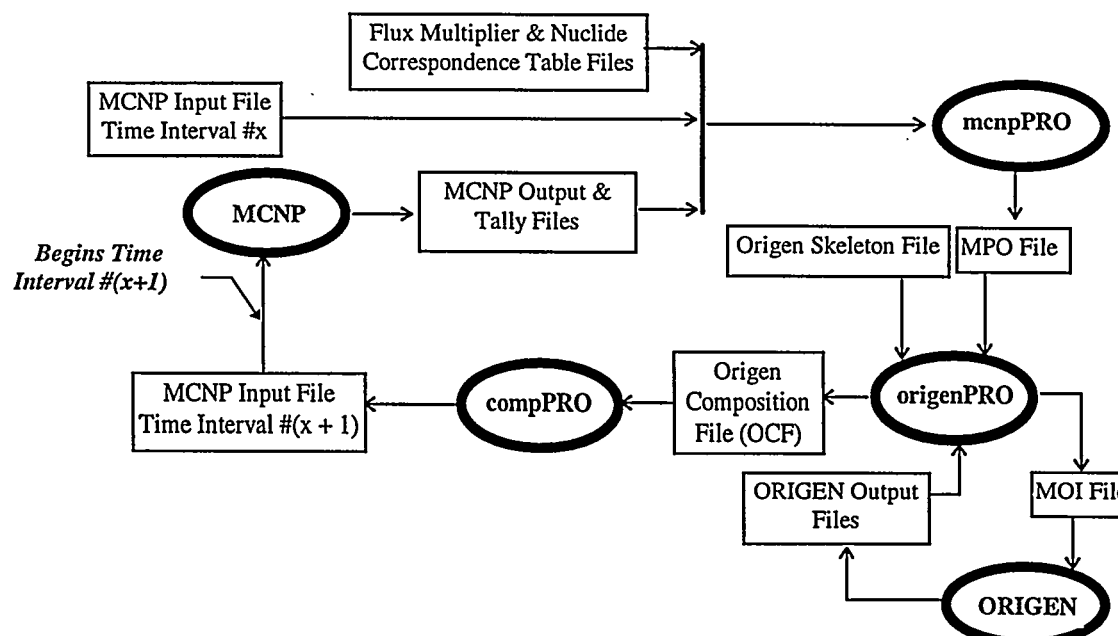


Figure 5.2 Detailed Flow Chart of MOCUP, MCNP, ORIGEN and User Supplied Files

The user specifies the cell flux, cell volume and nuclide reaction rates to be calculated via specifically formatted comment card text strings in the MCNP input file. The mcnpPRO module input includes the MCNP generated input and output files along with specifically formatted flux multiplier and nuclide correspondence tables generated by the user. The flux multiplier table contains flux normalization factors for each cell being depleted and the nuclide correspondence table provides the ORIGEN nuclide identifiers which correspond to MCNP nuclide identifiers (i.e. ZAIDs). The mcnpPRO module calculates one group cross sections by dividing each nuclide reaction rate by the flux, both of which it reads from the MCNP tally file. The cell volume, read from the MCNP output file, flux and one group cross sections are written to a MOCUP intermediate mcnpPRO output file (MPO).

The origenPRO module combines composition information, mcnpPRO output and a user supplied ORIGEN skeletal input file to produce the Modified ORIGEN Input file (MOI). Composition information is extracted from the MCNP input file for the time zero interval and thereafter from an ORIGEN Composition File, (OCF), it generates at the end of each ORIGEN depletion run. The ORIGEN skeletal file contains standard ORIGEN input parameters with the exception of composition and substitute cross section card information. The origenPRO module extracts the cross section and composition information from the MPO file and writes it to the MOI file; origenPRO then runs ORIGEN via a user modified script file, and uniquely renames the ORIGEN output files to correspond to the time step and MCNP cell depleted. It also extracts the composition information from the ORIGEN output file and generates the OCF to be integrated into the ORIGEN skeletal file by origenPRO during the next time interval.

The third module, compPRO, reads the composition information from the OCF files and updates the MCNP depletion cell nuclide compositions producing a new MCNP input file for the next time interval. One clockwise revolution around figure 5.2, beginning with the MCNP input files and ending with the compPRO output of the MCNP input file for the next time interval, equates to one time interval. The process is repeated for multiple depletion intervals ranging in

length from tenths of a GWd/MT during the initial burn-in period to several GWd/MT between cross section updates later in the cycle.

5.1.2 Selection of Key Nuclides. ORIGEN calculates the transmutation, decay and production of over 1700 nuclides. Thus, the composition information for virtually all nuclides are automatically tracked through the depletion calculations. However, a small subset are of specific interest or have a sufficient macroscopic cross section to significantly affect the reactivity and depletion behavior of the fuel. Hence, the number of nuclides for which one group cross sections must be calculated through MOCUP and MCNP can be greatly reduced without significant error.¹ The remaining nuclide cross sections can be drawn from the original ORIGEN library without appreciable effect on the resultant depletion reactivity and composition information.

The nuclides for which cross section information must be supplied to ORIGEN are selected based on four criteria: magnitude of effect on reactivity, importance of the nuclide itself or as part of a chain producing other important nuclides, and availability of MCNP cross section data. Actinides with $90 \leq Z \leq 96$ are tracked because they are of interest. Calculation of the cross sections for all the fission products would ensure that all reactivity effects were accounted for. However, this would be inordinately cumbersome and not all fission products need be tracked to account for the vast majority of fission product impact on reactivity. Selection of the key fission products most responsible for the overall fission product effect on reactivity is an iterative process.

ORIGEN produces an output table listing fractional neutron absorptions by fission product nuclides. Using this table, a list of fission products for which MCNP derived cross sections are to be used can be compiled. Initially, the set of fission product nuclides individually responsible for greater than 0.1% of neutron absorptions at the EOC are selected. The depletion calculations are then repeated, providing ORIGEN with MCNP derived cross sections for the nuclides selected. The ORIGEN neutron absorption table is re-checked, a new list compiled, and the depletion calculations repeated. After a few iterations, a definitive set of key fission products to be tracked

¹ A benchmark was conducted and errors quantified. See section 5.2.

can be distilled. The set of fission product nuclides listed in table 5.1 account for more than 95% of all fission product neutron absorptions. The cross sections for these fission products are calculated using MCNP data. The remaining fission product cross sections are used directly from the ORIGEN library: hence, no fission products are neglected. The less critical fission products are included on an approximate level.

Table 5.1 Selected Fission Products

Kr83	Ag109	Nd143	Sm150
Zr93	I129	Nd145	Sm151
Tc99	Xe131	Nd147	Eu151
Ru101	Cs133	Pm147	Sm152
Ru103	Cs134	Sm147	Eu153
Rh103	I135	Nd148	Eu154
Rh105	Xe135	Pm148	Eu155
Pd105	Cs135	Pm149	Gd157
Pd108	Pr141	Sm149	

5.2 Benchmark Calculations

A benchmark of the MCNP version 4A, ORIGEN version 2.1 and MOCUP depletion code system described in section 5.1 is presented. This section first describes the specifications and then the results of a PWR pin cell benchmark calculation..

5.2.1 Description of Benchmark and Specifications. Initial novel fuel compositions were screened using a PWR pin cell model benchmark described in EPRI report NP-6147 vol. 1 & 2 with amplifying information found in an ECN report ECN-C-93-088 [F-2, G-6]. Table 5.2 provides the pin cell specifications and table 5.3 lists the nuclide number densities used for the initial MCNP input file. The temperatures listed in table 5.2 indicate the temperature at which available MCNP ENDF V cross sections were evaluated. The temperature of the materials themselves were set equal to the benchmark value and the densities used were exactly those defined in the ECN report as listed in table 5.3.

The MCNP PWR pin cell model consists of a cylindrical fuel rod surrounded by a concentric cladding cylinder which is in turn encased in a square cell filled with light water moderator. The cell is modeled as 25 cm long with reflective boundary conditions at the axial ends and sides of the square cell (hence as an infinite lattice). The initial source neutron particle distribution is staggered every 4 cm to effect efficient sampling. The EPRI report pin cell differs in that the square water box is approximated by an equivalent diameter concentric annular cylinder and white or isotropic boundary conditions; this is known as the Wigner-Seitz approximation of an infinite square lattice. The square cell used here is a more precise physical representation of an infinite square lattice [G-6]. The impact of this difference is discussed in detail later. Figure 5.3 is a cross section of the cell as modeled with MCNP.

Table 5.2. Benchmark Pin Cell Specifications

Parameter	Benchmark Value	As Used Value
Dimensions (cm)		
Hot Fuel Radius	0.41169	0.41169
Hot Clad Inner Radius	0.41169	0.41169
Hot Clad O.R.	0.47587	0.47587
Hot Pin Pitch	1.25984	1.25984
Temperatures (°K)		
Fuel	922.04	900
Clad	614.04	600
Moderator	572.04	600
Materials		
Fuel	UO ₂	UO ₂
Fuel Density	10.142603	10.1431
Enrichment	3.9%	3.9%
Cladding	Zr-2	Zr-Nat
Moderator	light water	light water
Moderator Boron (ppm)	500	500
Specific Power (W/gU)	43.72	43.72

Table 5.3. Pin Cell Nuclide Densities

Nuclide	Density (nuclei/cm ³)
²³⁴ U	7.17941E+18
²³⁵ U	8.93440E+20
²³⁸ U	2.17301E+22
¹⁶ O	4.52432E+22
Zr-Nat	3.87351E+22
¹ H	4.87183E+22
¹⁶ O (mod)	2.43608E+22
¹⁰ B (mod)	4.01063E+19
¹¹ B (mod)	1.62861E+19

Table 5.4 presents the as-modeled specifications of the pin cell. As indicated in Table 5.3, a 43.72 W/gm U constant specific power is required. For a constant number density, the cell volume fixes the mass of the uranium in the MCNP pin cell. The 43.72 W/gmU equivalent for the ORIGEN fuel cell power is 5.204E-3 MW. The ORIGEN constant power IRP command was used. A pin power of 5.204E-3 MW equates to a burnup rate of 22.87 days per gigawatt-day/metric ton of heavy metal (GWd/MT). Thus, the ORIGEN skeletal files required by MOCUP were constructed based on a 22.87 day unit of time.

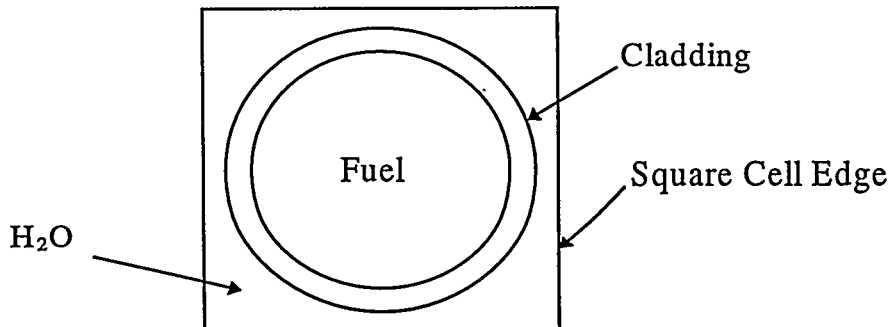


Figure 5.3. MCNP PWR Pin Cell Cross Section

The original purpose of the EPRI benchmark study was to investigate variations in reactivity and burnup results between the technical staffs of different utilities. A consortium of utilities performed controlled calculations on PWR pin cells. Infinite multiplication constant

(K_{inf}) values were reported as a function of burnup for five codes: Cell2 using ENDF/B-V cross section data, ECELL using STD cross section data, CASMO2 using both CASMO2 and alternately CPM cross section data, CPM2 with CPM data and CASMO3 with CASMO3 data. In the following discussion of results, reactivity (ρ) units were derived from K_{inf} values for plotting purposes due to the more convenient near-linear function of reactivity change with burnup.

Table 5.4. Pin Cell Model Specifications

Parameter	Value
Fuel Cell Volume	13.3116 cm ³
Fuel Mass	135.021 gms
Uranium (Heavy Metal) Mass	119.022 gms
Cell Power	5.20366E-3 MW
Burnup Rate	22.87 days = 1 GWd/MT

5.2.2 Benchmark Results. The largest and smallest reported ρ values were extracted from the EPRI report at each burnup to serve as reference brackets for comparison with MOCUP ρ values. Figure 5.4 and 5.5 present the results from an early benchmark run. Note in figure 5.4, the initial ρ is greater than the high reference value, indicating a need for model refinement. Figure 5.4 also shows some random oscillation in the values. These oscillations are more pronounced in figure 5.5. Figure 5.5 is a plot of the difference between the average reference value and the high benchmark, low benchmark and MOCUP reactivity values as a function of burnup. The oscillating line is the difference between the average reference reactivity and the MOCUP calculated pin cell reactivity. Note that the amplitude of the oscillations increases with burnup.

Figure 5.4. Benchmark PWR Pin Cell Reactivity vs Burnup

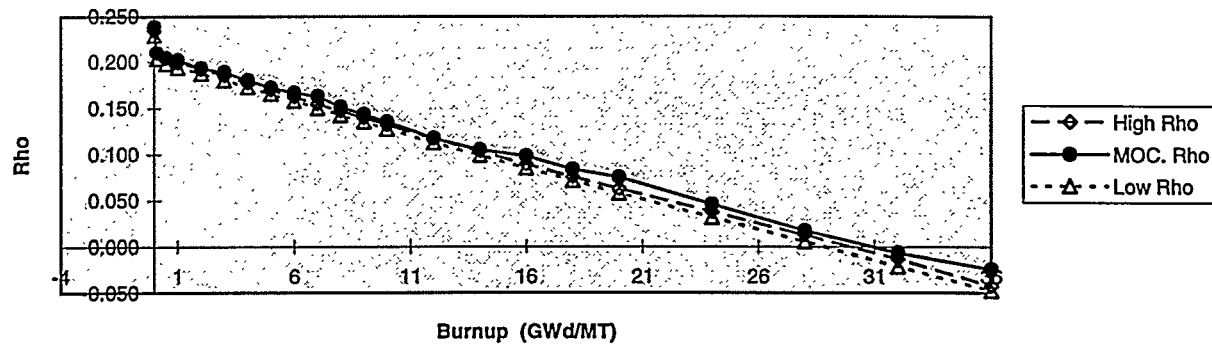
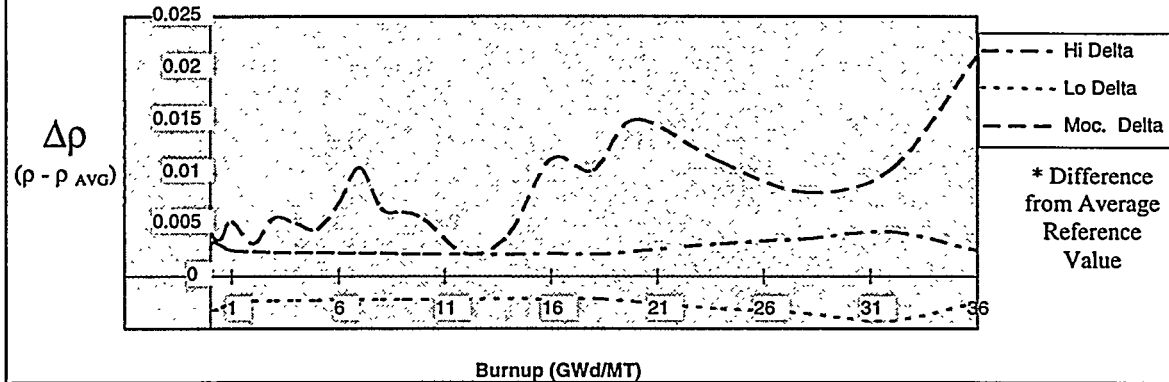


Figure 5.5. Hi Ref., Lo Ref. and MOCUP Reactivity Difference* vs. Burnup



Since MCNP is a Monte Carlo code, its results are statistical in nature. The precision of values is measured as a relative error and is dependent on the number of samples, known as neutron history tracks, used to produce the results [B-5]. This relationship is quantified by:

$$R \equiv S\bar{x} / \bar{X} \quad (5.1)$$

$$R \propto (1 / \sqrt{N}) \quad (5.2)$$

where N is the number of histories, R is the relative error, S_x is the standard deviation of the mean and X is the estimated mean value. The relative error is reported as a percentage of the mean. Thus, a value of 100 with a relative error of 0.10 means that there is 68% confidence that

the true value lies in the interval from 90 to 110 and 95% that the value is between 80 and 120. Equation 5.2 implies that in order to halve the relative error the number of histories run must be increased by a factor of four. The resulting increase in the computer processing unit time illustrates the weakness of Monte Carlo methods. This relative error in the MCNP flux and reaction rate calculations is passed on through MOCUP to ORIGEN where they are propagated in the depletion calculations and eventually result in the oscillations seen in figures 5.4 & 5.5. The import of these oscillations in terms of the reliability of the results is addressed in detail later.

Two modifications were made to the initial MCNP model and a second set of benchmark calculations conducted. First, the MCNP neutron thermal scattering tables option for the light water moderator was selected. These tables provide more exact scattering cross section values below 4ev. This refined light water thermal scattering treatment reduces the zero burnup K_{inf} from 1.13 to 1.30, which falls within the brackets of the lowest and highest EPRI reported values. Second, the number of MCNP histories per MOCUP time interval were increased from 52,250 to 300,000. This is expected to produce a reduction in the relative error for flux and reaction rate values by $\{1/(5.71)^{1/2}\}$ or a factor of 2.4. Table 5.5 compares the relative errors for the 52,250 and 300,000 history MCNP calculations for some key nuclide reactions calculated at a burnup of 10 GWd/MT. The reduction in relative error is slightly better than expected.

Figure 5.6 compares the reactivity results of this second set of benchmark depletion calculations with the reference benchmark values as a function of fuel burnup. There is better overall agreement due to the enhanced light water scattering treatment used in this set of MCNP calculations.

Table 5.5. Comparison of Relative Errors @ 10GWd/MT

# Histories used	52,250	300,000	Decrease Factor
Flux	0.0021	0.0008	2.63
(n, Gamma)			
^{235}U	0.0044	0.0017	2.59
^{238}U	0.0056	0.0023	3.29
^{239}Pu	0.0062	0.0025	2.48
^{240}Pu	0.00193	0.0072	2.68
^{241}Pu	0.0057	0.0023	2.48
Average	0.00866	0.0032	2.71
Total Fission			
^{235}U	0.0051	0.002	2.55
^{238}U	0.0073	0.0029	2.52
^{239}Pu	0.0058	0.0023	2.52
^{240}Pu	0.0046	0.0017	2.71
^{241}Pu	0.0053	0.0021	2.52
Average	0.00562	0.0022	2.55

Figure 5.6. Benchmark of Reactivity vs Burnup

(w/MCNP thermal scattering treatment)

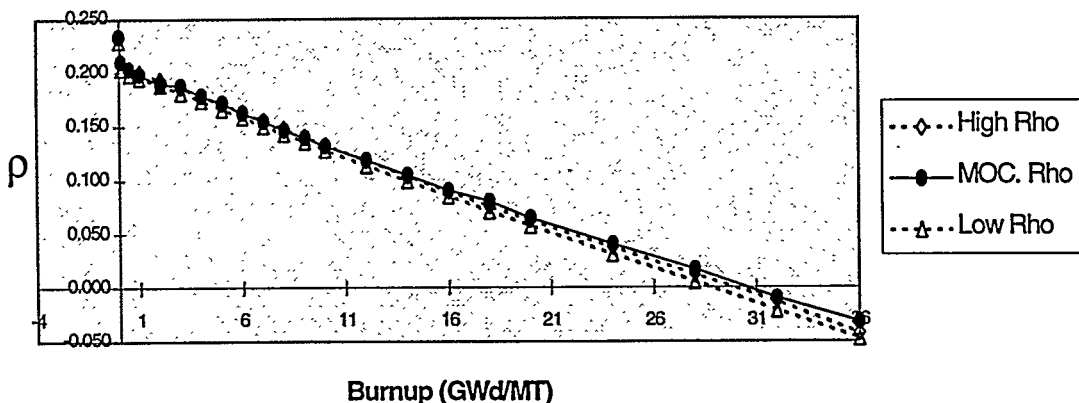


Figure 5.7 demonstrates the effect of reduced MCNP tally flux and reaction rate relative errors on the oscillations. Comparison of figures 5.5 & 5.7 reveals the effects of the two changes in the MCNP runs of the two set of benchmark calculations. First, figure 5.7 reactivity values start off

within the benchmark reference brackets. Secondly, although the oscillation patterns are similar, it is important to note the reduction in their magnitude from a maximum at 36 GWd/MT of approximately 0.021 to 0.013 (difference between MOCUP reactivity and the average of the reference values). This reduction can be attributed to reduced relative flux and reaction rate errors as a consequence of the larger number of MCNP histories run in the calculations represented in Figure 5.7. Producing accurate nuclide composition vs burnup data is critical to evaluation of deep burn plutonium disposition options. Hence, a CASMO-3 model of the PWR pin cell was also run to provide isotopic composition information as a function of burnup for comparison with the MOCUP system results. Figure 5.8 presents a comparison of results generated by the MOCUP system and CASMO for key nuclide and total fission product fuel weight percents at selected burnups. The shaded regions are the difference between the MOCUP and CASMO values. At the end of 36GWd/MT all nuclide compositions agree within 0.02% with the exception of ^{238}U . The discrepancy between MOCUP and CASMO3 ^{238}U composition grows consistently with burnup to reach a -0.11w% difference at 36GWd/MT. Likewise, the difference in fission product weight percents grow steadily with burnup to reach 0.07 w% at 36GWd/MT.

Figure 5.7 Hi, Lo, and MOCUP Reactivity Difference* vs Burnup
(w/MCNP thermal treatment and increased # of

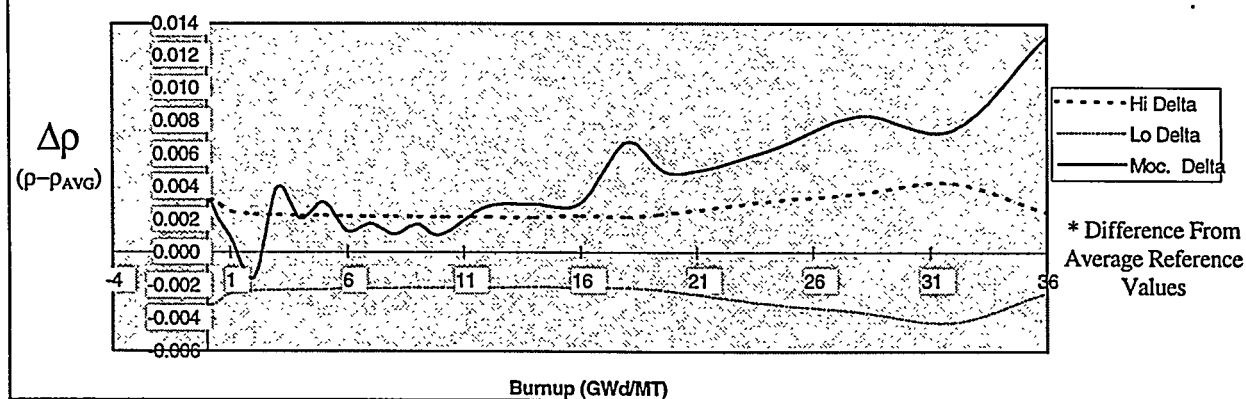


Figure 5.8 Comparison of CASMO and MOcup Normalized* Actinide & FP Weight %vs Burnup For PWR Pin Cell												
Nuclide GWd/MT:	Burnup (GWd/MT)				5							
	1		2		3		5		Casmo		Diff.	
Actinides	Casmo	Diff.	Moocup	Casmo	Diff.	Moocup	Casmo	Diff.	Moocup	Casmo	Diff.	Moocup
92235	3.784%	0.001%	3.785%	3.676%	-0.001%	3.675%	3.570%	-0.002%	3.568%	3.367%	-0.003%	3.364%
92238	96.113%	-0.013%	96.100%	96.149%	-0.009%	96.140%	96.183%	-0.003%	96.180%	96.252%	-0.012%	96.240%
94238	negligible		negligible	negligible		negligible	negligible		negligible	negligible		negligible
94239	0.046%	0.000%	0.047%	0.097%	-0.001%	0.097%	0.142%	0.000%	0.142%	0.224%	-0.002%	0.223%
94240	0.001%	0.000%	0.001%	0.003%	-0.001%	0.004%	0.007%	0.000%	0.008%	0.017%	0.001%	0.018%
94241	negligible		negligible	negligible		negligible	0.001%	0.000%	0.001%	0.004%	0.001%	0.005%
94242	negligible		negligible	negligible		negligible	negligible		negligible	negligible		negligible
Total Actinide Mass (gms):	118.90			118.70			118.60			118.40		
Fission Products												
Total gms:		1.22E-01			2.48E-01			3.72E-01			6.19E-01	
Weight %:	0.112%	-0.010%	0.102%	0.217%	-0.009%	0.208%	0.320%	-0.008%	0.312%	0.529%	-0.009%	0.520%
GWd/MT:		10			16			24			36	
Actinides	Casmo	Diff.	Moocup	Casmo	Diff.	Moocup	Casmo	Diff.	Moocup	Casmo	Diff.	Moocup
92235	2.906%	-0.002%	2.904%	2.425%	0.001%	2.426%	1.884%	0.007%	1.891%	1.252%	0.016%	1.268%
92238	96.416%	-0.016%	96.400%	96.597%	-0.027%	96.570%	96.814%	-0.054%	96.760%	97.083%	-0.113%	96.970%
94238	0.001%	0.000%	0.001%	0.002%	0.000%	0.002%	0.007%	-0.001%	0.006%	0.019%	-0.002%	0.017%
94239	0.381%	-0.004%	0.377%	0.508%	-0.004%	0.503%	0.611%	-0.002%	0.609%	0.687%	0.008%	0.695%
94240	0.052%	0.000%	0.052%	0.099%	0.000%	0.098%	0.160%	-0.001%	0.159%	0.242%	-0.001%	0.241%
94241	0.020%	0.002%	0.022%	0.051%	0.004%	0.055%	0.097%	0.005%	0.102%	0.161%	0.004%	0.166%
94242	0.001%	0.001%	0.002%	0.005%	0.002%	0.007%	0.016%	0.004%	0.020%	0.046%	0.006%	0.052%
Total Actinide Mass (gms):	117.80			117.00			116.00			114.6		
Fission Products												
Total gms:		1.24E+00			1.97E+00			2.95E+00			4.42E+00	
Weight %:	1.050%	-0.012%	1.038%	1.678%	-0.020%	1.658%	2.518%	-0.035%	2.483%	3.783%	-0.070%	3.713%

*Notes:

1. Actinide weight percents are self normalized to unity (not all actinides are listed in table)
2. Fission Product weight percents are normalized as follows:
Actinides weight % + Fission Product weight % = 100%

5.2.3 Discussion of Benchmark Results. Error propagation can be managed in two ways. Equation 5.1 shows that increasing the number of MCNP histories used in each time interval produces more precise reaction rate and flux values. Running a large number of MCNP histories is expensive in computer time and is not required for all depletions. In practice, rough screening calculations were completed using only a moderate number of histories. Promising results were subsequently checked and refined using a large number of histories. MCNP relative errors propagate with the number of ORIGEN time steps. However, too few ORIGEN time steps can produce errors resulting from the matrix exponential method used in ORIGEN [M-4]. A balance must be struck between the MCNP error propagation and the number of ORIGEN time steps to reduce the overall error.

Assuming valid modeling, MCNP tally results are considered precise and reliable if the relative error is ≤ 0.05 . However, the propagation of a 0.05 relative error through multiple ORIGEN depletion time steps results in an unacceptably high relative error in the output

composition as evidenced in figure 5.5. The MOCUP user manual recommends a relative error in the flux and reaction rate calculations of less than 1% [M-4]. Theoretically, a 1% relative error in the flux and cross section could propagate through five ORIGEN time steps to produce a 3.2% relative error in resultant ORIGEN output composition. Considering that the 36GWd/MT depletion of the PWR pin cell took 23 MOCUP time intervals with a total of roughly 200 ORIGEN depletion steps, one begins to question the validity of this depletion scheme. However, the composition data calculated via MOCUP shows stable trends and excellent agreement with CASMO data as a result of the self correcting nature of depletion calculations.

Relative error is a misnomer. What is really being described is confidence intervals. The true value could very well be the exact value calculated. In practice these errors will be random and will tend to be self correcting. Underestimation of a reaction rate and hence the cross section will result in under-depletion of that nuclide in a time interval. This will produce a reaction rate higher than the true value leading to accelerated depletion in the following time interval. The higher reaction rate will produce a larger cross section causing acceleration of the depletion of the nuclide in the next time step. This is why the error curves in figures 5.4 and 5.5 show oscillations that tend back toward zero. The random nature of the relative error in the MCNP calculations produces the irregular nature of the oscillations.

Note that at 36 GWd/MT, the figure 5.7, delta rho value is reduced by a factor of 1.6 relative to figure 5.5. This reduction is accomplished through an increase in the number of MCNP histories run by a factor of 5.7 which reduced the relative error of individual reaction rate calculations by a factor of approximately 2.6.

The EPRI report codes are multi-group, deterministic codes while MCNP uses fewer approximations because it is a continuous energy, Monte Carlo code. Thus, the EPRI codes and MCNP determine the quantities of interest through fundamentally different techniques. This results in some systematic differences in their results. MCNP is generally considered the reference tool against which other codes are checked [G-6].

The EPRI report codes were limited in capability to a Wigner-Seitz cylindrical pin cell approximation with white/isotropic boundary conditions. The square cell modeled in MCNP is a more accurate representation of actual square lattices found in PWRs. Comparisons of the results produced by these two cell models indicate that the Wigner-Seitz cell Kinf may be as much as 0.3% lower than a cell with identical specifications modeled as a square cell [G-6]. Further examination revealed that part of this difference may be found in differences in ^{238}U resonance absorptions. DE Kruijf et al. reported that two MCNP models, one with square cell reflective boundary conditions and one with cylindrical isotropic boundary conditions but identical in all other respects, were run using approximately 30 million histories to produce small relative errors [D-5, D-6]. The cylindrical model produced 1.3% higher absorptions resulting in an underestimation of the escape probability, p , of 0.34% and a 0.0034 lower Kinf value. This readily explains why the MCNP Kinf is at the upper edge of the benchmark range for fresh fuel. At 36 GWd/MT burnup, the MOCUP Kinf is 0.012 units or 1.25% greater than the average reference benchmark value. Thus, this systematic difference between the EPRI code techniques and MCNP cannot completely account for the high MOCUP Kinf value at the end of the burnup period.

The difference in fission product weight percent is not surprising. Fission products (as well as actinides) are handled explicitly in the MOCUP system. ORIGEN calculates fission production, decay and transmutation reactions during an individual burnup step for each nuclide and then sums the results to produce their new concentrations. Similar to the ECN and other benchmark work, thirty-five fission product nuclides were selected for MOCUP tracking. At the start of each time interval, the fission product absorption rates were calculated by MCNP, corresponding cross sections were calculated by mcnpPRO and input into ORIGEN by ORIGENPRO. The end of step compositions were updated in the MCNP input for the next time interval. These thirty-five fission products accounted for an average of 95% of the total fission product absorption. Thus, the MOCUP system allowed for very specific modeling of fission product composition and absorptions.

In contrast, CASMO uses decay and production chains to predict a cumulative yield of 23 individual nuclides and two lumped fission products. Significant differences in the ORIGEN and CASMO libraries have been reported. For example, Gruppelar et al. (1993) report a ^{155}Eu CASMO yield of 6.08E-7 as compared to the ORIGEN yield of 1.63E-8 [G-6]. This leads to a factor of two difference in the CASMO and ORIGEN ^{155}Eu concentrations. Surprisingly, the CASMO concentration is the lower of the two. The ^{155}Eu capture cross sections provides the answer. The CASMO ^{155}Eu cross section is 4.09E3 barns compared to ORIGEN's 3.63E3 barns. To further illustrate the potential magnitude of the differences in fission product cross section libraries, the WIMS cross section libraries have a ^{155}Eu capture cross section of 1.19E4, a factor of three higher than ORIGEN. These sorts of differences in fission product treatment and library values cause the consistently growing discrepancy between MOCUP and CASMO fission product weight percents. The lower fission product weight percent in MOCUP in turn leads to a trend of increasingly higher K_{inf} values relative to the benchmarks. The oscillations caused by the relative error propagation are superimposed on and somewhat mask this trend.

The very slightly low MOCUP ^{238}U concentration contradicts the higher ^{238}U resonance absorption caused by the previously discussed Wigner-Seitz approximation. This can not be readily explained but is not of sufficient magnitude to be of concern here. One possible explanation is that the resonance absorption difference is overcome by relative error oscillations. Similarly, the differences in ^{235}U and ^{239}Pu compositions are small and appear to be artifacts of the relative error oscillations.

5.2.4 Conclusions of Benchmark Calculations. The MCNP, ORIGEN, MOCUP code system has demonstrated a good ability to reproduce expected reactivity and isotopic results for PWR pin cell depletion. It has the advantage of not requiring multi-group and geometry approximations as well as an extensive cross section library. Relative error is a concern but can be managed through judicious use of ORIGEN time steps and specification of a sufficient number of MCNP histories to refine rough results.

Section 5.3 reviews the models and calculation techniques used to develop and evaluate the non-uranium plutonium deep burn PWR peripheral cycle advocated here.

5.3 Models and Techniques

This section describes the use of four different PWR models - an MCNP pin cell, an MCNP 34 pin model, a CASMO3 pin cell model, and an MCNP 1/8th symmetry core model - in the development of the proposed non-uranium fuel to be used in the periphery of PWRs to substantially eliminate plutonium. These models were used to determine the neutronic characteristics of the fuel as a function of burnup as well as to evaluate how it would interact with the non-peripheral fuel assemblies in the PWR core.

Chapter 4 discusses some of the specific neutronic challenges presented in using a PWR core partially loaded with non-uranium plutonium fuel. WGPu contains substantially less ^{240}Pu than RGPu. ^{240}Pu assists in holding down excess reactivity and providing resonance absorptions which make moderator and fuel temperature coefficients more negative. Thus, these neutronic challenges are greater for WGPu isotopics. Accordingly, all calculations were carried out using WGPu isotopics in order to be conservative. Specifically the following data are calculated: pin to pin power peaking factors, discharge isotopics, the fuel reactivity vs. burnup profile and reactivity coefficients. The following sections describe each of the four models and how they are used to calculate the required information. All the models are based on a PWR comprised of a standard 17 x 17 Westinghouse assemblies. The characteristics of the core and assemblies are listed in table 5.6. Fuel compositions are developed to support an 18 month fuel cycle with a capacity factor of 0.8. Burnup is usually measured in MWd/MT, however, non-uranium fuel has a much lower heavy metal content than standard UO_2 . Consequently, burnup is measured in units of effective full power days (EFPD) to provide a consistent basis for comparison. One EFPD is equal to the burnup achieved when one pin is run at core average 100% power (i.e. $q' = 5.688 \text{ Kw/ft}$) for one day. Thus, the base 18 month fuel cycle is repeated at 440 EFPD long periods. In other words,

the fuels must be developed to support core residence times which are multiples of 440 EFPD. The next sub-section details how depletion calculations were conducted.

Table 5.6 Westinghouse Core and Assembly Design Parameters

Design Parameter	Value
Number of Assemblies per Core	193 assemblies
Assembly Type	square, 17 x 17 rod slots
Number of Fueled Rods per Assembly	264 rods
Overall Outside Assembly Dimensions	21.4 cm
Number of Rods per Core	50,952 rods
Rod Pitch	1.26 cm
Rod Outside Diameter	0.9497 cm
Clad Thickness	0.0572 cm
Clad Material	Zircaloy-4
Gap Thickness	0.01651 cm
Core Average Linear Power	5.688 Kw/ft

5.3.1 MCNP 34 Pin Model Power Peaking Calculations. As discussed in chapter 4, the large thermal fission cross section of plutonium can produce significant power peaking in the plutonium pins adjacent to UO_2 assemblies. Thus, finding a plutonium fuel composition which produces acceptable pin to pin radial power peaking is a key development criteria. Figure 5.9 has two drawings of the same 34 pin model which simulates a single row of pins across two 1 x 17 assemblies; the upper picture is the full length 34 pin model and lower picture is a close-up truncated view. This 34 pin model is used to determine pin to pin power peaking and facilitates a detailed look at the interface region. The model simulates the interface between a peripheral assembly and its radially adjacent inboard assembly. The dashed line in the lower close-up view indicates where the row is truncated. Candidate non-uranium plutonium fuel compositions are loaded into the 17 peripheral assembly pins adjacent to the core reflector region. These 17 pins simulate a peripheral plutonium assembly. The left 17 pins adjacent to the core interior are loaded with standard 3.9 w% UO_2 . A reflected boundary condition is imposed on the left most

model surface adjacent to the core interior. Thus, the inner 17 UO₂ pins simulate the rest of the PWR core interior. The assembly dimensions, core baffle plate, reflector region and core barrel are explicitly modeled to simulate the Westinghouse Seabrook PWR. The moderator is H₂O with 500 ppm boron. This model is used in the first step of the depletion process.

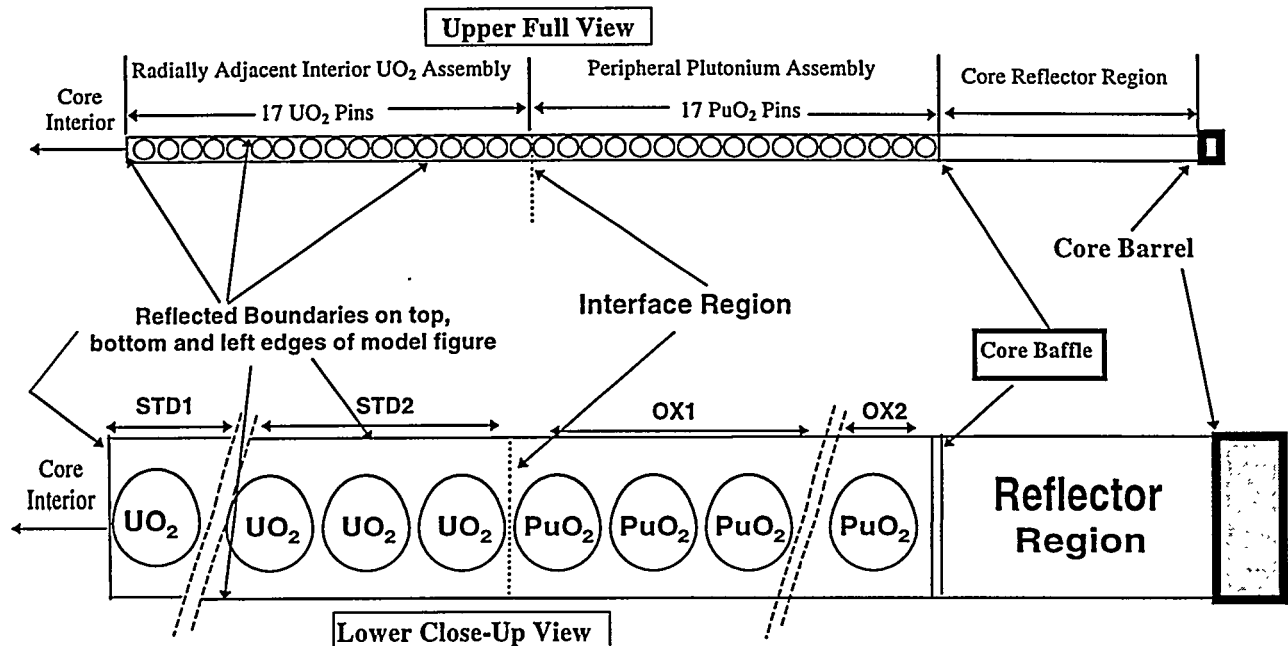


Figure 5.9. MCNP 34 Pin Row, Two Assembly Pin Model

Fresh non-uranium candidate fuels are loaded into the outer (right) 17 PuO₂ pin slots with fresh 3.9 w% UO₂ in the inner (left) 17 pin slots.. The MCNP model is run and the power deposited in each of the 34 pins is tallied. Peripheral assemblies comprise roughly 25% of the total number of assemblies in a core. Thus, the 17 interior UO₂ pins represent 3/4 and the 17 PuO₂ outer pins represent 1/4 of the total number of pins in the core. The power deposited in each pin is normalized to the core average pin power to produce a radial peaking factor for each pin. The core average pin power is calculated by:

$$\text{Core Average Pin Power} = \frac{\{[(\text{average power in UO}_2 \text{ pins}) \times 3] + (\text{average power in PuO}_2 \text{ pins})\}}{4} \quad (5.1)$$

The individual pin power radial peaking factors are then calculated relative to the core average pin power by:

$$\text{Radial Pin Power Peaking Factor} = \frac{\text{(individual pin power)}}{\text{(core average pin power)}} \quad (5.2)$$

The peaking factors are plotted against their radial location in the model. Seabrook fuel management calculations set a 1.5 maximum radial pin peaking factor to ensure that the overall highest peaking factor is less than 2.5 when combined with axial peaking factors. A 1.5 maximum radial peaking factor was adopted here. In addition to the power, the fast and thermal flux for each pin are also tallied and normalized to the core average. Figure 5.10 shows typical resultant power, thermal and fast flux profiles. The ordinate axis values are the pin values normalized to core average values. The abscissa values are the pin numbers from pin number one, which correlates to the left-most UO₂ pin directly adjacent to the reflected left vertical core interior surface in Figure 5.9, to pin number 34, which correlates to the right-most PuO₂ pin directly adjacent to the core baffle. The interface is marked by the dashed line to the left of the first PuO₂ pin (adjacent to the UO₂ assembly) which is pin number 18. As expected, the thermal flux decreases sharply at the interface due to the larger thermal absorption cross section of ²³⁹Pu relative to ²³⁵U. The fast flux remains unaffected by the interface, displaying a standard radial cosine flux shape at the core periphery. Looking at the power peaking moving radially outward from pin number 18 to 34, the power peaks in pin number 18 because of the plutonium fuel and still relatively large thermal flux. The power then drops in pin number 19 which has the same WGpu loading as pin number 18 but sees a lower thermal flux due to the shielding by pin number 18. Pin number 20 produces a second power peak because it has three times the ²³⁹Pu number density of pins number 19 and 18. The power drops off in pins 21 through 34 which have the same ²³⁹Pu number density as pin number 20 but see a decreasing thermal flux due to increased shielding by the inboard PuO₂ pins.

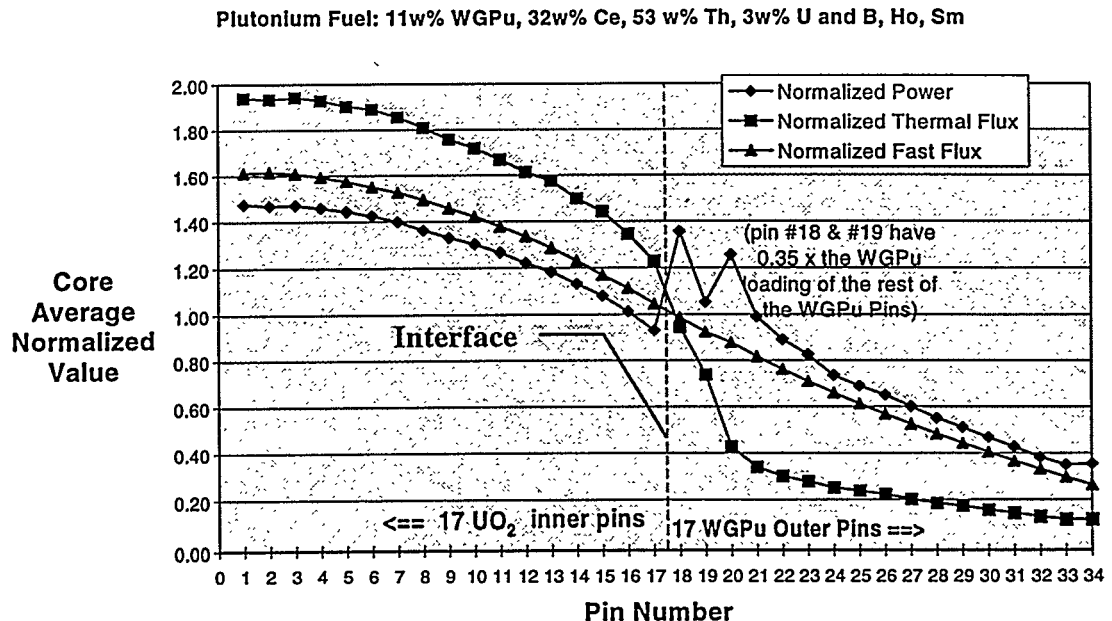


Figure 5.10 Example Pin Radial Power, Thermal and Fast Flux 34 Pin Model Results

The 34 pin model is used to determine the pin power relative to core average. The actual pin power is the product of the pin's peaking factor and the assumed core average linear power, 5.688 Kw/ft. This power is assumed constant over a MOCUP depletion time interval and used to perform depletion calculations using the MCNP Pin Cell model and ORIGEN. Running individual depletion calculations on each of the 34 pins would require 34 MCNP pin cell and ORIGEN calculations for each time interval. This is avoided by using the average power over a number of pins and depleting them as one composite pin. Four pin cell models are used to deplete the 34 pins. Referring to figure 5.9, UO₂ pins numbered 1 through nine are depleted as one pin labeled STD1. Similarly, UO₂ pins 10 through 17 are depleted as STD2, PuO₂ pins 18 through 24 are depleted as OX1 and pins 25 through 34 are depleted as OX2. These composite pins are depleted using the PWR Pin Cell Model.

5.3.2 Pin Cell Depletion & Reactivity Calculations. The MCNP pin cell model is similar to the benchmark pin cell described in section 5.2.1 with the addition of a concentric gap as shown in

figure 5.11. Table 5.7 lists the specifications. Depletions are carried out on the pin cell with the MOCUP MCNP-ORIGEN coupled codes as described in section 5.1.1.

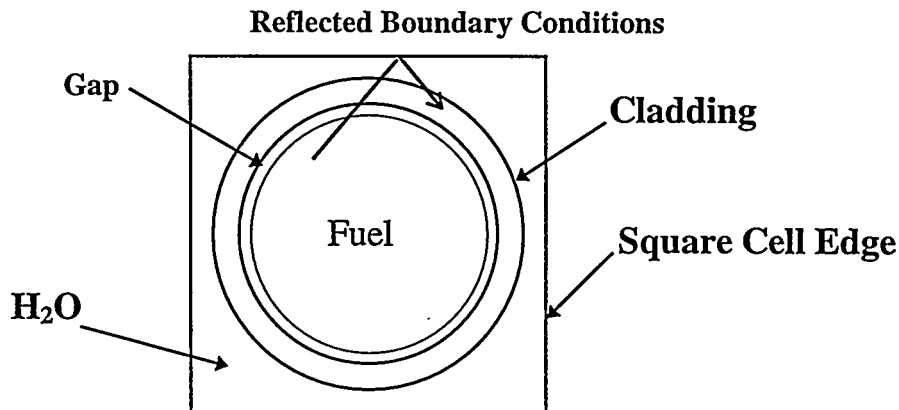


Figure 5.11 MCNP PWR Pin Cell Cross Section

Figure 5.12 summarizes the algorithm for using the 34 pin and pin cell MCNP models with MOCUP and ORIGEN to deplete fuel. The depletion cycle is started by loading the 34 pin model with fresh fuel compositions and determining individual and composite average pin powers. The fuel compositions for the four composite pins, STD1, STD2, OX1 and OX2, are subsequently loaded into four different MCNP pin cell models. Initially, the fresh fuel composition of STD1 and STD2 are the same and equal that of standard 3.9w% UO₂. Similarly, the compositions of fresh OX1 and OX2 plutonium oxide non-uranium fuels are the same. The average pin power of the pins represented by each of the four composite pins is calculated from the 34 pin model individual pin powers as described in sub-section 5.3.1. The corresponding average pin power is assigned to each of the four composite pins and is assumed constant during the subsequent ORIGEN depletion. The four pins are depleted at that power for a single MOCUP time interval following the process described in section 5.1.1. Since the pin powers for the four composite pins differ, the composition of all four pins will be different after the first depletion interval. The four resultant post-depletion composite pin compositions are loaded back into their associated 34 pin model pins, the radial peaking factors are checked and a new set of composite pin powers are calculated for the next time interval. The fuel is depleted via several time interval

cycles. The loop repeats until the fuel has been depleted to the desired number of EFPD or the maximum radial peaking factor of 1.5 is exceeded. The length of a MOCUP time interval depends on the previously accumulated burnup.

Table 5.7. MCNP Model Pin Cell Specifications

Parameter	Model Value
Dimensions (cm)	
Hot Fuel Radius	0.40132
Gap Outer Radius	0.41783
Hot Clad O.R.	0.47498
Hot Pin Pitch	1.2598
Temperatures (°K)	
Fuel	922.04
Clad	600
Moderator	600
Materials	
Fuel	non-uranium Pu fuel
Fuel Density	function of matrix
Enrichment	variable
Cladding	Zr-2
Moderator	light water
Moderator Boron (ppm)	500
Core Average Power (Kw/ft)	5.688

The length of the depletion time interval is chosen to be less than 10% of the total discharge burnup (as described in section 5.1.1) but also depends on the previously accumulated burnup. During the first approximately 50 EFPD, the composition of the fuel is rapidly changing. Initially, xenon and samarium equilibrium concentrations are burning in and the percentage changes in the fission product concentrations are large. Thus, the cross sections change more rapidly than later in the fuel cycle when the relative percentage of composition change is lower. Since the cross sections are assumed constant over a time interval, smaller depletion intervals are used to burn-in fresh fuel. Burn-in time intervals of one day for the first five days are used to allow xenon and samarium to reach equilibrium. Next, 10 and 20 EFPD

intervals are used until the accumulated burnup on the fuel reaches approximately 100 EFPD. After approximately 100 EFPD, the intervals are increased to 10% of the total EFPD. The next section discusses how the information gleaned from this algorithm is used to develop the non-uranium plutonium fuel.

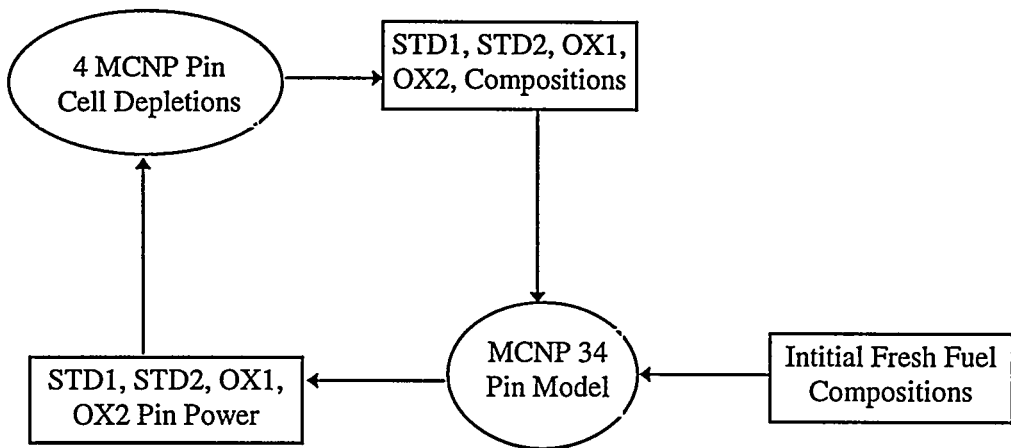


Figure 5.12 Pin Power - Depletion Algorithm

5.3.3 Analysis of Depletion and Pin Power Peaking Information. The algorithm depicted in figure 5.11 characterizes the fuel as a function of burnup. In addition to the pin to pin power peaking, reactivity and composition data are calculated. These two pieces of information are used to analyze the performance of candidate fuel compositions and to gain insight into how to alter the composition to improve performance.

An MCNP pin cell infinite medium multiplication factor, K_{inf} , is calculated for each MOCUP depletion interval. Individual fuel reactivity versus burnup profiles are constructed from these MCNP pin cell K_{inf} calculations. Figure 5.13 is an example profile for standard 3.9 w% UO_2 fuel and three different non-uranium fuel compositions, 10 w% WGpu with erbium as a poison, 10 w% WGpu with gadolinium as a poison and low loading non-uranium fuel at 3w% WGpu with erbium. These curves help determine how fuel performance can be improved. In general, the closer the UO_2 and PuO_2 pin reactivity profiles match, the more even the resultant power distribution over the cycle. A pin's reactivity profile is a function of how fast the fissile

plutonium is burning out relative to the poison. For example, the 10 w% WGPu non-uranium fuel with gadolinium pin reactivity is negative and relatively constant over the first 200 EFPD. This is because the 255,000 barn thermal capture cross section of ^{157}Gd dominates the neutron captures. By approximately 220 EFPD the ^{157}Gd is nearly burned out and the ^{155}Gd begins controlling the reactivity but it is also depleted rapidly. The pin's positive reactivity slope indicates that the poison is burning out much faster than the fissile material. By contrast, the 3w% WGPu non-uranium fuel with erbium poison has a shallow linear negative slope indicating that the rate at which positive reactivity is being added by the poison depletion is slightly less than the negative reactivity addition caused by fissile material depletion and fission product build-up. Thus, erbium provides longer term reactivity control. The 10 w% WGPu non-uranium fuel with erbium has a nearly constant reactivity profile due to the large initial fissile loading. As mentioned above, reactivity profile information correlates to pin power peaking information. Figure 5.14 shows the 0 and 620 EFPD pin radial power peaking profiles which correspond to the pin reactivity profiles in figure 5.13.

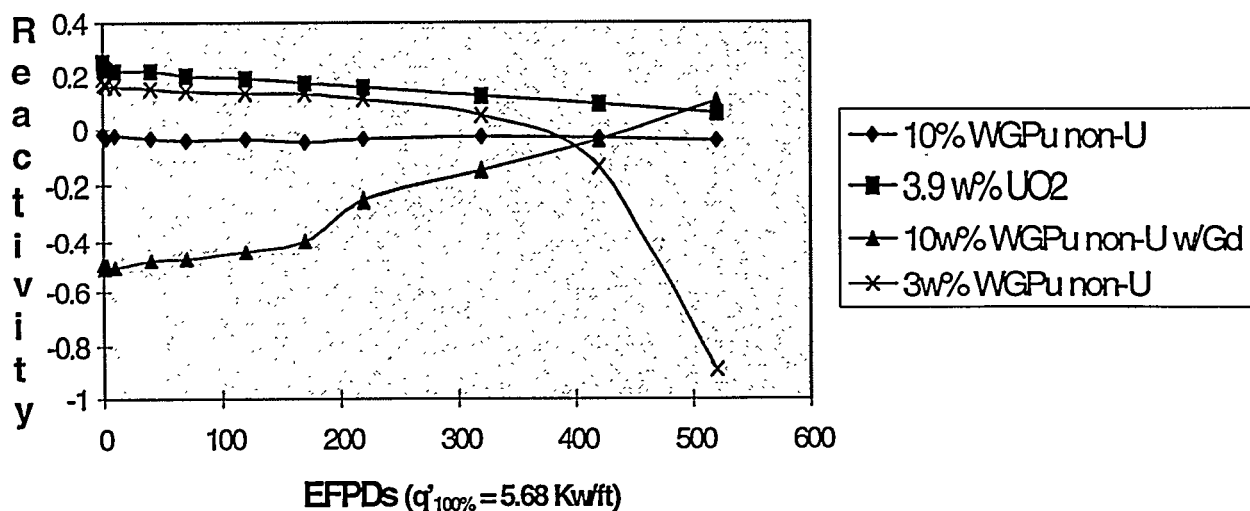


Figure 5.13 Example Reactivity vs. Burnup Profiles

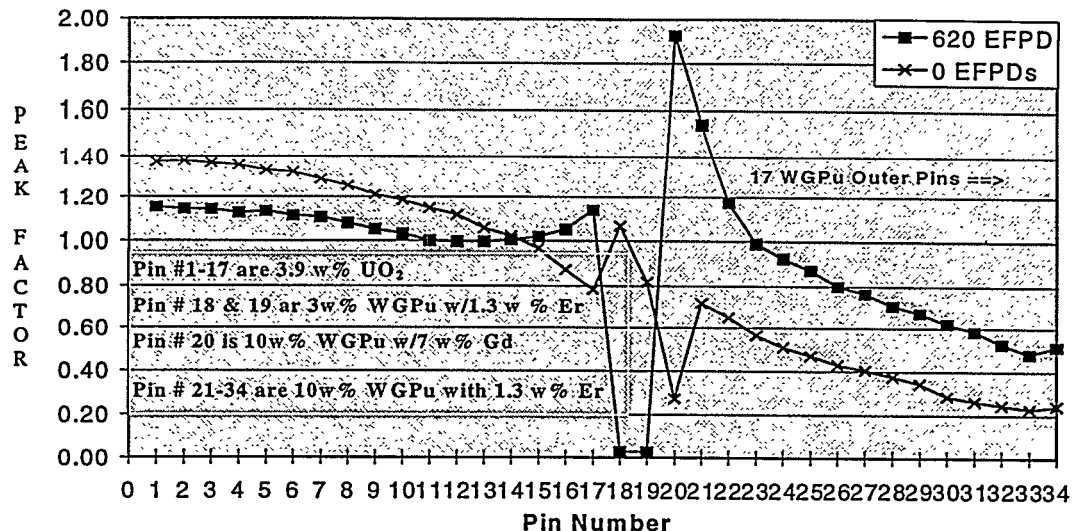


Figure 5.14 Pin to Pin Power Peaking for PuO_2 Assembly with Three Pu Pin Compositions

The 34 pin model loading configuration is described in the figure. Note that the power peaking of pins 18 and 19 are similar to that found in figure 5.10 and that pin number 20, which is loaded with gadolinium, has a very low peaking factor. The fresh fuel power peaks are acceptable. However, the gadolinium loaded pin produces an unacceptable power peak at 620 EFPD. Looking at figure 5.13, the power peak occurs because the gadolinium pin's reactivity is increasing while the other pins have negative reactivity vs burnup slopes. The composition vs burnup information generated by ORIGEN is also useful in understanding the causes for the observed characteristics. Review of the ORIGEN-generated compositions confirms that the ^{167}Gd shields ^{239}Pu reducing the ^{239}Pu consumption rate as it rapidly burns out. Thus, when the ^{167}Gd is completely depleted it leaves behind a relatively fresh plutonium pin composition. At 620 EFPD, the pin which contained Gd has a higher reactivity than the surrounding pins resulting in its unacceptable power peaking. The conclusion can be drawn that using a combination of high gadolinium and plutonium loading should be avoided because it results in problematic power peaking after about 1.5 cycles of exposure (in fixed position). Assembly rotation after one cycle can potentially ameliorate this problem.

Finally, it is interesting to note that pins #18 and 19 are producing very little power at 620 EFPD. Looking at the composition data, it is found that the pins generate little power because

most of the plutonium is destroyed by 620 EFPD. This conclusion is also of interest because the purpose of non-uranium fuel is to eliminate plutonium within the 880 EFPD base cycle. Thus, the plutonium content of the discharged fuel is a critical performance measure. Specifically, the goal is to minimize the ratio of residual plutonium to loaded plutonium for elemental plutonium and ^{239}Pu . Once a fuel which accomplishes this goal is found, its suitability for safe use in a core must be determined.

5.3.4 CASMO-3 Calculation of Core Average Reactivity Coefficients. In order to be feasible, a fuel which has acceptable power peaking vs burnup and which eliminates plutonium must also have acceptable reactivity coefficients. To be acceptable, peripheral PuO_2 fuel reactivity coefficients must be negative enough so that when they are averaged with the reactivity coefficients of the rest of the core, the whole core average reactivity coefficients are within PWR design limits. [C-5, F-4, M-6] The first step is to determine the reactivity coefficients of the candidate fuel composition in a pin cell configuration.

CASMO3 is specifically designed for depletion calculations. A CASMO3 pin cell model with the same specifications as found in table 5.7, is used to examine reactivity coefficients. First, base case depletions of both UO_2 and non-uranium compositions are run for a series of depletion steps under reference conditions as found in table 5.7. Then, several branch calculation depletions are run where a single reference parameter such as the fuel temperature is varied for each branch calculation. Table 5.8 lists the reference parameters varied and the associated reactivity coefficients calculated. A K_{inf} is calculated for each parameter value at each base case depletion step. The difference between the base case and branch calculation K_{inf} is used to determine the reactivity coefficient as shown in table 5.9.

Table 5.8 Summary of Pin Cell Reference Parameters and the Associated Reactivity Coefficient

Pin Cell Reference Parameter	Coefficient	Units
Fuel Temperature	Fuel Temperature	pcm/°K
Moderator Temperature	Isothermal Moderator Temperature	% delta rho / °K
Moderator Boron Concentration	Boron Worth	ppm/% delta rho
Moderator Percent Void	Void	%delta rho/% void

Table 5.9 Summary of Reactivity Calculations

Coefficient	Equation	Units
Fuel Temperature (FTC)	$FTC = 10^5 * [(K_{T1} - K_{T2})/K_{Tave}]$ (T1-T2)	pcm/°K
Isothermal Moderator Temperature (MTC)	$MTC = 10^4 * [(K_{T1} - K_{T2})/K_{Tave}]$ (T1-T2)	% delta rho * 10 ⁴ °K
Inverse Boron Worth (IBW)	$IBW = 100 * [(K_{B1} - K_{B2})/K_{B1}]$ (B1-B2)	ppm / % delta rho
Void (VC)	$VC = [(K_{V1} - K_{V2})/K_{V1}]$ (V1-V2)	%delta rho/% void

Once pin cell reactivity coefficients are calculated, they must be combined to produce core average parameters. Since this is a feasibility study rather than a licensing calculation, a weighted approximation of core average parameters is adopted.

Subject to the validity of approximations made in the derivation of the FLARE-type nodal codes, plus equality of the fast group flux and its adjoint (as confirmed by Mosteller [M-5] for typical PWR Cores), and neglecting certain leakage related terms, it can be shown that the neutron yield and reactivity coefficients should be weighted by the fast flux squared (or equivalently by the product of fast flux and neutron source rate) when aggregating assembly node values to obtain whole core average values [H-8]. From the near constancy of the energy release per fission neutron and fast group migration area, it also follows that power squared weighting is a useful, fairly accurate alternative [S-5]. A derivation of the power squared weighting scheme from the two group neutron balance equation can be found in appendix C.

The analytical support and numerical verification for power squared weighting are not as strong as for more conventional lattices because of the use of fertile-free fuel in a peripheral location. However, such weighting should be adequate for present purposes, particularly since it will be shown that the highly conservative arbitrary application of either power weighting or number weighting lead to results which do not move whole core kinetic parameters outside the currently acceptable design envelope for PWR cores.

Thus, the core average reactivity coefficients may calculated three ways as necessary: number weighting, power weighting and power squared weighting. Number weighting is most conservative because it assumes that the peripheral assembly pins, which on average produce less than 50% of core average assembly pin power, contribute equally in proportion to their number in the core as higher powered interior pins. Since the peripheral pins run at less than 100% power, core average power weighting is less conservative than number weighting but more conservative than the more accurate power squared weighting of individual pin contributions to core average kinetic parameters. The peripheral assemblies account for 25% of the core. Consequently, the core average reactivity coefficients are calculated using the appropriate pin cell reactivity coefficients as follows:

Let:

C_n \equiv Number Weighted Core Average Parameter,

C_p \equiv Power Weighted Core Average Parameter,

C_{p2} \equiv Power Squared Weighted Core Average Parameter,

C_u \equiv UO_2 Average Parameter

C_{Pu} \equiv Non-UraniumFuel Parameter

PW_u \equiv Average Power Generated in UO_2 Pins

and,

PW_{Pu} \equiv Average Power Generated in Non-Uranium Pins

$$C_n = [(C_u * 0.75) + (C_{Pu} * 0.25)], \quad (5.3)$$

$$C_p = \frac{\{[C_u * 0.75 * PW_u] + [C_{Pu} * 0.25 * PW_{Pu}]\}}{0.75 * PW_u + 0.25 * PW_{Pu}} \quad (5.4)$$

$$C_{p2} = \frac{\{[C_U * 0.75 * PW_u^2] + [C_{Pu} * 0.25 * PW_{Pu}^2]\}}{(0.25 * PW_u^2) + (0.75 * PW_{Pu}^2)} \quad (55)$$

Finally, a 1/8th symmetry MCNP PWR core model is used to check overall core reactivity at the beginning and end of the cycle to ensure it is within the envelope of current PWR fuel management practices. [C-5, F-4, M-6] The PWR Core model is an assembly level model using the MCNP repeated structures technique to model the pins and water holes in each assembly. The assembly specifications are the same as those listed for the 17 x 17 Westinghouse assembly listed in table 5.6. Figure 5.15 is a top down view of the 1/8th symmetry model with the assemblies numbered 1 through 31 showing the location of the peripheral assemblies and other features.

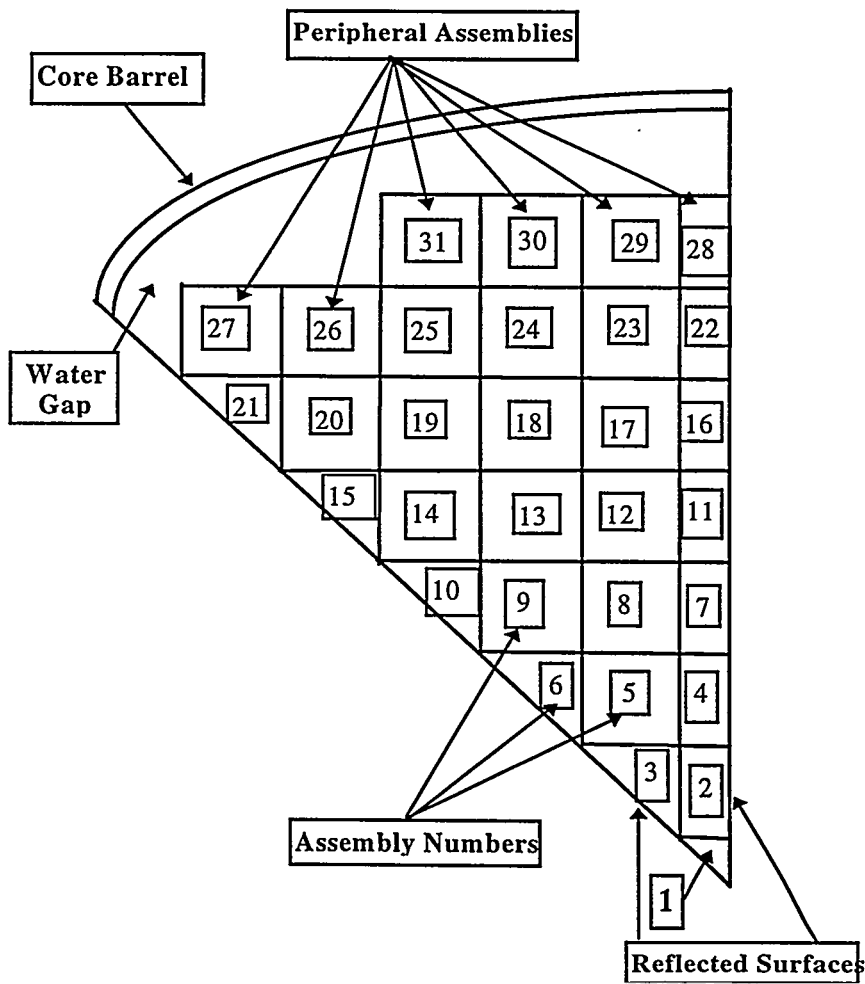


Figure 5.15 1/8th Symmetry MCNP PWR Core

5.4 Summary of Computer Codes, Models and Computational Techniques.

A 17 x 17 Westinghouse PWR assembly is used as the reference design for all computer models. Fuel compositions are developed to support an 18 month fuel cycle with a capacity factor of 0.8. Thus, fuels are developed to support core residence times for these peripheral assemblies which are multiples of 440 EFPD. Table 5.10 correlates models and codes with the required information they provide. All required information listed in table 5.10 is calculated as a function of burnup with the exception of the 1/8th core model effective multiplication constant (Keff).

A model with 34, 25 cm long pins arranged in a single row with reflected boundary conditions on the top, bottom and 3 sides and a core reflector region on the fourth side is used to model pin peaking at the interface between a peripheral PuO₂ assembly and the radially adjacent interior UO₂ assembly. Results of the 34 pin model are used to determine power peaking factors and actual pin powers. A 1.5 maximum radial power peaking factor is adopted. Four composite MCNP pin cells, representative of the 34 pins, are depleted at constant power. A satisfactorily benchmark MOCUP-MCNP-ORIGEN code system is used to perform the depletion calculations. The four pin cell models are used to generate one group cross sections for a selected group of actinides and fission products. These cross sections are substituted for ORIGEN library cross section information with the remainder of the nuclide cross sections coming directly from the ORIGEN libraries. ORIGEN performs depletion calculations on the fuel for a user-specified time period. The resultant new fuel compositions at each burnup step are used to generate a new set of cross sections for the next time interval. Hence, the fuel is depleted in a stepwise fashion. EFPD burnup units are used instead of MWd/MT to provide a consistent basis for comparison of non-uranium fuels and uranium fuels. The elimination of plutonium must be accomplished within the allowed peaking factor over a residence time that is a multiple of 440 EFPD. In addition, the presence of the fuel on the periphery must not alter the core average reactivity coefficients beyond design margins. Core reactivity coefficients of pin cells are calculated using

a CASMO3 model. Core average parameters can be approximated by power squared weighting of the contribution of individual pins to the core average parameter. For this application two more conservative weighting factors, the number of pins and the power of the pins are used as weighting constants in addition to power squared weighting. The next chapter presents the results of the calculations described here.

Table 5.10 Correlation of Required Information, Codes & Models

Information Required	Code(s)	Model	Output (→ Used As Input For)
Power Peaking	MCNP	34 Pin	Pin Powers (Depletion & Core Average Reactivity Calculations)
Depletion Compositions	ORIGEN	None	End of time interval fuel composition (Power Peak Calculations)
Reactivity Vs Burnup Flux Reaction Rates	MCNP	Pin Cell	Kinf Flux & Nuclide Reaction Rates (MOCUP)
Reactivity Coefficients	CASMO3	Pin Cell	Kinf vs Coeff. Parameter (Core Average Reactivity Calculations)
Assembly Residence Time	MCNP & ORIGEN	34 Pin & None	Reactivity & Composition (Fuel Cycle Planning)
Whole Core Reactivity	MCNP	1/8 th PWR Model	Keff at Specific Burnups

CHAPTER SIX: NON-URANIUM FUEL AND PERIPHERAL PWR CYCLE RESULTS

Chapter 5 described the computational tools and techniques used to determine the neutronic performance of a candidate non-uranium fuel relative to several fuel properties. The criteria listed in table 6.1 distill the performance criteria from proliferation , material and neutronic considerations, discussed in chapters 3, 4, and 5, which are appropriate for a non-uranium fuel used to eliminate plutonium in a peripheral PWR cycle. Candidate fuel form performance was evaluated based on the application of these criteria. Several WGPu and poison loading combinations were investigated leading to a recommendation of plutonium-erbium-oxide-inert diluent matrix for use in eliminating plutonium in a once through peripheral PWR cycle. Chapter 4 details the material considerations in the selection of candidate diluent matrices. This chapter presents the results of a neutronic evaluation of the recommended plutonium-erbium-oxide-inert diluent matrix fuel in the peripheral PWR fuel cycle. The first section describes the preferred fuel composition. The second section presents discharge properties and cycle feasibility results while the third section covers results relative to reactivity coefficients. The fourth section reviews other results from the analysis of fuel compositions which are not recommended. The final section summarizes these results and discusses implementation.

**Table 6.1 Neutronic Performance Criteria For Plutonium Disposition
Fuel Producing an Elimination Option**

Parameter	Definition	Specification	Comments
Discharge Properties (must substantially eliminate plutonium)			
Residual ^{239}Pu	$^{239}\text{Pu} / \text{Total Pu discharged}$	< 10	want to minimize weapons usability ^A
Residual Total Pu	$\text{Total Pu} / \text{Initial Pu Loaded}$	< 10	want to minimize weapons usability ^A
Fuel Cycle Feasibility (non-uranium Pu fuel must not impose any restrictions greater than those imposed if the periphery were loaded with twice burned UO_2)			
Residence Time	Number of EFPDs Fuel Remains in Core	multiple of 440 EFPDs	must support 18 month refueling cycle
Radial Power Peaking	Pin Power/core average pin power	< 1.5	must not be too large so as to cause total power peaking to exceed 2.5.
BOL and EOC Whole Core Reactivity	BOL & EOC Kinf values	≤ 1.3 & ≥ 1.0	Whole Core BOL and EOC reactivity must be within PWR design limits
Reactivity Coefficients (whole core average reactivity values must be within acceptable PWR design range)			
Fuel Temperature Coefficient (FTC)	$[((K_T - K_{900})/K_{900})/T - 900] * 10^5$ units = $(\text{pcm}/^{\circ}\text{F})$	BOC to EOC: -1.30 to -1.46	Typical PWR Design Values
Moderator Temperature Coefficient (MTC)	$[((K_{600} - K_T)/K_{600})/(600 - T)] * 10^4$ units = $\delta p / ^{\circ}\text{F} \times 10^{-4}$	BOC to EOC: -0.78 to -3.02	Typical PWR Design Values
Inverse Boron Worth (IBW)	$(1000 - \text{ppm}) / ((K_{1000} - K_{\text{ppm}})/K_{1000})$ units = $\text{ppm} / \% \delta p$	BOC to EOC: 108 to 96	Typical PWR Design Values
Void (VC)	$[((K_{0\%} - K_{V\%})/K_{0\%}) / (0\% - V\%)]$ units = $\delta p / \% \text{void} \times 10^3$	BOC to EOC: -0.41 ^B to -1.43 ^B	Typical PWR Design Values
A. Weapon's usability is described in chapter 3 section 3.3 B. Values are for critical moderator boron concentration			

6.1 Proposed Fuel and Cycle.

Chapter four discusses fuel matrix selection in detail. Choice of a proper matrix is critical to the practical in-core performance of the fuel. The matrix properties and composition determine suitability for fabrication as well as mechanical and thermal performance. An oxide fuel matrix is recommended over other fuel forms because it satisfies thermo-physical property requirements and is most readily adapted to current MOX

fabrication processes. The chapter four selection process recommends development of two candidate oxide matrices: alumina and zirconia. However, the neutronic performance of the fuel is not a significant function of the fuel matrix.

6.1.1 Importance of the Fuel's Inert Matrix Diluent. Several inert matrices were examined in the course of developing a fuel which would meet the requirements in table 6.1. The number density of the inert diluent element will necessarily be large relative to the fissile, fertile, fissionable and poison nuclide number densities of the fresh fuel. Thus, the diluent matrix constituents must be essentially neutronically inert to avoid depletion of the matrix and unacceptably large parasitic neutron losses. Therefore, only elements with thermal and resonance integral absorption cross sections less than 2 barns are considered to serve as diluents. Given that the matrix is specifically designed to be neutronically inert, the exact composition of that matrix has no impact on the resultant performance of the fuel. For example, the two fuels listed in table 6.2 have nearly the same plutonium and thorium number densities. However, one is a TRISO type fuel with an inert carbon matrix and the other is an oxide with an alumina matrix. The two fuels were depleted at the same power density for the same number of EFPDs. Figure 6.1 shows their reactivity versus burnup profiles. The two fuels behave similarly because their neutronically active constituents have similar number densities. The fact that they have totally dissimilar inert matrix compositions has no appreciable impact on their neutronic performance (different values of their scattering cross sections will change resonance self shielding slightly). The plutonium discharge isotopes and destruction performance are also nearly identical. The inert matrix is only a structural host for the plutonium and poison nuclides from a neutronic point of view. Thus, the results presented in this chapter for the fuel described in this section are equally applicable to any inert matrix fuel with similar plutonium and poison loading.

Table 6.2 Composition of Example Alumina and TRISO Fuels

Nuclide/Element	Alumina (atoms/b-cm)	TRISO (atoms/b-cm)
Neutronically Active Components		
^{239}Pu	1.42E-03	1.40E-03
^{240}Pu	9.07E-05	8.94E-05
^{241}Pu	7.53E-06	7.42E-06
^{232}Th	3.02E-03	3.71E-03
^{238}U	2.12E-04	1.31E-04
Inert Components		
Cerium	3.02E-03	0
Aluminum	3.09E-02	0
Carbon	0	6.37E-02
Oxygen	6.12E-02	1.07E-02

A zirconia (ZrO_2) inert matrix was used for the bulk of the evaluations reported here. The neutronic performance of zirconia was analyzed as a function of WG Pu loading, poison loading and poison type. Excellent performance was achieved using the fuel composition listed in table 6.3 which is designated Oxide5.

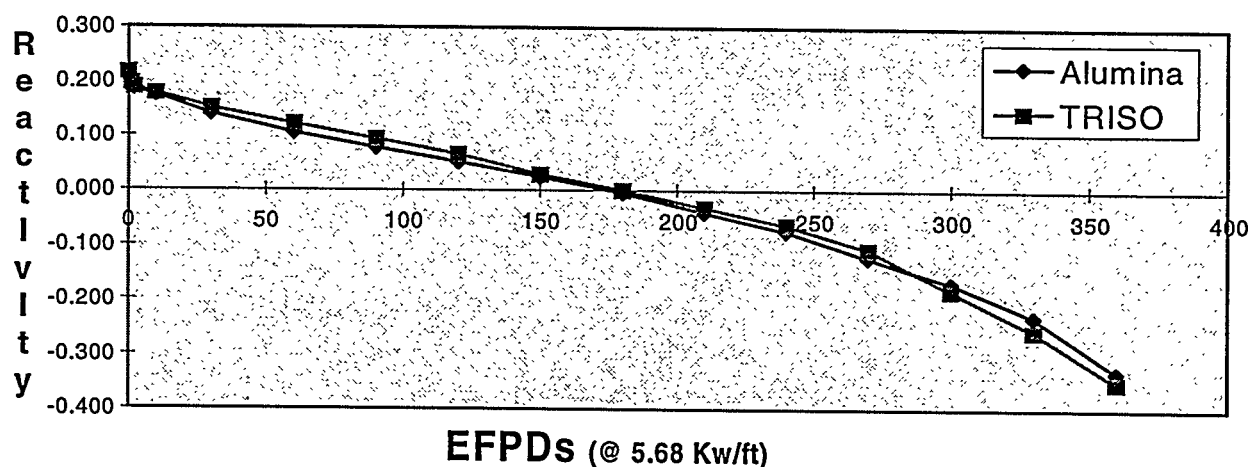


Figure 6.1 Comparison of the Reactivity Profiles of Similarly Loaded Fuels with Dissimilar Inert Matrices

MCNP cross section libraries were only available for ^{166}Er and ^{167}Er . However, table 6.4 demonstrates that the 166 and 167 erbium isotopes account for 99 and 86% of elemental

erbium macroscopic thermal and resonance absorption cross sections respectively. Thus, it is acceptable to use ORIGEN library cross sections for the mass 162, 164, 168 and 170 erbium

Table 6.3 Composition of Recommended Non-Uranium Fuel: Oxide 5

Nuclide/Element	Total Oxide Matrix w%
Neutronically Active Components	
²³⁸ Pu	3.49E-04
²³⁹ Pu	2.74E00
²⁴⁰ Pu	1.70E-01
²⁴¹ Pu	6.77E-03
²⁴² Pu	6.51E-04
²⁴¹ Am	3.83E-03
¹⁶⁶ Er	4.47E-01
¹⁶⁷ Er	3.61E-01
Inert Components	
Zirconium	7.04E01
Oxygen	2.53E01

Table 6.4 Erbium Cross Section^a and Abundance Data

Isotope	% Abundance	$\sigma_{abs}^{thermal}$	Macro-Product	% of Total
¹⁶² Er	0.14	19	2.66	0%
¹⁶⁴ Er	1.61	13	20.93	0%
¹⁶⁶ Er	33.6	20	672	4%
¹⁶⁷ Er	22.95	670	15376.5	95%
¹⁶⁸ Er	26.8	2.7	72.36	0%
¹⁷⁰ Er	14.9	5.8	<u>86.42</u>	<u>1%</u>
		Total:	16230.87	100%
Isotope	% Abundance	$\sigma_{abs}^{resonance}$	Macro-Product	% of Total
¹⁶² Er	0.14	500	70	1%
¹⁶⁴ Er	1.61	111	178.71	2%
¹⁶⁶ Er	33.6	100	3360	28%
¹⁶⁷ Er	22.95	300	6885	58%
¹⁶⁸ Er	26.8	37	991.6	8%
¹⁷⁰ Er	14.9	25	<u>372.5</u>	<u>3%</u>
		Total:	11857.81	100%
a. thermal neutron absorption cross sections in barns				
b. Macro-Product is defined as the % abundance x thermal cross section				

isotopes while using MCNP calculated cross sections for the more critical 166 and 167 erbium isotope cross sections. Once the composition of the fuel and the fuel cycle are defined, it is possible to determine the plutonium throughput of the recommended option.

6.1.2 Plutonium Cycle and Throughput. In the proposed fuel cycle, the periphery of the core is comprised of assemblies loaded with the Oxide5 fuel as listed in table 6.3. The remainder of the core is managed like a standard three batch UO₂ PWR core. The Oxide5 fuel composition is designed for a residence time of two 440 EFPD cycles, and is then discharged. Each Oxide5 assembly is rotated 180 degrees after the first cycle to achieve an even burnup of the plutonium in the pins. A single transition cycle is used to produce an equilibrium cycle where the core periphery is filled with alternating once burned and fresh Oxide5 assemblies. Since the purpose of this Oxide5 fuel in a peripheral loading is to destroy plutonium, the rate of plutonium consumption or throughput for this fuel and cycle is of interest.

The cycle model is based on the Westinghouse designed, Seabrook PWR core. The Seabrook core contains 48 peripheral assemblies of a total of 193 assemblies. Each assembly contains 289 pin slots. Nominally, an assembly is loaded with 264 pins and 25 water holes. Since the Oxide5 assemblies will remain on the periphery throughout their core residence time, it is assumed that the assemblies can be completely filled with 289 fuel pins. With the fissile density listed in table 6.3, each pin contains 26.7 gms of WGPu and there are 7.73 kilograms of WGPu in each assembly. Twenty four new assemblies are loaded into the core at the start of each cycle for a WGPu throughput of 186 kilograms per 18 month cycle. Thus, the 50 MT WGPu disposition mission would take 404 reactor years. Assuming all other existing constraints were removed, the 72 operating US PWRs could disposition the 50 MT of WGPu in 5.6 years [N-4]. Alternately, a 1000 MWe PWR with a 0.8 capacity factor produces 243 kgs of RGPU per year [B-3]. Assuming 1/4th of the core is fueled with Oxide5 assemblies, the remainder of the core would produce approximately 182 Kg of RGPU per year. Hence, the net plutonium production of a PWR loaded with Oxide5 fuel on the periphery and UO₂ assemblies in the interior would be only 58 kgs of RGPU per year. Thus,

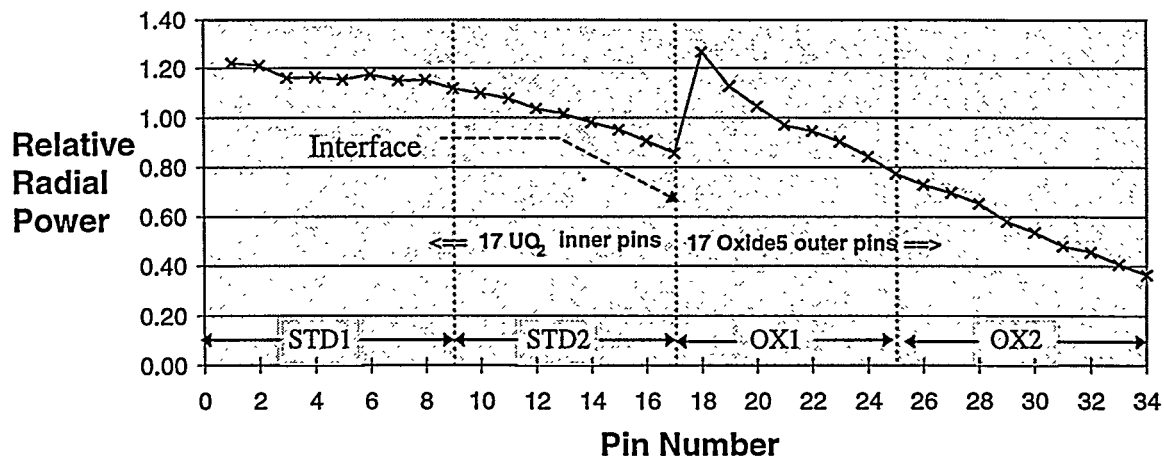
the growth of RGPU inventories could be significantly reduced. Fuel performance constraints require that the radial power peaking at the Oxide5-UO₂ assembly interface of the proposed peripheral cycle not exceed nominal PWR design limits.

6.2 Radial Power Peaking and Depletion of Oxide5 Fuel

Chapter 5 contains the details of how the radial power peaking and depletion calculations are carried out. This section presents the results of those calculations for Oxide5 fuel loaded in the periphery of a PWR.

6.2.1 Depletion Through Two Cycles. Figure 6.2 is the radial power profile for the 34 pin model loaded with fresh 3.9w% UO₂ in pins 1-17 and Oxide5 loaded in Pins 18-34.

Figure 6.2 Power Profile for Fresh 3.9w% UO₂ and Oxide5

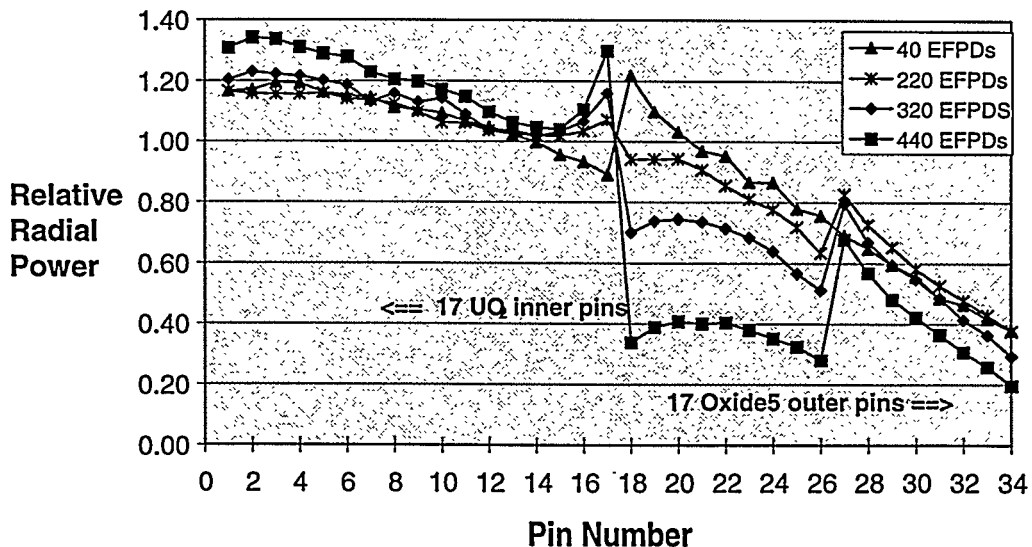


A maximum peak pin power of 1.27 times core average pin power occurs in the first Oxide5 pin: #18. This peak is well within the 1.5 maximum radial power peak value. The power peaks in pin #18 due to the greater cross section of ²³⁹Pu relative to ²³⁵U. As shown in figure 5.10, the larger plutonium cross sections result in thermal flux shielding of the outer Oxide5 by the inner Oxide5 pins. Since the plutonium number densities are the same for all the

Oxide5 pins, pin power decreases with increasing pin number moving radially outward from the interface. As described in chapter 5, the 34 pins are divided into four sets. An average pin power for each of the four sets is assigned to four corresponding composite pin cells which are used to model the depletion of all 34 pins. UO₂ pins numbered 1 through nine are depleted as one composite pin labeled STD1. Similarly, UO₂ pins 10 through 17 are depleted as STD2, PuO₂ pins 18 through 24 are depleted as OX1 and pins 25 through 34 are depleted as OX2.

The MCNP 1/8th core model loaded with fresh UO₂ and Oxide5 assemblies had a K_{eff} of 1.31. Thus, a core completely loaded with fresh fuel is within typical PWR values. Fresh core reactivity represents a conservative upper bound on the anticipated values. This peripheral fuel cycle is intended for incorporation into an equilibrium fuel cycle via a single transition cycle as described later in this subsection. Figure 6.3 tracks the development of the radial power profiles through the stepwise depletion of the UO₂ and Oxide5 pins.

Figure 6.3 Progression of Radial Power Peak for Oxide5 Through the First Cycle



As the plutonium in the inner Oxide5 pins is depleted, there is less shielding of the outer pins and the power peak moves radially outward. The magnitude of the peak in the Oxide5 pins

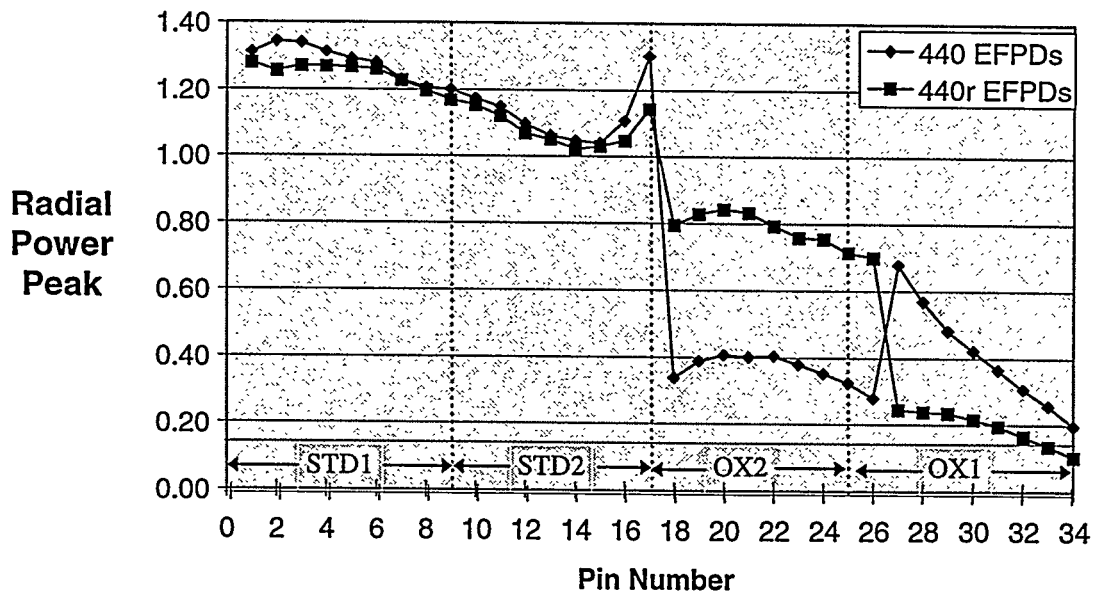
decreases relative to the fresh fuel pin #18 value for two reasons. First, the thermal flux remains partially shielded below that which is seen by pin #18 at the start of the cycle. Second, the pins are not as fresh as pin #18 was at the start of the cycle when they see the increase in thermal flux. Since there is relatively low fissile loading and no fertile material in the Oxide5 pins, there is a very sharp drop in power and reactivity during the first cycle. The complete pin reactivity profile over the two cycles is discussed in more detail later in this sub-section. At the EOC, the power in the OX1 pins has dropped well below core average. The discontinuities in the pin power profiles at pin 27 result from our use of region-average compositions in the assembly burnup scheme: zone average composition times the local flux consistently overestimates the local power here and also near pin #18.

It is interesting to note that the maximum radial power peak shifts from the Oxide5 pins to the last UO₂ pin adjacent to the Oxide5 assembly: pin #17. This is because the fissile content of OX1 pins is extremely depleted during the first cycle. Table 6.5 lists OX1 and OX2 plutonium destruction during the first and second fuel cycles. Note that there is greater destruction of plutonium in OX1 than OX2 because OX1 has shielded OX2 during the first fuel cycle. The first cycle ends with the maximum actual radial pin power peak well below the 1.5 limit. At the end of the first cycle, the Oxide5 assembly is rotated 180 degrees to facilitate an even burnout of the assembly. After the shift, the OX2 pins are numbered 17 through 24 and the OX1 pins are numbered 25 through 34. Figure 6.4 shows the radial power profile at the end of the first cycle, 440 EFPDs, and after the rotation of the Oxide5 assembly, 440r EFPDs. The change from the 440 to the 440r EFPDs radial power profile is only caused by the rotation of the Oxide5 assembly; there is no depletion difference between the 440 and 440r profiles. As expected, the 440r profile shows an increase in the OX2 average pin power because the fuel is now in a higher thermal flux region. The corresponding decrease in the OX1 average pin power peak is due to their rotation into the lower thermal flux outer region.

Table 6.5 OX1 & OX2 Pu Destruction

EFPDs	OX1		OX2	
	% ^{239}Pu	% $^{\text{Tot}}\text{Pu}$	% ^{239}Pu	% $^{\text{Tot}}\text{Pu}$
0	0.0%	0.0%	0.0%	0.0%
1	0.4%	0.2%	0.2%	0.1%
3	1.1%	0.7%	0.6%	0.4%
10	3.7%	2.2%	2.2%	1.3%
40	14.7%	9.1%	8.8%	5.4%
70	25.4%	15.8%	15.2%	9.4%
120	42.3%	26.9%	26.4%	16.4%
170	57.9%	37.8%	36.9%	23.3%
220	71.0%	47.9%	45.6%	29.1%
320	87.9%	63.6%	67.0%	44.6%
440	98.1%	79.8%	84.8%	60.2%
				<==End of First Cycle
540	99.3%	84.1%	97.3%	77.5%
640	99.8%	87.0%	99.8%	87.4%
740	99.9%	88.9%	100.0%	91.6%
880	100.0%	91.0%	100.0%	95.0%
				<==End of Second Cycle

Figure 6.4 Radial Power Shift as a result of Rotating the Oxide5 Assembly at EOC One

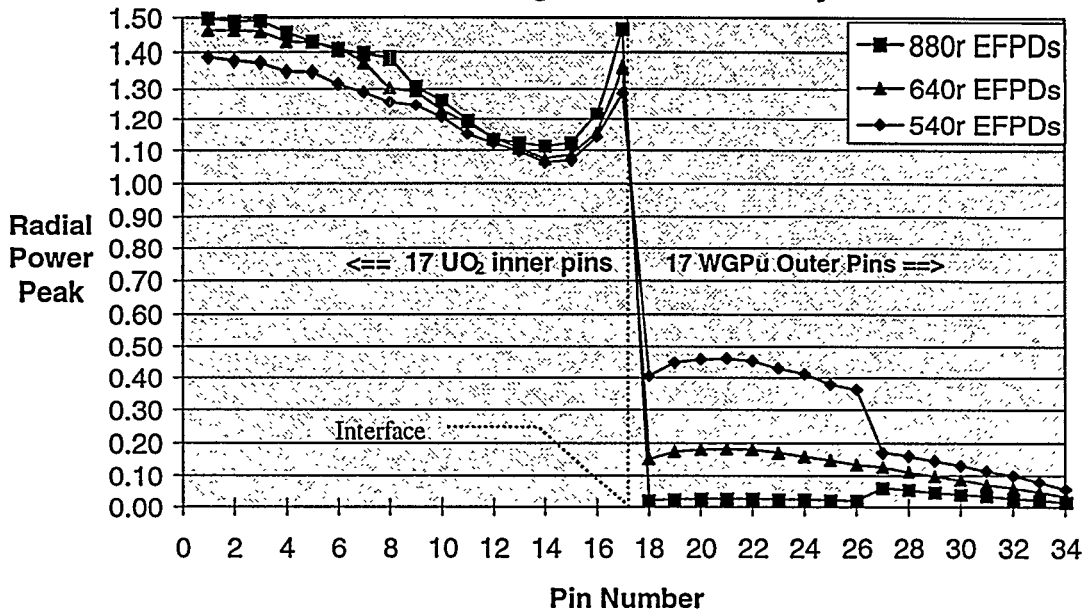


Rotating the Oxide5 assembly also reduces the power peak in the interface UO_2 pin #17. The second cycle begins with the 440r radial pin power peak profile.

The NAS classifies the PC-MHR as beyond the spent fuel standard but not a true elimination option because there is only 89% destruction of ^{239}Pu and 64% destruction of total plutonium. As indicated in table 6.5, the second cycle increases the Oxide5 pin plutonium destruction from values which are slightly better than non-uranium once-through cycles such as the PC-MHR or CANDU to a true elimination option with essentially 100% destruction of ^{239}Pu and 93% destruction of total plutonium. Thus, destruction of plutonium using Oxide5 in a two cycle peripheral PWR cycle meets the NAS discharge property specifications. Figure 6.5 shows radial power peaking profile development over the second cycle which ends at 880 EFPDs.

At 880 EFPDs, UO_2 pin #17 just reaches the 1.5 maximum allowable radial power peak. Thus, this fuel composition and cycle meet the radial power peak specification. When the plutonium becomes heavily depleted during the second cycle, the elimination of residual plutonium requires the rest of the core to provide the neutrons to burn out the residual plutonium. Thus, it must be possible for the peripheral assemblies to operate at low power without causing unacceptable power peaking. Assemblies producing so little power in the interior of the core would likely lead to unacceptable power peaking in adjacent assemblies. Using a radial blanket to burn out the residual plutonium is akin to reducing the effective size of the core. Thus, the lower power can be tolerated in the periphery of the core without causing unacceptable power peaking. Figure 6.5a shows the reactivity profile which correlates to the power peaking profiles of this two cycle depletion of Oxide5 and UO_2 .

Figure 6.5 Progression of Radial Pin Power Peaking Through the Second Cycle



The reactivity of the OXIDE5 fuel pins, OX1 and OX2, remains nearly constant and consistent with that of the UO₂ pins, STD1 and STD2, until the ¹⁶⁷Er is nearly completely depleted. These relatively flat OX1 and OX2 reactivity profiles provide the relatively benign radial peaking distributions of the first cycle. At about 300 EFPDs, the ¹⁶⁷Er is nearly completely depleted resulting in the loss of the positive reactivity contribution produced by ¹⁶⁷Er depletion.¹ Thus, the OX1 pins begin losing reactivity at a greater rate. The OX2 pins are shielded during the first cycle slowing their depletion of fissile material and ¹⁶⁷Er. Consequently, OX1 fuel burns out faster than the OX2 pins from 300 EFPDs to the end of the first cycle. Since the Oxide5 assembly is rotated 180 degrees at the end of the first cycle, the OX1 pins become shielded and the OX2 pins begin burning out at a faster rate over the second cycle. Since, the OX2 pins start the second cycle partially depleted, their reactivity drops very rapidly relative to OX1 pins.

¹ Figure 6.11 shows the depletion of 166 & 167 Erbium as a function of burnup.

Figure 6.5a Oxide5a & UO₂ Reactivity vs Burnup

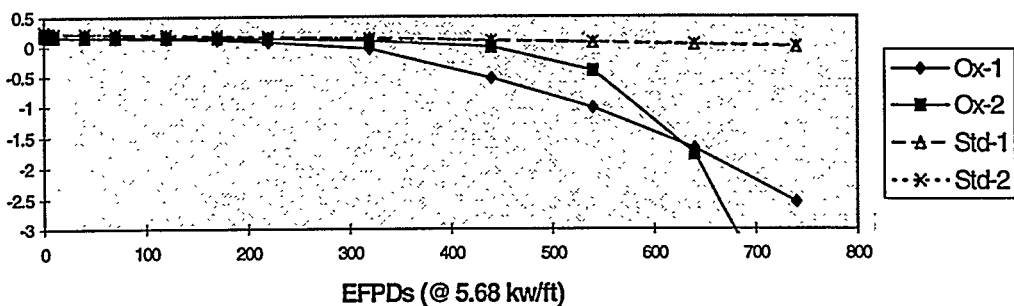


Table 6.6 presents the OX1 and OX2 average composite pin powers as a function of core EFPDs. Core EFPDs are the number of days the core is operating at 100% power which is generally equal to calendar days over an uninterrupted fuel cycle. At 440 EFPDs, the Oxide5 assembly pins are producing power at 39% of core average pin power. By the end of 540 EFPDs they are only producing about 22% of core average pin power. At the end of the second cycle, the Oxide5 assembly pins are producing less than 3% of core average power. However, the Oxide5 assembly pins still produce a two-cycle average power of 47.3%. This is a slight improvement over the average 30% produced in the periphery of PWRs using low leakage core fuel management. So, relative to current low leakage fuel management, there is a small net gain in neutron economy using this two cycle peripheral plutonium burning scheme. To assess potential changes in pressure vessel fluence, the net current into the reflector region was calculated using the MCNP 34 pin model. The net current was essentially the same for UO₂-UO₂ and UO₂-Oxide5 34 pin loadings. Thus, the pressure vessel fluence of the peripheral-Oxide5 cycle should be no more than that for standard full UO₂ cores. The plutonium fuel will not generate much power during the time it will take to destroy the residual plutonium. The power peaking in adjacent assemblies caused by the low power generation would be more difficult to manage if these assemblies were located on the interior of the core rather than on the periphery. Although probably not required, an alternating Oxide5 assembly loading scheme is recommended to reduce the power load on interior assemblies: i.e. every other peripheral assembly is replaced each cycle.

Table 6.6 Oxide5 Assembly Pin Power Over Two 440 EFPD Fuel Cycles

Core EFPDs	Kw/ft ^α			Avg. Net EFPDs	β	
	Ox1 Power	Ox2 Power	Avg. Power		Ox1 Net EFPDs	Ox2 Net EFPDs
0	4.98	2.88	3.93	0.84		
1	4.91	2.96	3.94	1.69	1.07	0.62
3	4.96	2.95	3.96	5.94	3.18	1.89
10	4.98	2.96	3.97	25.57	10.63	6.32
40	4.91	2.91	3.91	25.17	42.72	25.38
70	4.86	3.09	3.97	42.66	74.32	44.12
120	4.75	3.00	3.88	41.60	126.52	77.23
170	4.39	2.55	3.47	37.21	177.51	109.44
220	3.32	2.92	3.12	67.03	224.59	136.78
320	2.80	2.80	2.80	72.04	295.94	199.50
440	0.89	3.63	2.26	48.59	367.98	271.54
540	0.58	1.96	1.27	27.27	387.19	349.53
640	0.37	0.77	0.57	12.24	399.73	391.53
740	0.27	0.31	0.29	8.75	407.68	408.06
880	0.1752	0.1133	0.14425			
$\beta. \text{ Avg. Net EFPD} = (\text{Avg. Power}/5.88) \times (\text{# days})$		Total EFPDs: 416.62 Avg Power: 47.3%		Note: $\alpha. 5.688 \text{ Kw/ft} = 100\% \text{ core average power.}$		

The transition from an equilibrium PWR core to a core with the periphery loaded with plutonium can be completed via one transition cycle. For the transition cycle, fresh Oxide 5 assemblies are loaded into every other peripheral location with thrice burned UO_2 loaded into the other half of the periphery. At the end of the transition cycle, the UO_2 assemblies remaining in the periphery are replaced by fresh Oxide5 assemblies. Thus, an equilibrium cycle is reached with the periphery comprised of alternating once burned and fresh Oxide5 assemblies. Taken as a whole, the equilibrium periphery loading produces 54% of core average power at the start of each cycle and 21% of core average power at the end of each cycle. Thus, the alternating loading scheme would reduce the power burden on the interior assemblies relative to replacing the peripheral assemblies all at once.

The 1/8th MCNP core model loaded with UO_2 at a burnup of 1.5 cycles or 640 EFPDs and the entire periphery loaded with Oxide5 assemblies at a burnup of 880 EFPDs had a K_{eff} of 1.05. Thus, the core can still maintain criticality even if the entire periphery is loaded with exhausted Oxide5 fuel.

6.2.2 Summary of Radial Power Peaking and Depletion Results. Depletion calculation results show that the Oxide5 fuel composition meets the discharge property and fuel cycle feasibility performance criteria listed in table 6.1. Table 6.7 provides a summary.

Fresh Oxide5 has a relatively low fissile loading: about 1/3 that of standard PWR fuel. Consequently, power production during the last 220 EFPDs of the second cycle is minimal while residual plutonium is destroyed producing a true elimination option. Total plutonium destruction is in excess of 90% and 100% of ^{239}Pu is destroyed. The radial power peaking and core reactivity are within normal PWR limits throughout both cycles. Under current low leakage core fuel management, peripheral assembly power density is only about 30% of core average power. The end of the second cycle is an extension of that concept. The average power produced over the two cycles is 47%. Thus, there is a small net gain in average power produced in the periphery. The next step is to confirm the Oxide5 composition meets the reactivity coefficient specifications.

Table 6.7 Summary of Discharge Property and Fuel Cycle Feasibility Performance of Oxide5

Parameter	Definition	Specification	Calculated Value
Discharge Properties (must substantially eliminate plutonium)			
Residual ^{239}Pu	$^{239}\text{Pu} / \text{Total Pu discharged}$	< 10%	0.0 %
Residual $^{\text{Total}}\text{Pu}$	$\text{Total Pu} / \text{Initial Pu Loaded}$	< 10%	7.0 %
Fuel Cycle Feasibility (non-uranium Pu fuel must not impose any restrictions greater than those imposed if the periphery were loaded with twice burned UO_2)			
Residence Time	Number of EFPDs Fuel Remains in Core	multiple of 440 EFPDs	880 EFPDs
Radial Power Peaking	Pin Power/core average pin power	≤ 1.5	Max peak over two cycles = 1.5
BOL and EOC Whole Core Reactivity	BOL & EOC Kinf values	≤ 1.3 & ≥ 1.00	BOC Keff = 1.31 EOC Keff = 1.05

6.3 Oxide5 and Whole Core Reactivity Coefficients

Table 6.1 defines the reactivity coefficients and specifications of interest. The limits are based on meeting standard PWR design values. Chapter 5 details how these coefficients are calculated. This section presents the results of the reactivity coefficient calculations. Three algorithms for weighting the Oxide5 and UO₂ pin cell contributions to obtain core average reactivity coefficients are used: pin number, power and square power weighting.² Square power weighting is the most appropriate estimation technique. The Oxide5 pins run at a fraction of the core average 100% pin power. Thus, the Oxide5 relative pin power fraction is less than 1.0. Consequently, setting the weighting function equal to the power rather than the square of the power fraction assumes that the Oxide5 pins make a larger contribution to the core average parameters. Thus, power weighting is more conservative than square power weighting. Weighting the Oxide5 and UO₂ pin contributions based solely on the number of pins of each assumes that they contribute equally to core average parameters. Thus, number weighting is the most straightforward and also the most conservative algorithm. An additional degree of conservatism added to all of these calculations is that power increases in peripheral assemblies are partially offset by increased core leakage from those assemblies into the core reflector region. No credit is taken here for the contribution of this negative feedback to core average reactivity coefficients.

All Oxide5 and UO₂ coefficient calculations were done with a constant 500 ppm boron concentration in the coolant which is typical of mid-cycle concentrations. Note that CASMO3 cannot reliably calculate MTC, IBW or VC reactivity coefficients at 880 EFPDs. CASMO3 vendors indicated that the fissile density was too low for the code to consistently converge [B-3]. However, the power generated in the Oxide5 pins is so low by 740 EFPD, for which reactivity coefficient data was calculated, that Oxide5 pin contributions to core

² The algorithms for determining core average reactivity coefficients from pin cell values are explained in chapter 5. Appendix C derives the equations used in the algorithms.

average reactivity coefficients are negligible. This is exemplified in the fuel temperature coefficient results for the end of the second cycle which are presented next.

6.3.1 Fuel Temperature Reactivity Coefficient (FTC). CASMO3 branching Kinf calculations were run for 300, 600, 900, 1200, 1650 and 2100 °K fuel temperatures as a function of burnup. The reactivity added by the change in fuel temperature from 900 °K was calculated. Figure 6.6 shows the UO₂ and Oxide5 pin cell, and reference core average FTC vs Burnup curves. Note that the calculated UO₂ pin cell FTC is lower than the PWR core average “reference values”. However, since these are not meant to be licensing or even design level calculations, the small bias introduced into the determination of the core average FTC is acceptable. The Doppler coefficient becomes less negative as fuel temperature increase due to the reduced percentage increase in resonance broadening effect per degree change in temperature. The coefficient also becomes less negative with depletion and has a strongly positive value at the end of the second cycle. This positive value at the end of the second cycle is somewhat suspect because of problems experienced with CASMO3 at very low fissile densities and strongly subcritical conditions. However, even though these values were assumed to be accurate in order to be conservative, the core average FTC values were still acceptable. At 740 and 880 EFPDs, the Oxide5 pins are highly subcritical and only produce an average power of 0.29 and 0.14 Kw/ft respectively. Thus, based on a power weighting and squared power weighting, the positive Oxide5 FTC pin cell values make little contribution to core average FTC. Figure 6.7 shows the number weighted core average FTC values as compared to the dashed reference design average PWR values. Even using the very conservative number weighting algorithm described in chapter 5, the core average FTC values are consistent with the standard reference PWR values shown as dashed lines. Typical PWR values for the FTC under hot full power conditions are $-1.30 \delta\rho/{}^{\circ}\text{F} \times 10^{-5}$ at BOC and $-1.46 \delta\rho/{}^{\circ}\text{F} \times 10^{-5}$ at EOC [M-6].

Figure 6.6 UO₂ and Oxide5 Pin Cell FTCs vs Burnup

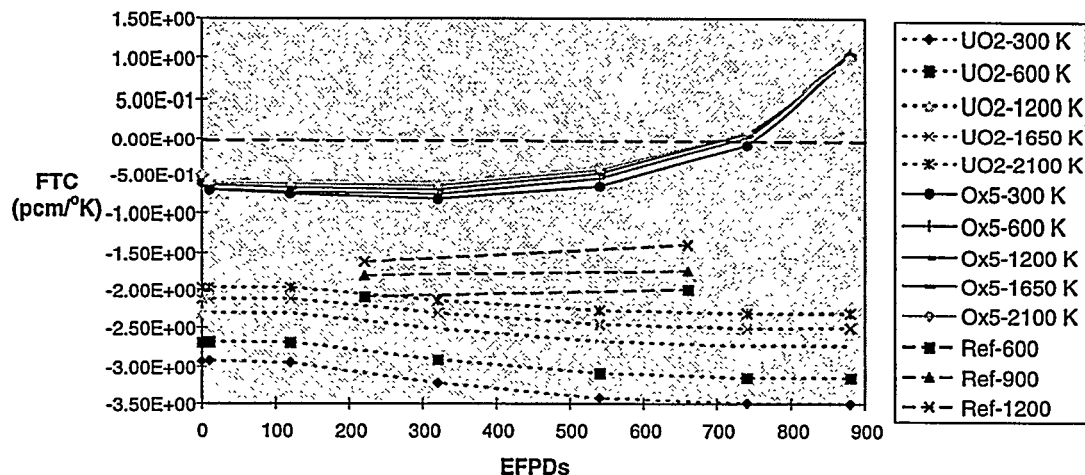


Figure 6.7 Number Weighted and Reference Core Average FTC's vs Burnup

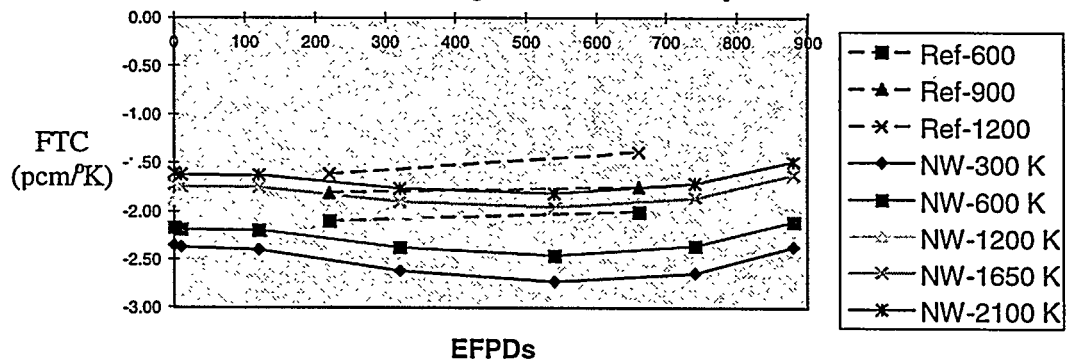


Figure 6.8 shows the power weighted core average FTC values. The effect of the Oxide5 assemblies on the EOC FTC values is reduced due to the lower power contribution of the plutonium pins above 600 EFPDs.

Figure 6.8 Power Weighted and Reference Core Average FTC vs. Burnup

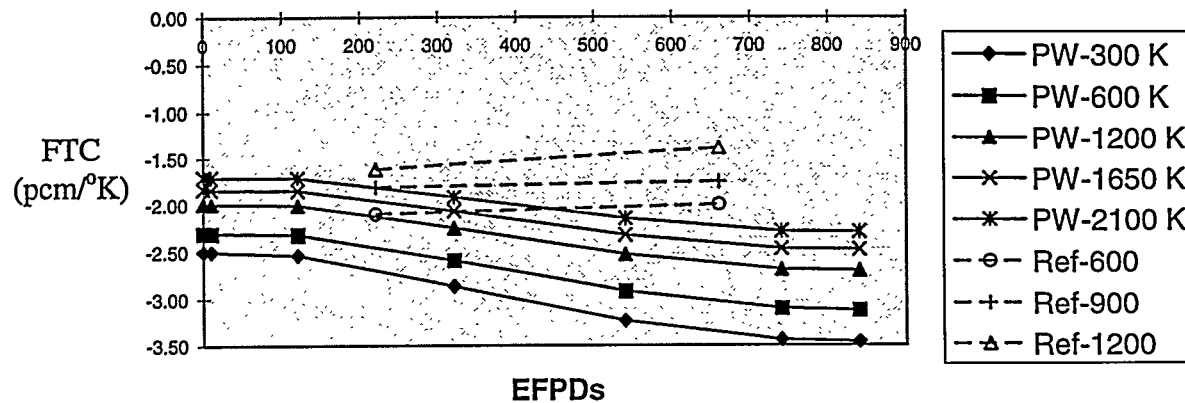
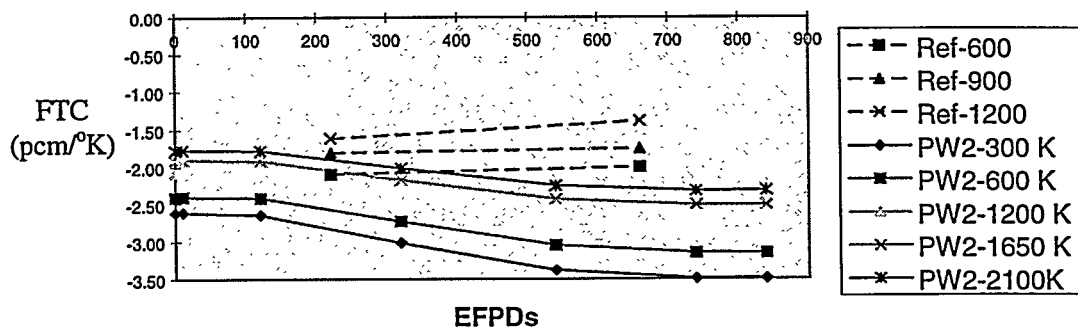


Figure 6.9 shows the results of the most accurate (but least conservative) power squared core average coefficient algorithm. These values are the most negative of those produced by the three algorithms. Thus, the FTC values produced by all three algorithms indicate that the core average FTC with peripherally loaded Oxide5 assemblies is within normal PWR FTC values. The next reactivity coefficient of interest is the Moderator Temperature Coefficient.

Figure 6.9 Square Power Weighted and Reference Core Average FTC vs. Burnup



6.3.2 Moderator Temperature Coefficient Results. The equation for the pin cell moderator temperature coefficient is defined in table 6.1. The CASMO3 Oxide5 and UO₂ pin cell MTCs are plotted as a function of burnup in figure 6.10. Figure 6.11 shows the depletion of erbium with burnup, which directly correlates to the shape of the MTC curves. As discussed in chapter 4, erbium was selected as a burnable poison because its resonances around 0.46 and 0.58 ev provide a negative MTC. Consequently, the Oxide5 MTC becomes less negative in direct correlation to the depletion of ¹⁶⁷Er. Note that there appears to be no UO₂ pin cell bias relative to the reference PWR core average parameters.

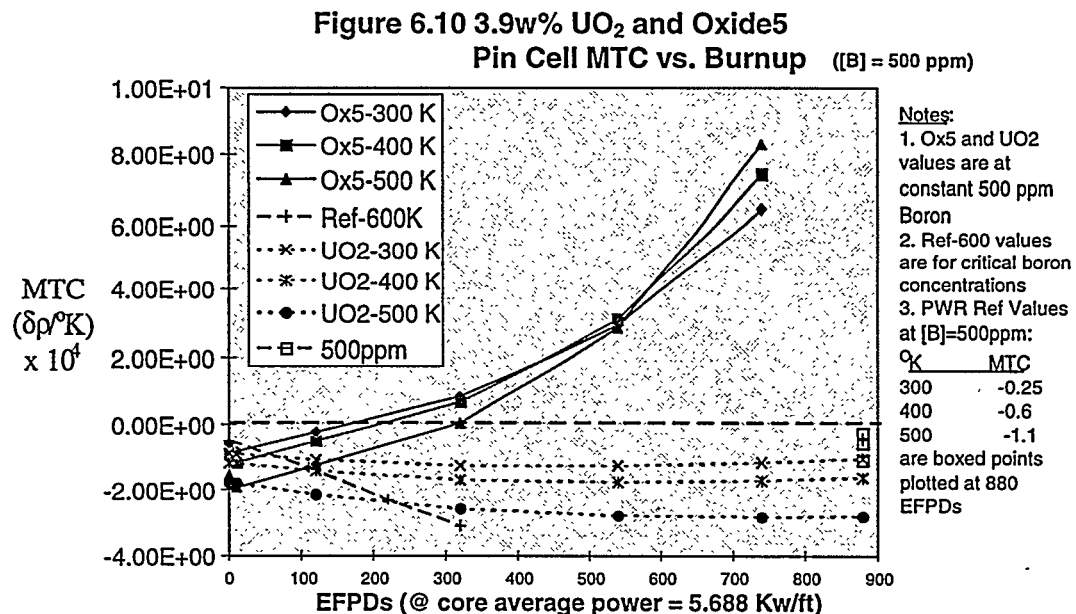
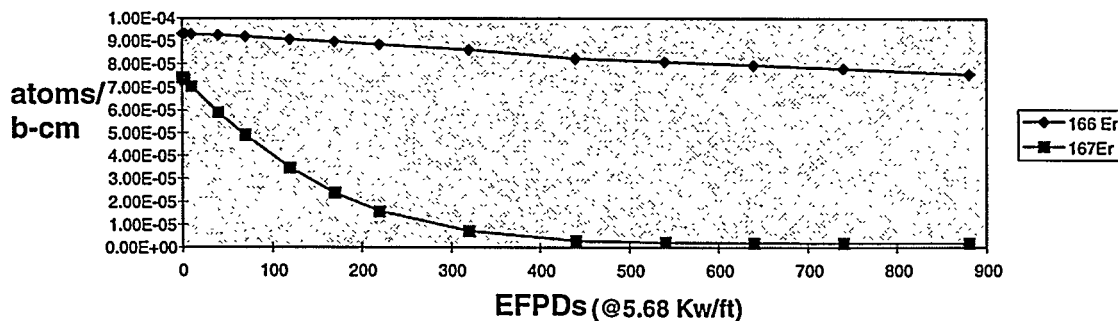


Figure 6.11 Erbium Composition vs EFPDs



The positive Oxide5 MTC values at > 300 EFPDs, which is near the end of the first cycle, appears troubling at first glance. Table 6.6 shows that at the start of the second cycle

the OX2 pins produce as much as 63% core average pin power. However, table 6.6 also shows that due to the shielding by the OX1 pins during the first cycle, the OX2 pins have actually only accumulated 271 EFPDs of burnup by the end of the first cycle. Thus, the OX2 pin's MTC is still slightly negative at the start of the second cycle when they are still producing significant power. By 540 EFPDs, the Oxide5 pins average only 22% of the 100% core average pin power. Consequently their contribution to core average properties is greatly diminished by the time their MTC goes strongly positive at the end of the second cycle.

Figure 6.12 shows the number weighted core average MTC. The dashed 600 °K line is a reference value of MTC for a core where the boron concentration is adjusted to maintain the core exactly critical. Thus, as the boron concentration is reduced with increasing burnup, the magnitude of the MTC increases in the negative direction. Thus, this line is not directly comparable with the calculated Oxide5 values which are for a constant boron concentration of 500 ppm. The vertical lines at the right of the chart are standard PWR EOC MTC values for a constant 500 ppm boron concentration at the temperatures listed in the figure notes [C-5]. The very conservative number weighted MTC values result in a positive temperature coefficient at the end of the second cycle. Thus, we must look to the more accurate power and power squared weighted algorithm results plotted in figure 6.13 for acceptable values.

Figure 6.12 Number Weighted and Core Average MTC vs. Burnup [B] = 500 ppm

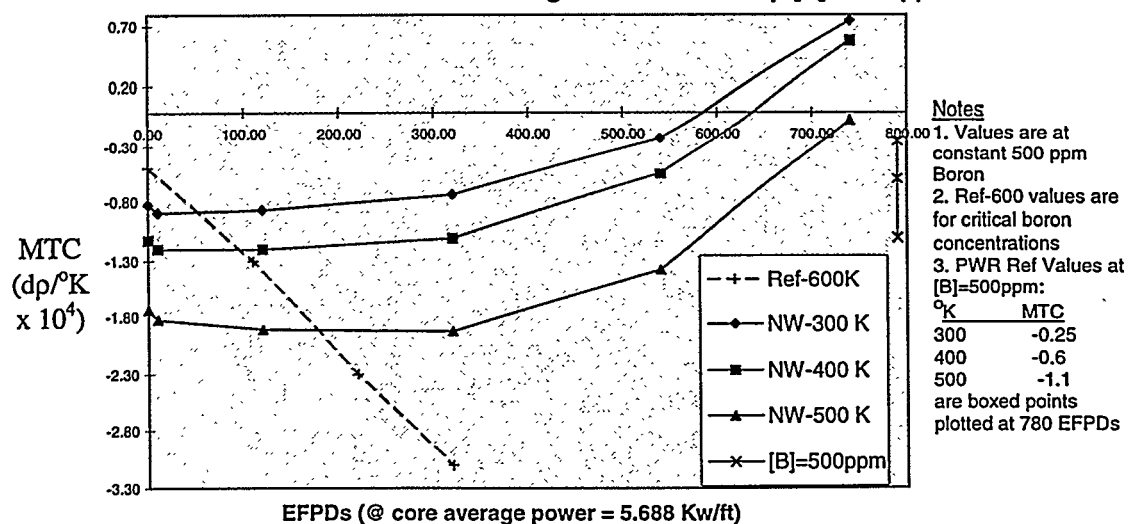
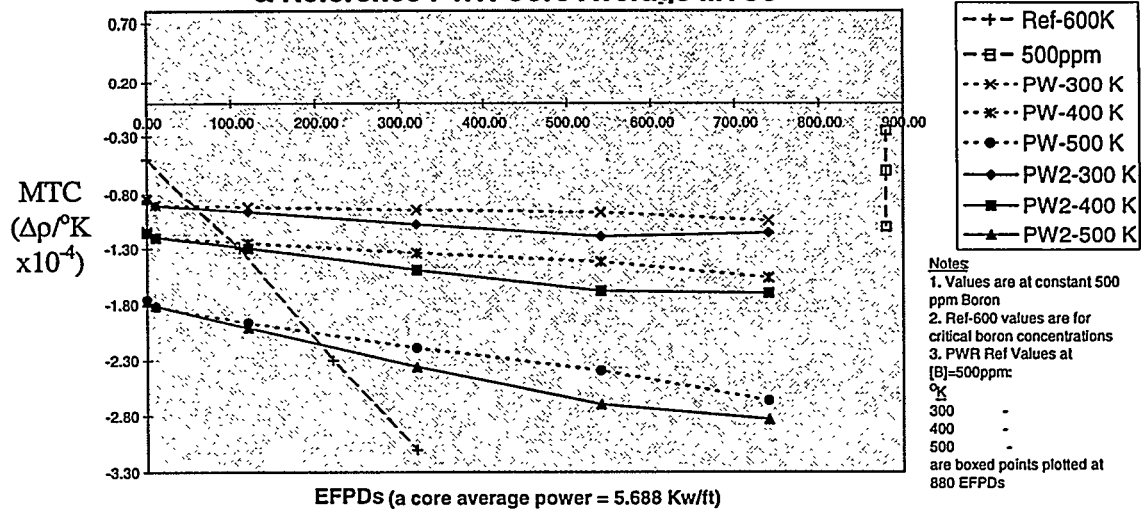


Figure 6.13 Power and Square Power Weighted & Reference PWR Core Average MTCs



Both the power and square power weighting schemes produce acceptable MTC values. The square power MTC values are a more negative and more accurate estimation of core average MTC. The next sub-section examines the inverse boron worth (IBW) and void coefficient (VC) results

6.3.3 Inverse Boron Worth (IBW) and Void Coefficient (VC). The inverse boron worth is calculated in units of ppm/change in reactivity. Thus, a small value equates to a larger boron worth. Figure 6.14 plots the results for the Oxide5 pin cell. These values are not significantly different from the plotted reference PWR values. The Oxide BOC value is approximately 160 as compared to the reference value of 108 and the 740 EFPD Oxide5 value of 50 compares to the 96 reference EOC value. The low BOL Oxide5 IBW is the result of the harder spectrum produced by the large thermal plutonium cross sections. The 740 EFPD Oxide5 IBW of 50 results from the highly thermal spectrum of the over moderated condition and almost completely depleted Oxide5 fuel. Note that the UO₂ pin cell values have a conservative bias relative to the reference core values taken from the literature: i.e.

more ppm boron per % δp . Thus, Oxide5 is not the limiting factor for core average boron worth. Figure 6.15 plots the number and power weighted values.

Figure 6.14 UO_2 and Oxide5 Pin cell and Reference PWR Core Average IBW vs Burnup

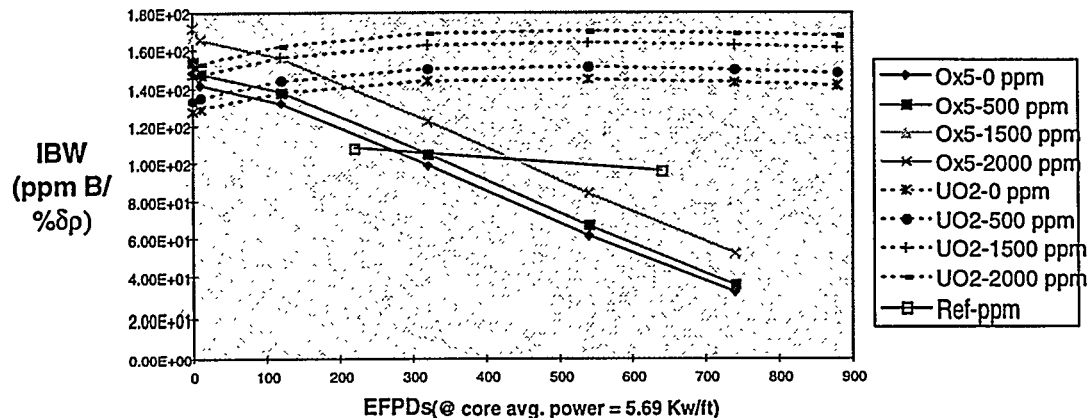
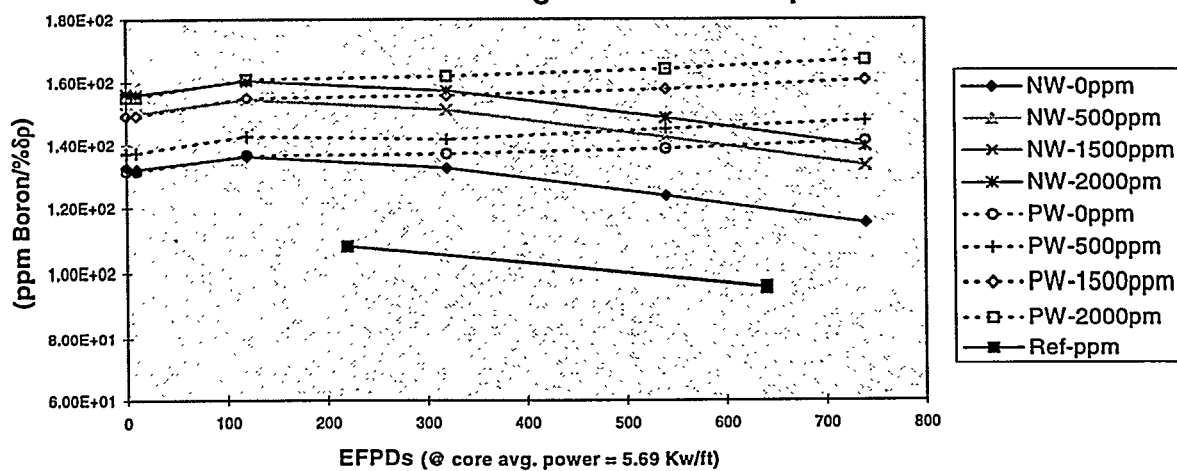


Figure 6.15 plots number and power weighted IBW core average values in. The UO_2 is not depleted like the Oxide5 fuel and has a lower EOC boron worth. The Oxide5 fuel contributes little to the power weighted core average parameter at the end of the second cycle. Consequently, the core average IBW is lower than the Oxide5 IBW at greater than approximately 440 EFPDs. Also, the power weighting IBW is less than the number weighted IBW due to the power weights of the Oxide5 and UO_2 contributions. Thus, the Oxide5 fuel is not a limiting factor with respect to acceptable core average IBW reactivity coefficients.

Figure 6.15 Number & Power Weighted Core Average IBW vs. Burnup



The final reactivity coefficient of interest is the VC. Figure 6.16 shows the Oxide5 VC as a function of burnup for several void percents. Similar to the MTC, the Oxide5 pin cell void coefficient becomes positive for higher burnups because the low fissile material density results in an over-moderated condition. However, lower fissile density also equates to lower power generation in the pins during the second cycle. As with MTC core average values, the power weighted core average VC values are acceptable. Figure 6.17 shows the power weighted and number weighted core average void coefficients [F-4].

Figure 6.16 UO_2 and Oxide5 Pin Cell Void Coefficient vs Burnup

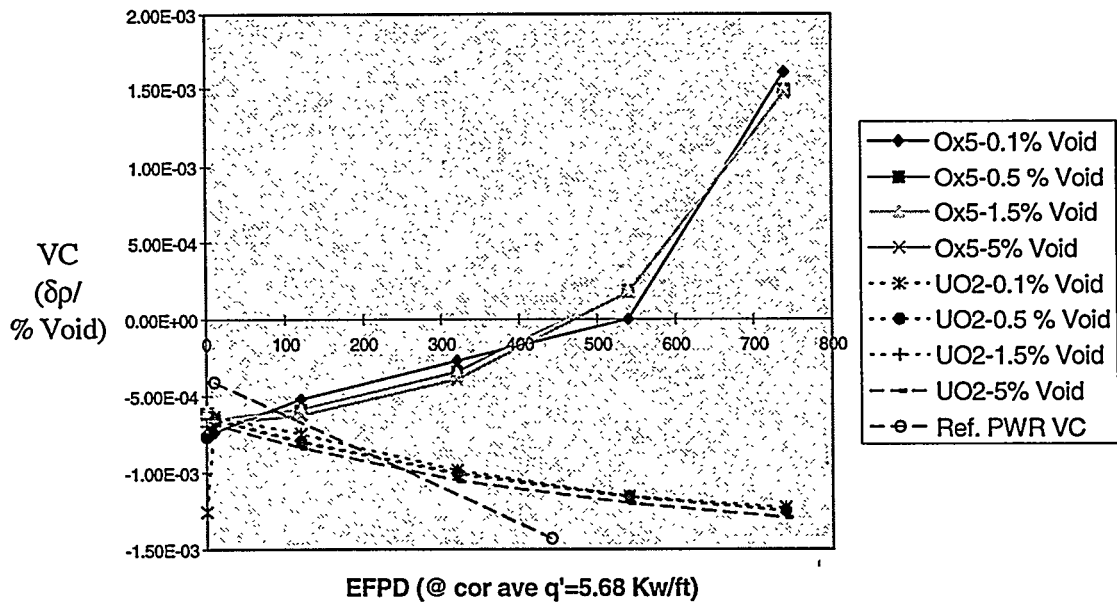
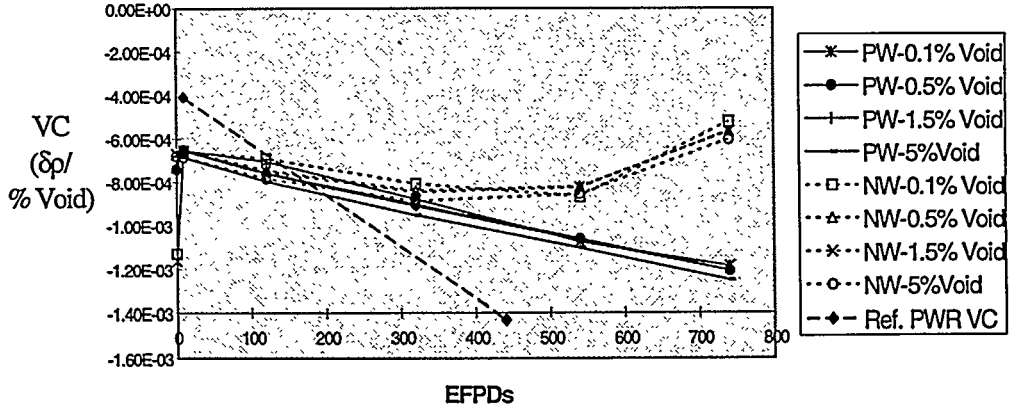


Figure 6.17 Number and Power Weighted Core Average Void Coefficients vs Burnup



6.3.4 Summary of Reactivity Coefficient Results. Table 6.8 summarizes core average reactivity coefficient performance relative to reference PWR values [C-5]. All reference values are for hot full power conditions with calculated core average values produced using the power weighting algorithm. All calculated values are for a moderator boron concentration of 500 ppm and hot full power conditions.

The algorithms used for calculating the core average values from the pin cell values produces results comparable to reference core values. The core average values calculated using the power weighted algorithm are acceptable when compared to reference core average values despite the added conservatism of using power vice square power weighting and taking no credit for the effect of leakage on the periphery reactivity coefficients. The IBW is a bit higher than reference PWR values but is not unreasonable. In conclusion, the Oxide5 periphery PWR core reactivity coefficients are within the design limits. The next section reviews some analysis results for less successful fuel compositions.

Table 6.8 Summary of Core Average Reactivity Coefficient Results [C-5, F-4]

Coefficient	Condition	Reference Values		Calculated Values	
		BOL	EOL	BOL	EOL
FTC $\times 10^5$ $\delta\rho/^\circ\text{F}$	600 $^\circ\text{F}$	-2.1	-2.0	-2.3	-3.12
FTC $\times 10^5$ $\delta\rho/^\circ\text{F}$	1200 $^\circ\text{F}$	-1.6	-1.4	-2.0	-2.7
MTC _{[B]=500ppm} $\times 10^4$ $\delta\rho/^\circ\text{F}$	300 $^\circ\text{F}$		-0.25	-0.85	-1.0
MTC _{[B]=500ppm} $\times 10^4$ $\delta\rho/^\circ\text{F}$	400 $^\circ\text{F}$		-0.6	-1.14	-1.6
MTC _{[B]=500ppm} $\times 10^4$ $\delta\rho/^\circ\text{F}$	500 $^\circ\text{F}$		-1.1	-1.76	-2.7
IBW ppm / $\delta\rho$		108	96	137	148
VC $\times 10^3$ $\delta\rho/\%$ void		-0.41 ^a	-1.43 ^a	-0.816	-1.21

a. Values are for critical moderator boron concentration

6.4 Other Results.

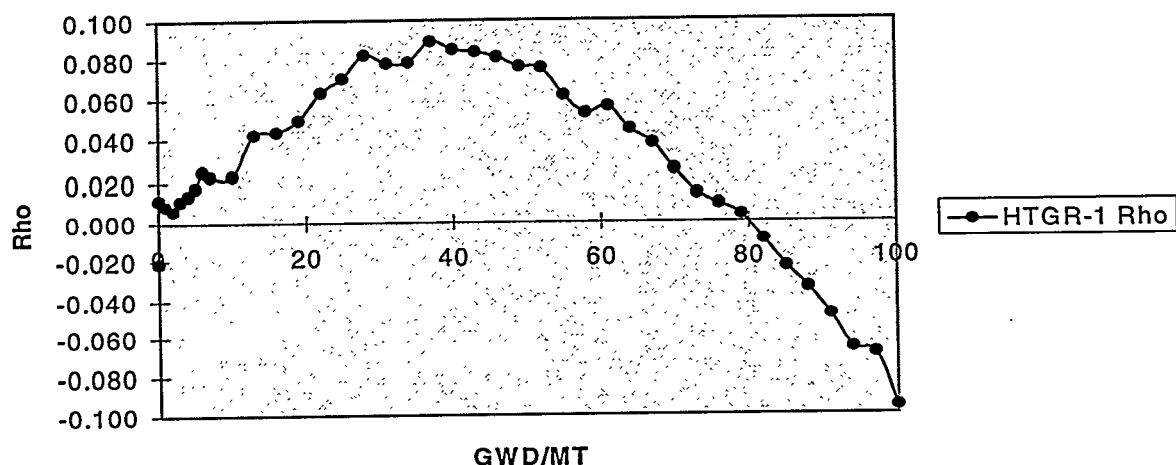
The development of the Oxide5 fuel composition was an iterative process guided by analysis of unacceptable results and intuition. The chapter 5, section 5.3.3, discussion of figure 5.12 is an example of the sort of analysis done. This section presents results and conclusions derived through the analysis of unacceptable fuel compositions.

6.4.1 High Plutonium and Poison Loading. Initial fuel compositions were based on a high, 10w%, WGpu loading with a corresponding high poison loading to hold down initial reactivity. Higher loading provides greater throughput which reduces the number of reactor-years required to complete disposition. This is a key advantage for a WGpu spent fuel standard disposition mission. However, MOX LWR disposition options already produce a spent fuel standard product and are a significantly more mature technology. The advantage of the non-uranium fuel lay in its ability to produce an elimination option. Unfortunately, there are several disadvantages to high plutonium loading with respect to an elimination option.

Higher plutonium loading necessarily means that a larger number of fissions per length of fuel are required to achieve a given level of plutonium destruction. A larger number of fissions can be produced by either leaving the pins in the core longer or increasing the power density. Both techniques place more stringent performance burdens on a novel fuel development effort. In addition, higher plutonium loading forces greater reliance on burnable poison control. This reduces the feasibility of using erbium as the burnable poison because of its relatively smaller thermal and resonance cross sections. The erbium number density would have to be nearly 10 times that of Eu and more than a factor of 20 higher than that of Gd to provide the same reactivity hold down. However, both Eu and Gd burn out much faster and produce a less negative MTC than Er, as explained in chapter 4 section 4.3.4. Thus, the probability of developing radial power peaking problems midway through the cycle is increased with Eu and Gd use. Lower radial power peaking is possible with lower plutonium loading. For example, HTGR1 fuel had three times the fissile density of Oxide5 and used Eu to hold down excess BOC reactivity. Figure 6.18 shows the resultant peak in

reactivity at approximately 40 GWd/MT. The burnup units are Giga-Watt-Days/Metric-Ton Heavy Metal (GWd/MT). This increase and then decrease in reactivity is typical of high plutonium loading fuel with Eu or Gd poison. It is also important to note that at 100 GWd/MT, there remains substantial quantities of plutonium. Table 6.10 shows the depletion composition summary for HTGR1.

Figure 6.18 HTGR-1 Reactivity vs Burnup



At 100 GWd/MT the HTGR1 fuel is very subcritical and yet < 51% of the total plutonium and 48% of the ^{239}Pu has been destroyed. Eliminating the plutonium would require significantly higher burnups and longer core residence times. Thus, the fuel would have to be taken to very high burnups and spend a significant portion of its residence time placing a negative reactivity load on the core. Consequently, increasing the plutonium loading usually results in increased plutonium residuals in the discharged spent fuel. Also, the reactivity peak mid cycle caused by rapid burnup of the Eu, tends to produce unacceptable radial power peaking. Lower loadings produce less BOL excess reactivity; thus, the excess reactivity is small enough to be controlled by erbium without having to resort to large erbium number densities. Erbium burns out slower and lower radial power peaking is observed. Thus, low plutonium loading is preferred to create an elimination option fuel.

Table 6.9 HTGR-1 Depletion Isotopic Summary

Depleted @ :80% Core Ave Specific Power = 30.65 MW/MT (73 kW/I)

Gwd/MT:	0	40	100			
	gms	w%	gms	w%	gms	w%
Fissile:						
U233			1.22E-01	0.49%	2.28E-01	0.92%
Pu239	4.72E+00	19.30%	3.19E+00	12.76%	1.24E+00	5.03%
Pu241	2.00E-02	0.08%	1.79E-01	0.72%	3.30E-01	1.33%
Total Fissile w%:	19.38%		13.96%		7.28%	
Fertile:						
Th232	1.83E+01	74.68%	1.81E+01	72.34%	1.78E+01	72.07%
U238	6.63E-01	2.71%	6.27E-01	2.51%	5.75E-01	2.33%
Pu240	1.65E-01	0.67%	5.07E-01	2.03%	7.25E-01	2.93%
Total Fertile w%:	78.06%		76.87%		77.33%	
Actinides:						
Total Pu	4.91E+00		3.89E+00		2.39E+00	
Total U	6.63E-01		7.55E-01		8.29E-01	
Pu238					2.16E-03	
Pu242						
Poisons:						
Total FP	0.00E+00	0.00%	1.70E+00	6.79%	3.33E+00	13.48%
Eu151	2.98E-01	1.22%	4.45E-02	0.18%		0.00%
Eu152			9.50E-02	0.38%	1.23E-02	0.05%
Eu153			3.62E-01	1.45%	3.04E-01	1.23%
Eu154			7.58E-02	0.30%	1.17E-01	0.47%
Eu155	3.26E-01	1.33%	1.68E-02	0.07%	3.86E-02	0.16%
Eu w%:	2.55%		2.38%		0.16%	
Total gms:	2.45E+01		2.50E+01		2.47E+01	
$^{233}\text{U}/\text{U}_{\text{tot}}$:	0.0%		16.1%		27.5%	
$^{239}\text{Pu}/\text{Pu}_{\text{tot}}$:	96.2%		82.0%		52.0%	
$^{239}\text{Pu}/^{239}\text{Pu}_0$:	100.0%		67.6%		26.3%	
$^{239}\text{Pu}_{\text{tot}}/\text{Pu}_{\text{tot}}$	100.0%		79.3%		48.7%	

6.4.2 Comparison of Thorium and non-Thorium Fuels. PWR pin cell calculations of the reactivity profile and depletion isotopics of two candidate fuel compositions are presented. Discussion of an alumina non-fertile fuel composition is followed by review of a thorium loaded TRISO fuel.

The fresh composition of the non-fertile alumina fuel is given in table 6.11. The fuel consists of a Pu-CeO₂ fluorite phase dispersed in an peroskovite matrix. The Cerium, Ce, atom density is five times that of plutonium in order to enhance the chemical separation barrier of the fresh fuel. Note that this fuel has no control poison in the alumina matrix; none is necessary. Figure 6.19 compares the reactivity profiles of the alumina fuel with that of standard 3.9w% enriched UO₂ fuel. The composition of the UO₂ is identical to that used in the code benchmark discussed earlier. Figure 6.19 shows that the fresh non-fertile alumina fuel reactivity is slightly lower than that of UO₂ and the slope of the burnup curve is similar to the that of the standard UO₂ fuel until late in the cycle.

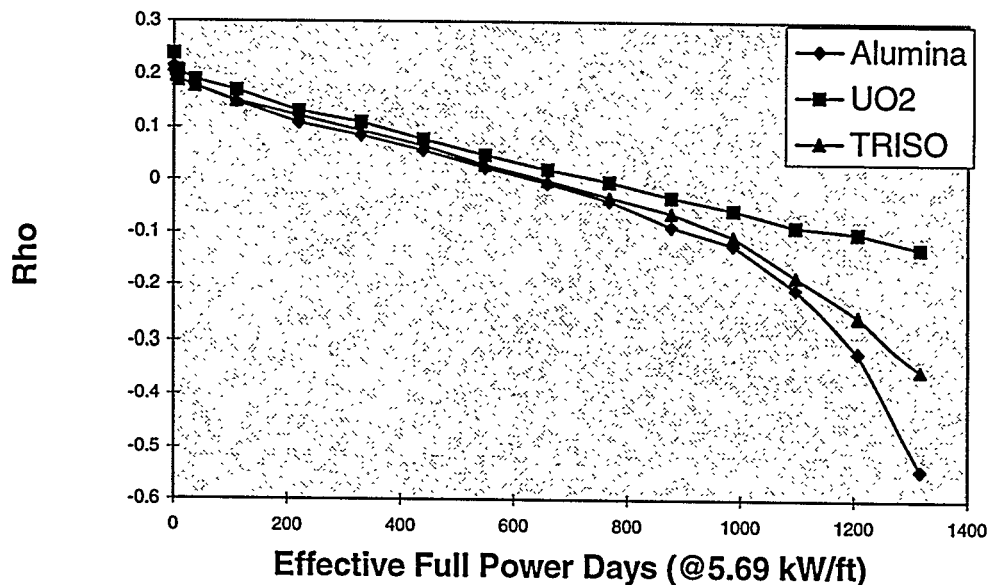
These two facts seem counter-intuitive. First, the alumina fuel fissile atom density is 1.6 times that of 3.9 w% UO₂ and contains no poison; thus, a higher initial alumina reactivity might be expected. However, the absorption cross section of ²³⁹Pu is 1.7 times that of UO₂. The higher cross section coupled with the higher loading leaves the fresh alumina fuel undermoderated. Examination of the spectrum confirms that it is highly epithermal. Thus, the fresh fuel reactivity is suppressed below that of the UO₂. Second, UO₂ produces ²³⁹Pu which reduces the rate of fissile consumption, and hence, the rate of reactivity loss. The lack of fertile material in the alumina might suggest that its reactivity would decrease at a rate greater than that of the standard UO₂. However, the slope of the reactivity profile is proportional to the decrease in mass of fissile material per total mass of fissile material present. Since the ²³⁹Pu loading is 1.6 times that of ²³⁵U in UO₂, there is a smaller percentage decrease of total fissile material per gram of fissile material consumed, thereby reducing the slope of the profile making it comparable to 3.9 w% UO₂. A smaller additional effect may be that as the ²³⁹Pu is depleted, the moderator to fissile fuel ratio increases, thus adding reactivity. Dilute

^{239}Pu has nearly three times the thermal microscopic capture cross section as ^{238}U and ^{240}Pu 's thermal capture cross section is nearly 100 times that of ^{238}U .

Table 6.10 Non-Fertile Alumina Composition

Isotope/Element	Weight %	Density (gm/cm ³)
^{239}Pu	9.31	5.63E-1
^{240}Pu	0.60	3.61E-2
^{241}Pu	0.050	3.01E-3
^{151}Eu	0.00	0.00E0
^{153}Eu	0.00	0.00E0
Ce	29.11	1.76E0
Al	33.72	2.04E0
O	27.20	1.64E0
Total	1.00	6.04

Figure 6.19 Alumina and TRISO Reactivity vs. Burnup



Thus, the fissile ^{241}Pu production in WG Pu fuel is comparable to that of ^{239}Pu density in UO_2 fuel. The number densities of 240 & ^{241}Pu in Alumina and ^{239}Pu in UO_2 as a function of EFPDs in table 6.12 add some credence to this argument. A combination of these factors may explain the parallel slope in the reactivity vs. burnup curves of UO_2 and non-fertile alumina.

fuels. As the total ^{239}Pu atom density decreases, the rate of reactivity decrease per gram of ^{239}Pu consumed increases and the production of ^{241}Pu decreases leading to the divergence in slopes at higher burnups.

Table 6.11 Comparison of Fertile Production of Fissile Material in UO_2 and Alumina Fuels

EFPDs	Alumina		UO_2
	^{240}Pu (atom/b-cm)	^{241}Pu (atom/b-cm)	^{239}Pu (atom/b-cm)
0	9.65E-5	7.52E-6	0.0E0
329	1.63E-4	3.72E-5	9.51e-5
658	2.17E-4	1.13E-4	1.34E-4
988	2.018E-4	1.33E-4	1.50E-4

Table 6.13 lists isotopic results for depletion of non-fertile alumina and TRISO fuels. Nearly all of ^{239}Pu and approximately 80% $^{\text{Tot}}\text{Pu}$ is destroyed. The best reported MOX PWR once through cycle isotopics results were approximately 0.1w% ^{238}Pu , 50w% ^{239}Pu , 30w% ^{240}Pu , 16w% ^{241}Pu and 4w% ^{242}Pu but with a net plutonium destruction of less than 35% [D-4]. Next, the thorium loaded TRISO fuel pin results are considered.

Table 6.12. TRISO and Alumina Fuel Depletion Isotopics

EFPDs	^{238}Pu w%	^{239}Pu w%	^{240}Pu w%	^{241}Pu w%	^{242}Pu w%	^{239}Pu Dest.	$^{\text{Tot}}\text{Pu}$ Dest.
Non-Fertile Alumina							
0	0.00	93.5	6.00	0.50	0.00	0.00	0.00
768	0.01	48.4	29.5	18.3	3.65	75.20	72.60
1317	0.17	11.9	37.6	27.9	22.4	97.4	79.60
Thorium-Loaded TRISO							
0	0.00	93.5	6.00	0.51	0.00	0.00	0.00
768	0.01	58.3	24.6	14.7	2.19	66.87	43.27
1317	0.01	21.7	36.7	27.1	14.2	93.70	72.80

The TRISO fuel pin is assumed to have a packing density of 90 volume % of which 68% is filled with carbon from either the PyC or SiC layers or carbon compact fill material.

The fuel kernels occupy only 22 volume % of the pin. However, the fuel kernel ^{239}Pu w% was increased to maintain an overall pin fissile density similar to that of the alumina fuel. The kernel composition is listed in table 6.14. Thorium provides fissile ^{233}U . Thorium is also an excellent aqueous plutonium analog. Special units had to be added to the PUREX process to effect adequate separation of thorium from uranium and plutonium product streams in thorium fuel cycles: the result was the THOREX process. ^{238}U is loaded to maintain end of cycle ^{233}U w% below 20% of the total U in the spent fuel; however, use of the minimum loading which achieves that end is required to minimize ^{239}Pu production. At this low loading no significant ^{239}Pu production was observed. The TRISO fuel is also depleted at a constant q' of 5.68 Kw/ft, producing the reactivity profile seen in figure 6.19. The profile closely follows the alumina reactivity except at higher burnups where the fertile conversion has a larger effect due to the depleted ^{239}Pu inventory in the TRISO fuel. This further supports the assertion that the slope of the reactivity burnup curve can be controlled to a large extent through manipulation of the fissile density. The TRISO and alumina have similarly high fissile densities and thus similar reactivity profiles.

Table 6.13 Thorium TRISO Fuel Composition

<u>Isotope/Element</u>	<u>Kernel HM Weight %</u>	<u>HM Density (gm/cm³)</u>
^{239}Pu	26.65	5.55E-1
^{240}Pu	1.71	3.601E-2
^{241}Pu	0.14	3.00E-3
^{232}Th	67.93	1.43E0
^{238}U	3.58	5.2E-2
Total	100.0	2.067

A review of table 6.12 shows that the TRISO fuel also performs significantly better than MOX LWR burning options but not as well as the alumina fuel. Some of the power is provided by ^{233}U rather than ^{239}Pu fissions. Thorium production of ^{233}U reduces the total plutonium and ^{239}Pu destruction and reduces the isotopic dilution. Thus, thorium is rejected for use in plutonium elimination fuel. Although both the TRISO and Alumina fuels produce

plutonium destruction much greater than that of UO_2 , neither could be considered an elimination option.

6.4.3 Summary of Other Results. Three major conclusions were drawn based on the results presented in this section and the discussion in chapter 5 section 5.3.3 of figure 5.12. First, lower plutonium loading has major advantages for producing an elimination option. Second, lower plutonium loading reduces the required poison loading allowing the use of erbium. Thus, a flatter reactivity profile and lower radial power peaking are possible. Third, thorium reduces the rate of plutonium destruction and is therefore rejected for use in an elimination option.

6.5 Summary of Oxide5 Results. The Oxide5 fuel composition, listed in table 6.3, is designed to be resident on the periphery of the core for two 440 EFPD cycles and then discharged. The assembly is rotated 180 degrees after the first cycle. A single transition cycle is used to produce an equilibrium cycle where the core periphery is filled with alternating once burned and fresh Oxide5 assemblies. The interior of the core is filled with three batch UO_2 assemblies. Table 6.15 summarizes the criteria performance results for the Oxide5 fuel.

The Oxide5 composition starts out with low plutonium loading. Consequently, it produces significant power through the first, but only half of the second, cycle. During the last 220 EFPDs in the core the residual plutonium is destroyed producing a true elimination option. Total plutonium destruction is in excess of 90% and eventually all of the ^{239}Pu is destroyed. The radial power peaking and core reactivity are within normal PWR limits throughout both cycles. The average power produced over the two cycles is 47%. Thus, there is a small net gain in average power produced in the periphery. The throughput of the proposed cycle is acceptable.

The WGPu throughput of this cycle is 124 kilograms per year; a 50 MT WGPu disposition mission would take 404 reactor years and assuming all other existing constraints were removed, the 72 operating US PWRs could disposition the 50 MT of WGPu in 5.6 years [N-4]. Alternatively, loading Oxide5 fuel on the periphery of otherwise standard UO₂ cores would reduce plutonium production by 75%. Thus, the growth of RGPU inventories could be significantly reduced.

Table 6.14 Summary of Oxide5 Neutronic Performance

<u>Parameter</u>	<u>Oxide Peripheral</u> <u>Calculated Core</u> <u>Average Value</u>	<u>Specification</u>	<u>Comments</u>
Discharge Properties (must substantially eliminate plutonium)			
Residual Pu	0%	< 10%	want to minimize weapons usability ^A
Residual Plutonium	7%	< 10%	want to minimize weapons usability ^A
Fuel Cycle Feasibility (non-uranium Pu fuel must not impose any restrictions greater than those imposed if the periphery were loaded with twice burned UO₂)			
Residence Time	880 EFPDs	multiple of 440 EFPDs	must support 18 month refueling cycle
Radial Power Peaking	Max peak over two cycle = 1.5	< 1.5	must not be too large so as to cause total power peaking to exceed 2.5.
BOL and EOC Whole Core Reactivity	BOC Keff = 1.31 EOC Keff = 1.05	≤ 1.3 & ≥ 1.00	Whole Core BOL and EOC reactivity must be within PWR design limits
Reactivity Coefficients (whole core average reactivity values must be within acceptable PWR design range)			
FTC ^c units = (pcm/°F)	BOC to EOC: -1.85 to -1.7	BOC to EOC: -1.30 to -1.46	Typical PWR Design Values
MTC ^c units = $\delta\mu/^\circ F \times 10^4$	BOC to EOC: -1.76 to -2.7	BOC to EOC: -0.78 to -3.02	Typical PWR Design Values
IBW units = ppm / % $\delta\mu$	BOC to EOC: 137 to 148	BOC to EOC: 108 to 96	Typical PWR Design Values
VC units = $\delta\mu / \% \text{void} \times 10^3$	BOC to EOC: -.86 to -1.21	BOC to EOC: -0.41 ^B to -1.43 ^B	Typical PWR Design Values

A. Weapon's usability is described in chapter 3 section 3.3.

B. Values are for critical moderator boron concentration.

C. Values at normal operating temperatures.

The calculated reactivity coefficients for the PWR core with Oxide5 assemblies loaded in the periphery are comparable to reference PWR core average values. This is despite the added conservatism of using power rather than square power weighting. Thus, Oxide5 assemblies can be used in the periphery of a PWR to eliminate plutonium.

CHAPTER SEVEN: SUMMARY AND CONCLUSIONS

7.1 Scope and Objectives

The risk of nuclear proliferation associated with the liberation of 100 metric tons of weapons grade plutonium (WGPu) from US and Russian nuclear arsenals and increasing world reactor grade plutonium (RGPu) stockpiles has led proliferation experts to call for world-wide management of plutonium [B-1, N-1, M-3, V-1]. One of the key tenets of proposed plutonium management plans is the reduction of stockpiles to the minimum levels consistent with needs. The only way to irrevocably reduce stockpiles is to destroy the plutonium through fission and transmutation. The most promising method for effecting large scale transmutation of plutonium in a timely manner is through burning it in light water reactors.

This thesis examined the feasibility of using non-uranium fuel in a pressurized water reactor radial blanket to eliminate plutonium of both weapons and civilian origin. Several constraints are considered including impact on proliferation risk, acceptability of resultant core physics parameters, and fuel performance and manufacturing feasibility. Elimination is defined as substantially complete destruction of plutonium. Large scale use of non-uranium

fuels for plutonium disposal will require a significant research and development effort. The goal of this work is to suggest a starting point for that development.

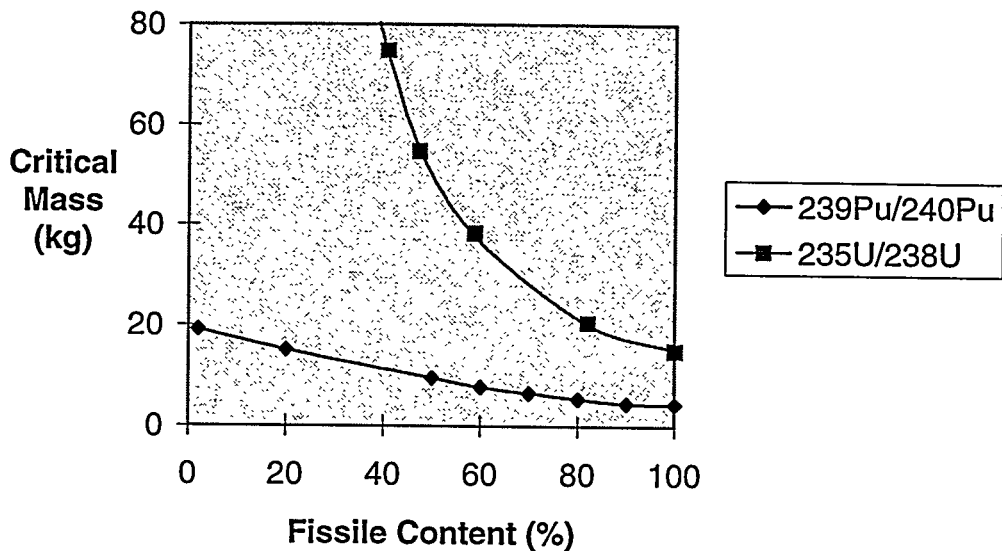
7.2 Background and Motivation for Work

Plutonium of nearly any isotopic composition can be used to produce an explosive critical mass.¹ Figure 1.1 plots the critical mass for a simple nuclear weapon design consisting of a metal sphere surrounded by a thick neutron reflecting uranium metal shell, as a function of the metallic uranium or plutonium sphere isotopes [R-2]. The difficulties in producing such a weapon with RG⁹⁰Pu are not appreciably greater than those encountered with WGPu [M-1]. Approximately 10 kilograms of the plutonium found in typical once-through light water reactor spent fuel would be sufficient to build a simple nuclear explosive which would have an approximate yield of one kiloton. A one kiloton yield would have a lethal range roughly one third that of the Hiroshima explosion [N-2]. Thus, a very simple RG⁹⁰Pu weapon could be used to destroy a significant portion of a large city and cover the rest in radioactive fallout. Plutonium theft by a non-national entity is the reference nuclear proliferation scenario of concern in this thesis.

The basic information required to assemble a nuclear weapon from its raw materials has been public for many years [T-2]. Unlike uranium, plutonium can not be denatured to prevent its use as weapons material and as such is uniquely suited to support fast chain reactions. Therefore, physical control of plutonium and other weapons usable fissile materials is the primary means of limiting the proliferation of nuclear destruction capabilities.

¹ Plutonium which is comprised primarily of ^{238}Pu or ^{242}Pu is of little practical use in nuclear explosives. However, these exceptions are inconsequential since the vast majority of the world's plutonium is of an isotopic composition which makes it of practical weapons use.

Figure 7.1 Critical Mass of Uranium and Plutonium as a Function of Isotopic Mix [R-2]



The world inventory of plutonium is already large and is growing rapidly at a rate of 70 MTs/year [N-1]. Total plutonium stockpiles will reach 1700 MTs by the year 2000. Separated RGPU is being produced at the rate of 20 MT/year which exceeds consumption and will result in a stockpile of approximately 170 MTs by the year 2000. In addition, the INF and START treaties will liberate approximately 100 MTs of WGpu for disposal. The reliability of international safeguards in deterring and detecting diversion of plutonium for non-peaceful purposes is a function of the size and physical form of the stockpile which must be safeguarded.² Consequently many experts have called for reduction of world inventories of plutonium [M-2, N-1, V-1]. The primary way currently available to reduce plutonium stockpiles is to fission it in light water reactors.

Unfortunately, neutron capture in the ^{238}U present in MOX produces ^{239}Pu , thereby reducing the maximum net plutonium destruction possible. Plutonium destruction in a light water reactor with a mixed oxide core destroys only approximately 30-40% of the total

² For example, Pu in the form of fuel assemblies which can be counted are easier to safeguard than Pu in the separations part of a reprocessing plant where it is dissolved in various radioactive solutions [M-2].

plutonium loaded while non-uranium plutonium fuel can destroy nearly twice that amount [D-4].

7.3 Summary of Proposed US WGPu Reactor Disposition Options and the RGPu Mission

This section summarizes the proposed options for burning 50 MT of US WGPu. Table 7.1 summarizes the key destruction capabilities of example reactor vendor proposals for disposal of 50 MT of WGPu in 25 years. The Combustion Engineering System 80+ PWR and the General Electric BWR-5 designs represent currently operating LWRs. The Westinghouse PDR1400 is an evolutionary PWR design and the General Electric ABWR is an advanced BWR design. The General Atomics Plutonium Consumption - Modular High Temperature Gas Reactor (PC-MHR) is most efficient for plutonium destruction because it uses non-uranium fuel. However, the PC-MHR reactor and fuel technology is the least mature option. The Canadian Deuterium Uranium (CANDU) reactors have extremely flexible reactivity control systems and are estimated to require the shortest lead time before WGPu burning operations could begin. These reactors produce spent fuel which makes the plutonium roughly as inaccessible as the plutonium in conventional spent fuel; thus, they meet the NAS defined "spent fuel standard". WGPu accounts for 6% of the worlds plutonium stockpile. Thus, making the metallic WGPu pits more unattractive for weapons use than RGPu in spent fuel provides little additional proliferation risk reduction unless the larger RGPu stockpile is also subject to elimination. However, the NAS states in its 1994 report on weapons grade plutonium disposition that "Further steps should be contemplated, however, to move beyond the spent fuel standard and reduce the security risk posed by all the world's plutonium stocks, military and civilian, separated and unseparated; the need for such a step already exists and will increase with time" [N-1]. This suggests that there are two distinct plutonium disposal missions: WGPu disposal and RGPu disposal.

WGpu plutonium disposal mission proposals are designed to convert 50 MTs of metal pits into a product which meets the spent fuel standard in approximately 25 years. The RGpu mission involves reducing the proliferation risk of the complete world stockpile of all plutonium [M-2, N-1, V-1]. To reach a condition of no net production of RGpu, 60-70MT of RGpu must be destroyed annually. This will require a broad application of plutonium elimination technology. Over 60% of operating US light water reactors are PWRs [N-4]. A fuel which could eliminate plutonium in a once-through PWR cycle could be used for an ongoing RGpu disposal mission as well to complete a WGpu mission. In the present work, metrics for quantifying the proliferation risk associated with the disposition products were developed and WGpu MOX spent fuel, WGpu borosilicate glass and WGpu non-uranium spent fuel were compared.

Table 7.1 Summary of US WGpu Reactor Disposition Options						
Metric	Reference Designs					
	System-80	BWR-5	PDR1400	ABWR	PC-MHR	CANDU
Throughput (MT WGpu/Rx-yr)						
	1.5	1.06	1.56	1.2	0.28	1.05
Discharge Isotopes (kgm Isotope /kgm total Pu Mass)						
²³⁸ Pu	0	0.010	0.02	0.006	0.003	0.001
²³⁹ Pu	0.609	0.421	0.54	0.590	0.275	0.513
²⁴⁰ Pu	0.234	0.353	0.227	0.270	0.302	0.375
²⁴¹ Pu	0.137	0.151	0.151	0.105	0.327	0.086
²⁴² Pu	0.027	0.066	0.062	0.028	0.093	0.024
Destruction Fraction (kgm loaded/kgm discharged)						
²³⁹ Pu	0.49	0.71	0.53	0.61	0.89	0.63
Total Pu	0.22	0.36	0.18	0.38	0.64	0.34
Average Burnup (GWd/MTHM)						
	32.5	39.2	40.0	39.0	590.2	9.7
% Pu in HM						
	3.7	2.0	1.1	4.1	96.1	1.0
Discounted (4%) Life Cycle Cost (Revenue) in \$M - Government Ownership						
	not avail.	not avail.	(759)	(552)	(1324)	not avail.
Discounted (4%) Life Cycle Cost (Revenue) in \$M - Utility Ownership						
	not avail.	1313	1111	1113	(660)	1481

7.4 Quantification of the Proliferation Resistance Inherent in Disposition Products

Quantification of proliferation resistance is controversial [N-2]. However, it is important to be able to gauge approximately how proliferation resistant the end product of a disposition option is relative to other products and the spent fuel standard. Such quantification can not only help in selecting which options are most useful for plutonium disposition but it can also illuminate where the emphasis of future improvements to fuel cycle proliferation resistance can be made. This section details an approach for such quantification. It is offered as a logical and objective starting point for discussion and modification rather than the definitive method. The intent is to quantify the inherent resistance of disposition option products themselves. Inherent proliferation resistance refers to the barriers that prevent a terrorist with access to a disposition product from making a nuclear device.

7.4.1 Definition of Metrics. Table 7.2 lists the metrics proposed for quantifying the proliferation resistance of final disposal products. The metrics measure disposition product properties which act as a barrier to producing a weapon from the plutonium contained in the product. Two barrier types were identified: disposition product matrix barriers and plutonium weapons usability. Disposition product matrix barriers are those barriers presented by the matrix against recovery of the plutonium contained in it. Plutonium weapons usability barriers are those barriers against using the plutonium once it is recovered from the matrix.

7.2 Inherent Plutonium Disposition Product Barrier Metrics

Criteria	Type of Measurement	Units/Scale
Disposition Product Matrix Barriers		
Fissile Density	Quantitative	kg fissile Pu/m ³ host
Dissolution	Quantitative	gms/liter
Separation	Quantitative	dimensionless
Radiation Barrier	Quantitative	years
Plutonium Weapons Usability		
Isotopic	Quantitative	gms fissile/gm Pu
Critical Mass	Quantitative	kg Pu
Neutron Emission	Quantitative	n/sec-kg Pu
Decay Heat	Quantitative	w/gm Pu
1. The separation metric is calculated by ratioing separation distribution coefficients if the data can be found. Alternately it is calculated as an ionic radius ratio as described in section 3.2.3.		

7.4.2 Example Computation and Comparison of Proliferation Resistance of Spent WG⁹⁴Pu MOX, a WG⁹⁴Pu Borosilicate Glass Log and Spent WG⁹⁴Pu Non-Uranium Fuel. Table 7.3 lists the metric values for the three disposition products. Metric values are converted into scores using scoring functions. The spent fuel standard was used as the minimum acceptable proliferation barrier performance. Consequently, metric values equivalent to those for spent fuel received a score of zero with a negative score given for sub-spent fuel performance and a positive score for proliferation resistance beyond spent fuel's. Investigating the optimum shape for these scoring functions was beyond the scope of this work. Simple linear scoring functions were used similar to the example critical mass scoring function in figure 7.2.

Table 7.3 Raw Metric Values

Metric (units in Table 7.2)	Spent LEU	HLW Glass Log	Spent WGPu MOX	WGPu Non-U Fuel
Disposition Product Matrix Barriers				
Fissile Density	158	18.34	97.48	1.55
Dissolution	167	not applicable	167	211
Separation	40	0.12	40	0.37
Radiation Barrier	160	145	160	160 ^a
Plutonium Weapons Usability				
Isotopic	68.6	94.5%	69.1%	10.2%
Critical Mass	15.4	12.0	16.6	48.3
Neutron Emission	3.3×10^5	5.3×10^4	4.4×10^5	1.4×10^6
Decay Heat	10.3	2.3	14.4	10.3

a. The non-uranium radiation barrier is assumed to be the same as MOX spent fuel.

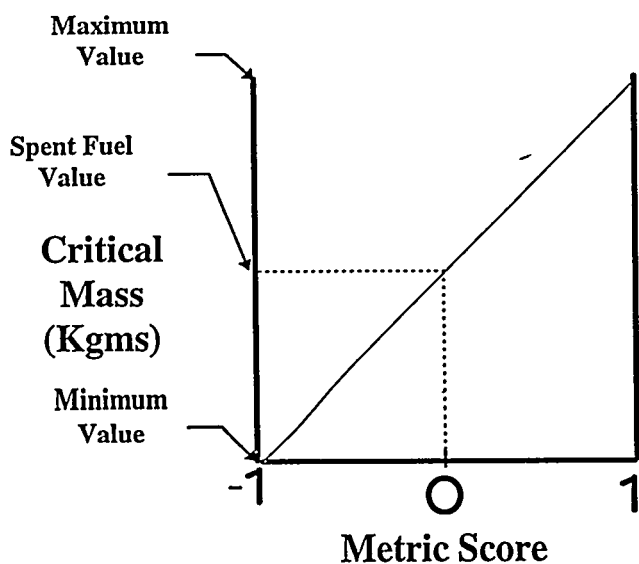


Figure 7.2 Example Critical Mass Metric Scoring Function

Table 7.4 presents the results of scoring of each metric for the three disposition products.

Within the two barrier types, individual metric scores were weighted from zero to one based on their relative importance in creating the barrier. For example, the neutron emission rate of RGPU will not prevent producing a one kiloton terrorist weapon. However, a weapon can not work unless a critical mass has been accumulated. Thus, from a terrorist threat scenario viewpoint, the critical mass metric is more important and its contribution to the weapons barrier is given greater weight. The weights within each barrier type sum to unity; hence, equal weight is given to matrix and plutonium weapons usability barriers. The relative resistance of each barrier type for each disposition product is quantified by the sum of the associated metric scores and weights. Table 7.5 presents the results for the three disposition products considered here.

Table 7.4 Metric Score Summary

Metric	Spent LEU	HLW Glass Log	Spent WGPU MOX	WGPU Non-U Fuel
Disposition Product Matrix Barriers				
Fissile Density	0.00	0.89	0.39	1.00
Dissolution	0.00	0.00	0.00	-0.26
Separation	0.00	-1.00	0.00	-0.99
Radiation Barrier	0.00	-0.19	0.00	0.00
Plutonium Weapons Usability				
Isotopic	0.00	-0.82	-0.02	1.00
Critical Mass	0.00	-0.22	0.04	1.00
Neutron Emission	0.00	-1.00	0.10	1.00
Decay Heat	0.00	-1.00	0.51	0.00

The barrier scores are added to produce a single number rating of the proliferation resistance of an individual disposition product. The products are then ranked. Table 7.6 lists the final results for the example comparison of WGPU disposition products of spent MOX, a borosilicate glass log and spent non-uranium fuel. The top scoring product is ranked number 1 and is the most inherently proliferation resistant product while the lowest scoring product is ranked number 3 and is the least inherently proliferation resistant product.

Table 7.5 Metric Weights, Contributions and Barrier Type Scores

Metric	Weight Functions	HLW Glass Log	Spent WGPu MOX	WGPu Non-U Fuel
Disposition Product Matrix Barriers				
Fissile Density	0.3	0.27	0.12	0.30
Dissolution	0.1	0.00	0.00	-0.03
Separation	0.1	-0.10	0.00	-0.10
Radiation Barrier	0.5	-0.094	0.00	0.00
Matrix Barrier Score	-0.074		0.12	0.18
Plutonium Weapons Usability				
Isotopic	0.4	-0.33	0.01	0.40
Critical Mass	0.4	-0.09	0.01	0.40
Neutron Emission	0.1	-0.10	0.00	0.10
Decay Heat	0.1	-0.10	0.051	0.00
Usability Barrier Score	-0.62		0.07	0.90

Table 7.6 Overall Ranking of Inherent Proliferation Resistance

	HLW Glass Log	Spent WGPu MOX	WGPu Non-U Fuel
Matrix Barrier Score	0.074	0.12	0.18
Weapons Usability Score	-0.62	0.07	0.90
Overall Score	-0.49	0.19	1.08
Ranking	3	2	1

7.4.3 Discussion of Example Proliferation Resistance Quantification. Although all the options exceed the spent fuel standard for fissile density, the non-uranium spent fuel clearly offers greater proliferation resistance as a result of eliminating more plutonium. The selection of 1.1 w% plutonium in the glass log is based on proposed options but is probably on the low end of loadings being considered [N-2]. A lower or higher loading would produce larger and

smaller fissile density respectively. The chemical barrier matrix metrics, dissolution and solubility, show that MOX meets the spent fuel standard based mainly on the properties of UO₂. The glass and non-uranium zirconia matrix options appear less chemically resistant than the MOX. However, these numbers are the most suspect in the group because they are based on data which was not specifically derived for this application and consequently has a limited applicability. Finally, as expected, all the options meet the spent fuel standard for a radiation barrier and the differences in the barrier metric scores are small.

The advantages of near complete elimination of plutonium in the non-uranium fuel substantially enhances the plutonium weapons usability barrier. The non-uranium spent fuel residual plutonium is mostly ²⁴²Pu making it quite useless for nuclear explosive purposes. On the other extreme, the fact that no plutonium is transmuted shows up as a strong weakness of the vitrification option. The MOX option falls between the two as might be expected since plutonium usability metrics essentially measure the degree of plutonium transmutation accomplished.

As a result of the enhanced plutonium weapons usability barrier, the non-uranium spent fuel provides the best proliferation resistance. The MOX spent fuel provides the next best performance but scores only slightly above the spent fuel standard which equates to a score of zero. The vitrified waste form is the least proliferation resistant product because of the low barrier to use of the separated plutonium, which remains weapons grade. This substandard performance of the vitrified waste form is based on the assumption that both the matrix level and plutonium usability barriers are of equal merit. However, the matrix level barriers would have to be considered approximately 8 times more important than the plutonium usability barrier for the vitrified waste form to meet the spent fuel standard: an improbable assumption.

7.5 Material and Neutronic Considerations and the Selection of a Non-Uranium Fuel Matrix.

The goal is to develop a fuel which eliminates plutonium and can be integrated into current LWR fuel cycles with minimum perturbation to existing cycles. Thus, there are two primary sets of in-core performance criteria such a fuel must satisfy: thermo-physical performance and neutronic. Acceptable thermal and mechanical performance means that the presence of non-uranium fuel in the core does not impose any additional operational or transient restrictions beyond those which normally apply to a standard PWR core. Peripheral assemblies comprise approximately 25% of a PWR core. Consequently, as long as the non-uranium fuel loaded into the periphery performs at least as well as standard UO_2 , no additional restrictions should be required. Thus, UO_2 characteristics are used as baseline minimum performance standard. A long term fuel development and testing effort will be required to ascertain the performance of a non-uranium fuel.

To be neutronically acceptable, the fuel must not alter core physics parameters and power distribution beyond acceptable PWR design limits. Neutronic considerations are the subject of the next section and neutronic performance results are covered in section 7.7.

7.5.1. Non-Uranium Plutonium Fuel Neutronic Considerations. Plutonium neutronic properties differ significantly from those of uranium. This presents some problems at the interface between Pu and UO_2 assemblies. In addition, the absence of ^{238}U in non-uranium Pu fuels necessitates that a substitute must be found to perform the neutronic functions of ^{238}U in UO_2 fuel. Table 7.7 presents a summary of these neutronic challenges.

Thorium is rejected as a matrix constituent because the production of ^{233}U detracts from the destruction of ^{239}Pu . Burnable poisons are one potential fuel design solution to compensate for the potentially unacceptable nuclear design characteristics of non-uranium plutonium fuels.

Burnable poisons (BP) serve three purposes: they provide beginning of cycle (BOC) excess reactivity control; allow increased fissile loading; shape the reactivity vs. burnup curve over the cycle; and provide resonance absorption negative contributions to FTC and MTC. A BP with a thermal cross section that is larger than the fissile nuclide is preferred because it will burn out faster, leaving less residual negative reactivity at the EOC. However if the thermal cross section is too large, the poison burns out too quickly, causing an unacceptably high excess reactivity peak early in the cycle. A rule of thumb relationship between the poison and fissile cross sections can be derived from the basic depletion equation. The result is that a BP for

which $\frac{\sigma_a^{BP}}{\sigma_a^F} \geq 2.5$ is preferable for cycle reactivity control. The second function of the BP is to

provide negative FTC and MTC. Thus, the poison's absorption cross section vs energy profile must have a sufficient resonance cross section, preferably around the 0.3 ev ^{239}Pu resonance energy, and must not decrease significantly in the epithermal range. Application of these two criteria to the list of potential poisons produces three primary candidates: Europium, Gadolinium and Erbium. All three are rare earths and so have similar chemical properties. Erbia is the preferred poison because it was found to be more effective for cycle reactivity and reactivity coefficient management. Section 7.8 contains more details of the neutronic performance of these poisons.

The next sub-section proposes a logical means of filtering through the large number of possible fuel matrices to identify promising candidates with which to begin a research and development effort.

Table 7.7 Comparison of Non-Uranium Plutonium and Standard Uranium Nuclear Design Characteristics

Parameter	Plutonium Core	Reason for Difference	Potential Consequence
Isothermal Moderator Temperature Coefficient (MTC)	1. WGPu compositions are much less negative 2. RGPU compositions are slightly less negative	1. Reduced resonance absorption plus spectral shift 2. Same as above but with increased ^{240}Pu resonance absorptions	1. Unacceptable transient behavior 2. Unacceptable transient behavior
Prompt Fuel Temperature Coefficient (FTC)	1. WGPu compositions are much less negative 2. RGPU compositions are slightly less negative	1. Reduced resonance absorption 2. same as above but with increased ^{240}Pu resonance absorptions	1. Unacceptable transient behavior 2. Unacceptable transient behavior
Cold to Hot Reactivity Swing	Reduced	Less Negative MTC	Reduced cold born requirements
Installed Reactivity	Reduced	Lower allowable fissile loading	Shorter cycle length
Control Rod Worth	Reduced	More epithermal flux	Possible increase in number of rods
Boron Worth	Reduced	More epithermal flux	Increased boron requirements
Xenon Worth	Reduced	More epithermal flux	Improved stability
Fission Product Poisons	Increased	Increased yields	Reactivity penalty - shorter cycle
Local Power Peaking	Increased	Increased water worth	More complex fuel management
Delayed Neutron fraction	Reduced	$\beta_{\text{Pu}} < \beta_{\text{U}}$	Unacceptable transient behavior

7.5.2 Narrowing the field. This sub-section presents the filter logic used to narrow the field of candidate fuel matrices. A fluorite type oxide fuel matrix is recommended for further study. Figure 7.3 is a flow chart showing the decision points leading to a recommendation of three candidate fuels for development: zirconia, alumina and TRISO.

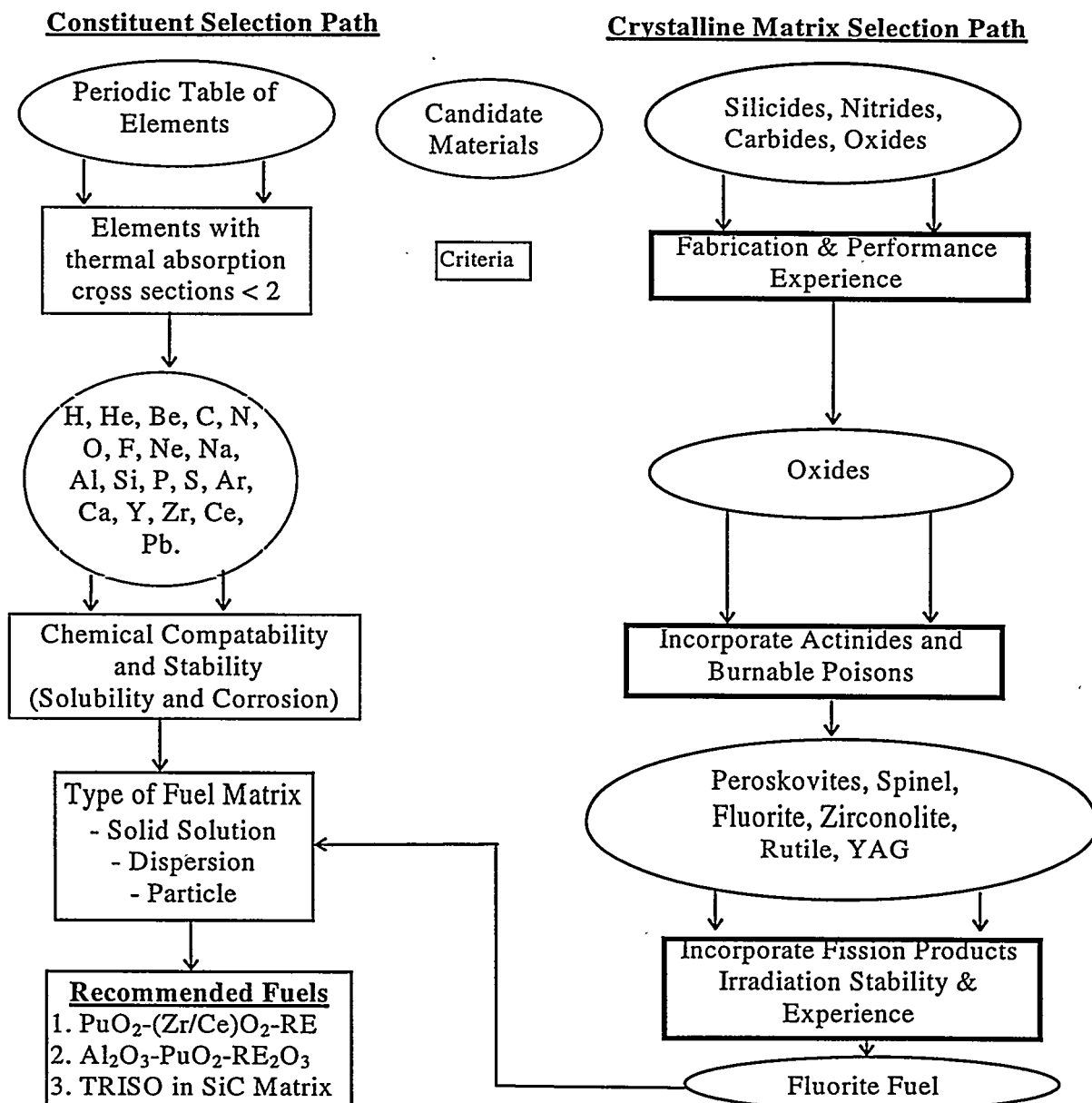


Figure 7.3 Fuel Constituents and Crystalline Matrix Selection Logic Flow Chart

7.5.3 Thermal Performance Criteria. The non-uranium ceramic material which will incorporate the plutonium and absorber atoms must possess thermo-physical properties which give it in-service performance as good or better than UO_2 . It is therefore worthwhile to develop a set of metrics to compare properties of potential plutonium fuel ceramics to UO_2 . Thermal performance is defined by the licensing and design limits imposed on fuel. Three performance areas are of specific interest: thermal margin to melting, transient time constant for quenching, and stored energy.

1. Thermal Margin to Melting: Let T_{CL} , T_{MP} be the normal operating centerline temperature and the ceramic melting point respectively. Figure 7.4 illustrates the relationship of these temperatures:

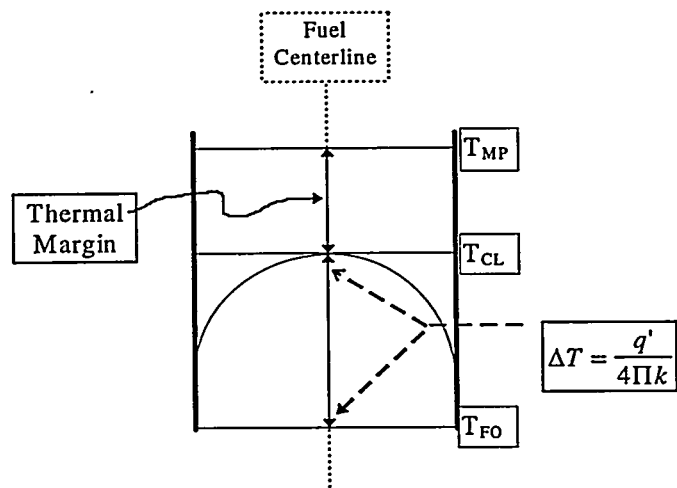


Figure 7.4 Fuel Temperature Profile

ΔT is the difference between fuel outside edge temperature, T_{FO} , and T_{CL} . ΔT is therefore equal to the linear heat generation rate, q' , divided by the product of the thermal conductivity of the material, k , and 4π . The relative thermal margin to melting can be calculated by the following expression:

$$\text{Thermal Margin} = \frac{T_{\text{MP}} - T_{\text{CL}}}{T_{\text{MP}}} \quad (7.1)$$

Thus, for the same q' a material with a larger value of kT_{MP} will have a larger thermal margin to melting.

2. Stored Energy. Stored energy must be removed via emergency cooling systems in the event of a Loss of Coolant Accident, LOCA. The more energy stored in the fuel during normal operation the greater the heat load on cooling systems. The stored energy, E_s , is approximately equal to the product of the heat capacity, c_p , the density, ρ , and the average fuel temperature $\overline{\Delta T} = 1/2(\Delta T)$:

$$E_s \approx \rho c_p \overline{\Delta T} = \frac{q' \rho c_p}{8 \Pi k} \quad (7.2)$$

In this expansion, one recognizes the thermal diffusivity parameter α as:

$$\alpha \equiv \frac{k}{\rho c_p} . \quad (7.3)$$

Thus, ceramic material α values can be used as a comparison metric. A larger value of α is preferable from a stored energy consideration.

3. Transient Time Constant. The transient time constant characterizes the rate of decay of the fundamental mode during quenching. It is determined by the thermal diffusivity, α , in expressions of the form:

$$P = P_0 e^{-\alpha \lambda^2 t} \quad (7.4)$$

where λ is in units of inverse length.

Table 7.8 summarizes the above considerations. The ratio of the metric values to that of UO_2 must exceed or equal that of UO_2 to ensure adequate performance. It is important to note that the thermal conductivity is a strong function of crystalline structure, purity, fluence and temperature and quoted values vary considerably in the literature. Thus, the values presented are more illustrative of potential performance and must be confirmed as part of the fuel development and testing program.

Table 7.8 Summary of Proposed Thermo-physical Performance Criteria

Thermal Limit or Consideration	Performance Constraint	Metric	New Matrix Value UO ₂ Matrix Value
No Fuel Melt	- normal operating thermal margin to melting	kT_{MP}	≥ 1.0
LOCA Performance	- maximum allowable stored energy	α	≥ 1.0

Table 7.9 presents the properties and resultant metric ratios for the recommended zirconia, alumina and TRISO (considered as a SiC matrix). Alumina and SiC matrices have acceptable performance metrics. Zirconia's substandard performance is primarily due to its low thermal conductivity. Erbia, which is added primarily for reactivity control and which helps to stabilize zirconia in the preferred mono-clinic fluorite structure, may also improve the thermal conductivity of the zirconia. CaO can also be used to stabilize zirconia and at 15 mol% has been reported to increase conductivity to above 2.0 W/m-⁰K[S-1] at 1500 ⁰K. However, zirconia's thermal conductivity must be increased by a factor of two to achieve UO₂ margin ratios ≥ 1.0 . Consequently, annular pellets may be required to reduce the centerline temperature. An annulus of half the pellet diameter was found to drop the centerline fuel temperature by 600 degrees to 1300 ⁰C at a 400 w/cm power density [D-1].

Table 7.9 Summary of Recommended Fuels Thermo-physical Performance

Candidate Matrix	ρ (gm/cm ³)	T_{MP} (°C)	k (W/m-K)	C_p (J/ ⁰ K-kg)	kT_{MP}	α_{UO_2}
ZrO ₂	5.85	2770	2.0	457.2	0.5	0.5
Al ₂ O ₃	3.97	2000	7.0	775.7	1.4	1.6
SiC	3.22	1950	15	666.6	2.9	5.0
UO ₂	10.97	2820	3.6	235.7	1.0	1.0

7.6 Computational Codes, Models and Techniques

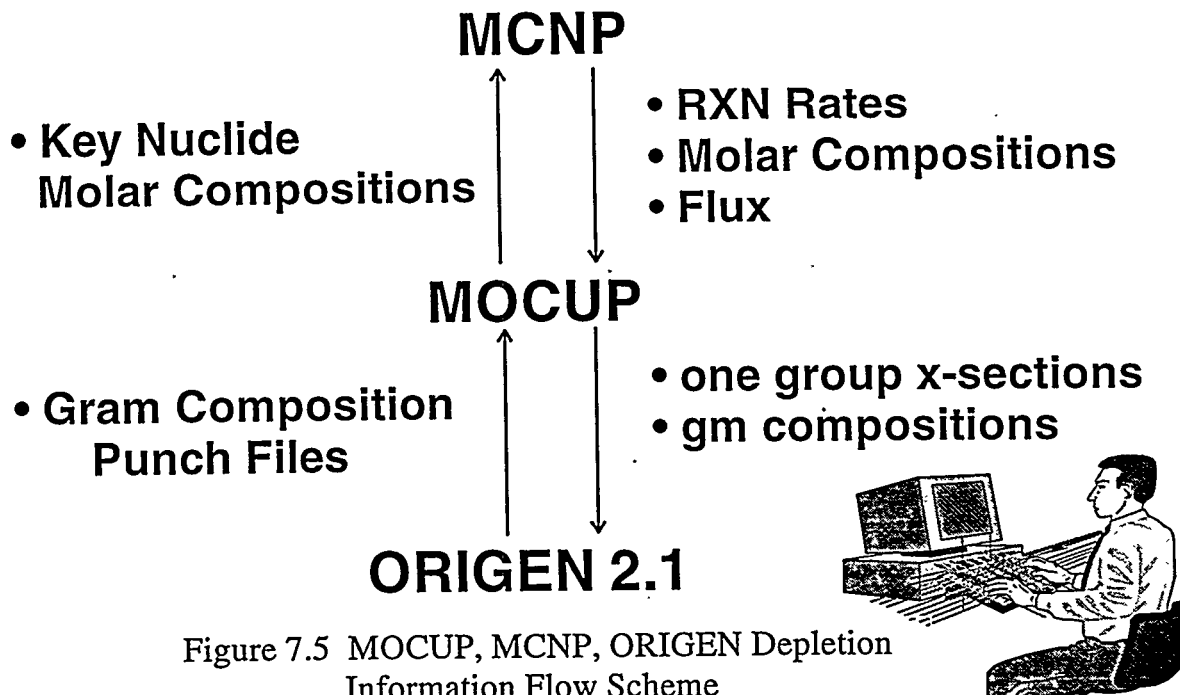
This section discusses the models, codes and calculations used to develop and evaluate the non-uranium plutonium oxide fuel. The neutronic challenges of a PWR core partially loaded with non-uranium plutonium fuel are greater for WGPu isotopes than for RGPU. Consequently, all calculations were carried out using WGPu isotopes in order to be conservative. Specifically the following data are calculated: pin to pin power peaking factors, discharge isotopes, the fuel reactivity vs. burnup profile, core average reactivity coefficients and whole core reactivity. All models used are based on a PWR core comprised of standard 17 x 17 Westinghouse assemblies. Fuel compositions are developed to support an 18 month fuel cycle with a capacity factor of 0.8, which equates to 440 EFPD.

7.6.1 Depletion Calculations. Three computer codes were used to perform depletion calculations: ORIGEN version 2.1, MCNP version 4A and MOCUP [C-4, B-5, M-4]. CASMO-3 was used for depletion benchmark comparison and temperature coefficient calculations.

As the name implies the MCNP-ORIGEN2 Coupled Utility Program (MOCUP) serves as a conduit for passing information between MCNP and ORIGEN. Nuclide-specific cross section information calculated by MCNP is manipulated by MOCUP and provided to ORIGEN. Depletion composition changes calculated by ORIGEN are tracked by MOCUP and used to create MCNP input decks. Thus, composition and reactivity changes are calculated as a function of burnup. No modification to either ORIGEN or MCNP is required to treat nuclides explicitly in depletion calculations. This allows accurate depletion of novel fuels and geometries through a series of MOCUP time intervals and ORIGEN time steps. Time intervals refer to the change in burnup between MCNP reaction rate calculations and subsequent ORIGEN nuclide cross section updates. Time steps refer to the individual ORIGEN depletion commands, IRP or IRF, within each MOCUP time interval. Several ORIGEN time steps are

used to complete the burnup specified for a single MOCUP time interval. Figure 7.5 shows the flow of depletion calculation information between MOCUP, ORIGEN and MCNP.

ORIGEN contains one-group cross section libraries and fission product yields for all the nuclides of potential interest. However, these one-group cross section libraries are produced using sophisticated reactor physics codes which collapse multi-group libraries based on specific standard reference reactor geometries and fuel compositions. Consequently, the accuracy of the results that can be produced using these one group cross sections decreases as the actual system being evaluated moves further away from the reference basis for the particular library being used. Consequently, the ORIGEN cross section libraries are of limited use in evaluating new fuel compositions.



Fortunately, ORIGEN has a built in feature which allows substitution of user supplied one group cross sections for ORIGEN cross sections. In the present instance, substitute cross sections are derived for the actual composition and geometry from MCNP flux and nuclide reaction rate tallies. A new set of accurate one-group substitute cross sections are generated and

supplied to ORIGEN each depletion interval. The cross sections are assumed constant over the depletion interval. The resultant ORIGEN output composition is then incorporated into a new MCNP input and a new set of fluxes and reaction rates calculated. The entire depletion cycle is completed in stepwise fashion.

A benchmark comparison of the MCNP version 4A, ORIGEN version 2.1 and MOCUP depletion code system was conducted against a published EPRI benchmark and excellent agreement was found.

7.6.2 Models and Techniques. Four different PWR models - an MCNP pin cell, an MCNP 34 pin model, a CASMO3 pin cell model, and an MCNP 1/8th symmetry PWR core model - were used to determine the neutronic characteristics of the fuel as a function of burnup as well as to evaluate how it would interact with the non-peripheral fuel assemblies in the PWR core.

Figure 7.6 shows two drawings of the 34 pin model which simulates a single row of pins across two 17 x 17 assemblies; the upper picture is the full length 34 pin model and the lower picture is a close-up truncated view. This 34 pin model is used to determine pin power and pin to pin power peaking for each depletion step. The moderator is H_2O with 500 ppm boron. Four composite pin cell models are used to deplete the 34 pins. UO_2 pins numbered 1 through nine are depleted as one pin labeled STD1. Similarly, UO_2 pins 10 through 17 are depleted as STD2, PuO_2 pins 18 through 24 are depleted as OX1 and pins 25 through 34 are depleted as OX2. These composite pins are depleted using the MCNP Pin Cell Model. This model is used in the first step of the depletion process.

The depletion cycle begins by loading the 34 pin model with fresh fuel compositions and determining individual and composite average pin powers. The fuel compositions for the four composite pins, STD1, STD2, OX1 and OX2, are subsequently loaded into four different MCNP pin cell models. The corresponding average pin power is assigned to each of the four composite pins and is assumed constant during the subsequent ORIGEN depletion. The four

pins are depleted at that power for a single MOCUP time interval following the process described in figure 7.7.

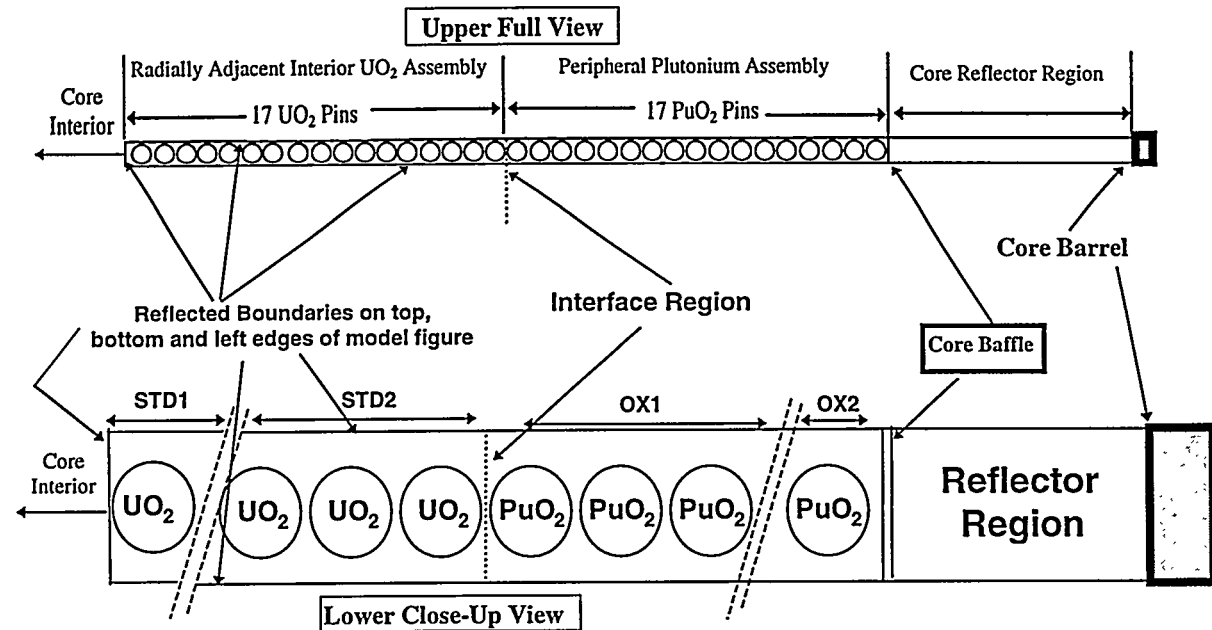


Figure 7.6 MCNP 34 Pin Row, Two Assembly Model

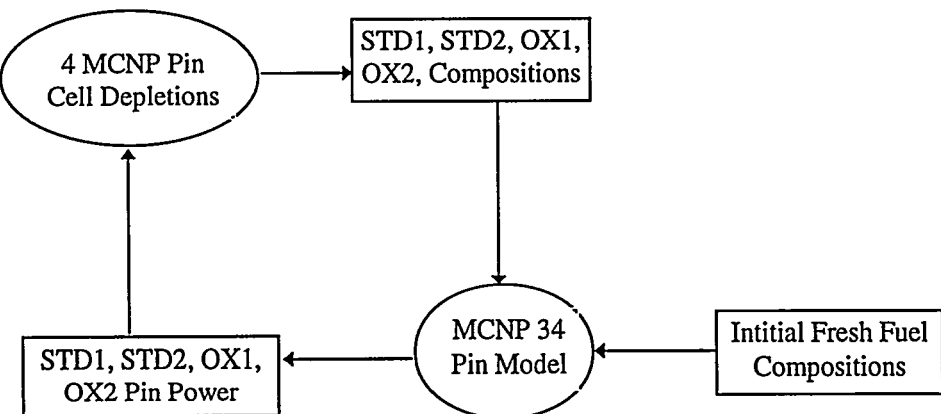


Figure 7.7 Pin Power - Depletion Algorithm

7.6.3 CASMO-3 Calculations and Core Average Reactivity Coefficients. In order to be feasible, a fuel which has acceptable power peaking vs burnup and which eliminates plutonium must also have acceptable reactivity coefficients. To be acceptable, peripheral

PuO_2 fuel reactivity coefficients must be negative enough so that when they are averaged in with the reactivity coefficients of the rest of the core, the whole core average reactivity coefficients are within PWR design limits. The first step is to determine the reactivity coefficients of the candidate fuel composition in a pin cell configuration.

CASMO3 pin cell models are used to determine the standard 3.9w% UO_2 and PuO_2 reactivity coefficients listed in table 7.10. Once pin cell reactivity coefficients are calculated, they must be combined to produce core average parameters. Since this is a feasibility study rather than a licensing calculation, a weighted approximation of core average parameters is adopted.

Table 7.10 Summary of Reactivity Calculations

Coefficient	Equation	Units
Fuel Temperature (FTC)	$\text{FTC} = \frac{10^5 * [(K_{T1} - K_{T2})/K_{Tave}]}{(T1 - T2)}$	pcm/ $^{\circ}\text{K}$
Isothermal Moderator Temperature (MTC)	$\text{MTC} = \frac{10^4 * [(K_{T1} - K_{T2})/K_{Tave}]}{(T1 - T2)}$	$\frac{\% \text{ delta rho} * 10^4}{^{\circ}\text{K}}$
Inverse Boron Worth (IBW)	$\text{IBW} = \frac{100 * [(K_{B1} - K_{B2})/K_{B1}]}{(B1 - B2)}$	ppm / $\% \text{ delta rho}$
Void (VC)	$\text{VC} = \frac{[(K_{V1} - K_{V2})/K_{V1}]}{(V1 - V2)}$	$\% \text{ delta rho} / \% \text{ void}$

Subject to the validity of approximations made in the derivation of the FLARE-type nodal codes, plus equality of the fast group flux and its adjoint (as confirmed by Mosteller [M-5] for typical PWR Cores), and neglecting certain leakage-related terms, it can be shown that the neutron yield and reactivity coefficients should be weighted by the fast flux squared (or equivalently by the product of fast flux and neutron source rate) when aggregating assembly node values to obtain whole core average values [H-8]. From the near constancy of the energy release per fission neutron and fast group migration area, it also follows that power squared weighting is a useful, fairly accurate alternative [S-5]. A derivation of the power squared weighting scheme from the two group neutron balance equation can be found in appendix C.

The analytical support and numerical verification for power squared weighting are not as strong as for more conventional lattices because of the use of fertile-free fuel in a peripheral location. However, such weighting should be adequate for present purposes, particularly since it will be shown that the highly conservative arbitrary application of either power weighting or number weighting lead to results which do not move whole core kinetic parameters outside the currently acceptable design envelope for PWR cores.

7.7 Results.

This section presents the results of analysis of the proposed fuel cycle and PuO₂ fuel composition. The performance criteria listed in table 7.11 were distilled from proliferation, material and neutronic considerations. The neutronically inert matrix is only a structural host for the plutonium and poison nuclides and has negligible impact on the neutronic performance of the fuel. Thus, the results presented are equally applicable to any inert matrix fuel with similar plutonium and poison loading. Several WGPu and poison loading combinations were investigated. A plutonium-erbium-oxide inert-diluent matrix is recommended for use in eliminating plutonium in a once through peripheral PWR cycle. Gd and europium burned out too fast resulting in unacceptable power peaking in the middle of the cycle.

**Table 7.11 Neutronic Performance Criteria For Plutonium Disposition
Fuel Producing an Elimination Option**

Parameter	Definition	Specification	Comments
Discharge Properties (must substantially eliminate plutonium)			
Residual ^{239}Pu	$^{239}\text{Pu} / \text{Total Pu discharged}$	< 10	want to minimize weapons usability ^a
Residual Total Pu	$\text{Total Pu} / \text{Initial Pu Loaded}$	< 10	want to minimize weapons usability ^a
Fuel Cycle Feasibility (non-uranium Pu fuel must not impose any restrictions greater than those imposed if the periphery were loaded with twice burned UO_2)			
Residence Time	Number of EFPDs Fuel Remains in Core	multiple of 440 EFPDs	must support 18 month refueling cycle
Radial Power Peaking	Pin Power/core average pin power	< 1.5	must not be too large so as to cause total power peaking to exceed 2.5.
BOL and EOC Whole Core Reactivity	BOL & EOC Kinf values	≤ 1.3 & ≥ 1.00	Whole Core BOL and EOC reactivity must be within PWR design limits
Reactivity Coefficients (whole core average reactivity values must be within acceptable PWR design range)			
Fuel Temperature Coefficient (FTC)	$[(K_T - K_{900})/K_{900}]/(T-900)] * 10^5$ units = (pcm/ $^{\circ}\text{F}$)	BOC to EOC: -1.30 to -1.46	Typical PWR Design Values
Moderator Temperature Coefficient (MTC)	$[(K_{600} - K_T)/K_{600}]/(600-T)] * 10^4$ units = $\delta\mu/\text{F} \times 10^{-4}$	BOC to EOC: -0.78 to -3.02	Typical PWR Design Values
Inverse Boron Worth (IBW)	$(1000-\text{ppm})/((K_{1000} - K_{\text{ppm}})/K_{1000})$ units = ppm /% $\delta\mu$	BOC to EOC: 108 to 96	Typical PWR Design Values
Void (VC)	$[(K_{0\%} - K_{V\%})/K_{0\%}]/(0\% - V\%)$ units = $\delta\mu / \% \text{void} \times 10^3$	BOC to EOC: -0.41 to -1.43	Typical PWR Design Values ^b

a. Weapon's usability is described in chapter 3 section 3.1

b. Values are for critical moderator boron concentration

7.7.1 Description of the PuO₂-Er₂O₃-inert matrix Fuel and Peripheral Cycle. A zirconia (ZrO₂) inert matrix was used for the bulk of the evaluations reported here. The neutronic performance of zirconia was analyzed as a function of WGPu loading, poison loading and poison type. Excellent performance was achieved using the fuel composition listed in table 7.12 which is designated Oxide5.

Table 7.12 Composition of Recommended Non-Uranium Fuel: Oxide 5

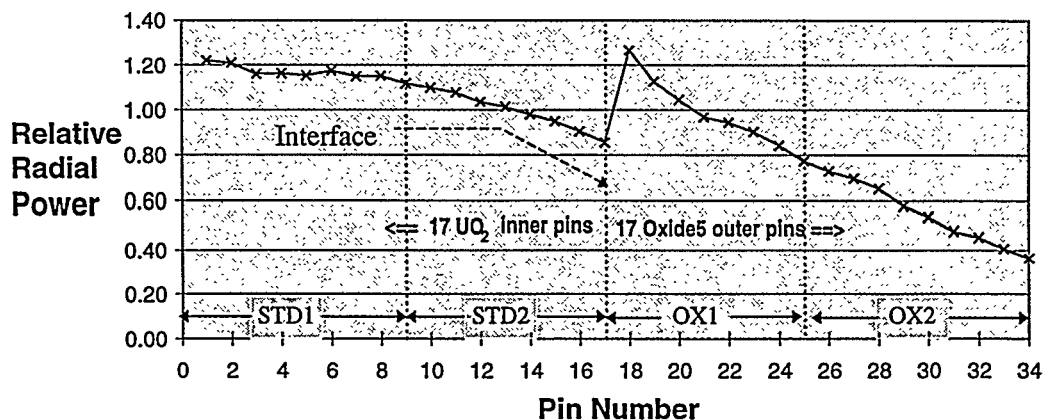
Nuclide/Element	w%
Neutronically Active Components	
²³⁸ Pu	3.49E-04
²³⁹ Pu	2.74E00
²⁴⁰ Pu	1.70E-01
²⁴¹ Pu	6.77E-03
²⁴² Pu	6.51E-04
²⁴¹ Am	3.83E-03
¹⁶⁶ Er	4.47E-01
¹⁶⁷ Er	3.61E-01
Inert Components	
Zirconium	7.04E01
Oxygen	2.53E01

In the proposed fuel cycle, the periphery of the core is comprised of assemblies loaded with the Oxide5 fuel as listed in table 7.12. The remainder of the core is managed like a standard three batch UO₂ PWR core. The Oxide5 fuel composition is designed for a residence time of two 440 EFPD cycles and then discharged. Each Oxide5 assembly is rotated 180 degrees after the first cycle to facilitate an even burnup of the plutonium in the pins. A single transition cycle is used to produce an equilibrium cycle where the core periphery is filled with alternating once burned and fresh Oxide5 assemblies. Since the purpose of this Oxide5 fuel and peripheral cycle is to destroy plutonium, the rate of plutonium consumption or throughput for this fuel and cycle is of interest.

Twenty four new assemblies are loaded into the core at the start of each cycle for a WGpu throughput of 124 kilograms per year. Thus, the 50 MT WGpu disposition mission would take 404 reactor years. Assuming all other existing constraints were removed, the 72 operating US PWRs could disposition the 50 MT of WGpu in 5.6 years [N-4]. Alternately, a 1000 MWe PWR with a 0.8 capacity factor produces 242 kgs of RGpu per year [B-3]. Assuming 1/4th of the core is taken up by Oxide5 assemblies, the remainder of the core would produce only 182 Kg of RGpu per year. The net plutonium production of a PWR loaded with Oxide5 fuel on the periphery and UO₂ assemblies in the interior 24% of that of a standard UO₂ core. Thus, the growth of RGpu inventories could be significantly reduced. Implementation of this solution to the growth of RGpu stockpiles requires that the radial power peaking at the Oxide5-UO₂ assembly interface must not exceed nominal PWR design limits.

7.7.2 Radial Power Peaking and Depletion Cycle Results. Figures 7.8 and 7.9 are the radial power peaking factor profiles (pin power divided by core average pin power) for the 34 pin model loaded with fresh 3.9w% UO₂ in pins 1-17 and Oxide5 loaded in Pins 18-34 and the progression of the profile with burnup over the first 440 EFPD cycle.

Figure 7.8 Radial Power Profile for Fresh 3.9w% UO₂ and Oxide5



A maximum peak pin power of 1.27 times core average pin power occurs in the first Oxide5 pin: #18. This peak is well within the 1.5 maximum radial power peak value. Power peaks in

pin #18 due to the greater cross section of ^{239}Pu relative to ^{235}U . As shown in figure 7.8, the large plutonium cross section results in thermal flux shielding of the outer Oxide5 by the inner Oxide5 pins. Since the plutonium number densities are the same for all the Oxide5 pins, pin power decreases moving radially outward from the interface. The 1/8th MCNP core model loaded with fresh UO_2 and Oxide5 assemblies had a K_{eff} of 1.31.

As the plutonium in the inner Oxide5 pins is depleted, there is less shielding of the outer pins and the power peak moves radially outward. At the EOC, the power in the OX1 pins has dropped well below core average. The discontinuities in the pin power profiles at pin 27 result from our use of region-average compositions (i.e. OX1 and OX2) in the assembly burnup scheme: zone average composition times the local flux consistently overestimates the local power here and also near pin #18. The first cycle ends with the maximum actual radial pin power peak well below the 1.5 limit.

Figure 7.9 Progression of Radial Power Peak for Oxide5 Through the First Cycle

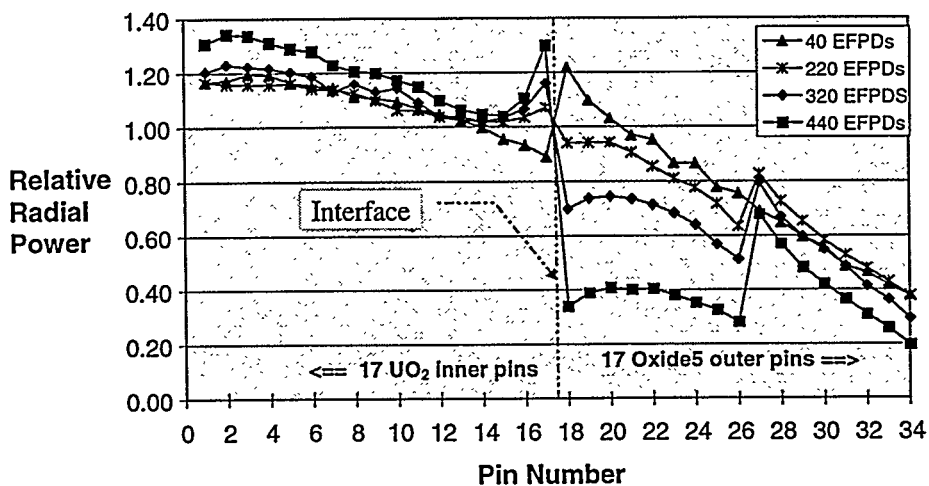


Table 7.13 lists OX1 and OX2 plutonium destruction during the first and second fuel cycles. Note that there is greater destruction of plutonium in OX1 than OX2 because OX1 has shielded OX2 during the first fuel cycle.

Table 7.13 OX1 & OX2 Pu Destruction

EFPDs	OX1		OX2	
	% ^{239}Pu	% $^{\text{Tot}}\text{Pu}$	% ^{239}Pu	% $^{\text{Tot}}\text{Pu}$
0	0.0%	0.0%	0.0%	0.0%
1	0.4%	0.2%	0.2%	0.1%
3	1.1%	0.7%	0.6%	0.4%
10	3.7%	2.2%	2.2%	1.3%
40	14.7%	9.1%	8.8%	5.4%
70	25.4%	15.8%	15.2%	9.4%
120	42.3%	26.9%	26.4%	16.4%
170	57.9%	37.8%	36.9%	23.3%
220	71.0%	47.9%	45.6%	29.1%
320	87.9%	63.6%	67.0%	44.6%
440	98.1%	79.8%	84.8%	60.2%
540	99.3%	84.1%	97.3%	77.5%
640	99.8%	87.0%	99.8%	87.4%
740	99.9%	88.9%	100.0%	91.6%
880	100.0%	91.0%	100.0%	95.0%

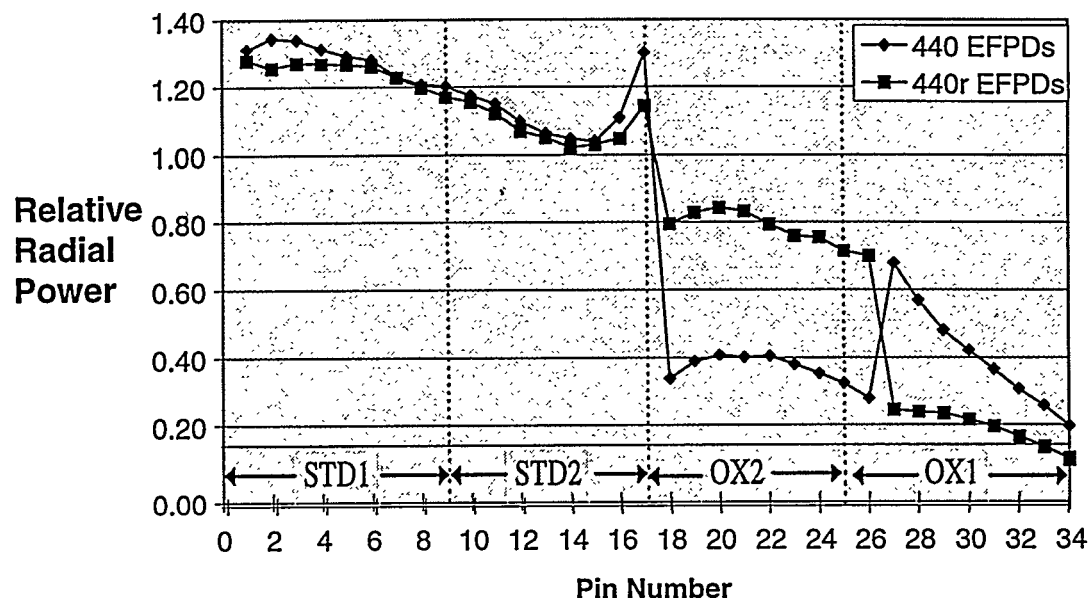
<==End of First Cycle

<==End of Second Cycle

The NAS classifies the PC-MHR as beyond the spent fuel standard but not a true elimination option because there is only 89% destruction of ^{239}Pu and 64% destruction of total plutonium.. As indicated in table 7.13, the second cycle increases the Oxide5 pin plutonium destruction from values which are slightly better than non-uranium once-through cycles such as the PC-MHR or CANDU to a true elimination option with 100% destruction of ^{239}Pu and 93% destruction of total plutonium. Thus, destruction of plutonium using Oxide5 in a two cycle peripheral PWR cycle meets the discharge property elimination option specifications in table 7.11.

At the end of the first cycle, the Oxide5 assembly is rotated 180 degrees to facilitate an even burnout of the assembly. After the shift, the OX2 pins are numbered 17 through 24 and the OX1 pins are numbered 25 through 34. Figure 7.10 shows the radial power peak profile at the end of the first cycle, 440 EFPDs, and after the rotation of the Oxide5 assembly, 440r EFPDs.

Figure 7.10 Radial Power Profile Shift Between First and Second Cycles Due To Oxide5 Assembly Rotation



Rotating the Oxide5 assembly also reduces the power peak in the interface UO₂ pin #17. The second cycle begins with the 440r radial pin power peak profile. Figure 7.11 shows radial power peaking profile development over the second cycle which ends at 880 EFPDs.

At 880 EFPDs, UO₂ pin #17 just reaches the 1.5 maximum allowable radial power peak. Thus, this fuel composition and cycle meet the radial power peak specification. The elimination accomplished during the second cycle necessitates Oxide5 pin power reduction to near zero as the rest of the core provides the neutrons to burn out the residual plutonium. An assembly producing so little power in the interior of the core would likely lead to unacceptable power peaking in adjacent assemblies. The assemblies on the periphery normally run at lower powers. Using a radial blanket to burn out the residual plutonium is akin to reducing the effective size of the core. Thus, the lower power can be tolerated in the periphery of the core without causing unacceptable power peaking. At the end of the second cycle, the Oxide5 assembly pins are producing less than 3% of core average power. However, a single assembly of Oxide5 pins still produces a two cycle average power of 47.3%. Thus, there is a slight increase over the average 30% produced in the periphery of

PWRs using low leakage core fuel management, but, the increase is not so large as to cause significant changes in core vessel fluence. To further assess potential changes in pressure vessel fluence, the net current into the reflector region was calculated using the MCNP 34 pin model. The net current was essentially the same for UO₂-UO₂ and UO₂-Oxide5 34 pin loadings. Thus, the pressure vessel fluence of the peripheral-Oxide5 cycle should be no more than that for standard full UO₂ cores. Taken as a whole, the equilibrium periphery loaded with fresh and once burned Oxide5 assemblies produces 54% of core average power at the start of each cycle and 21% of core average power at the end of each cycle. Thus, the alternating loading scheme would reduce the power burden on the interior assemblies relative to replacing the peripheral assemblies all at once.

Figure 7.11 Progression of Radial Pin Power Peaking Through the Second Cycle

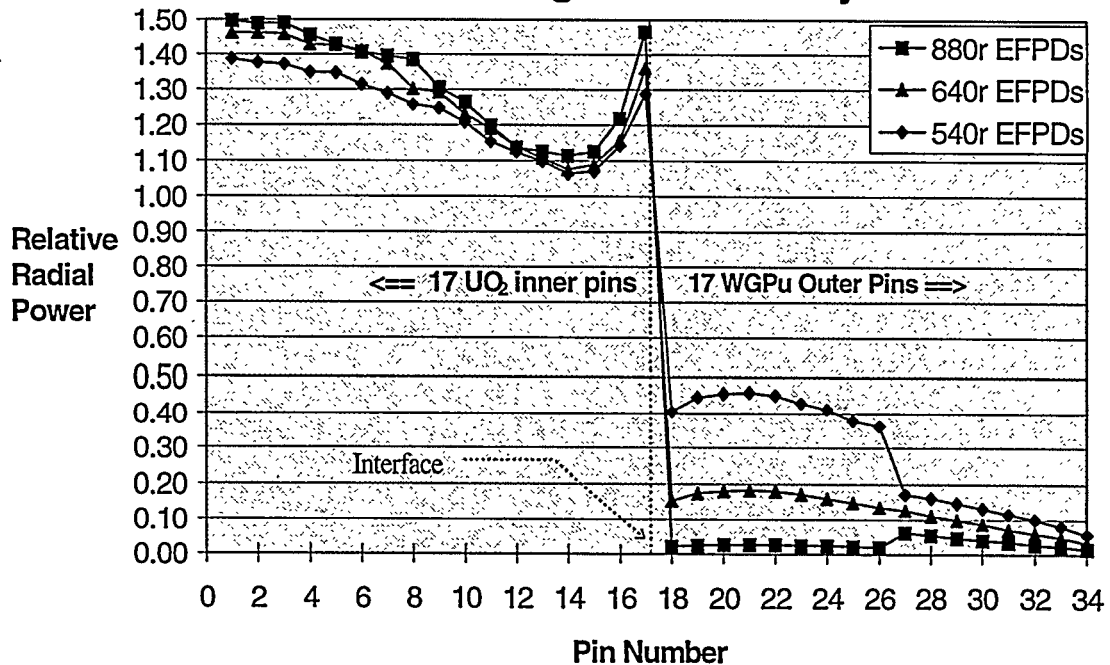


Figure 7.12 shows the reactivity profile which correlates to the power peaking profiles of this two cycle depletion of Oxide5 and UO₂. The reactivity of the OXIDE5 fuel pins, OX1 and OX2, remains nearly constant and consistent with that of the UO₂ pins, STD1 and STD2, until the ¹⁶⁷Er is nearly completely depleted as shown in figure 7.13. These relatively flat OX1 and OX2 reactivity profiles provided by the erbium depletion rate result in the relatively

benign radial peaking distributions of the first cycle and demonstrate why Er is the preferred burnable poison. Erbium also provides a negative influence on the FTC and MTC providing acceptable core average reactivity temperature coefficients.

Figure 7.12 Oxide5 & UO₂ Reactivity vs Burnup

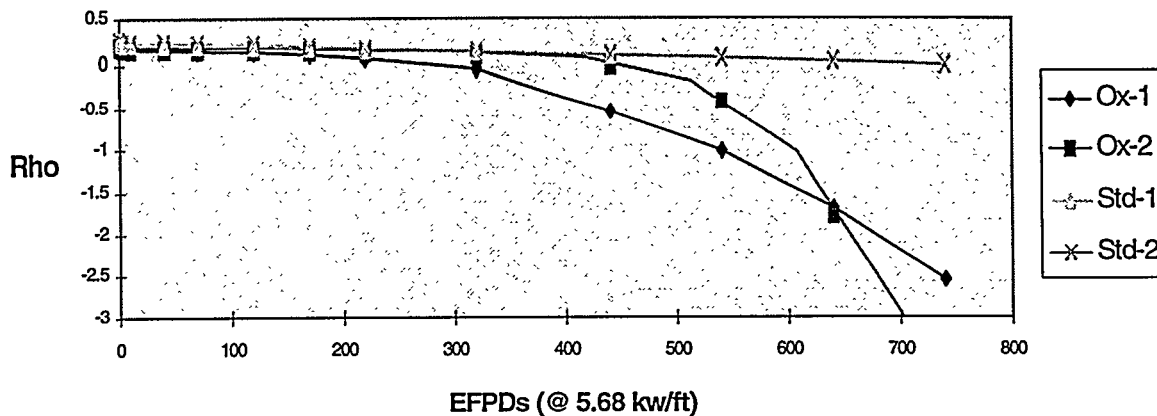
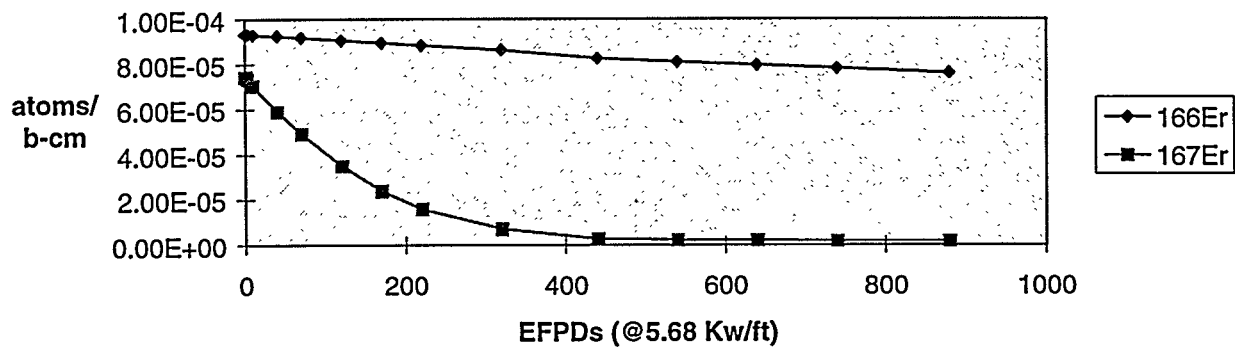


Figure 7.13 Er Composition vs EFPD



7.7.3 Oxide5 Core Average Reactivity Coefficient Results. As described in sub-section 7.6.3, three algorithms for weighting the Oxide5 and UO₂ pin cell contributions to core average reactivity coefficients are used: number of pins (NW), power (PW) and square power weighting (PW2). Square power weighting is the most accurate estimation technique. However, the Oxide5 pins run at a fraction of the core average 100% pin power so that power weighting is more conservative than square power weighting. Weighting the Oxide5 and

UO_2 pin contributions based solely on the number of pins of each assumes that they contribute equally to core average parameters. Thus, number weighting is the most straightforward and also the most conservative algorithm. All Oxide5 and UO_2 coefficient calculations were done with a constant 500 ppm boron concentration in the coolant. The fuel temperature coefficient results, commonly referred to as Doppler coefficient, are presented first.

Figure 7.14 shows the UO_2 and Oxide5 pin cell, and reference core average FTC vs Burnup curves. The FTC becomes less negative with depletion and has a strongly positive value at the end of the second cycle. At 740 and 880 EFPDs, the Oxide5 pins are highly subcritical and only produce an average power of 0.29 and 0.14 Kw/ft respectively. Thus, based on a power weighting or squared power weighting the positive Oxide5 FTC pin cell values make little contribution to core average FTC. Note that the calculated UO_2 pin cell FTC is lower than the PWR core average “reference” values. However, since these are not meant to be licensing or even design level calculations, the small bias introduced into the determination of the core average FTC is acceptable.

Figure 7.14. 3.9w% UO_2 , and Oxide5 Pin Cell FTC vs. Burnup

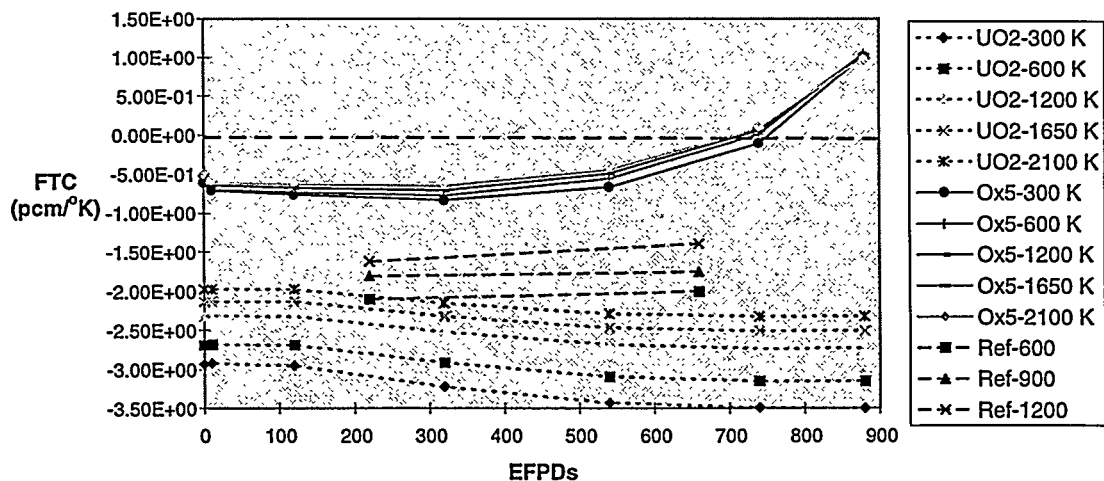


Figure 7.15 shows the number weighted core average FTC values as compared to the dashed reference design average PWR values. Even following the very conservative number

weighting algorithm, the core average FTC values are consistent with standard reference PWR values shown at 600, 900 and 1200K. Power weighting further improves the FTC relative to standard PWR values as shown in figure 7.16.

Figure 7.15 Number Weighted and Reference Core Average FTC vs Burnup

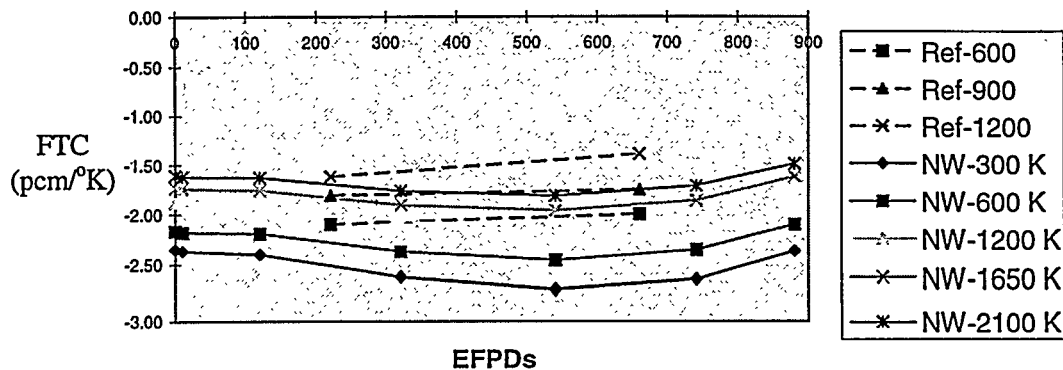
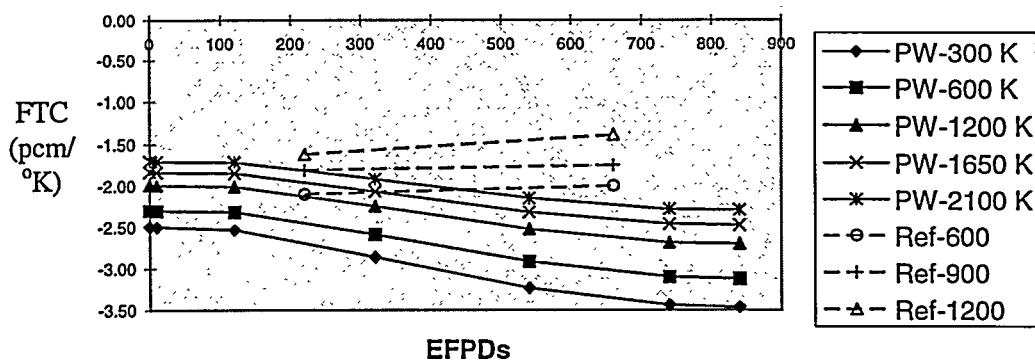
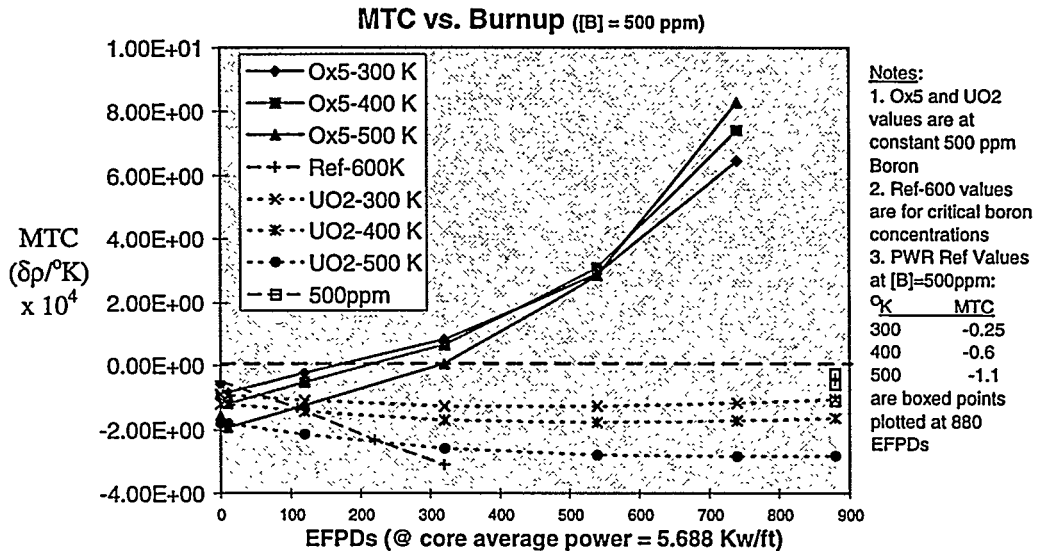


Figure 7.16 Power Weighted and Reference Core Average FTC vs Burnup



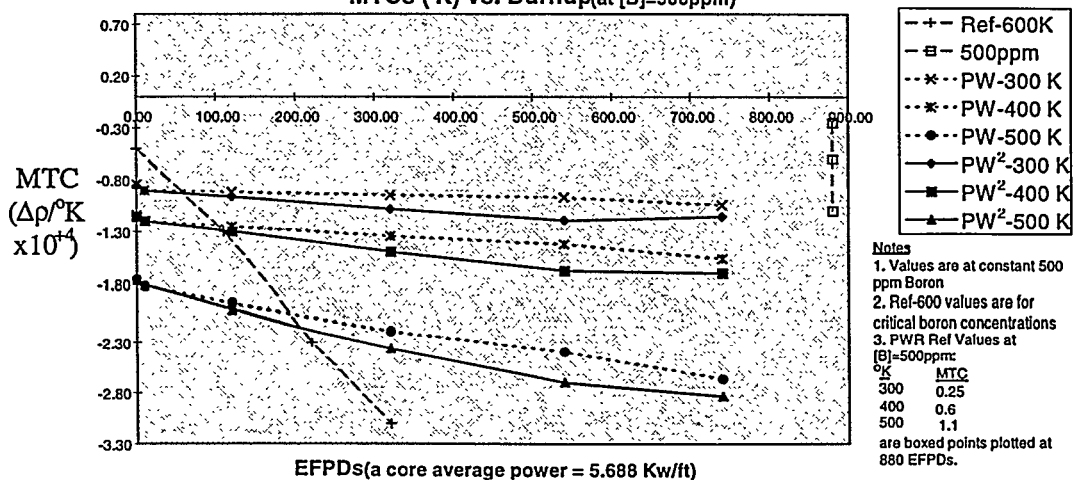
The CASMO3 Oxide5 and UO₂ pin cell and reference PWR core average MTCs are plotted as a function of burnup in figure 7.17. The depletion of erbium with burnup, given in figure 7.13, directly correlates to the shape of the MTC curves. As discussed in section 7.6.1, erbium was selected as a burnable poison because its resonances around 0.46 and 0.58 ev provide a negative MTC. Consequently, the Oxide5 MTC becomes less negative in direct correlation to the depletion of ¹⁶⁷Er. Note that there appears to be no UO₂ pin cell bias relative to the reference PWR core average parameters.

Figure 7.17 3.9w% UO₂ and Oxide5 Pin Cell



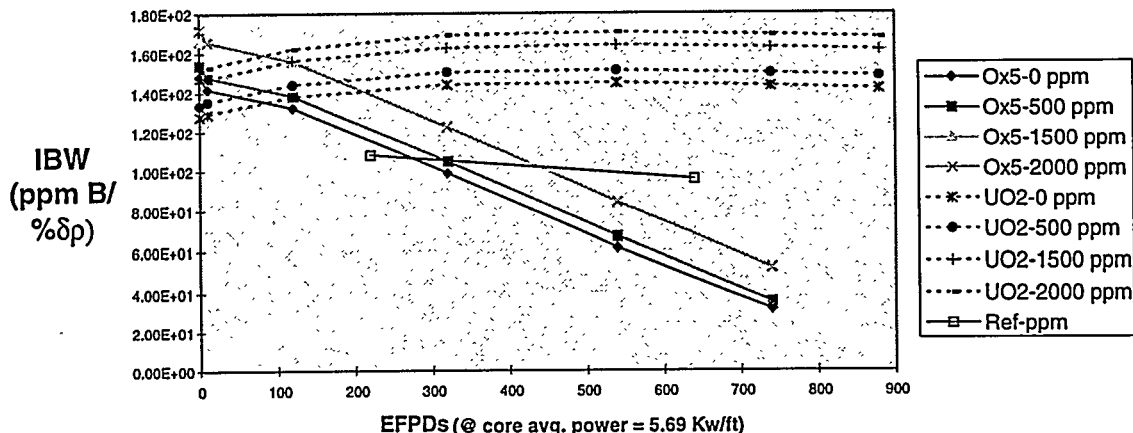
Fortunately, by the time the pins lose all their erbium they are sufficiently depleted so that they are producing relatively little power. Thus, their contribution to the core average MTC is minimal as can be seen in figure 7.18 of the power and square power weighted MTCs which fall close to the reference PWR values.

Figure 7.18 Power and Square Power Weighted & Reference PWR MTCs (°K) vs. Burnup(at [B]=500ppm)



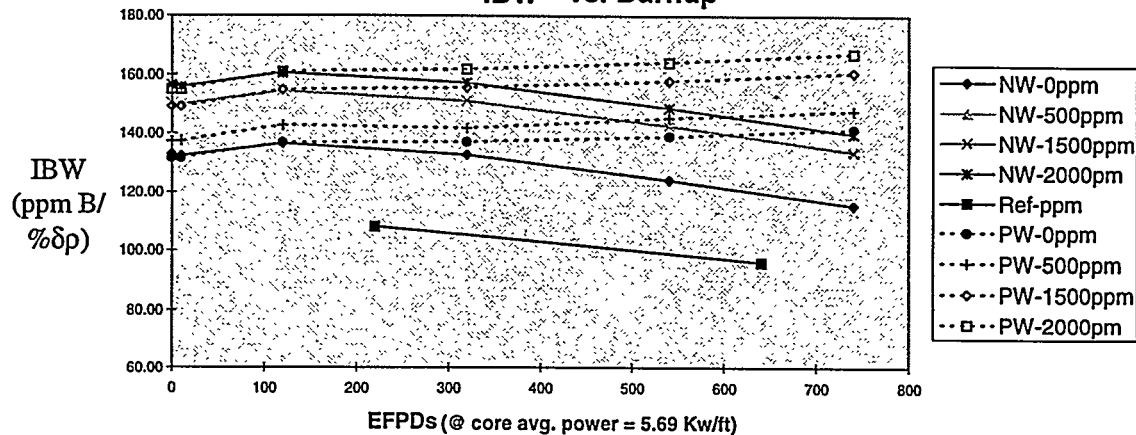
Inverse boron worth (IBW) is calculated in units of ppm/change in reactivity. Thus, a small value equates to a larger boron worth (which is desirable). Figure 7.19 plots the results for the UO₂ and Oxide5 pin cell and reference PWR core average. These values are not significantly different from the plotted reference PWR values. The Oxide BOC value is approximately 160 as compared to the reference value of 108 and the 740 EFPD Oxide5 value of 50 is to be compared to the 96 reference EOC value. The high BOC Oxide5 IBW at the BOC is the result of the harder spectrum produced by the large thermal plutonium cross sections. The 740 EFPD Oxide5 IBW of 50 results from the highly thermal spectrum of the over moderated condition and almost completely depleted Oxide5 fuel.

Figure 7.19 UO₂ and Oxide5 Pin cell and Reference PWR Core Average IBW vs Burnup



Note that the UO₂ pin cell values have a conservative bias relative to the reference core values taken from the literature: i.e. more ppm boron per % $\delta\rho$. The core average power weighted IBW values, shown in figure 7.20, are higher than those for Oxide5 but by less than the computational bias. Thus, Oxide5 is not the limiting factor for core average boron worth.

Figure 7.20 Number & Power Weighted IBW vs. Burnup



The final reactivity coefficient of interest is the void coefficient (VC). Figure 7.21 shows the Oxide5 and UO₂ VCs as a function of burnup for several void percents. UO₂ pin cell values fall close to the core average PWR values. The Oxide5 pin cell void coefficient becomes positive for higher burnups because the low fissile material density results in an over-moderated condition. However, lower fissile density also equates to lower power generation in the pins during the second cycle.

Figure 7.21 UO₂ and Oxide5 Pin Cell Void Coefficients (VC) vs Burnup

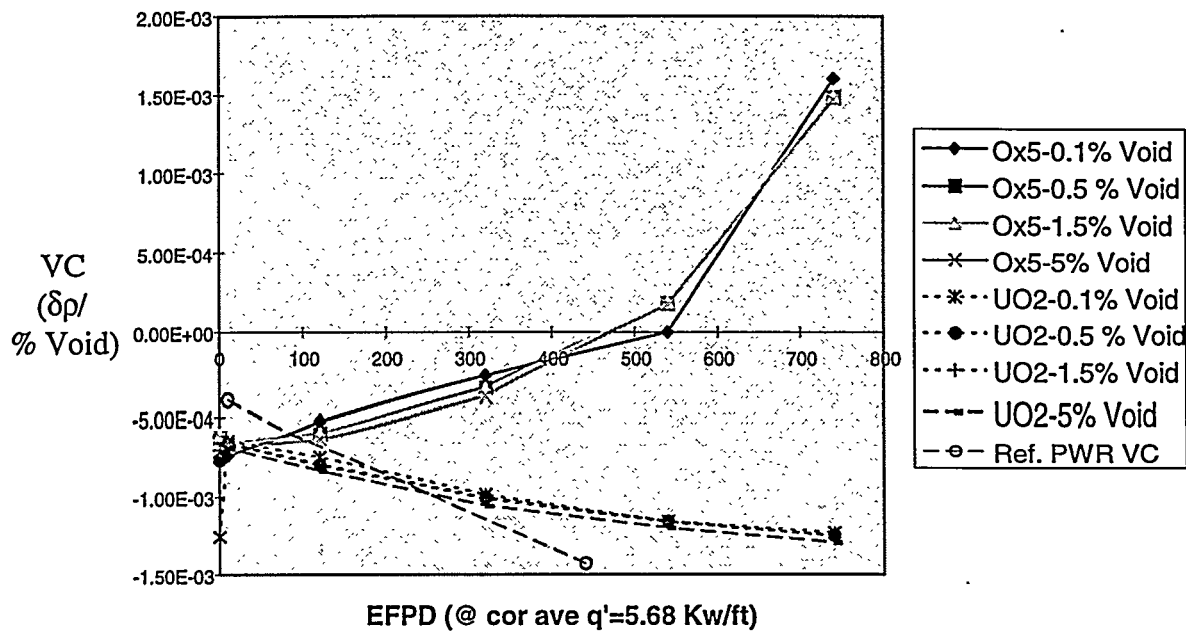
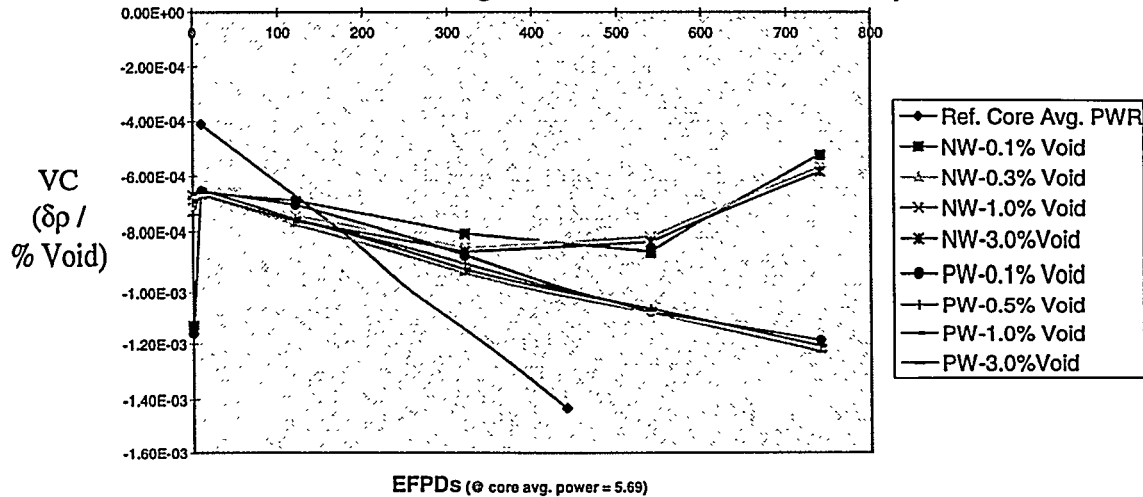


Figure 7.22 shows the power weighted and number weighted core average void coefficient [F-4]. As with the MTC, the low power of the higher burnup Oxide5 pins reduces their contribution to core average values and results in void coefficient values comparable to standard PWR averages.

Figure 7.22 Number and Power Weighted and Reference Core Average Void Coefficients vs. Burnup



7.7.4 Conclusions on Oxide5 Performance. Table 7.14 summarizes Oxide5 performance relative to the selected criteria. The Oxide5 composition starts out with low plutonium loading. Consequently, it produces significant power through the first but only half of the second cycle. During the last 220 EFPDs in the core the residual plutonium is destroyed producing a true elimination option. Total plutonium destruction is in excess of 90% and essentially all of the ^{239}Pu is destroyed. The radial power peaking and core reactivity are within normal PWR limits throughout both cycles. There is a small net gain in average power produced in the periphery. The throughput of the proposed cycle is acceptable.

The Oxide5 periphery PWR core reactivity coefficients are comparable to reference PWR values.

Table 7.14 Summary of Oxide5 Neutronic Performance

<u>Parameter</u>	<u>Oxide Peripheral Calculated Core Average Value</u>	<u>Specification</u>	<u>Comments</u>
Discharge Properties (must substantially eliminate plutonium)			
Residual ^{239}Pu	0 %	< 10 %	want to minimize weapons usability ^A
Residual Plutonium	7 %	< 10 %	want to minimize weapons usability ^A
Fuel Cycle Feasibility (non-uranium Pu fuel must not impose any restrictions greater than those imposed if the periphery were loaded with twice burned UO_2)			
Residence Time	880 EFPDs	multiple of 440 EFPDs	must support 18 month refueling cycle
Radial Power Peaking	Max peak over two cycle = 1.5	< 1.5	must not be too large so as to cause total power peaking to exceed 2.5.
BOL and EOC Whole Core Reactivity	BOC Keff = 1.31 EOC Keff = 1.05	≤ 1.3 & ≥ 1.00	Whole Core BOL and EOC reactivity must be within PWR design limits
Reactivity Coefficients (whole core average reactivity values must be within acceptable PWR design range)			
FTC ^c units = $(\text{pcm}^{\circ}\text{F})$	BOC to EOC: -1.85 to -1.7	BOC to EOC: -1.30 to -1.46	Typical PWR Design Values
MTC ^c units = $\delta p^{\circ}\text{F} \times 10^4$	BOC to EOC: -1.76 to -2.7	BOC to EOC: -0.78 to -3.02	Typical PWR Design Values
IBW units = ppm / % δp	BOC to EOC: 137 to 148	BOC to EOC: 108 to 96	Typical PWR Design Values
VC units = $\delta p / \% \text{void} \times 10^3$	BOC to EOC: -0.86 to -1.21	BOC to EOC: -0.41 ^B to -1.43 ^B	Typical PWR Design Values
A. Weapon's usability is described in chapter 3 B. Values are for critical moderator boron concentration C. Values at normal operating temperatures.			

7.8 Conclusions

Plutonium, both WGPu and RGPU, can be used to produce nuclear explosives. One of the primary means for preventing proliferation is through plutonium safeguards and security measures. The production of RGPU in current once-through LWR fuel cycles exceeds consumption, resulting in growing global stockpiles of plutonium, which will strain these measures. The bulk of this RGPU is in spent fuel but spent fuel radiation barriers will diminish below IAEA minimum self protecting levels in less than 160 years after discharge [N-1]. Proliferation experts call for world-wide management of plutonium [B-1, N-1, M-3, V-1]. One of the key tenets of proposed plutonium management plans is the reduction of stockpiles to minimum levels consistent with needs. The only way to irrevocably reduce stockpiles is to destroy the plutonium through fission and transmutation. LWRs dominate the population of reactors worldwide; thus, the most promising method for effecting large scale transmutation of plutonium in a timely manner is through burning it in light water reactors.

MOX technology in current light water reactors is sufficient to reduce the risk of proliferation posed by WGPu to the level of the much larger stockpiles of RGPU. Consequently there is no need to develop a new technology to disposition WGPu. However, current LWR WGPu disposition options are limited in their ability to destroy plutonium because they use fertile MOX fuel. The PC-MHR has nearly double the WGPu destruction capabilities of the MOX options because it uses a non-uranium fuel. However, the PC-MHR option also requires new reactor technology and it does not eliminate plutonium. The RGPU mission will require the disposal of 60-70 MTs/year in order to halt the growth of stockpiles. A large number of new reactors would be required; thus, reliance on new reactor technology to complete the RGPU mission is impractical. Non-uranium fuel could provide the ability to eliminate plutonium with current reactors. Plutonium disposition products in which the plutonium has been substantially eliminated with a non-uranium fuel provide significant and quantifiable additional barriers to proliferation.

Development of non-uranium fuels for PWR use will require a large research and development effort. Based on material considerations, stabilized zirconia, alumina or TRISO particle inert fuel matrices are promising candidates for the start of the development effort. The plutonium-erbium-oxide-inert-matrix composition, designated here as Oxide5, is recommended. Using the periphery of the PWR allows the non-uranium fuel to be run at low power which is necessary during the destruction of residual plutonium. Oxide5 used in the periphery of a PWR will destroy essentially 100% of the ^{239}Pu and > 90% of the total plutonium loaded in the fuel in two 440 EFPD core burnup cycles. The resultant core average and cycle properties are comparable to nominal PWR core parameters. Thus, the proposed cycle is feasible. The net plutonium production of this cycle is only 24% that produced in current once-through PWR LEU cycles. Thus, the rate of plutonium stockpile growth can be significantly reduced.

7.9 Future Work.

This thesis was a scoping and feasibility study intended to serve as a starting point for a much larger fuel development and qualification program that would have to be completed before non-uranium fuels could be used to eliminate plutonium in PWRs. As such there is a great deal of refinement that must be accomplished to turn the proposed fuel and fuel cycle into a working cycle.

The primary area of work outstanding is material development and testing of non-uranium matrices. The work done here was purely a paper study. Non-uranium fuels must be fabricated and irradiated. Fabrication processes must be developed and scaled to production levels. In addition, the recommended Oxide5 fuel composition represents one possible solution rather than a complete list of all possible solutions. Thus, more scoping studies looking at different fuel and poison combinations are possible. More precise calculation of core average parameters using NRC licensing level codes will also be required. In particular,

a specific reactor should be selected and a realistic sequence of future core loading cycles examined to effect transition to and operation of an “equilibrium cycle”. Finally, this study has demonstrated that the periphery of the core can be used to destroy plutonium nuclides at low powers. Thus, it may be possible to extend this technique to the destruction of other undesirable highly radiotoxic actinides such as Np, Am and Cm which are limiting nuclides for high level waste repository design [S-6].

The crude metrics and weighting functions used to evaluate the WGPu glass log, spent MOX fuel and spent non-uranium fuel in chapter 3 are probably adequate for selecting between an array of widely different options as in the given examples. More refined versions are probably called for if one is to discriminate within a given category of options (such as between different non-U fuel types). This could well be a profitable subject for future work, in which case attention is recommended to evaluation of more appropriate (e.g. non-linear) scoring functions, and to better metrics for dissolution.

Appendix A Nomenclature

Al ₂ O ₃	-	Alumina
BP	-	Burnable Poison
CANDU	-	Canadian Deuterium Uranium reactor
CE	-	Combustion Engineering
CS	-	Containment and Surveillance
D	-	Chemical Distribution Coefficient
Dy	-	Dysprosium
EOC	-	End of Fuel Depletion Cycle
Er	-	Erbium
Eu	-	Europium
FMEF	-	Fuel Manufacturing and Evaluation Facility (located in Hanford, WA.)
PPF	-	Fuel Processing Facility (located in Idaho Falls, ID)
FSU	-	Former Soviet Union
FTC	-	Fuel Temperature Reactivity Coefficient or Doppler Coefficient
Gd	-	Gadolinium
GWd/MT	-	Gigawatt-days/Metric Ton of Heavy Metal
Ho	-	Holmium
HLW	-	High Level Waste
IBW	-	Inverse Boron Worth
IFBA	-	Integrated Fuel Burnable Absorbers
IAEA	-	International Atomic Energy Agency
INF	-	Intermediate-range Nuclear Forces Treaty
Kinf	-	Infinite Medium Multiplication Constant
Keff	-	Effective Multiplication Constant
LWR	-	Light Water Reactor
MOI	-	Modified ORIGEN Input file
MPO	-	MOCUP mcnpPRO Output File

MHR	-	Modular High Temperature Gas Reactor
MTC	-	Isothermal Moderator Temperature Coefficient
MWd/MTHM	-	Mega-Watt-Days per Metric Ton of Heavy Metal
NPT	-	Nuclear Non-Proliferation Treaty
OCF	-	MOCUP Origen Composition Files
PC-MHR	-	Plutonium Consumption - Modular High Temperature Gas Reactor (by General Atomics)
PWR	-	Pressurized Water Reactor
Pu	-	Plutonium
RE	-	Rare Earth Poisons
RGPu	-	Reactor Grade Plutonium
Rho	-	Reactivity
SiC	-	Silicon Carbide
Sm	-	Samarium
START	-	Strategic Arms Reduction Treaty
Th	-	Thorium
US	-	United States
VC	-	Void Coefficient
W	-	Tungsten
WF	-	Weight Function
WNF	-	WGpu Non-Uranium Fuel
WNP1	-	Washington Nuclear Project Unit #1
WNP2	-	Washington Nuclear Project Unit #2
WNP3	-	Washington Nuclear Project Unit #3
w%	-	weight percent
ZrO ₂	-	Zirconia

Appendix B Detailed Metric Values and Scoring Calculations

Introduction

This appendix is provided to give a clear example of the calculations supporting the comparison of the inherent proliferation resistance barriers of HLW spiked vitrified logs, spent WGPu MOX fuel and spent WGPu non-uranium fuel (WNF) disposition products. Detailed calculations are presented only for the WNF disposition product. The calculations for the other two disposition products are similar. Chapter 5 details the computer code models and methods used to derive the data from which the metric values are calculated.

B.1 WGPu Non-Uranium Fuel (WNF) Raw Metric Values. Table B.1 lists a summary of the metrics proposed to evaluate the inherent proliferation resistance of plutonium disposition products.

B.1 Inherent Plutonium Disposition Form Barrier Metrics		
Criteria	Type of Measurement	Units/Scale
Disposition Product Matrix Barriers		
Fissile Density	Quantitative	kg fissile Pu/m ³ host
Dissolution	Quantitative	gms/liter
Separation	Quantitative	dimensionless
Radiation Barrier	Quantitative	years
Plutonium Weapons Usability		
Isotopic	Quantitative	gms fissile/gm Pu
Critical Mass	Quantitative	kg Pu
Neutron Emission	Quantitative	n/sec-kg Pu
Decay Heat	Quantitative	w/kgm Pu
1. The separation metric is calculated by ratioing separation distribution coefficients if the data can be found. Alternately it is calculated as an ionic radius ratio as described in section 3.2.3.		

The first metric value is fissile density. The fissile density is derived from the WNF discharge composition in grams and the volume of the MCNP pin cell model used for depletion calculations. The WNF pin cell contains 1.026×10^{-3} grams of ^{239}Pu and

1.961×10^{-2} grams of ^{241}Pu . The pin cell is 13.3116 cm^3 resulting in a fissile density of 1.55 Kgs of fissile Pu/m³ of disposition product.

The dissolution metric value is the solubility of $\text{Zr}(\text{NO}_3)_2$ listed in Lange's chemistry handbook as 211 grams/100 grams of H_2O at 40 °C [L-2]. Also listed in the same table is the solubility of $\text{UO}_2(\text{NO}_3)_2$ as 167 grams/100 grams of H_2O . Thus, the two metric values are directly comparable and used for metric scoring without further manipulation. Plutonium is removed from borosilicate glass by leaching rather than dissolution. Thus, the dissolution metric is not applicable to the borosilicate glass log. A neutral value will be assigned in the metric scoring step. Were it available, data on the rate of dissolution or leaching for all the forms considered might be a more appropriate choice.

The separation metric values are derived from reported distribution coefficients for relevant metal ions dispersed between phases of tri-butylphosphate in an organic solvent and aqueous nitric acid [B-3]. The coefficients are dimensionless measures of moles of an ion in the organic phase per moles of the same ion in the aqueous phase. The distribution coefficients are normalized to that of plutonium. The normalized value indicates how the ion will be distributed relative to plutonium, and hence, how easily separable it is. If the ratio of the ion distribution coefficient to that of plutonium is relatively small, the ions will be easily separable. Table B.2 lists the relevant raw and normalized coefficients. Pu and U clearly separate into the organic phase leaving the other elements in the aqueous phase. The relative number of ions will also influence the absolute distribution of the metals. An ion with a small distribution coefficient may still wind up in the organic phase if it is present in significant enough quantities. This will force multiple separation stages to effect a given separation. Therefore, the metric value is the sum of the products of the normalized distribution coefficients and the component mole ratio (i.e. the number of moles of each non-plutonium metal in the disposition form divided by the number of moles of plutonium). Mole ratios for spent WNF are calculated directly from final molar composition data listed in an ORIGEN depletion code output table. The HLW vitrified glass log form is designed with

20 w% fission products. The separation metric for MOX was dominated by uranium because of both its large normalized distribution coefficient and the large uranium content in MOX. Table B.2 shows the WNF separation metrics calculation. Uranium is not part of the WNF, however, the values for uranium are included in table B.2 to show why the MOX separation coefficient is so large relative to the vitrified log or WNF.

Table B.2 Separation Metric Calculation					
Type of Ion	Significance/ Representative of	Mole Ratio	Distribution Coefficient	Normalized Distribution Coefficient	Product (Mol x Norm)
Pu	Plutonium	1.0	18.5	1.0	N/A*
Zr	Matrix Constituent	63.1	0.09	0.0049	0.34
Rare Earths	Fission Products	24.0	0.022	0.0012	0.029
U	MOX fuel constituent	0.00	33	1.78	0.00
* Not Applicable				WNF Separation Matrix Value	0.37

The next metric is the radiation barrier. The radiation barrier over the time scales of interest here is set by the fission products. Thus, it is assumed that spent LEU, WGpu MOX and WNF all have similar radiation barriers. Short lived fission products are essentially gone 15 years after discharge. Since the average half life of long-lived fission products is 30 years, the radiation emissions of spent fuel decrease by 50% every 30 years. Assuming a 2000 rem/hr at 1 meter barrier remains 15 years after discharge, the radiation barrier is 125 rem/hr at 135 years and 62.5 rem/hr at 165 years after discharge [N-1]. Therefore, we conservatively assume that the barrier of all three spent fuels will be below 100 rem/hr by 160 years after discharge. The glass log is designed to start out with a 2,000 rem/hr @ 1m barrier; thus, its barrier will last 15 years less than spent fuel barriers. The metric value is the number of years for the radioactive barrier to decay to the 100 rem/hr at 1 meter threshold.

The first weapons usability barrier metric is the isotopic measure of percentage of fissile plutonium isotopes discharged in the WNF. WNF discharge isotopes w% are 1.54, 0.51, 18.1, 9.66 and 70.2 for 238, 239, 240, 241, and 242 Pu, respectively. Consequently, the

isotopic metric value is $(9.66 + 0.51) = 10.17\%$. The critical mass of the plutonium mix was determined using an MCNP model of a bare plutonium metal sphere of the WNF discharge isotopic composition and a density of 19.8 gm/cm^3 . The radius of the sphere was adjusted through several iterations to reach an effective multiplication constant (K_{eff}) of 1.00. At a radius of 8.35 cm, the WNF spent plutonium has a metal sphere MCNP K_{eff} of 1.00233 ± 0.00600 . This equates to a plutonium mass of 48.28 kgs.

The neutron emission and decay heat rate were calculated the same way. Each isotope of plutonium has an associated neutron emission and decay heat rate as indicated in table B.3 (values are taken from table 1.1). Individual decay heat and neutron emission rate contributions to total values were calculated for each isotope based on their weight fraction of total plutonium. Thus, the neutron emission and decay metric values for WNF were $5.21 \times 10^6 \text{ neutrons/sec-kg}$ and 10.3 Kw/ton respectively.

Table B.3 WNF Discharge Isotopics; Neutron Emission and Decay Heat Calculations

Isotope	Discharge Isotopics weight fraction	Neutron Emission (neutrons/sec-kg)	Neutron Emission Contribution	Decay Heat (kW/ton)	Decay Heat Contribution
^{238}Pu	1.54E-02	2.60E+06	4.00E+04	5.60E+02	8.62E+00
^{239}Pu	5.00E-03	2.20E+01	1.10E-01	1.90E+00	9.50E-03
^{240}Pu	1.81E-01	9.10E+05	1.65E+05	6.80E+00	1.23E+00
^{241}Pu	9.66E-02	4.90E+01	4.73E+00	4.20E+00	4.06E-01
^{242}Pu	7.02E-01	1.70E+06	1.19E+06	1.00E-01	7.02E-02
	Total:	5.21E+06			Total: 1.03E+01

Table B.4 lists the plutonium isotopics for spent LEU, spent WGpu MOX and borosilicate glass logs.

Table B.4 Spent LEU, Spent MOX and Borosilicate Glass Log Isotopics

Isotope	Spent LEU (from table 1.1)	Spent WGpu MOX (Westinghouse PDR 1400)	Borosilicate Glass Log (WGpu isotopics)
^{238}Pu	1.3	2.00	0.012
^{239}Pu	60.30	54.00	93.80
^{240}Pu	24.30	22.70	5.80
^{241}Pu	8.30	15.10	0.23
^{242}Pu	5.00	6.20	0.22

Table B.5 summarizes all the WNF metric values, as well as for the borosilicate glass log and the WGPu MOX spent fuel.

Table B.5 Raw Metric Values				
Metric (units in table B.1)	Spent LEU	HLW Glass Log	Spent WGPu MOX	WGPu Non-U Fuel
Disposition Product Matrix Barriers				
Fissile Density	158	18.34	97.48	1.55
Dissolution	167	not applicable	167	211
Separation	40	0.12	40	0.37
Radiation Barrier	160	145	160	160 ^a
Plutonium Weapons Usability				
Isotopic	68.6	94.5%	69.1%	10.2%
Critical Mass	15.4	12.0	16.6	48.3
Neutron Emission	3.3×10^5	5.3×10^4	4.4×10^5	5.21×10^6
Decay Heat	10.3	2.3	14.4	10.3

a. The non-uranium radiation barrier is assumed to be the same as MOX spent fuel.

B.2 Conversion of Metric Values into Metric Score. The next step in the evaluation process is to convert the metric values into metric scores via metric scoring functions. Since spent fuel is defined as the minimum performance standard, spent fuel scores zero for all metrics. The slope of the linear scoring functions are derived by taking the inverse of the range from 0 to 1 or 1 to zero. All functions are of the form shown in figure B.1.

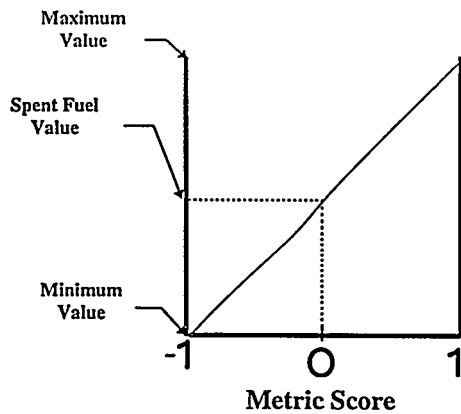


Figure B.1 Example Metric Scoring Function

All the disposition products have a lower fissile density than spent LEU resulting in only positive values. The 1.55 non-uranium value is the best and so defines the upper bound of the range and equates to a 1.00 score. The difference between LEU spent fuel and non-uranium fissile densities is 156.45 Kg/m^3 . Taking the inverse produces a linear slope of 6.4×10^{-3} score units/unit difference in density of the option form and spent fuel. Thus, the MOX score is $[(158.0 - 97.5) \times (6.4 \times 10^{-3})] = 0.387$. The score for the vitrified log is similarly calculated $[(158.0 - 18.4) \times (6.4 \times 10^{-3})] = 0.893$. All of the options perform better than spent LEU, hence, all fissile density scores are greater than 0. Figure B.2 shows the associated scoring metric.

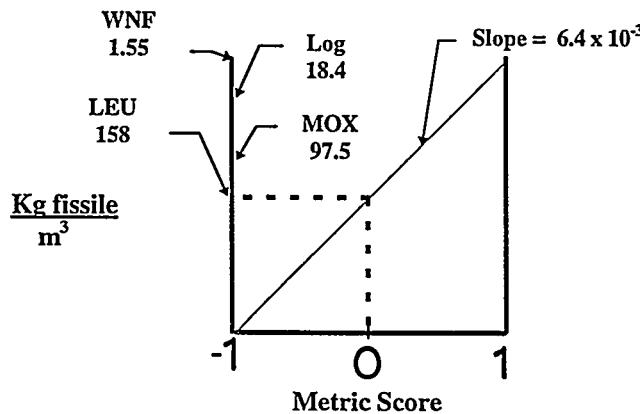


Figure B.2 Fissile Density Scoring Function

The dissolution metric scoring function ranges from 0 to 1 and 0 to -1 are based on the spent fuel metric value thus defining boundary values of 0 and 334 gm of matrix constituent/liter of H₂O on either end of the ordinate axis. Since a lower solubility is preferable, a -1 metric score equates to the higher solubility of 334 gm of matrix constituent/liter of H₂O. This metric value range produces a linear scoring function slope of 6.0×10^{-3} score units/relative difference in solubility as shown in figure B.3. Since the matrix of spent fuel and LEU is the same, the solubility difference is zero and so MOX scores zero. The 211 gm Zr(NO₃)₂/liter of H₂O solubility of a zirconia matrix is larger than that for a UO₂ matrix. The score is calculated by: $[6.0 \times 10^{-3} \times (167 - 211)] = -0.264$. Note that selection of the range was somewhat arbitrary and selection of a different range would alter the function slope, and hence, produce a different WNF score. Plutonium is removed from borosilicate glass by leaching rather than dissolution. Hence, the glass log is assigned a neutral spent fuel value of zero. Figure B.3 shows the associated scoring metric.

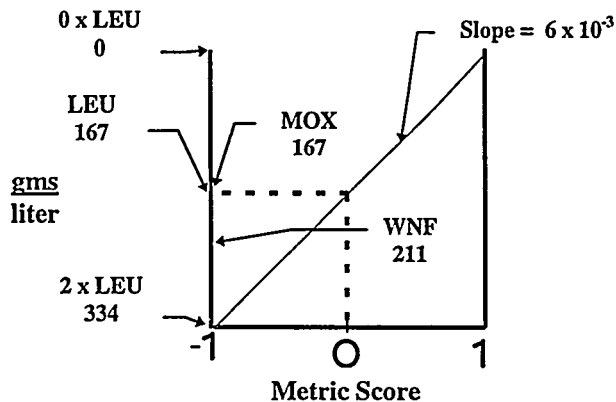


Figure B.3 Dissolution Scoring Function

The 2.5×10^{-2} score units/unit difference slope in the separation metric value is defined by assigning a -1 score to the 0.12 low vitrified log value; thus the log receives a score of -1. The WNF does not fair much better with a score $[2.5 \times 10^{-2} \times (0.368 - 40)] = -0.99$. Both the non-uranium zirconia fuel and the vitrified log have significantly lower separation scores than MOX as a result of their lack of significant quantities of uranium. Figure B.4 shows the associated scoring metric.

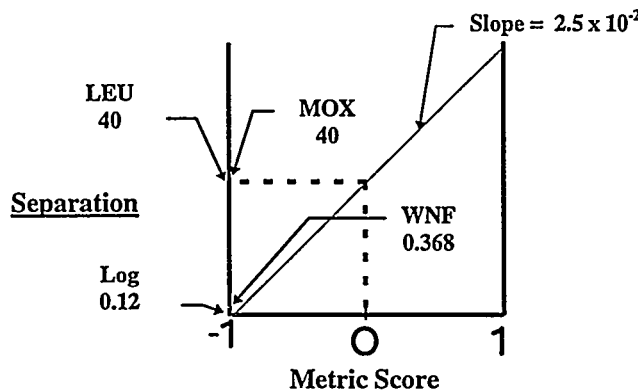


Figure B.4 Separation Scoring Function

There is little difference in radiation barrier metric values. The +1 score is defined as 150% of the spent fuel radiation barrier or 240 years. Likewise, the -1 score is equated to 80 years for an equivalent slope of 1.25×10^{-2} . As described above, MOX, LEU and non-uranium fuel are assumed to all have approximately the same radiation barrier resulting in metric scores of 0.00 for all three. The vitrified log's radiation barrier metric value is 15 years less and so earns a slightly negative score: $[1.25 \times 10^{-2} * (145 - 160)] = -0.188$. Figure B.5 shows the associated scoring metric.

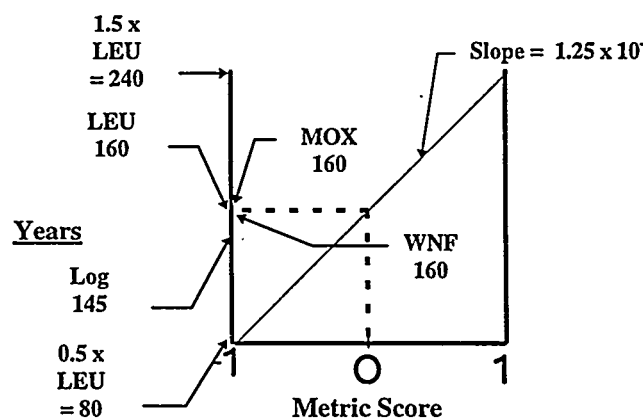


Figure B.5 Radiation Scoring Function

The isotopic scores are calculated with two different scoring function slopes. The 0 to 1 abscissa score range is defined by the 68.6% spent LEU fuel value, at 0, and non-uranium fuel value of 10.17 % yielding a 1.0 value for WNF. The 0 to -1 ordinate range is limited by a maximum of 100% fissile plutonium. Thus, there are two different slopes: 3.2×10^{-2} from 0 to -1 and 1.71×10^{-1} from 0 to 1. The MOX score is $[(68.6 - 69.1) * 3.18 \times 10^{-2}] = -0.016$ and the glass log score is $[(68.6 - 94.5) * 3.18 \times 10^{-2}] = -0.824$. Figure B.6 shows the associated scoring metric.

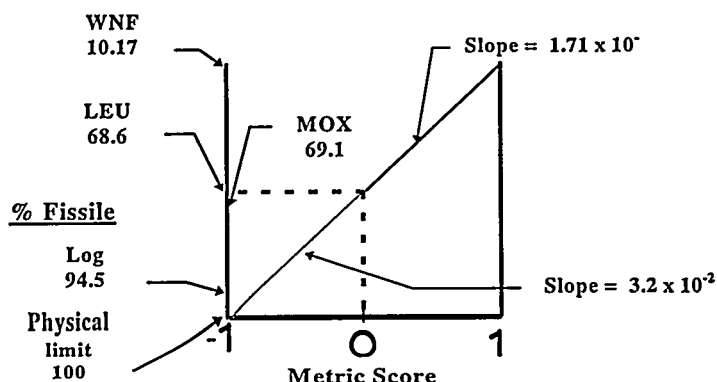


Figure B.6 Isotopic Scoring Function

Similarly, the critical mass slope from -1 to 0 is limited by a zero critical mass constraint which produces a slope of 6.5×10^{-2} . The positive score slope, from 0 to 1, is defined by the 48 kg non-uranium fuel critical mass for a slope of 3.0×10^{-2} . The resultant Log score is $[(12.0 - 15.4) * 6.5 \times 10^{-2}] = -0.22$ and the MOX score is $[(16.6 - 15.4) * 3.0 \times 10^{-2}] = 0.036$. Figure B.7 shows the associated scoring metric.

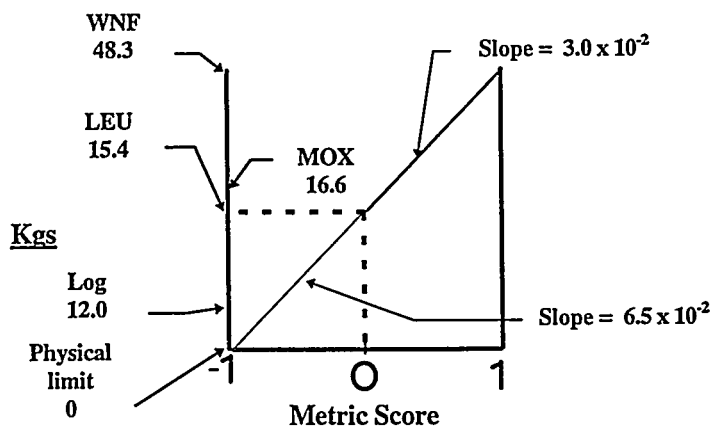


Figure B.7 Critical Mass Scoring Function

On a log scale, the range of metric values for neutron emissions results in a slope equal to $[1/(WNF - LEU)] = 8.3 \times 10^{-1}$ defined by the $\log(5.21 \times 10^6) = 6.72$ WNF values. If the same slope is maintained for the 0 to -1 range, the low limit becomes $5.52 - (6.72 - 5.52) = 4.27$. Thus, the log score is a -1 and the MOX score is $[(5.64 - 5.52) * 8.3 \times 10^{-1}] = 0.10$. Figure B.8 shows the associated scoring metric.

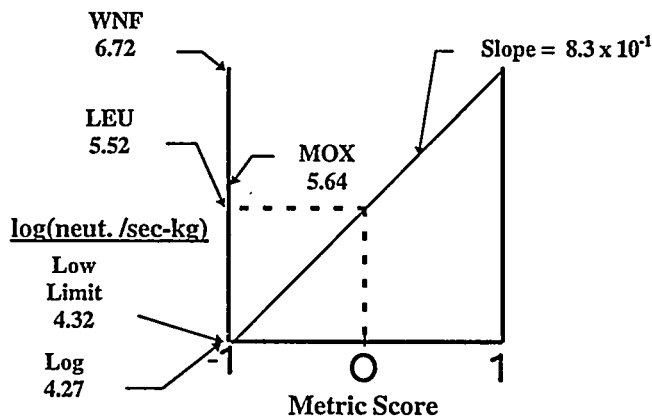


Figure B.8 Neutron Emission Scoring Function

Finally, the decay heat scoring function ordinate range is defined by the low value of the vitrified log decay heat generation, producing a uniform slope for 0 to -1 and 0 to 1 of 0.125 score units/watt. MOX earns a score of $[(14.4 - 10.3) * 0.125] = 0.513$, the log earns -1 and WNF earns 0.00.

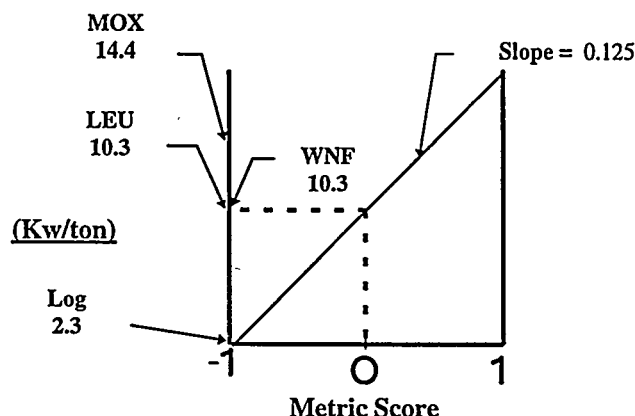


Figure B.9 Decay Heat Scoring Function

Table B.6 Summarizes all the metric scores.

Table B.6 Metric Score Summary				
Metric	Spent LEU	HLW Glass Log	Spent WGPu MOX	WGPu Non-U Fuel
Disposition Product Matrix Barriers				
Fissile Density	0.00	0.89	0.39	1.00
Dissolution	0.00	0.00	0.00	-0.26
Separation	0.00	-1.00	0.00	-0.99
Radiation Barrier	0.00	-0.19	0.00	0.00
Plutonium Weapons Usability				
Isotopic	0.00	-0.82	-0.02	1.00
Critical Mass	0.00	-0.22	0.04	1.00
Neutron Emission	0.00	-1.00	0.10	1.00
Decay Heat	0.00	-1.00	0.51	0.00

B.3 Barrier Type and Overall Scoring Results. Individual metric values and scores are derived above; two steps remain to determine the final ranking of the relative inherent proliferation resistance of the three disposition products. First the proliferation score of the disposition product matrix and plutonium weapons usability barriers types must be determined. Then the options must be ranked in terms of their overall proliferation resistance.

Barrier type scores are the sum of the product of the associated individual metric contributions. The contributions are determined by weighting the importance of each metric in determining the strength of the associated barrier. It is recognized that how the metrics are weighted is subject to great debate. Weighting of the metrics is heavily dependent on the perspective of the decision maker and many different valid solutions can result. The

viewpoint chosen here is to minimize a sub-national or terrorist threat. The weight functions (WF) and contribution of each metric, as assigned by the author, are listed in table B.7 & B.8. The WFs sum to 100% so that the product matrix and plutonium weapons usability barrier types both have an equal total weight of 1. Table B.7 explicitly calculates the barrier level scores for WNF and table B.8 provide the resultant barrier scores for all three disposition products.

Table B.7 WNF Barrier Type Scores

	WF	Metric Score	Product Score
Disposition Product Matrix Barriers			
Fissile Density	0.3	1.00	0.30
Dissolution	0.1	-0.26	-0.026
Separation	0.1	-0.99	-0.10
Radiation Barrier	0.5	0.00	0.00
Matrix Barrier Score			0.18
Plutonium Weapons Usability			
Isotopic	0.4	1.00	0.40
Critical Mass	0.4	1.00	0.40
Neutron Emission	0.1	1.00	0.10
Decay Heat	0.1	0.00	0.00
Usability Barrier Score			0.9

A disposition product which exactly met the spent fuel standard would have an overall score of 0.00. Table B.9 presents the overall scores and subsequent final ranking of the disposition products. The overall scores are just the sum of the barrier scores. The disposition products are then ranked in order of decreasing total score. The top scoring product is ranked number 1 and is the most inherently proliferation resistant product while the lowest scoring product is ranked number 3 and is the least inherently proliferation resistant product.

Table B.8 Metric Weights, Contributions and Barrier Type Scores

	WF	HLW Glass Log	Spent WGPu MOX	WGPu Non-U Fuel
Disposition Product Matrix Barriers				
Fissile Density	0.3	0.27	0.12	0.30
Dissolution	0.1	0.00	0.00	-0.03
Separation	0.1	-0.10	0.00	-0.01
Radiation Barrier	0.5	-0.09	0.00	0.00
Matrix Barrier Score		-0.074	0.12	0.18
Plutonium Weapons Usability				
Isotopic	0.4	-0.33	-0.01	0.40
Critical Mass	0.4	-0.09	0.01	0.40
Neutron Emission	0.1	-0.10	0.01	0.10
Decay Heat	0.1	-0.10	0.051	0.00
Usability Barrier Score		-0.62	0.069	0.90

The crude metrics and weighting functions are probably adequate for selecting among an array of widely different options as in the given examples. More refined versions are probably called for if one is to discriminate within a given category of options (such as between different non-U fuel types). This could well be a profitable subject for future work, in which case attention is recommended to evaluation of more appropriate (e.g. non-linear) scoring functions, and to better metrics for dissolution.

Table B.9 Overall Scores and Ranking of Inherent Proliferation Resistance

	HLW Glass Log	Spent WGPu MOX	WGPu Non-U Fuel
Matrix Barrier Score	0.07	0.12	0.18
Weapons Usability Score	-0.62	0.07	0.90
Overall Score	-0.55	0.19	1.08
Ranking	3	2	1

Appendix C Weighting to Determine Core Average Reactivity

Coefficients

Subject to the validity of approximations made in the derivation of the FLARE-type nodal codes, plus equality of the fast group flux and its adjoint (as confirmed by Mosteller [M-5] for typical PWR Cores), and neglecting certain leakage related terms, it can be shown that the neutron yield and reactivity coefficients should be weighted by the fast flux squared (or equivalently by the product of fast flux and neutron source rate) when aggregating assembly node values to obtain whole core average values [H-8]. The result is:

$$\frac{\partial \rho}{\partial T_f} = \sum_p \frac{\delta \rho}{\delta T_f^p} = \frac{\sum_p \bar{\Phi}^p S^p \left(\frac{\delta k_{\text{inf}}^p}{k_{\text{inf}}^p \delta T_f^p} \right)}{\sum_p \bar{\Phi}^p S^p} \quad (\text{C1})$$

From the near constancy of the energy release per fission neutron and fast group migration area, it also follows that power squared weighting is a useful, fairly accurate alternative [S-5]. An alternative derivation of the power squared weighting scheme from the two group neutron balance equation follows. Refer to chapter 3 of Reference [D-9] for supporting details.

Beginning with the two group neutron balance equations,

$$-D_1 \nabla^2 \Phi_1 + \sum a_1 \Phi_1 + \sum_{12} \Phi_1 - \frac{1}{k} (\nu \sum_{f1} \Phi_1 + \nu \sum_{f2} \Phi_2) = 0 \quad (\text{C2})$$

$$-D_2 \nabla^2 \Phi_2 + \sum a_2 \Phi_2 - \sum_{12} \Phi_1 = 0 \quad (\text{C3})$$

and making the one and one-half group approximation:

$$\sum a_2 \Phi_2 \cong \sum_{12} \Phi_1 \quad (\text{C4})$$

One can combine Eqs. C2, C3 & C4 and manipulate the results, using the definition of reactivity, namely:

$$\rho = \frac{(\nu \Sigma f_1 \Phi_1 + \nu \Sigma f_2 \Phi_2) - (\Sigma_{a1} \Phi_1 + \Sigma_{a2} \Phi_2)}{(\nu \Sigma f_1 \Phi_1 + \nu \Sigma f_2 \Phi_2)} . \quad (C5)$$

To obtain the critical system (k=1) equation:

$$\nabla^2 \Phi_1 + \frac{1}{M^2} \left(\frac{\rho}{1 - \rho} \right) \Phi_1 = 0 . \quad (C6)$$

where,

$$M^2 \equiv \left(\frac{D_1}{\Sigma_{a1} + \Sigma_{i2}} \right) \quad (C7)$$

The fast flux can be eliminated by an energy balance:

$$\Phi_1 = \frac{q}{\kappa \left(\Sigma_{f1} + \frac{\Sigma_{f2} \Sigma_{i2}}{\Sigma_{a2}} \right)} \quad (C8)$$

where q = the local power density and κ is the energy per fission (i.e. Mev/fission) such that:

$$q = \kappa \left(\Sigma_{f1} + \Sigma_{f2} \frac{\Sigma_{i2}}{\Sigma_{a2}} \right) \Phi_1 . \quad (C9)$$

Thus, combining C6 and C8:

$$\nabla^2 [q(1 - \rho)] + \frac{\rho q}{M^2} = 0 . \quad (C10)$$

Normalizing Eqn. C9 by the total power for an assembly with reactivity ρ_i and power fraction f_i :

$$\nabla^2 [f_i(1 - \rho_i)] + \frac{\rho_i f_i}{M^2} = 0 . \quad (C11)$$

and approximating the Laplacian as the difference between the local assemblies' average value r and assembly i :

$$\frac{f_r(1 - \rho_r) - f_i(1 - \rho_i)}{0.25h^2} + \frac{\rho_i f_i}{M^2} = 0 \quad (C12)$$

where h is defined as the assembly width, f_i is the fractional power of assembly i and M is the migration length. Assuming the assembly is surrounded by core average assemblies with $\rho_r = \rho_s = 0$ and taking the first order terms of a series expansion:

$$f_i \approx 1 + \theta \rho_i \quad (C13)$$

where

$$\theta = 1 + \frac{1}{4} \left(\frac{h}{M} \right)^2. \quad (C14)$$

One also has:

$$\bar{\rho}_{core} = \sum_{i=1}^N f_i \rho_i \quad (C15)$$

which follows directly from the definition of reactivity. To this point we have merely reproduced the sequence of equations from chapter 3 of reference [D-9].

Differentiating Eqn. C14 with respect to temperature,

$$\frac{\delta \bar{\rho}_c}{\delta T_c} = \sum_1^N f_i \frac{\delta \rho_i}{\delta T_c} + \sum_1^N \rho_i \frac{\delta f_i}{\delta T_c} \quad (C16)$$

but, relative to core-average power fraction ($f_{avg} = 1/N$) Eqn C12 can be rewritten:

$$f_i = \bar{f}(1 + \theta \rho_i) \quad (C17)$$

Substituting Eqn. C17 into Eqn. C16 and manipulating the results leads to:

$$\frac{\delta \bar{\rho}_c}{\delta T_c} = \sum_1^N \frac{f_i}{\bar{f}} (f_i + \theta \bar{f} \rho_i) \frac{\delta \rho_i}{\delta T} \quad (C18)$$

For peripheral assemblies $\rho_i = \rho_{inf} - \rho_L$, where ρ_L is a leakage reactivity penalty

($\rho_L \sim 0.12$). Finally since,

$$\theta \rho_i \ll 1 , \quad (C19)$$

Eqn. C17 becomes,

$$\frac{\delta \bar{\rho}_c}{\delta \bar{T}_c} \approx \sum_i^N \left(\frac{f}{\bar{f}} \right)^2 \left(\frac{\delta \rho_i}{\delta T_i} \right) . \quad (C20)$$

Thus, the change in core reactivity due to a change in temperature can be calculated by summing the contributions of the changes in reactivity of the individual assemblies weighted by the square of their power. Since the ratio $\left(\frac{f}{\bar{f}} \right)$ is less than one for the peripheral assemblies considered in this application, using power weighted contributions (i.e. using $\left(\frac{f}{\bar{f}} \right)$ instead of $\left(\frac{f}{\bar{f}} \right)^2$ times the pin cell reactivity coefficient) to obtain core average values overestimates the effect of the peripheral assemblies on core average reactivity coefficients. Thus, it is more conservative for this application. Using straight number weighted contributions assumes the ratio $\left(\frac{f}{\bar{f}} \right)$ equals 1.0 and that all assemblies contribute equally to the core average reactivity coefficients. Thus, number weighting produces the most conservative core average values of the three weighting schemes.

REFERENCES

[A-1] Akie, H., Muromura, T., Takano H., Matsuura, S., 1994, "A New Fuel Material For Once -Through Weapons Plutonium Burning", Nuclear Technology, vol. 107, no. 2, pp 182-191.

[A-2] *Atoms in Japan*, " NSC Gives Green Light to Pu-Thermal Utilization", Atoms in Japan, July 1995, pp. 16.

[A-3] AECL Technologies, "Plutonium Consumption Program CANDU Reactor Project", DOE Contract #AC03-94SF20218, AECL Technologies Inc, July 31, 1994.

[A-4] ABB-Combustion Engineering , "DOE Plutonium Disposition Study: Screening Study for Evaluation of the Potential for System 80+ to Consume Excess Plutonium" Volume 1 and 2, DOE Contract #DE-AC03-93 SF19682, ABB-Combustion Engineering, April 30, 1994.

[A-5] ABB-Combustion Engineering , "DOE Plutonium Disposition Study: Analysis of Existing ABB-CE Light Water Reactors For the Disposition of Weapons-Grade Plutonium.", DOE Contract #DE-AC03-93 NSF19682, ABB-Combustion Engineering, June 1, 1994.

[A-6] Ayoub A., Driscoll M., Todreas N. , "A Strategy For Extending Cycle Length to Improve Pressurized Water Reactor Capacity Factor", MIT-ANP-TR-032, Jun. 1995.

[B-1] Berkout F., Diakov A., Fieveson H., Hunt H., Lyman E., Miller M., vonHipple F., "Disposition of Separated Plutonium", *Science and Global Security*, vol. 3, pp. 161-213 , 1993.

[B-2] Beard C., Buksa J., Chidchester K., Eaton S., Motley F., Siebe D., "Evaluation of Existing United States' Facilities for Use as a Mixed-Oxide (MOX) Fuel Fabrication Facility for Plutonium Disposition", Los Alamos National Laboratory, ICONE4, March 1-14, 1996.

[B-3] Benedict M., Pigford T. H., Levi H. W., Nuclear Chemical Engineering, pp. 462, McGraw Hill, 1981

[B-4] Burgess J., "Ions in Solution: Basic Principles of Interaction", Ellis Horwood Limited, 1988.

[B-5] Briesmeister, J. M., 1993 "MCNP - A General Monte Carlo N-Particle Transport System Version 4A", editor, Los Alamos National Laboratory, LA 12625-M.

[B-6] Bahadir T., Studsvick of America, Newton MA., personal consultation, March 1996.

[C-1] Chang G. S., "Physics Analysis of Tungsten in Weapons-Grade U/Pu Fuels for LWR U/Pu burning/power Reactors", Trans. Am. Nucl. Soc., 70, 90-91, (June 1994).

[C-2] Clinnard, F. W., Hurley G.F., Hobbs. L.W., 1982, "Neutron Irradiation Damage in MgO, Al₂O₃ and MgAl₂O₄ Ceramics", Journal of Nuclear Materials, vol. 108-109, pp. 655-670.

[C-3] Clinnard F. W., 1979, "Ceramic for Applications in Fusion Systems", Journal of Nuclear Materials, vol. 85&86, pp. 393-404.

[C-4] Croff, A. G., 1980, "ORIGEN2 - A Revised and Updated Version of the Oak Ridge Isotope Generation and Depletion Code", Oak Ridge National Laboratory, ORNL/TM-7175.

[C-5] Cumo M., Afgan N., "Post Graduate Course on Energy Engineering: Nuclear Power Plant", CATTID, 1995.

[C-6] Crump M., Flynn E., "System 80+ Plutonium Disposition Capability," Global '93 International Conference, Seattle, Sept. 1993.

[D-1] Degueldre C., Kasemeyer U., Botta F., "Study of Plutonium Incineration in LWRs employing a Uranium Free Fuel Inert Matrix-Burnable Poison-Actinide Approach", Paul Scherrer Institute, TM-43-95-12, May 1995.

[D-2] Department of Energy Office of Fissile Materials Facts Release, "Department of Energy Declassifies Location and Forms Of Weapons-Grade Plutonium And Highly Enriched Uranium Inventroy Excess To National Security Needs", DOE Office of the Press Secretary, Feb. 8 1996.

[D-3] DOE press release, Reuters News Agency, Washington, 8 Feb. 1996.

[D-4] Department of Energy Report, 1993, "US. Department of Energy Plutonium Disposition Study, Technical Committee Report, Volumes I & II, July 2 1993" Office of Nuclear Energy, US DOE, Washington DC, 1994.

[D-5] DE Kruijf W. J. M., Janssen , A. J., 1993a "Benchmark Calculations on Resonance Absorption By ²³⁸U in A PWR Pin Cell", Netherlands Energy Research Foundation , ECN-R-93-016.

[D-6] DE Kruijf, W. J. M., Janssen, A. J., 1993b, "Detailed Resonance Absorption Calculations with Monte Carlo Code MCNP and a Collision Probability Version of the Slowing Down Code Rolaids", Netherlands Energy Research Foundation , ECN-RX--93-109.

[D-7] Department of Defense, "Military Plutonium From Commercial Spent Nuclear Fuel", Congressional Hearings, Subcommittee on Interior and Insular Affairs, US House of Representatives, October 1, 1981.

[D-8] Driscoll, M.J., MIT Department of Nuclear Engineering Nuclear Fuel Cycle Issues Course Class Notes, course #22.351, spring 1995.

[D-9] Driscoll, M.J., Downar T.J., Pilat E.E., 1990, "The Linear Reactivity Model for Nuclear Fuel Management", American Nuclear Society, La Grange Park, pp 69-101.

[E-1] Eckhart L., Christenson J., "Reevaluation of the Feasibility of Stainless Steel Cladding for LWR Applications", Trans. Am. Nucl. Soc., 34, 354, 1980.

[E-3] Edinus M., Forssen B., "CASMO-3, A Fuel Assembly Burnup Program: User's Manual Version 4.7", Studsvik of America Inc., Newton MA, 1993.

[E-2] Erlich E., H., Wadekamper D., "Capability of the Advanced Boiling Water Reactor to Operate with MOX Fuel", General Electric Nuclear Systems, ICONE4, March 1-14, 1996.

[F-1] Feinroth H., "Feasibility Study on Use of Ceramic Cladding to Reduce the Severity of Reactor Accidents", Gamma Eng. Corp. Report to NRC, # 8533-1, June 1990.

[F-2] Fisher , J. R., Grow, R.L., Hodges, D. Rapp, J.S., Smolinske, K.M., 1989, "Evaluation of Discrepancies in Assembly Cross Section Generator Codes", Electric Power Research Institute NP-6147, vols. 1 & 2.

[F-3] "Reversing the Arms Race: How to Achieve and Verify Deep Reductions in the Nuclear Arsenals", ed. von Hippel F., Sagdeev R., Gordon and Breach Science Publishers, New York, 1990, pp. 265.

[F-4] "Final Saftey Analysis Report: Maine Yankee Atomic Power Station", Volume1, Chapter 3, rev 4, 1971.

[F-5] Flipot A., et. al., "Burnable Poison Dispersion in UO₂ Fuel", Nucl. Eng. Int., Vol. 15, No. 167, April 1970.

[G-1] Gitzen W.H., "Alumina as a Ceramic Material", Alcoa Research Laboratories, The American Ceramic Society, 1970.

[G-2] General Atomics, "MHTGR Plutonium Consumption Study: Phase I Report", report for DOE, GA/DOE-051-94, May 1993.

[G-3] General Atomics, "MHTGR Plutonium Consumption Study: Phase II Final Report", report for DOE, GA/DOE-051-94, April 29, 1994.

[G-4] General Electric, "Study of Plutonium Disposition Using GE Advanced Boiling Water Reactors", DOE Contract #DE-AC03-93SF19681, GE Nuclear Energy, April 30th, 1994.

[G-5] General Electric, "Study of Plutonium Disposition Using Existing GE Boiling Water Reactor (ABWR)", DOE Contract #DE-AC03-93SF19681, GE Nuclear Energy, June 1, 1994.

[G-6] Gruppelaar H., Klippe, H.T.H., Kloosterman, J.L., Hoogenboom, J.E., De Leege, P.F., Verhagen, F.C., Bruggink, J.C., 1993, "Evaluations of PWR and BWR Assembly Benchmark Calculations, Status report of EPRI computational benchmark results, performed in the framework of the Netherlands' PINK programme", Netherlands Energy Research Foundation ECN-C-93-088.

[G-7] Gavin P., et al., "Lead Test Fuel Assembly Physics for Erbium at the San Onofre Nuclear Generation Station", Trans. Am. Nuc. Soc., vol. 68, June 1993.

[H-1] Hejzlar N.E., Todreas N. E., Driscoll M.J., "Evaluation of Materials For The Fuel Matrix of a Passive Pressure Tube LWR Concept", MIT Nuc. Eng. Dept., MIT-ANP-TR-017, DOE/ER/75785-2, December 1993.

[H-2] Holden R. B., "Ceramic Fuel Elements", United Nuclear Corporation, Gordon and Breach Science Publications, N.Y., 1966.

[H-3] Horn F.L., Fillo J.A., Powell J.R., "Performance of Ceramic Materials in High Temperature Steam and Hydrogen", Journal of Nucl. Mat., Vol. 85 & 86, 1979, pp. 439-443.

[H-4] Herbig R., Rudolph K., Lindau B., Skiba O.V., Maershin, A.A., 1993, " Vibratory Compacted Fuel for the Liquid Metal Reactor BOR-60", Journal of Nuc. Mat., vol. 204, pp. 93-101.

[H-5] Haag, "Development of Reactor Graphite", Journal of Nuc. Mat., vol. 171, 1990, pp41-48.

[H-6] Hopkins G. R., " Carbon and Silicon Carbide as First Wall materials in Inertial Confinement Fusion Reactors", GA-A14894, General Atomic Company, March 1978.

[H-7] Hansen C., US Nuclear Weapons, Orion Books, New York, 1988.

[H-8] Henry A. F., Professor of Nuclear Engineering, MIT Nuclear Engineering Department, personal consultation, March 1996.

[H-9] Haas D., Vandergheynst A., Van Vliet J., Lorenzelli R., "Mixed-Oxide Fuel Fabrication Technology and Experience at the Belgonucleaire and CFCA Plants and Further Developments For the MELOX Plant", Nuclear Technology, Vol. 106, Apr. 1994, pp. 60-82.

[J-1] Journal of Commerce Staff Report April 3, 1996, pp. 5B.

[J-2] Jonsson A., "Initial Physics Evaluation of Erbium as a Burnable Absorber in a PWR", Trans. Am. Nucl. Soc., vol. 68, June 1990.

[K-1] Kilbourn, B. T., 1993, "A Lanthanide Lanthology: Part I, A-L", Molycorp Corporation, White Plains, NY pp. 6-9.

[K-2] Kingery W.D., Bowen H.K., Ulhman D.R., "Introduction to Ceramics; 2nd Edition", John Wiley and Sons, Inc., New York, 1976.

[K-3] Kinoshita C., Fukumoto K., Fukada K., Garner F.A., Hollenburg G.W., 1995, "Why is Magnesia Spinel a Radiation Resistant Material?", J. of Nuc. Mat., vol. 219, pp. 143-151.

[K-4] Krief, R.A., 1992, "Nuclear Engineering: Theory and technology of Commercial Nuclear Power", Second Edition, Hemisphere Publishing, Washington DC, pp. 77.

[L-1] Lovins A. B., "Nuclear Weapons and Power-Reactor Plutonium", Nature, vol. 283, 822 (Feb. 1980).

[L-2] "Lange's Handbook of Chemistry", Dean J. A., Ed., McGraw Hill, New York, 1985, pp. 10-21.

[M-1] Mark, J. C., 1990, "Explosive Properties of Reactor Grade Plutonium", Science and Global security, vol. 4, no. 1, pp. 111-128.

[M-2] Miller M. M., "Are IAEA Safeguards on Plutonium Bulk Handling Facilities Effective?", Nuclear Control Institute, August 1990.

[M-3] Meyer W., Loyalka S. K., Williams R., "The Homemade Nuclear Bomb Syndrome", Trans. Am. Nucl. Soc., 22, 834-835, Nov., 1975.

[M-4] Moore, R., Schnitzler, B.G., Wemple C.A., Babcock, R.S., Wessol, D.E., "MOCUP: MCNP-ORIGEN2 Coupled Utility Programs", Idaho National Engineering Laboratory, Idaho Falls ID, INEL-95/0523, 1995.

[M-5] Mosteller R.D., "Self Adjointness of the Fast Flux in a Pressurized Water Reactor", Trans. Am. Nucl. Soc., vol. 50, Nov, 1985.

[M-6] Matzie R. A., "Licensing Assessment for PWR Extended Burnup Fuel Cycles", Combustion Engineering Report for DOE #CEND-381, UC-78, March 1981.

[M-7] Miller M. M., "The Iraqi Nuclear program: Past Present and Future?", IGCC Conf. on Non-Proliferation, Limasol, Cyprus, August 1995.

[N-1] NAS 1994: National Academy of Sciences, Committee on International Security and Arms Control, "Management and Disposition of Excess Weapons Plutonium", National Academy Press, Washington DC.

[N-2] NAS 1995: National Academy of Sciences, Committee on International Security and Arms Control , Panel on Reactor Related Options for the Dispositioning of Excess Weapons Plutonium, "Management and Disposition of Excess Weapons Plutonium, Reactor Related Options", National Academy Press, Washington DC.,

[N-3] Nuclear Engineering International, "Japanese Long Term Plan: Back-peddling on Recycling", vol. 39, No. 483, pp. 110-113, Oct. 1994.

[N-4] Nuclear News, " The World List of Nuclear Power Plants." Am. Nuc. Soc. LaGrange Park, IL, vol. 38, no. 3, March 1995.

[P-1] Paratte, J.M., Chawla, R., 1995 "On the Physics and Feasibility of Light Water Reactor Plutonium Fuels Without Uranium", Annals of Nuclear Energy, vol., no. 7, Jul. 1995.

[P-2] "Physics of Plutonium Recycling, Volume 1: Issues and Perspectives", OECD Documents, Paris, France, vol. I, pp. 149-165, 1995.

[R-1] Reeve H.R., Gailor O.H., "Cell Depletion and Spectrum Recalculations", Trans. Am. Nucl. Soc., 13, 172, (June 1970).

[R-2] Rochlin G. I., Plutonium, Power, and Politics: International Arrangements for the Disposition of Spent Nuclear Fuel, University of California Press, Berkeley CA., 1979.

[S-1] Sterbenz, J. W., Olsen C.S., Sinha U.P., "Weapons Grade Plutonium Disposition, Volume 4: Plutonium Dispositioning in Light Water Reactors," DOE/ID-10422, pg. 14-15, June 1993.

[S-2] Serber R., The Los Alamos Primer, The First Lectures on How to Build An Atomic Bomb, University of California Press, 1992.

[S-3] The Economist, "Uranium Plutonium and Pandemonium", June 5th 1993, pp. 98-100.

[S-4] Selvaduray. G., Goldstein, M., Anderson, R., 1978, " Separation Technologies Reviewed", Nuclear Engineering International, Vol. 23, No. 275, pp. 35-40.

[S-5] Sauer I. L., Driscoll M. J., "A core Related Pattern and Composition Optimization Methodology for PWRs", MITNE-266, MIT Nuclear Engineering Department, March 1985.

[S-6] Salvatores M., Prunier C, Guerin Y., Zaetta A., "Transmutation Studies at CEA in Frame of the SPIN Program Objectives, Results and Future Trends", Proceed. of American Institute of Physics Int'l. Conf. on Accelerator-Driven Transmutation Technologies and Applications, Las Vegas, NV. 1994.

[S-7] Secker J., Erwin R., "ZrB₂: The Optimum Integral Fuel Burnable Absorber for PWRs", Trans. Am. Nuc. Soc., vol. 62, Nov. 1990.

[T-1] Todreas, N. E., Kazimi, M. S., Nuclear Systems I, Thermal Hydraulic Fundamentals, Hemisphere Publishing Inc., New York, 1990, pp. 296.

[T-2] Taylor T. B., "Nuclear Disarmament and Peaceful Nuclear Technology - Can We Have Both?", Nuclear Disarmament and Nuclear Technology.

[T-3] Taylor T. B., "Disarmament and Fissile Material", Reversing the Arms Race: How to Achieve and Verify Deep Reductions in the Nuclear Arsenals, ed. von Hippel F. Sagdeev R., Gordon and Breach Science Publishers, New York, 1990, pp. 91.

[T-4] Tang J., Driscoll M., Todreas N. , "Physics Considerations in a Passive Light Water Pressure Tube Reactor", MIT-ANP-TR-009, Nov. 1991.

[V-1] "Reversing the Arms Race: How to Achieve and Verify Deep Reductions in the Nuclear Arsenals", edited by von Hippel F., Sagdeev R., Gordon and Breach Science Publishers, New York, 1990.

[W-1] Westinghouse, "PDR Plutonium Disposition Study Phase II Final Report", DOE Contract #DE-AC03-93SF19683, Westinghouse Electric Corporation, April 30th, 1994.

[Y-1] Yario W., "Boron-Containing Burnable Poisons, " Trans. Am. Nucl. Soc. Vol. 39, Nov. 1981.